



<https://theses.gla.ac.uk/>

Theses Digitisation:

<https://www.gla.ac.uk/myglasgow/research/enlighten/theses/digitisation/>

This is a digitised version of the original print thesis.

Copyright and moral rights for this work are retained by the author

A copy can be downloaded for personal non-commercial research or study, without prior permission or charge

This work cannot be reproduced or quoted extensively from without first obtaining permission in writing from the author

The content must not be changed in any way or sold commercially in any format or medium without the formal permission of the author

When referring to this work, full bibliographic details including the author, title, awarding institution and date of the thesis must be given

Enlighten: Theses

<https://theses.gla.ac.uk/>
research-enlighten@glasgow.ac.uk

Characterisation and Analysis of PDE4A
Phosphodiesterase Isoforms

Moira Ann Wilson (B.Sc Hons.)

Thesis submitted to the University of Glasgow
for the degree of Doctor of Philosophy
in the Faculty of Science

Institute of Biomedical and Life Sciences
University of Glasgow

December 1995

ProQuest Number: 10391316

All rights reserved

INFORMATION TO ALL USERS

The quality of this reproduction is dependent upon the quality of the copy submitted.

In the unlikely event that the author did not send a complete manuscript and there are missing pages, these will be noted. Also, if material had to be removed, a note will indicate the deletion.



ProQuest 10391316

Published by ProQuest LLC (2017). Copyright of the Dissertation is held by the Author.

All rights reserved.

This work is protected against unauthorized copying under Title 17, United States Code
Microform Edition © ProQuest LLC.

ProQuest LLC.
789 East Eisenhower Parkway
P.O. Box 1346
Ann Arbor, MI 48106 – 1346

Thesis
10464
Copy 2



	<u>PAGE</u>
LIST OF CONTENTS	ii
LIST OF FIGURE LEGENDS	vii
LIST OF TABLES	xii
ABBREVIATIONS	xiii
ACKNOWLEDGEMENTS	xiv
SUMMARY	xv

1.	<u>Introduction</u>	1
1.1	Cyclic adenosine 3', 5'- monophosphate as a Second Messenger.....	1
1.2	Cyclic AMP Dependent Protein Kinase.....	1
1.3	Biological Effects Mediated by Cyclic AMP.....	2
	(i)Cyclic AMP as a Hormonal Second Messenger	2
	(ii)Cyclic AMP in the Central Nervous System.....	4
	(iii)Cyclic AMP in the Immune System.....	4
	(iv)Cyclic AMP in the Cardiovascular System.....	4
1.4	Adenylyl Cyclase.....	6
	(i)Synthesis of Cyclic AMP.....	6
	(ii)Adenylyl Cyclase Structure.....	6
	(iii)Adenylyl Cyclase regulation by G-Proteins.....	7
1.5	Inactivation of the Cyclic AMP Signal.....	9
1.6	Cyclic Nucleotide Phosphodiesterases.....	9
1.7	Cyclic GMP Metabolising Phosphodiesterases.....	10
	(i)PDE1 - Calmodulin Stimulated PDE.....	10
	a)Cellular Distribution.....	10
	b)Structure.....	11
	c)Substrate Specificity and Regulation	11
	(ii)PDE5 Cyclic GMP Specific Phosphodiesterase.....	12
	(a)Characteristics.....	12
	(b)Phosphorylation by Protein Kinase A and Protein Kinase G.....	13
	(c)Isolation of Murine cDNAs Representing PDE5.....	14
	(iii)PDE6 Retinal Rod and Cone Phosphodiesterases.....	14
	(a)Visual Pathway	15
	(b)Rod Cyclic GMP Phosphodiesterases	15
1.8	Cyclic AMP Phosphodiesterases	16

	(i)PDE2 - Cyclic GMP Stimulated Phosphodiesterase.....	16
	(a)Kinetics	16
	(b)Physiological Role	17
	(ii)PDE3 - Cyclic GMP Inhibited Phosphodiesterase.....	18
	(a)Structure and Kinetics.....	18
	(b)Regulation of Cyclic GMP Inhibited Phosphodiesterase	19
1.9	PDE4 Cyclic AMP Specific PDEs.....	21
	(i)Isolation and Purification of PDE4	21
	(ii)Peripheral Plasma Membrane PDE	22
1.10	PDE Activities isolated from <i>Drosophila melanogaster</i>	22
	(i)Mutants of <i>Drosophila melanogaster</i>	24
	(ii)Identification of the <i>dunc</i> Gene Product.....	24
	(iii)Molecular Analysis of the <i>dunc</i> Gene.....	24
1.11	Rat Homologues of the <i>Drosophila dunc</i> Gene	25
	(i)Isolation of RD1 (PDE4A1) by Cross-Hybridisation With <i>dunc</i> Gene Probe.....	27
	(ii)Isolation of DPD (PDE4B1) by Suppression of the <i>ras</i> 2 ^{val19} Mutation of <i>Saccharomyces Cerivisiae</i>	28
	(iii)Biochemical Analysis of DPD (PDE4B1) and RD1 (PDE4A1)	30
	(iv)Unique N-Terminal Region of RD1	31
	(v)Functional Role for PDE4 Species in the CNS.....	32
1.12	Molecular Analysis of Rat PDE4	33
1.13	Human Multigene Family Encoding Cyclic AMP Specific Phosphodiesterases	34
1.14	Cellular Regulation of PDE4.....	36
1.15	Pharmacological Effects of PDE4 Inhibition.....	38
	(i)(a)PDE4 Inhibition in the Treatment of Asthma.....	38

	(b)PDE4 in Monocytes	38
	(c)PDE4 in Eosinophils and T-lymphocytes.....	39
	(ii)PDE4 in the CNS	40
	(iii)PDE4 in Smooth Muscle	41
1.16	Isolation of a Human Monocyte Cyclic AMP Specific Phosphodiesterase - hPDE4A _{Livi}	41
1.17	Isolation of a PDE4 PDE From Human Brain	42
1.18	Isolation of a Human PDE4D.....	43
1.19	Kinetics of Cyclic AMP Hydrolysis and Inhibition by Rolipram of PDE4	43
	(i)Kinetics of Cyclic AMP Hydrolysis.....	44
	(ii)Inhibition by Rolipram	44
	(iii)High Affinity Rolipram Binding Site Detected in Rat Brain.....	44
	(iv)The Rolipram Binding Site of Human PDE4.....	46
	(v)High Affinity Rolipram Binding Outwith the CNS.....	47
1.20	PDE7 High Affintity Cyclic AMP Specific PDE	49
2 .	<u>Materials and Methods</u>	60
2.1	Solutions	60
2.2	Chemicals	60
2.3	Preparation of Soluble and Pellet Associated Enzyme From Yeast.....	60
2.4	Phosphodiesterase Assay.....	60
2.5	Thermal Denaturation.....	62
2.6	Protein Determination.....	62
2.7	Preparation of Synaptosomes.....	63
	(i)Tissue preparation	63
	(ii)Percoll-Sucrose Solutions	63
	(iii)Fraction Collection.....	63

2.8	Subcellular Fractionation of Synaptosomes by Continuous Sucrose Gradients.....	64
	(i)Cell Lysis.....	64
	(ii)Preparation of Membranes.....	64
	(iii)Continuous Sucrose Gradient	65
2.9	Acetylcholinesterase Assay.....	65
2.10	Lactate Dehydrogenase Assay	66
2.11	5'-nucleotidase Assay.....	66
2.12	Assay of Adenylate Cyclase Activity.....	67
2.13	Cyclic AMP Determination.....	67
2.14	Preparation of Cyclic AMP Binding Protein from Bovine Adrenal Glands.....	69
	(i)Dissection.....	69
	(ii)Homogenisation.....	69
	(iii)Centrifugation	69
2.15	SDS-PAGE Electrophoresis	69
2.16	Western Blotting.....	70
2.17	Concentration of Protein Samples.....	70
3.	<u>Results - Chapter 3 - Characterisation of Human PDE4A</u>	
	<u>h6.1</u>	
3.1	Introduction	72
3.2	Results.....	74
3.3	Conclusions and Discussion	78
4.	<u>Results - Chapter 4 - Analysis of Truncated Versions of</u> <u>h6.1, Chimeric PDE HYB1 and an N-terminal Domain</u> <u>Extension PDE 10AORF</u>	
4.1	Introduction.....	112
4.2	Results.....	116
4.3	Conclusions and Discussion	120

5.	<u>Results - Chapter 5 - Analysis of Rat PDE4A RD1</u>	
5.1	Introduction.....	150
5.2	Results.....	155
5.3	Conclusions and Discussion.....	159
6.	<u>Final Discussion and Conclusions</u>	175
7.	<u>References</u>	183
	<u>Appendix 1</u>	202

Fig. 3.2.5	Dose-Response to RO-20-1724 of Pellet h6.1	96
Fig. 3.2.6	Dose-Response to IBMX of Soluble and Pellet h6.1	97
Fig. 3.2.7	Dose-Response to Cilostimide of Pellet h6.1	98
Fig. 3.2.8 a	Kinetics of Rolipram Inhibition of Soluble h6.1	99
Fig. 3.2.8 b	Kinetics of Rolipram Inhibition of Pellet h6.1	100
Fig. 3.2.9 a	Dixon Replot of Rolipram Inhibition of Soluble h6.1	101
Fig. 3.2.9 b	Dixon Replot of Rolipram Inhibition of Pellet h6.1	102
Fig. 3.2.10 a	Slope Replot of Rolipram Inhibition of Soluble h6.1	103
Fig. 3.2.10 b	Slope Replot of Rolipram Inhibition of Pellet h6.1	104
Fig. 3.2.11	Kinetics of IBMX Inhibition of Pellet h6.1	105
Fig. 3.2.12	Dixon Replot of IBMX Inhibition of Pellet h6.1	106
Fig. 3.2.13	Slope Replot of IBMX Inhibition of Pellet h6.1	107
Fig. 3.2.14	Measurement of Increasing h6.1 Protein Concentration vs Activity	108
Fig. 3.2.15	Schematic Representation of Competitive Inhibition	109
Fig. 3.2.16	Slope Replot of Rolipram Inhibition of hPDE4A _{Livi}	110

Fig. 3.2.17	Schematic Representation of Partial Competitive Inhibition	111
Fig. 4.1.1	Schematic Alignment of Mammalian PDE Isoform Families	132
Fig. 4.1.2	Alignment of Human and Rat PDE4 mRNA	133
Fig. 4.2.1	Schematic Representation of Truncations of h6.1	134
Fig. 4.2.2	Alignment of the Sequences of h6.1, HYB1 and 2EL	135
Fig. 4.2.3	Alignment of the Sequences of 10AORF and PDE46	136
Fig. 4.2.4	Alignment of the Sequences of h6.1, HYB1, 2EL, YMS10, YMS11, YMS12, 10AORF and PDE46	137
Fig. 4.2.5	Determination of K_m cyclic AMP For Soluble 10AORF	138
Fig. 4.2.6	Determination of K_m cyclic AMP For Soluble HYB1	139
Fig. 4.2.7	Determination of K_m cyclic AMP For Soluble YMS11	140
Fig. 4.2.8	Determination of K_m cyclic AMP For Soluble YMS12	141
Fig. 4.2.9	Dose-Response to Rolipram of Soluble 10AORF	142
Fig. 4.2.10	Dose-Response to Rolipram of Soluble HYB1	143
Fig. 4.2.11	Dose-Response to Rolipram of Soluble YMS11	144

Fig. 4.2.12	Dose-Response to Rolipram of Soluble YMS12	145
Fig. 4.2.13	Kinetics of Rolipram Inhibition of Soluble 10AORF	146
Fig. 4.2.14	Dixon Replot of Rolipram Inhibition of Soluble 10AORF	147
Fig. 4.2.15	Slope Replot of Rolipram Inhibition of Soluble 10AORF	148
Fig. 4.2.16	Thermostability of Soluble 10AORF, HYB1 and YMS12 at 45°C	149
Fig. 5.1.1	Formation of Synaptosomes	166
Fig. 5.2.2	Lactate Dehydrogenase Activity in Rat Cerebellum Synaptosomal Fractions	167
Fig. 5.2.3	Distribution of Lactate Dehydrogenase Activity as Determined by Thorne et al (1991)	168
Fig. 5.2.4	Acetylcholinesterase Activity in Rat Cerebellum Synaptosomal Fractions	169
Fig. 5.2.5	Distribution of Acetylcholinesterase Activity as Determined by Thorne et al (1991)	170
Fig. 5.2.6	Western Blot of RD1 Immunoreactivity in Fractions obtained from Rat Cerebellum Synaptosomes	171
Fig. 5.2.7	Distribution of 5' Nucleotidase Activity In Synaptosomal Subcellular Fractions Obtained from a Sucrose Density Gradient	172

Fig. 5.2.8	Distribution of Adenylyl Cyclase Activity In Synaptosomal Subcellular Fractions Obtained from a Sucrose Density Gradient	173
Fig. 5.2.9	RD1 Immunoreactivity in Fractions Obtained from Subcellular Fractionation of Synaptosomes (F2 & F3)	174

<u>List of Tables</u>		<u>Page</u>
Table 1	Expression of PKA Subtypes I and II	51
Table 1a	Comparison of Characteristics of <i>Drosophila dunc</i> PDE with RD1 and DPD	52
Table 1b	Detection of Human PDE4 in Human Tissues and Defined Cell Lines	53
Table 1c	Nomenclature for Rat PDE4 Species	
Table 2	IC ₅₀ and EC ₅₀ Values for Inhibition / Activation of Pellet h6.1 Activity by EDTA and Divalent Cations	54
Table 3	K _m , Inhibitor Profile and Thermostability Values for Soluble and Pellet Forms of h6.1	84
Table 4	Comparison of h6.1 Activity Expressed in the Soluble Fractions of COS-1 Cells and <u><i>Saccharomyces Cerivisiae</i></u>	85
Table 5	Specific Activities of PDE Activity in <u><i>Saccharomyces cerivisiae</i></u> Expressing HYB1, YMS11, YMS12 and 10AORF	129
Table 6	K _m ^{cyclic AMP} and IC ₅₀ ^{rolipram} Data for Soluble HYB1, YMS11, YMS12 and 10AORF, in Comparison with h6.1	130
Table 7	Thermostability Values Calculated for Soluble YMS12, 10AORF and HYB1 at 45°C, and Comparison with h6.1	131
Table 8	Lactate Dehydrogenase (LDH) Activity Determined from Rat Cerebellum Synaptosome Preparation	165

Abbreviations

G _i	Inhibitory guanine nucleotide regulatory protein
G _s	Stimulatory guanine nucleotide regulatory protein
ATP	Adenosine triphosphate
BSA	Bovine Serum Albumin
Cyclic AMP	Adenosine 3'5' cyclic monophosphate
EDTA	Ethylene diaminetetracetic acid
EGTA	Ethylene glyco-bis (beta-aminoethyl ether) N,N,N',N' - tetracetic acid
GTP	Guanosine triphosphate
NAD	Nicotinamide adenine dinucleotide
Tris	2-amino-2-hydroxymethyl-propane-1,3-diol
PDE	Phosphodiesterase
LDH	Lactate dehydrogenase
RO-20-1724	4-(3-butoxy-4-methoxybenzyl)-2-imidazolidine
Rolipram	4-[3-(cyclopentoxy)-4-methoxyphenyl]-2-pyrrolidine

Acknowledgements

I would like to thank the Division of Biochemistry and Molecular Biology, IBLS, University of Glasgow for the use of the facilities throughout this Ph.D. I would also like to thank my supervisor, Professor Miles Houslay for his help, understanding, patience and guidance throughout this thesis.

I would like to take this opportunity to thank Dr. Mike Sullivan, formerly of Sandoz, for providing all of the cloned PDEs analysed in this study.

I would like to thank those in A3 and A20 who have helped me in any way during this project. Special, heartfelt thanks goes to my good friend Sandra who has helped me in my times of need, and has been a fine friend despite having to work beside me. Thanks also goes to Fraser, with whom I shared the good and bad times of Ph.D student life, and was always there with a hearty laugh to cheer up your day.

An extra-special thanks goes to my Dad and my sister Elizabeth for their love, support and encouragement throughout my first degree and Ph.D. I could not have managed without you guys!

Last, but by no means least, I would like to thank Mervyn who has suffered the most I think! I thank him for his love, his patience and for putting up with me during the most trying time of my life.

Thanks!

Summary

Studies were performed on a human cyclic AMP specific phosphodiesterase (PDE) of the PDE4A family. The cDNA for this isoform had been isolated from a human T-lymphocyte cDNA library and engineered for expression in *Saccharomyces cerevisiae* (Dr M.Sullivan, Sandoz). Characterisation of the PDE activity of h6.1 demonstrated that both pellet and soluble forms were kinetically identical, hydrolysing cyclic AMP specifically. Substrate hydrolysis was unaffected by low concentrations ($2\mu\text{M}$) of cyclic GMP or calcium / calmodulin but was selectively inhibited by the PDE4 class selective inhibitors rolipram and RO-20-1724. The PDE3 class inhibitor cilostimide and the non-selective inhibitor IBMX served as weak inhibitors. Both rolipram and IBMX were shown to inhibit pellet and soluble h6.1 activities in a simple competitive manner. EDTA-treated h6.1 could be dose-dependently activated by the divalent cations Mg^{2+} and Mn^{2+} . This suggested that there was a site specific interaction between the divalent cations and h6.1.

Pelleted h6.1 was not affected by NaCl or detergent treatment. Thus PDE activity was neither peripherally bound or an integral membrane protein. Indeed, the only difference found between pellet and soluble h6.1 was that the pellet activity was more thermostable. In each case, activity decayed as a single exponential, which suggested that only a single population of enzyme was expressed in each compartment

The function of the distinct N and C terminal domains of h6.1 were investigated. The N-terminal region of h6.1 was shown to be important in such functions as substrate hydrolysis, inhibitor interaction and thermostability. This analysis of a human PDE4A isoform (10AORF) which differed from h6.1 in having a larger N-terminal domain, showed that it exhibited a significantly lower K_m for cyclic AMP ($1.9\pm 0.2\mu\text{M}$, $p=0.025$) compared to h6.1 ($4.1\pm 1.7\mu\text{M}$). In addition, 10AORF exhibited an IC_{50} ($0.19\pm 0.02\mu\text{M}$, $p=0.004$) for rolipram which was considerably lower than that for

h6.1($0.5 \pm 0.15 \mu\text{M}$). Importantly, it has been suggested that a conformational change, induced by the larger N-terminal region of 10AORF occurred, which resulted in a change in the way in which rolipram inhibited enzyme activity. Whilst rolipram was a simple competitive inhibitor of h6.1, partial competitive inhibition was seen with 10AORF. The enzyme 10AORF also showed increased thermostability with a $t_{0.5}$ (>30 mins) significantly greater than that of h6.1 at 45°C (10mins). The role of the N-terminal region in modulating PDE properties was emphasised further upon the analysis of HYB1. The chimeric PDE, HYB1 was a construct formed by the substitution of the N-terminus of h6.1 with that of the inactive splice variant 2EL. Whilst this had no significant effect on the $K_{\text{M}}^{\text{cyclic AMP}}$, it significantly increased the IC_{50} for rolipram ($1.93 \pm 0.23 \mu\text{M}$) and reduced the thermostability of HYB1 (3 mins), compared to h6.1. Thus, the distinct N-terminal domain of 10AORF contributed to changing the potency of rolipram action, the K_{M} for cyclic AMP hydrolysis and thermostability. The C-terminal domain was shown to be involved in the interaction with rolipram also, since the truncation of this region (YMS12) resulted in a significantly greater IC_{50} ($1.7 \pm 0.14 \mu\text{M}$, $p=0.0001$) for rolipram inhibition compared to h6.1.

The cellular expression of an analogous PDE4A rat isoform, RD1, was investigated in rat brain. The *in vivo* expression of the rat PDE4A splice variant, RD1 was studied in rat cerebellum synaptosomal fractions. Sub-fractionation of those synaptosomal fractions which contained the greatest amount of RD1 immunoreactivity, determined that RD1 was enriched in the plasma membrane fraction. The location of RD1 was identified with the plasma membrane markers 5'-nucleotidase and adenylyl cyclase. This has been previously shown in COS-1 cells transfected with RD1 cDNA (Shakur et al 1993). Location at the plasma membrane, along with adenylyl cyclase, places RD1 at a site alongside other components of the cyclic AMP signalling

pathway, and provides a route for the termination of the signal generated by cyclic AMP.

Chapter - 1

Introduction

1. Introduction

1.1 Cyclic adenosine 3', 5'- monophosphate as a Second Messenger

Signal transduction can be defined as the mechanism by which a primary messenger, such as a hormone, binds to a specific receptor on the cells surface coupled to an effector system and generates an intracellular signal resulting in the biochemical response. The intracellular signal triggers a cascade of molecular reactions the result of which culmanates in the biochemical response. One such intracellular signal, or second messenger, is cyclic adenosine 3', 5'- monophosphate (cyclic AMP). Since the discovery of cyclic nucleotides their synthesis, modulation by hormones, neurotransmitters and pharmacological agents are mechanisms which are now among the most well established in cellular signalling.

1.2 Cyclic AMP Dependent Protein Kinase

The biochemical response to cyclic AMP is initiated by the binding of the second messenger to its intracellular 'receptor', cyclic AMP dependent protein kinase (PKA). PKA is the only known receptor protein for cyclic AMP in eukaryotic cells (Krebs 1985) and exists as 2 holoenzyme forms types I and II. The inactive holoenzyme form of PKA is a cytoplasmic, tetrameric complex of both regulatory (R) and catalytic (C) subunits. High affinity binding of 4 molecules of cyclic AMP to the R subunit, activates the complex by dissociation of the two catalytic subunits from the R subunit dimer (Beebe and Corbin 1986), therefore, liberating the catalytic subunits to phosphorylate substrate proteins or to migrate to the nucleus (Nigg 1990). This can be summerised in the reaction scheme:



Studies have shown that the RII subunit has an additional function, namely the localisation of PKA (Scott 1991).

Specificity of PKA for a particular substrate protein, may be explained by the hypothesis that individual pools of PKA are compartmentalised

to a subcellular location in close proximity to that particular substrate protein (Scott and Carr 1992). Therefore, activation of a particular PKA pool can only arise when elevation of cyclic AMP occurs in response to an appropriate hormone. Activation of a particular PKA isoform is dependent on the hormone and tissue involved (table 1). Each subtype exists as an alpha and beta isoform, the alpha isoform is expressed in most cell types but the beta isoform is expressed preferentially in brain tissue (Scott and Carr 1992). In general, type I isoforms are primarily cytoplasmic whereas most (~75%) type II activity is found associated with the particulate fraction.

1.3 Biological Effects Mediated by Cyclic AMP

Cellular activity, and its control, is dependent upon a variety of neurotransmitters, growth factors and hormones which transduce their effects through the extracellular binding to specific plasma membrane spanning receptors. The mechanism by which receptor occupation, by such ligands, leads to an intracellular response has been the subject of much investigation. Work by Sutherland and Rall in the 1950's demonstrated that, in the presence of glucagon or adrenaline, then phosphorylase present in the supernatant fraction of liver homogenates was activated by a heat stable factor. For this activation to occur it was noted that the plasma membrane fraction was required (Rall et al 1957). Later work identified this heat stable factor as cyclic AMP. The observation that glucagon and adrenaline could not activate phosphorylase directly, suggested that the point of hormonal regulation was at adenylyl cyclase, the enzyme which catalyses the formation of cyclic AMP from ATP, (Rall et al 1957). This work was the basis of the "second messenger hypothesis", namely, a secondary messenger e.g. cyclic AMP is formed in response to a ligand binding to its specific receptor and, once formed, this intracellular messenger can then alter cell function.

(i)Cyclic AMP as a Hormonal Second Messenger

Since its discovery, the second messenger cyclic AMP has shown to be central in the functioning of a diverse range of biological systems. Of great importance is the role of cyclic AMP in the hormonal control of blood glucose and fatty acid levels. Cyclic AMP has a dual effect in the hormonal control of lipolysis in adipocytes. On the one hand, cyclic AMP mediates the lipolytic action of hormones such as catecholamines, corticotrophin and glucagon (Steinberg et al 1975). The second messenger promotes lipolysis through the activation of cyclic AMP-dependent protein kinase, which phosphorylates and activates hormone sensitive lipase resulting in hydrolysis of stored triglyceride to glycerol and free fatty acids (Stråfors et al 1984). Conversely, the degradation of cyclic AMP and the subsequent reduction in cyclic AMP-dependent protein kinase has been shown to be of functional importance in the antilipolytic action of insulin (Smith and Manganiello 1988, Vasta et al 1992 and Anderson et al 1989).

Homeostatic control of blood glucose levels has been shown to be a cyclic AMP mediated event. Glucagon, the hormone produced by the alpha cells of the pancreas is involved in the promotion of glycogenolysis, gluconeogenesis and the release of free fatty acids. The receptor for glucagon is coupled to the cyclic AMP synthesising enzyme adenylyl cyclase through the stimulatory G-protein G_s . In the liver, elevation of the intracellular levels of cyclic AMP, via activation of the glucagon receptor, triggers an enzymatic cascade initiated by PKA mediated phosphorylation (Cohen 1985). Primarily this is the phosphorylation of glycogen phosphorylase, leading to the breakdown of glycogen and glucose release, and of glycogen synthase which results in the inactivation of the enzyme. This cyclic AMP signal in response to glucagon in hepatocytes has been shown to be transient (Heyworth et al 1983). Following the initial increase in cyclic AMP, rapid desensitisation of adenylyl cyclase occurs (Heyworth and Houslay 1983), in which the glucagon receptor uncouples from G_s . Several lines of evidence have shown that the uncoupling

is due to a protein kinase C mediated phosphorylation of the receptor (Murphy et al 1987, Murphy & Houslay 1988).

(ii)Cyclic AMP in the Central Nervous System

A role for cyclic AMP in the central nervous system (CNS), associated with the processes of learning, memory, neurotransmission and mood regulation has been highlighted. In particular numerous genetic mutations in genes associated with learning in *Drosophila melanogaster* have been isolated. These genetic mutations have been associated with alterations of the cyclic AMP signalling pathway including *dunc*, which encodes a cyclic AMP specific phosphodiesterase, and *rut* which encodes a calcium-calmodulin stimulated adenylyl cyclase (Dudai 1988, Levin et al 1992, Qiu et al 1991). These studies have shown alterations in olfactory learning (Byres et al 1981) associated with mutations of the *dunc* gene, resulting from altered cyclic AMP metabolism (Nighorn et al, 1991). In the mammalian CNS the role of cyclic AMP is less well characterised, however it has been associated with the processes of neurotransmission by virtue of its synaptic localisation (Therien and Mushynski 1979) and in mood regulation (Schneider et al 1986).

(iii)Cyclic AMP in the Immune System

In the mammalian immune system, cyclic AMP is known to be an important regulator of such functions as attenuation of lymphocyte blastogenesis (Epstein et al 1984), lymphocyte proliferation and differentiation (Coffey et al 1978, Hadden 1988), inhibition of release of inflammatory mediators histamine and leukotriene C₄ from basophils (Peachell et al, 1992) and the blockade of the cytokine pathway due to the suppression of tumour necrosis factor alpha production from human mononuclear cells (Semmler et al 1993).

(iv)Cyclic AMP in the Cardiovascular System

Cyclic AMP has been shown to be crucial in the control of cardiac contraction (Trautwein & Heschler 1990) and diastolic relaxation (Morgan 1991b).

The force of cardiac contraction is related to the cross-linking of the actin and myosin filaments of the myocardium which, in turn, shortens the contractile apparatus (Robertson et al 1982) and results in the actual contraction. Cross-linking of actin and myosin is itself dependent upon the availability of intracellular calcium to bind to the regulatory protein troponin C (Fabiato & Fabiato 1979). Cyclic AMP mediates the contraction through the elevation of intracellular calcium via the PKA mediated phosphorylation of voltage dependent calcium channels of the sarcolemma. This in turn causes the release of more calcium from the sarcoplasmic reticulum (Morgan et al 1991a). Indeed it has been shown that agents which elevate intracellular levels of cyclic AMP are therapeutically useful as positive inotropic agents (Brunkhorst 1989).

Relaxation of cardiac muscle is initiated by the phosphorylation of troponin C by PKA, causing a decrease in the affinity of the calcium binding site, and of the sarcoplasmic calcium pump. Therefore there is reduced availability of calcium for the contractile proteins (Morgan et al 1991b).

Contractile agonists such as PAF (platelet activation factor), induce the contraction of airway smooth muscle via phospholipase C catalysed hydrolysis of phosphatidylinositol (4,5) biphosphate into inositol (1,4,5) triphosphate and sn - 1,2-diacylglycerol (Rodger & Pyne 1992). Vascular smooth muscle relaxation (Chasin 1972) and airway smooth muscle relaxation (Torphy 1988) are both under the influence of cyclic AMP, in that, this nucleotide inhibits contraction by causing a net efflux of calcium from the cell, which is necessary for contraction (Kukovetz et al 1981).

Stimulation response of platelets involves the adhesion to sub-endothelial tissues, secretion of secretory granule components, the formation of platelet aggregates, increased glycogenolysis and the rapid synthesis of

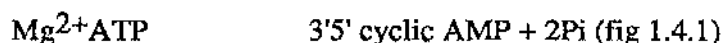
oxidative metabolites of arachidonic acid, all of which are dependent in one way or another on intra/extra cellular calcium. Cyclic AMP itself, and agents which elevate cyclic AMP, inhibit these responses by regulation of the free calcium level in the platelet, or by the control of calcium-dependent reactions which are essential for these responses. Cyclic AMP is therefore central to the control of platelet activation (Feinstein et al 1981).

The above summary of the processes involving cyclic AMP is by no means expansive, however it highlights the complex systems within which cyclic AMP is a major component.

1.4 Adenylyl Cyclase

(i) Synthesis of Cyclic AMP

Synthesis of cyclic AMP from ATP is dependent upon the regulation of the enzyme adenylyl cyclase [E.C. 4.6.1.1; ATP pyrophosphatase (cyclising)]. The reaction catalysed by this enzyme can be represented by :-



(ii) Adenylyl Cyclase Structure

The adenylyl cyclases comprise a diverse family of enzymes with variations both within and between species. With regard to cellular location adenylyl cyclase is exclusively plasma membrane associated with exception of certain bacterial forms which are cytosolic.

Three general classes of adenylyl cyclase exist which are distinct with respect to the way in which they are associated with the membrane and include the periphally membrane bound form of *Saccharomyces cerevisiae* and *Escherichia coli*, the form of the enzyme from Dictyostelium which has a single transmembrane spanning region and the integral membrane enzyme found in eukaryotic cells. (Tang and Gilman 1992). Eight isoforms (types I - VIII) of the eukaryotic integral membrane adenylyl cyclase are known (Krupinski et al 1992) and have been shown to be the products of distinct genes. An overall,

well conserved structure for this enzyme can be seen throughout the eight isoforms, comprising a short amino-terminal region (N) and two 40kDa cytoplasmic domains, C₁ and C₂, between which lies two alternating extremely hydrophobic stretches, M₁ and M₂, each of which are predicted to contain six transmembrane helices (Ishikawa et al 1992).

Among the eight adenylyl cyclases considerable sequence homology exists between the C_{1a} and C_{2a} regions (fig 1.4.2). These regions are reputed to be the catalytic sites due to the similarity (~35% identity) to what is known to be the catalytic domain of guanylyl cyclases (Chinkers and Garbers 1991). Presumably the hydrophobic domain is involved in the anchorage of the enzyme to the membrane for accessibility to the membrane receptors.

(iii) Adenylyl Cyclase regulation by G-Proteins

The signal between receptor and effector (adenylyl cyclase) is transduced by the heterotrimeric guanine nucleotide-binding proteins or G-proteins (Gilman 1987). Adenylyl cyclase activity is modulated by receptors interacting with either G_s (stimulatory) or G_i (inhibitory) which are bound to the inner surface of the plasma membrane. Heterotrimeric G-proteins consist of three subunits, alpha which is the largest and which confers G-protein specificity, together with beta and gamma.

In the resting state the alpha, beta and gamma subunits are complexed together with GDP (guanosine diphosphate) bound to the alpha subunit. Receptor occupancy results in the activation of the G-protein complex and release of the GDP from the alpha subunit, which is in turn replaced by GTP (guanosine triphosphate). The alpha-GTP subunit dissociates from the beta-gamma and diffuses along the inner plasma membrane surface and couples with the effector. After a few seconds the signal is 'switched off' by the intrinsic GTPase activity of the alpha subunit which hydrolyses the bound GTP to GDP, hence rendering the alpha subunit inactive. Once inactivated the alpha subunit reassociates with the beta-gamma and the complex returns to its resting

state (fig 1.4.3). There is evidence of cross-talk between the phospholipase C signalling system where it has been shown that activators of PKC, phorbol esters, increase basal adenylyl cyclase activity (Pyne et al 1993). Phorbol esters have also been shown to enhance the ADP-ribosylation of the G_s -alpha sub-unit by cholera toxin (Pyne et al 1993). Indeed, PKC itself has been shown to phosphorylate alpha G_s *in vitro*, in which it was shown that the substrate of the reaction was the guanine nucleotide free form of the alpha sub-unit (Pyne et al 1992).

Regulation of adenylyl cyclase is not an exclusive role for the alpha subunit, for, adenylyl cyclase activity can be modulated by beta-gamma subunits but in a type-specific fashion. Whereas beta-gamma inhibits type-I adenylyl cyclase when stimulated by either G_s -alpha or calcium-calmodulin, beta-gamma greatly potentiates the stimulatory effect of G_s -alpha on either type-II or type-IV adenylyl cyclase (Tang and Gilman 1991). These interactions are dependent on the prenylation of the G-protein gamma subunit (Iñiguez-Lluhi et al 1992). Recent evidence also suggests a role for the beta-gamma subunits in the activation of mitogen-activated protein kinases (MAPK), or extracellular signal-regulated kinases (ERKS), in COS-7 cells transfected with muscarinic receptor (Crespo et al 1994) and the alpha_{2A} adrenoceptor (Van Bleszen et al 1995).

Inhibition of the adenylyl cyclases is mediated by the G_i family of G-proteins. These include G_{i1} , G_{i2} , G_{i3} and G_o (Milligan 1988). Considerable evidence suggests that the major trigger for the inhibition of adenylyl cyclase is G_i -alpha 2, which has been implicated in a variety of receptor systems including the thrombin receptor in P9 cells (Watkins et al 1992), leukotriene B4 receptors in HI-60 cells (Goetzel et al 1994), 5-HT_{1A} receptors in CHO-K1 cells (Raymond et al 1993) and with the glucagon receptor in hepatocytes (Bushfield et al 1990 and 1991). As with the G_s family, the beta-gamma complex of G_i proteins plays an important role in adenylyl

cyclase regulation. In platelet and the S49 cell line, exogenously added beta-gamma complex of G_i proteins was able to inhibit adenylyl cyclase by a mechanism involving the deactivation of G_s-alpha (Katada et al 1984).

1.5 Inactivation of the Cyclic AMP Signal

In this introduction the mechanisms by which cyclic AMP synthesis is regulated, the range of biological effects the second messenger is involved and the functions of PKA have been discussed. Another vital component of the cyclic AMP signalling pathway is its degradation. The only way in which the cells of eukaryotic organisms can terminate the cyclic AMP signal is through its hydrolysis catalysed by a heterologous family of enzymes known as the cyclic nucleotide phosphodiesterases (PDEs) (EC 3.1.4.17). Certainly some organisms such as Dictyostelium (Pitt et al 1992) can extrude cyclic AMP from the cell, however, the most important method of control of intracellular concentration of cyclic AMP are the PDEs.

1.6 Cyclic Nucleotide Phosphodiesterases

General Introduction

Following the first experiments by Butcher and Sutherland in the early 1960's demonstrating enzymatic degradation of cyclic nucleotides, it was soon apparent, based on the studies by Appleman and co-workers, that multiple forms of PDE could catalyse the same reaction (Butcher and Sutherland 1962, Thompson and Appleman 1971, Appleman and Terasaki 1975). We now know that at least seven different isoenzyme families of PDEs exist which differ in respect of substrate specificity, regulation, kinetics and inhibitor profile.

Originally PDEs were classified simply on the basis of substrate hydrolysing ability into cyclic GMP and cyclic AMP PDEs. However, with the realisation that multiple forms of each class existed it was necessary to develop a more sophisticated system. The classification system used in this thesis is as described by Beavo et al (1994). Most of the individual types of PDE have closely related subfamilies, that is, are products of distinct but highly

homologous genes, which give rise to alternatively spliced mRNAs. Indeed, members of one family generally share ~20-25% sequence similarity with members of another family, which occurs in the region thought to be involved in catalysis (Chen et al 1986, Charbonneau et al 1986). Therefore, PDEs are classified into species (capital letter), gene family (PDE + Arabic numeral), gene (capital letter) and splice variant, for example HSPDE4A1.

The functional relevance for the existence of so many isoenzymes of PDEs can be explained by the differential expression in selected cell types, and the regulation of the different isoenzyme forms by a variety of intracellular components, which allow the manipulation of specific isoforms in an individual cell type. Also the opportunity is there for the development of specific pharmacological tools which could be used to target an isoenzyme form, and therefore be potentially useful from a therapeutic perspective.

1.7 Cyclic GMP Metabolising Phosphodiesterases

(i)PDE1 - Calmodulin Stimulated PDE

The family of calmodulin (CaM) stimulated PDEs (PDE1) is one of the best characterised. Discovered in the 1960s from experiments on bovine brain (Cheung 1967), it was one of the first cyclic nucleotide PDEs to be purified to homogeneity and characterised in terms of molecular properties. Although detected in various tissues the enzyme is predominantly found in mammalian brain (Sharma et al 1980) and heart (La Porte 1979).

a)Cellular Distribution

Although CaM stimulated PDE is generally considered to be cytosolic, as shown in neuronal cytoplasmic preparations (Kincaid et al 1987), the precise cellular location varies with tissue type. For example PDE1 activity has been localised to the synaptic density membrane fraction of rat brain (Grab 1981) and to particulate fractions of heart and kidney (Kakiuchi et al 1978). The differences noted in cellular distribution occur because of tissue specific differential isoenzyme expression.

b)Structure

Structural characterisation studies have shown the CaM stimulated PDE to be a dimer composed of identical subunits which vary in molecular weight between 58 to 63kDa with each individual isoenzyme. Each subunit can bind 2 molecules of CaM in the presence of Ca^{2+} , with CaM and Ca^{2+} synergistically interacting to activate the PDE. Therefore, an elevation of the intracellular concentration of Ca^{2+} results in the increased affinity of the enzyme for CaM (Richman and Klee 1978).

c)Substrate Specificity and Regulation

Basal PDE1 activity can be increased up to 20 fold in the presence of Ca^{2+} and CaM with both the basal and stimulated activities showing Mg^{2+} dependency (Wang et al 1990). Kinetic analysis on purified preparations have shown that although PDE1 can utilise both cyclic AMP and cyclic GMP as substrate the predominant isoenzyme species show a higher affinity for cyclic GMP in vitro (Kakurchi et al 1973), hence these enzymes are classified as cyclic GMP PDEs.

Hormonal regulation of PDE1 has been reported in studies in which agonists which increase intracellular Ca^{2+} , cause a decrease in intracellular cyclic nucleotide (Sumners and Myers 1991). This was shown to be independent of adenylyl or guanylyl cyclase inhibition, therefore the regulation of PDE1 is an essential component of the Ca^{2+} signal transduction pathway. The PDE1 isoenzyme is selectively inhibited by vinpocetine with inhibition resulting in effects on the central nervous system (de Noble et al 1986) and vasculature (Hidaka and Endo 1984).

Recent evidence (Spence et al 1995) has identified a novel link between the lipid and cyclic AMP signalling systems involving PDE1. Spence et al (1995) has shown that upon selective overexpression of PKC isoforms in chinese hamster ovary cells, an induction of PDE1 activity occurred. It has been

suggested that this PKC mediated induction, was via regulation of PDE1 gene expression by the AP-1 (*fos/jun*) complex.

(ii) PDE5 Cyclic GMP Specific Phosphodiesterase

Originally the PDE5 family encompassed subgroups including the retinal cyclic GMP PDE rod outer segment PDE (ROS) (Yamazaki et al 1980), cone PDE (Gillespie and Beavo 1988) and the cyclic GMP specific PDE from lung (Francis et al 1980). However on the basis of distinct sequence differences between the retinal and lung PDEs these were categorised as PDE6 and PDE5 respectively.

The cyclic GMP-binding-cyclic GMP-specific PDE (cGBPDE) or PDE5 was first recognised in the supernatant fractions from lung preparations by Lincoln et al (1976). This PDE isoenzyme family is characterised by the hydrolytic activity being highly specific for hydrolysis of cyclic GMP with the inability to hydrolyse cyclic AMP. PDE5 is present in tissues including rat (Thomas et al 1990a) and bovine lung (Francis and Corbin 1988), human platelets (Hamet and Coquil 1978), rat spleen (Coquil 1983), guinea-pig lung (Burns et al 1992) and vascular smooth muscle (Hamet et al 1984).

(a) Characteristics

The native molecular weight of PDE5 from rat and bovine lung has been delineated to be ~177 kDa (Francis et al 1980) and from guinea-pig lung ~90kDa (Burns & Pyne 1992). PDE5 has been partially purified from guinea-pig lung (Burns et al 1992), and has been characterised by its specificity for cyclic GMP with a K_m of ~2.2 μ M and V_{max} of 1.2nM / min / mg. Purification of the enzyme from guinea-pig lung has shown it to be kinetically similar to, and with an inhibitor profile resembling, that isolated from bovine (Francis & Corbin 1988) and rat lung (Thomas et al 1990a,b).

PDE5 has in addition to the catalytic site a non-catalytic binding site, to which, a function has not yet been clearly attributed. Thomas et al

(1990a,b) suggest that the function of the non-catalytic site may be to stimulate the hydrolytic activity of the PDE. The non-specific PDE inhibitor IBMX, which potently and competitively inhibits PDE5, binds to the catalytic site of PDE5 and is known to increase the binding of cyclic GMP to the non-catalytic site (Frances and Corbin 1988). It is thought that this situation can work in reverse, in that, binding of compounds to the non-catalytic site can increase the binding and hydrolysis of cyclic GMP at the catalytic site (Thomas et al 1990a,b).

(b) Phosphorylation by Protein Kinase A and Protein Kinase G

Partially purified PDE5 from guinea-pig lung (Burns et al 1992) has been shown to be phosphorylated *in vitro* by both protein kinase A and protein kinase G (Burns et al 1992, Burns & Pyne 1992, Thomas et al 1990a,b). PKA mediated increase in PDE activity was sensitive, in a dose dependant manner, to alkaline phosphatase treatment (Burns & Pyne 1992). Burns and Pyne (1992) suggest that it is not necessary for cyclic GMP to bind to the enzyme prior to the activation by PKA. This is in contrast to the study by Thomas et al (1990b), in which it was shown that cyclic GMP binding was a pre-requisit to activation by PKA. Burns and Pyne (1992) propose that either the differences are due to different PDE5 isoforms, or that a regulatory protein which binds to the non-catalytic site, is present in the purified preparations which enables the phosphorylation to occur.

Phosphorylation by PKA increases the V_{max} of the reaction of cyclic GMP hydrolysis and also decreases the sensitivity of PDE5 to inhibition by zaprinast (Burns et al 1992). The loss of sensitivity to zaprinast is shown through the loss of non-competitive inhibition when phosphorylated by PKA. Thus, PDE activation via PKA, may involve a mechanism where the non-catalytic sites to which zaprinast binds are perturbed (Burns & Pyne 1992).

The physiological consequences of PKA mediated phosphorylation are unknown. There is evidence however, of cross-talk between the cyclic AMP and cyclic GMP signalling systems. Agonists which induce contraction of smooth muscle are known to accumulate cyclic GMP (Nakatuso & Diamond 1989). Thus, an increase in cyclic AMP, for example via beta-adrenoceptor agonists in smooth muscle, would decrease the inhibitory cyclic GMP pool by activating PDE5 in a PKA dependent manner (Burns et al 1992).

(c) Isolation of Murine cDNAs Representing PDE5

A full length cDNA clone has been isolated from a bovine lung cDNA library, which upon expression in COS-7 cells was shown to encode a protein kinetically similar to that isolated and purified from bovine lung (Burns et al 1995). Partial clones from a murine lung cDNA library have been subsequently isolated using the bovine cDNA ³²P-labelled clone as a probe. Two partial clones isolated were of interest and were shown to encode the PDE catalytic domain found throughout the PDE family, and a region which is proposed to contain the cyclic GMP binding site. These mouse clones are the subject of present study and are being used to isolate the full length mouse clone, to identify the localisation of the mouse PDE5 in tissues and the identity of any spliced variants which may exist (Burns et al 1995).

Corbin and coworkers have cloned and expressed bovine PDE5 and have shown that the enzyme is phosphorylated in the whole cell. Mutagenesis studies by this group have also shown that at least two different types of cyclic GMP binding sites are present. This group have also noted a conserved motif in all PDEs, Hx₃Hx-20E, which is thought to function as a zinc binding site (Francis et al 1994). Of interest, Pyne and coworkers have shown that the inhibitory effect of zaprinast on PDE5 could be due to its ability to chelate zinc (Beavo et al 1994).

(iii) PDE6 Retinal Rod and Cone Phosphodiesterases

The mammalian visual pathway is modulated by cyclic GMP specific PDE6 isoenzyme family, which hydrolyses cyclic GMP in response to light in both rod and cone photoreceptors.

(a) Visual Pathway

In rod photoreceptors the visual pathway is triggered when the protein rhodopsin absorbs a photon of light (Wald 1968). This converts the rhodopsin into its activated form which in turn activates transducin. Transducin is a heterotrimeric guanine-nucleotide-binding protein of three subunits T_{α} which has GDP bound in its inactive state, T_{β} and T_{γ} . Activation of transducin by rhodopsin involves the exchange of GDP bound to the T_{α} subunit with GTP. Once GTP is bound the T_{α} subunit dissociates from the T_{β} - T_{γ} complex to activate the PDE through the removal of its inhibitory subunit and leaves the PDE free to hydrolyse cyclic GMP (Fung et al 1981). A cation channel in the plasma membrane of rod photoreceptors, which primarily transports Na^{+} , is gated and activated by cyclic GMP, therefore lowering the cyclic GMP concentration by PDE decreases the Na^{+} influx by closing the channel (Yau and Nakatani 1985, Matthews 1987). This membrane hyperpolarisation generates the neuronal signal and constant Na^{+} flow maintains depolarisation of the membrane in the dark. A Ca^{2+} sensitive guanylate cyclase is stimulated by low levels of Ca^{2+} , which results from the action of a Na^{+}/Ca^{2+} exchanger, and restores cyclic GMP levels after illumination (Zuckermann 1973).

Little is known about the role of the cone PDEs in photoperception. Obvious physiological differences occur between rods and cones which come into play in low and high luminescence situations respectively. Despite this, cone specific PDE isoenzymes exist and it is expected that cone visual transduction processes are similar to that of rods.

(b) Rod Cyclic GMP Phosphodiesterases

The bovine rod cyclic GMP PDEs are composed of three types of subunit, the 88kDa alpha subunit, the 84kDa beta subunit and two inhibitory 13kDa gamma subunits which keep the PDE in an inactive state during resting (Baehr et al 1979, Deterre et al 1988). Evidence suggests that all three types of subunit undergo significant post translational modification. Relevance of these post translational modifications are unclear however, the C-terminal cysteine modification presumably orientate the PDE correctly in the membrane and are necessary for the normal function of the PDE. Both the alpha and beta subunits are methylesterified at a C-terminal cysteine and are differentially prenylated by farnesylation and geranylgeranylation respectively. In addition, PDE alpha and gamma can be phosphorylated by a protein kinase C (PKC) isoenzyme but no change in activity was noted (Udovichenko 1993, Anant et al 1992).

1.8 Cyclic AMP Phosphodiesterases

(i)PDE2 - Cyclic GMP Stimulated Phosphodiesterase

After initial identification of a cyclic GMP stimulated PDE (cGsPDE) or PDE2 activity in soluble fraction of a rat liver preparation (Beavo et al 1970), several other tissues were similarly studied for evidence of this PDE. cGsPDE was found in rat brain (Beavo et al 1971), adipose tissue (Klotz and Stock 1972) and human platelets (Hidaka and Asano 1976).

The PDE2 family is characterised by the allosteric regulation of cyclic AMP and cyclic GMP hydrolysis with positive co-operative kinetics. Two distinct subfamilies of this enzyme exist, PDE2A1 the heart / adrenal isoenzyme (Martins et al 1982), PDE2A2 the membrane bound form (Yamamoto et al 1983) and the PDE2B1 liver form (Pyne et al 1986) which may be a proteolytic product of PDE2A due to its smaller molecular size. However, both membrane and soluble phosphorylated proteins are found, which might imply the existence of two distinct splice variants.

(a)Kinetics

Studies on the purified enzyme have shown that the PDE is dimeric and hydrolyses both cyclic GMP and cyclic AMP. Cyclic GMP however, is both the preferred substrate and activator of cyclic AMP hydrolysis. Allosteric regulation of the enzyme is considered to occur distal to the catalytic site (Moss et al 1977). Reports on the bovine adrenal isoenzyme have shown that stimulation of cyclic AMP hydrolysis correlates with the binding of ^3H -cyclic GMP at a distinct site (Miot et al 1985). It is as yet unclear as to whether cyclic AMP and cyclic GMP are hydrolysed at the same or different sites.

b) Physiological Role

One important aspect of this enzyme family is the ability to hydrolyse both cyclic AMP and cyclic GMP. In situations where both cyclic nucleotide concentrations are elevated, then the hydrolysis of one cyclic nucleotide can be stimulated by the other. Studies have shown that cyclic GMP is a more potent activator of cyclic AMP hydrolysis (Moss et al 1977) than vice versa. This unique situation has been shown to be of key physiological significance in the adrenal gland, particularly associated with aldosterone production. Stimulation of the atrial natriuretic factor receptor, coupled to the guanylate cyclase effector system in the adrenal gland results in an elevated cyclic GMP concentration with a concomitant decrease in cyclic AMP, ultimately effecting cyclic AMP mediated responses (MacFarland et al 1987). The search for an isoenzyme selective inhibitor of this PDE has been relatively unsuccessful, except for the compound EHNA (erythro-9-(2-hydroxy-3-nonyl)-adenine) which is commonly used as an adenosine deaminase inhibitor (Méry & Fischmeister 1994). EHNA was reported to be the same compound as previously described (MEP-1) by Podzuweit (1995). The IC_{50} for PDE inhibition ($\sim 1\mu\text{M}$) is significantly less than the concentration of EHNA used to inhibit adenosine deaminase. EHNA was shown to antagonise cyclic GMP effects, mainly inhibition of L-type Ca^{2+} current, in isolated frog ventricular

myocytes (Méry et al 1995). It would therefore seem that this compound will be invaluable in determining other functions of cGsPDE.

In addition cGsPDE functions as an important transducer of cyclic GMP as a second messenger in the brain. Evidence to support this comes from the abundance of the enzyme responsible for cyclic GMP formation, guanylate cyclase (Nakane et al 1983) in various neuronal cell types. Expression of the molecular target for cyclic GMP the cyclic GMP dependent protein kinase (Lohmann et al 1981) and a more widespread expression of cGsPDE (Repaske et al 1993, Sonnenberg et al 1991) has also been demonstrated in mammalian brain.

(ii)PDE3 - Cyclic GMP Inhibited Phosphodiesterase

The PDE3 cyclic GMP inhibited enzymes (cGIPDE) form an isoenzyme class of cyclic AMP hydrolysing enzymes which are characteristically inhibited by micromolar concentrations of cyclic GMP. This isoenzyme form has been identified in and purified from tissues such as adipose (Degerman et al 1987, Saltiel and Steigerwalt 1986), bovine cardiac ventricle (Harrison et al 1986) and rat liver (Pyne et al 1987).

(a)Structure and Kinetics

From tissues which have been studied so far, with the exception of the 'dense-vesicle' PDE, the PDE3 family appear to be peptides of native molecular size 105 - 135 kDa. However, these PDEs are particularly sensitive to endogenous proteolysis producing fragments of around 30 - 80 kDa in size.

'Dense-vesicle' PDE has been purified to apparent homogeneity from rat liver (Pyne et al 1987), and is activated in hepatocytes by glucagon in a cyclic AMP dependent manner (Heyworth et al 1983) and also by insulin through an unknown mechanism (Loten et al 1978, Loten et al 1983, Heyworth et al 1983, Houslay et al 1983). The rat liver hormonally activated 'dense-vesicle' PDE was shown to be an integral membrane protein anchored to the membrane bilayer via a 5 kDa peptide (Pyne et al 1987). Native 'dense-vesicle'

enzyme has a molecular mass of approximately 62 kDa. However, during purification this 5 kDa membrane anchor becomes cleaved yielding a 57 kDa clipped species (Pyne et al 1987). Evidence also suggests that the PDE may exist as a 110kDa dimer in situ (Pyne et al 1987).

Similar K_m values have been reported for the hydrolysis of cyclic AMP and cyclic GMP by the PDE3 PDEs isolated, with concentrations ranging from 0.1 - 0.8 μ M for both substrates and V_{max} values greater for cyclic AMP than cyclic GMP. These enzymes also exhibited linear Michaelis-Menten kinetics for substrate hydrolysis (Degerman et al 1986, Degerman et al 1988 and Harrison et al 1986). On analysis of the 'dense-vesicle' PDE it was shown to be unusual in its class by virtue of it being a high-affinity cyclic AMP PDE which has low K_m and V_{max} values for cyclic GMP, suggesting a high affinity for cyclic GMP (Pyne and Anderson 1987, Marchmont et al 1981 and Pyne et al 1986).

The hallmark of the PDE3 class, including the 'dense-vesicle' PDE, is the potent competitive inhibition by cyclic GMP with an IC_{50} value in the range of < 1 μ M. Similarly the compound cilostimide is selective for the inhibition of PDE3 with reported IC_{50} values of < 0.1 μ M for PDE3 from human and bovine platelets (MacPhee et al 1986, Grant and Colman 1984). Functional effects of pharmacological inhibition of PDE3 include inhibition of platelet aggregation (Simpson 1988) and stimulation of lipolysis (Elks and Manganiello 1984).

(b) Regulation of Cyclic GMP Inhibited Phosphodiesterase

Hormonal regulation of PDE3 has been investigated and well characterised in rat adipocytes (Anderson et al 1989), in 3T3-L1 adipocyte cell line (Vasta et al 1992) and in hepatocytes (Heyworth et al 1983). In adipocytes, lipolysis is promoted by hormones such as adrenaline via beta adrenoceptor stimulation (Anderson et al 1989) which results in the elevation of the intracellular cyclic AMP concentration. Conversely stimulation of these cells by

insulin causes an antilipolytic effect by reduction of cyclic AMP within the cell. Thus, in adipocytes there is a fine balance between cyclic AMP production by adenylyl cyclase and cyclic AMP degradation via PDEs. Reduction in cyclic AMP levels in adipocytes has been shown to be centrally controlled by a PDE3 which is found exclusively associated with the endoplasmic reticulum subfraction and is stimulated by both insulin and isoproterenol, a beta adrenoceptor agonist (Anderson et al 1989).

The activation of PDE3 in adipocytes is the result of phosphorylation of specific serine residues (Smith et al 1991). The kinase involved in the activation of the PDE via beta adrenoceptor occupancy is thought to be PKA (see chapter section 1.2) (Vasta et al 1992), however the identity of the kinase involved *in vivo* mediating the action of insulin is more intriguing. *In vitro* experiments with 3T3-L1 cells have shown PDE3 phosphorylation and activation through PKA. However, it is unlikely that insulin promotes PDE3 phosphorylation via PKA *in vivo* since the challenge of adipocytes with insulin inhibits lipolysis through cyclic AMP reduction.

An analogous PDE3 to the hepatocyte 'dense-vesicle' form (Heyworth et al 1983) is present in adipocytes (Anderson et al 1989). Both adipocyte and hepatocyte cGIPDE are phosphorylated by PKA *in vitro* and are similarly activated by insulin and isoproterenol.

Inhibition of PDE3 is thought to be the underlying mechanism of action of PDE3 inhibitors such as milrinone (Brechler et al 1992). In light of this a human PDE3 has been cloned from myocardial tissues (Meacci et al 1992). Subcellular fractionation studies on mammalian myocardium by other investigators has shown a PDE3 activity associated with the sarcoplasm (Smith et al 1993), which presumably has functional relevance in controlling intracellular Ca^{2+} leading to a positive inotropic response. This has been shown to be the case for the positive inotropy produced by glucagon, which activates a

specific Ca^{2+} channel type in myocytes, mediated by the inhibition of PDE3 (Méry et al 1990) in a pertussis toxin sensitive manner (Brechler et al 1992).

1.9 PDE4 Cyclic AMP Specific PDEs

The PDE4 cyclic AMP specific enzymes are, like the other PDE classes, a diverse isoenzyme family which are characterised by a high specificity and affinity for cyclic AMP. In view of their complexity the PDE4 family have been known by a variety of names, namely peak III PDEs due to their elution profile from DEAE - cellulose (Weishaar et al 1985), cyclic AMP PDEs and high-affinity or low K_m PDEs (Weishaar et al 1985, Thompson et al 1984), type IV PDEs (Strada and Thompson 1985, Beavo 1990) and PDE4 (Beavo et al 1994). Their substrate specificity aside, cyclic AMP specific PDEs are also distinguishable by their inhibition by a selective group of compounds including the antidepressant drug rolipram and Ro-20-1724 and their insensitivity to inhibition by cyclic GMP.

(i) Isolation and Purification of PDE4

Most cells possess cyclic AMP PDEs which hydrolyse substrate with both 'high' and 'low' affinity (Erneaux et al 1980). At cyclic AMP concentrations in the lower range of 0.1 - 10 μM the 'high' affinity PDEs rapidly reach V_{max} , whereas the 'low' affinity PDEs operate in the range of 10 - 50 μM . Therefore, it seems likely that the 'high' affinity cyclic AMP PDEs play a key role in the signal transduction initiated by hormones which produce only a minor change in the cyclic AMP intracellular concentration. However, it should be noted that the labelling of cyclic AMP PDEs as either 'low affinity' or 'high affinity' is indeed a simplification, where it is possible that even one enzyme can possess both properties giving rise to anomalous kinetics (Marchmont et al 1981) or, that the cyclic AMP hydrolysing activity in a given cell type could be made up of PDE4 isoforms hydrolysing substrate at different rates. It is therefore necessary to isolate the PDE to characterise its activity, which is possible by physical separation such as DEAE-cellulose (Weishaar et

al 1985, Lavan et al 1990), by analysis with a specific inhibitor or by the cloning the PDE activity using sequence specific probes.

Prior to molecular cloning technology the isolation of PDE4 isoforms proved to be difficult because of various factors including the PDE4 isoforms being present only in trace amounts, they can be compartmentalised within the cell, and like other PDEs are unstable and easily proteolysed. Despite this, PDE4 isoforms have been isolated from a variety of tissues and species including human heart (Reeves et al 1987) and rat liver and hepatocytes (Marchmont et al 1981, Lavan et al 1990). One of the first characterised and purified to apparent homogeneity was the peripheral plasma membrane (PPM) PDE from rat liver (Marchmont et al 1981, Houslay & Marchmont 1981, Pyne et al 1987, Pyne et al 1989).

(ii) Peripheral Plasma Membrane PDE

The PPM PDE has been purified to apparent homogeneity from rat liver and is hormonally activated by insulin (Marchmont et al 1981). Marchmont et al (1981) have shown this PDE to be a 52 kDa monomer which is associated with the cytosolic surface of the plasma membrane through ionic interactions, and is localised via an integral membrane protein (Houslay & Marchmont 1981). PPM PDE is also found, and expressed in similar levels, in rat kidney, heart and white adipose tissue (Pyne et al 1987). This PDE was shown to be distinct from the 'dense vesicle' liver PDE by virtue of their different subcellular locations (Heyworth et al 1983) and that the PPM PDE is activated by insulin via tyrosyl phosphorylation (Pyne et al 1989). Most important was the observation that the PPM PDE was insensitive to inhibition by cyclic GMP (Marchmont et al 1981) or ICI118233 (Pyne et al 1987) which are known to inhibit the 'dense vesicle' PDE but it was sensitive to inhibition by the type IV PDE inhibitor Ro 20-1724.

1.10 PDE Activities isolated from *Drosophila melanogaster*.

One of the early approaches into studying PDE4 isoforms was concerned with the cyclic AMP specific PDE from *Drosophila melanogaster*. Early observations by Davis and Kiger in 1978, demonstrated that cyclic AMP levels could be genetically manipulated in *Drosophila* adults. It was shown that the levels of cAMP in these flies were dependent on the presence of the region 3D3-3D4 of the X-chromosome, and that by varying the number of doses of chromomere 3D3-3D4, the activity of the cyclic AMP PDE could be controlled in a dose dependent manner. Flies completely deficient in chromomere region 3D3-3D4, had elevated levels of cyclic AMP compared to those flies with 1, 2 or 3 doses of this chromomere region. However, cyclic GMP levels were not altered by the absence of chromomere region 3D3-3D4. These observations demonstrated that the cyclic AMP levels in these flies were genetically determined, and suggested that this particular chromomere region contained a structural or regulatory gene necessary for cyclic AMP PDE activity.

Subsequent studies (Kiger and Golanty 1979, Davis and Kiger 1980, Davis and Kiger 1981) supported the idea that chromomere region 3D3-3D4 did contain the gene or genes which conferred PDE activity. It was shown that two distinct forms of PDE activity, Forms I and II, could be isolated from normal adult *Drosophila*. Form I was characterised as a heat stable enzyme, which hydrolyses both cyclic AMP and cyclic GMP with equal affinity, and is activated by calcium. PDE Form II was also a heat labile enzyme with a lower molecular weight than Form I but was specific for hydrolysis of cyclic AMP only. The activity of the Form II enzyme was dependent on high magnesium concentrations but unlike Form I was insensitive to calcium activation. Form II was shown to be absent in flies deficient in chromomere region 3D3-3D4. Therefore, genetic dosage of chromomere region 3D3-3D4 affects the activity of Form II, in a manner which suggests this region may include the structural gene. However, the calcium / calmodulin dependent enzyme, Form I, was not affected. Using present day isoenzyme nomenclature, Form I could be

characterised as a member of PDE1 (see section 1.7.(i), and Form II, the PDE deficient in flies with a genetic deletion of chromomere region 3D3-3D4, a PDE4 isoenzyme.

(i) Mutants of *Drosophila melanogaster*.

Mutant flies carrying a genetic deletion at the chromomere region 3D3-3D4 are termed dunce mutants. This arose from the observations that deletions of this region of the X-chromosome results in a particular phenotypic learning defect. Dunce mutants fail to learn in olfaction tests associated with electric shock (Byres et al 1981) Other physiological characteristics of dunce mutants are known and include, female (Mohler 1973 and 1977) and male (Kiger 1977) infertility . The absence of imaginal disc derivatives such as legs, halteres, hemitergites and genitalia (Kiger 1977) has been shown to be a maternal defect in the dunce mutants. The connection between each of the aforementioned phenotypic characteristics is a genetic mutation of the dunce gene which results in an aberration of cyclic AMP metabolism.

(ii) Identification of the *dunc* Gene Product

Previous reports have implied that cyclic AMP metabolism is closely involved in reproduction and learning/memory in *Drosophila*. However some ambiguity existed as to the identity of the dunce gene product. Originally it was suggested that either the gene encoded a cyclic AMP PDE (Davis and Kiger 1981), or that the dunce gene encodes a protein which has an effect post-translationally to interact and activate the PDE catalytic activity. The later was a possibility considered by Chen et al (1986) who conducted experiments screening *drosophila* adult, pupal and embryonic cDNA libraries using unique genomic restriction fragments of *dnc*⁺ as probes. The *dnc*⁺ gene was isolated by the chromosome walking technique (Davis and Davidson 1984) which generated six RNAs subsequently reported as *dnc*⁺ gene products (Davis and Davidson 1986).

(iii) Molecular Analysis of the *dunc* Gene

Molecular analysis of cDNAs isolated by Chen et al (1986) revealed that the open reading frame of *dnc*⁺ showed similarity to other protein encoding genes which suggests that *dnc*⁺ does indeed encode protein in vivo. Comparison of the protein sequence of *Drosophila dunce* gene (Chen et al 1986) with the protein sequences from other PDEs such as the calcium / calmodulin stimulated PDE from bovine brain, the cyclic GMP stimulated PDE from bovine heart and the yeast PDE2 gene (Sass et al 1986), revealed a 200-270 residue segment in each that is homologous to the others and which appears to be constrained to the carboxyl segment of this protein (Charbonneau et al 1986) (fig 1.10.4). The homologous segment is proposed to comprise the catalytic domains in the set of enzymes analysed. Bacterial expression systems used to express truncated cDNA clones lacking this ~270 amino acid sequence are devoid of PDE activity (Swinnen et al 1989). Within the ~270 amino acid sequence several residues are conserved, in particular histidine which could determine protein folding or substrate interaction. However, outside this region of homology which is proposed to contain the catalytic region, there are no common sequences found throughout the PDE superfamily, however sequence similarities are known to exist within an isoform family. The *dunce* gene product was found to share a seven amino acid sequence with the RII sub-unit of the cyclic AMP-dependent protein kinase that is predicted to be part of the cyclic AMP binding site. Thus, considering the region of sequence homology with other PDEs and with the cyclic AMP dependent protein kinase, this evidence strongly suggested that the *dunce* encoded protein is a functional PDE (Chabonneau et al 1986, Chen et al 1986).

1.11 Rat Homologues of the *Drosophila dunce* Gene

Further evidence in support of the *Drosophila dunce* gene encoding a functional PDE, came from studies which involved the molecular cloning of rat homologues of the *Drosophila* gene (Swinnen et al 1989, Swinnen and Joseph et al 1989, Swinnen et al 1991). The approach used to

isolate mammalian dunc gene counterparts involved the screening of a rat cDNA library of rat testis origin, with a ^{32}P -labelled *Drosophila dunc* cDNA clone (Swinnen et al 1989). Four cDNA clones (ratPDE 1 - 4) were subsequently isolated and demonstrated that not only were the four clones homologous to each other, they also contained within the sequences the 270 amino acid region discussed in section (iv) (fig 1.10.4). Differential tissue expression of the PDE clones, and the existence of little homology outwith the 270 amino acid region suggested that the cDNAs originated from genes which were distinct and related, as opposed to products of alternative splicing of the one gene. The existence of distinct PDE genes provides some basis, at least from a molecular point of view, for the heterogeneity observed throughout the PDE superfamily. These studies resulted in the isolation of four groups of cDNA clones of rat testis origin with considerable homology to the *Drosophila dunc* gene. Three of these cDNA clones were used for transformation of bacteria (Swinnen and Joseph 1989). These transformations increased PDE activity in the bacterial extracts suggesting that the cDNA clones were derived from transcripts encoding functional enzymes. This can also be said of the *Drosophila dunc* gene product due to the significant sequence homology with the cDNA clones. The sequence analysis of *dunc* cDNA clones (Chen et al 1986) therefore confirms the initial biochemical studies which suggested the gene encoded a PDE ((Davis and Kiger 1978, Kiger and Golanty 1979, Davis and Kiger 1980).

The significance of the isolation of these homologous cDNA clones of the *Drosophila dunc* gene is in the origin of the cDNA library - a rat testis cDNA library. This suggested a role for cyclic AMP PDEs in gametogenesis in a mammalian species. It is therefore interesting to note that deficiency of the *dunc* gene in *Drosophila* has an effect on both male and female fertility (Mohler 1973 and 1977, Kiger 1977)

Certain ambiguity arose from the initial biochemical analysis of these enzymes which highlighted specific problems in the isolation of these isoforms, such as inconsistent reports of molecular size due to sensitivity of PDEs to proteolysis, which resulted in the purification of catalytically active fragments, and the isolation of a mixture of PDEs as opposed to one isoform. The instability of the PDE4 family is one of the many problems encountered when analysing these proteins. However, studies using *Drosophila melanogaster* and *Saccharomyces cerevisiae* have had a particular important role to play in the study of PDE4 from a molecular genetic perspective. Two independent groups using different strategies have isolated two cDNA clones RD1 (rat *dunc-1*) (Davis et al 1989, Davis and Henkle-Tigges 1989) and DPD (*dunc* - like phosphodiesterase) (Colicelli 1989) from a rat brain cDNA library.

(i) Isolation of RD1 (PDE4A1) by Cross-Hybridisation with
dunc Gene Probe

Given that cyclic AMP PDEs play such a central role in the neuronal processes of learning and memory in *Drosophila*, and their involvement in the control of reproduction of these flies, the investigation for mammalian homologues was considered critical. The strategy undertaken by Davis et al (1989) involved screening genomic libraries from different species. Initially, a cDNA probe was constructed which corresponded to a section of the *Drosophila dunc* gene, and was used to screen a variety of genomic cDNA libraries including rat. Subsequently the rat *dunc* -1 gene was isolated. A fragment of the rat *dunc* -1 genomic clone, which had a high degree of homology to the *Drosophila dunc* gene, was used to probe a rat brain cDNA library and resulted in the isolation of the clone RD1. The homology of the predicted product of RD1 with other PDEs was compared (Davis et al 1989). Sequence comparison of cDNA clones RD1 and DPD have shown a high degree of homology in the conserved 270 amino acid region. However within this homologous region, approximately half of the identical residues use

alternative codons, and outwith the region little sequence similarity is seen either upstream or downstream suggesting they are products of distinct genes (Davis et al 1989, Colicelli et al 1989).

(ii) Isolation of DPD (PDE4B1) by Suppression of the *ras 2^{val19}*

Mutation of *Saccharomyces cerevisiae*

In the study which reported the isolation of DPD (Colicelli et al 1989) a different strategy to that used in the isolation of RD1 was employed. The second strategy involved searching for cDNA clones whose expression would suppress the phenotype associated with the *ras 2^{val19}* mutation in *Saccharomyces cerevisiae*.

Saccharomyces cerevisiae encodes two genes *RAS 1* and *2* homologous to the mammalian *RAS* oncogene family. *RAS* genes represent the transforming genes found in many human tumours, and encode for 21kDa GTP binding proteins (p21) which are associated with the plasma membrane (Gibbs et al 1984 and 1985). In *Saccharomyces cerevisiae* disruptions of both genes results in growth failure, however, normal growth patterns are restored if double mutants are transformed to express either human (Kataoka et al 1985) or viral (DeFeo-Jones et al 1985) *RAS*.

RAS functions to modulate adenylyl cyclase activity in *Saccharomyces cerevisiae* as removal of the influence of *RAS* has been shown to result in deficient adenylyl cyclase activity (Toda et al 1985). Purified yeast *RAS 1* or *2*, or the human counterparts have been shown to activate yeast adenylyl cyclase in reconstitution experiments (Broek et al 1985), where the *RAS* protein is replaced in mutant cells by *RAS* from either mammalian or yeast origin.

Regulation of adenylyl cyclase by *RAS* in yeast can be attributed to the similarities between G-proteins and *RAS*, that is, concerning their membrane association, ability to bind guanine nucleotides (Shih et al 1980) and have intrinsic GTPase activity (McGrath et al 1984). Gilman (1984) has

suggested that on the basis of this and of sequence homology between *RAS* and the alpha subunit of G-proteins that both proteins do share a similar function. Guanine nucleotide binding is associated with the activation of yeast cyclase (Casperson 1983) and with the cloned yeast *RAS-2* product (Tamanoi et al 1984) which is a protein of similar size to the alpha subunit of G-proteins.

An analogous situation to the loss of G-protein alpha subunit, that is the loss of cyclase activation, is reported when the *RAS-2* gene is disrupted (Toda et al 1985). This supports the notion that the *RAS-2* gene encodes a protein similar to the G-protein alpha subunit. Indeed, in *Saccharomyces cerevisiae* *ras 2^{val19}* mutants which encodes valine at the nineteenth codon instead of glycine, cyclase is constitutively activated (Toda et al 1985) presumably due to the loss of GTPase activity, therefore the activation of cyclase is not terminated by the return to the resting GDP bound *RAS*. Similar levels of adenylyl cyclase activation to the result of the *ras 2^{val19}* mutation are seen with the non-hydrolysable GTP analogue guanosine 5'-(beta-gamma-imido)triphosphate (Gpp(NH)p) (Broek et al 1985).

The *ras 2^{val19}* missense mutants are typified by a particular phenotype which is manifested as an abnormal response to nutrient stress summarised by Toda et al 1985. When the *ras 2^{val19}* mutants are nutritionally deprived of nitrogen and sulphur they lose viability and terminally arrest at all growth phases whereas the wild-type arrest in the unbudded state. Correlation exists between the *ras 2^{val19}* mutation and the inability to accumulate glycogen and trehalose when entering the stationary phase of growth. Adenylyl cyclase activity in *ras 2^{val19}* mutants is increased ~4 fold which would correspond to the increase in cyclic AMP levels and the increased PKA dependent control of metabolism, that is glycogen levels. The *ras 2^{val19}* mutation renders yeast unable to respond to changes in the nutritional environment and intolerant to heat shock (Toda et al 1985, Sass et al 1986). Therefore the overexpression of any of the contributory elements of the cyclic AMP signalling pathway in yeast,

for example, high level expression of adenylyl cyclase (Kataoka et al 1985), overexpression of PKA (Sass et al 1986) or the deletion of the regulatory subunit of PKA (Matsumoto et al 1982) produce the same phenotype as that seen with the *ras 2^{val19}* mutation. In order to overcome these nutritional restrictions the yeast has to reduce the level of intracellular cyclic AMP, and the only mechanism by which the cell can do this is by a cyclic AMP PDE. As in the study by Collicelli et al (1989) cDNA clones which encode a PDE can be isolated in this system, hence the isolation of DPD and the yeast PDE2 gene (Sass et al 1986).

The mammalian DPD cDNA was shown to encode a protein with a high degree of amino acid sequence identity (~80%) with the cognate *Drosophila dunc* species within the conserved region. Protein sequence analysis of the gene products of RD1 and DPD showed little sequence conservation with other known PDEs (Charbonneau 1986). However the amino acid sequences of RD1 and DPD have approximately 90% homology within the conserved domain, and 67% in the upstream region, but regions of identical residues are separated by intermittent amino acid sequences. Up to 50% of identical amino acid residues within the conserved domain utilise alternative codons, which suggest that the two cDNA clones are encoded by distinct but related genes (Swinnen et al 1989).

(iii) Biochemical Analysis of DPD (PDE4B1) and RD1

(PDE4A1)

The homology of RD1 and DPD to the *Drosophila dunc* gene product predicted similar properties for the rat homologues to the *Drosophila* cAMP PDE. RD1 and DPD were both shown to encode high affinity cyclic AMP PDEs similar to the *Drosophila dunc* PDE upon expression in a yeast system (Davis and Henkle-Tigges 1989). Kinetic analysis of the *Drosophila dunc* PDE and the cognate mammalian species RD1 and DPD characterised these proteins as having a high affinity for cyclic AMP (Henkel-Tigges and

Davis 1989, Shakur et al 1993). This study confirmed early reports that the *Drosophila* cyclic AMP PDE did not hydrolyse cyclic GMP, even at substrate concentrations of up to 1mM (Kiger and Golanty 1979, Davis and Kiger 1980, Chen et al 1986).

A summary of the properties of RD1 and DPD as compared to the *Drosophila* counterpart is shown in (fig 1.11.6) The most striking observation was that the mammalian homologues were potently inhibited by rolipram and RO 20-1724 whereas the dunce PDE was insensitive. Hence, the sequence divergence between the *Drosophila* and mammalian proteins allow one to speculate the existence of a binding site for pharmacologically important compounds (Henkel-Tigges and Davis 1989).

(iv) Unique N-Terminal Region of RD1

The idea that the amino terminal region of RD1 encoded a membrane association motif has been the subject of much investigation (Shakur et al 1993, and 1995). Expression of the RD1 cDNA in COS-1 cells resulted in an increased cyclic AMP specific PDE activity which was selectively inhibited by the PDE4 inhibitors rolipram and RO-20-1724 and was located predominantly (~85%) to the plasma membrane (Shakur et al 1993). An N-terminally truncated RD1 species which lacked the first 25 amino acids (the met²⁶RD1), was shown to be characteristically similar to the full length RD1 in that they shared inhibitor and substrate specificity however, the met²⁶RD1 was found exclusively in the cytosolic fraction. These 25 N-terminal amino acids conferred membrane integration which allowed the solubilisation of RD1 with the non-ionic detergent TX-100, but not by either washing the membrane with high concentrations of NaCl or rehomogenisation (Shakur et al 1993). Additionally, the N-terminal 25 amino acids of RD1 have been shown to be regulatory in the catalytic function of the enzyme in parallel with membrane anchorage (Shakur et al 1995). The engineered deletion of the first 25 amino acids of RD1 were previously shown not to alter either the K_m for cyclic AMP

or the selectivity for, or sensitivity to, inhibitors of PDE activity (Shakur et al 1993). Using C-terminal specific antisera to RD1, Shakur et al (1995) have been able to determine the relative amounts of both RD1 and the N-terminal truncated enzyme the met²⁶RD1 expressed in transfected COS-1 cells. The unique N-terminal region of RD1 was shown to be inhibitory on catalytic function, where deletion of this domain resulted in a ~2 fold increase in the V_{max} value. In addition, Shakur et al (1993) have shown that in thermostability experiments, membrane associated RD1 was more resistant to denaturation either detergent solubilised RD1 or the met²⁶RD1. It is believed therefore, that association of RD1 with the plasma membrane through this N-terminal region regulates both the structure and activity of the enzyme.

(v) Functional Role for PDE4 Species in the CNS

Rolipram and RO20-1724 are both compounds with anti-depressant properties. Indeed Rolipram has been evaluated in clinical trials as an effective drug for the treatment of depression. The most surprising observation was that many of the patients tested in the trial did not previously respond to other anti-depressant therapy (Watchel 1983). It is intriguing that *dunc* mutants lacking the gene encoding a PDE exhibit a learning and memory (Dudai 1983) defect, whereas in humans the anti-depressant drug Rolipram elevates mood, possibly by the inhibition of PDEs. If the anti-depressant action of Rolipram is indeed via PDE inhibition as has been suggested (Watchel 1983), then a role for the *Drosophila* cyclic AMP PDE and its mammalian homologues in the complex processes underlying the neurobiochemical events of mood regulation in mammals, and learning / memory in insects has been recognised. Further evidence to support this suggestion comes from a study by Nighorn et al (1991), in which it was found that the *dunc* PDE was markedly concentrated in the neurophil associated with mushroom body cells. These areas have been previously implicated in the processes of learning and memory. A parallel

study in rat brain has shown *in vivo* expression of DPD and RD1 (Lobban et al 1994, Shakur et al 1995) in particular brain areas.

1.12 Molecular Analysis of Rat PDE4

Four distinct PDE4 genes representing the four isoform subfamilies found in rat have been isolated (Swinnen et al 1990) (fig 1.10.4). The full length cDNAs of RD1 (PDE4A1) (Davis et al 1989), DPD (PDE4B1) (Collicelli et al 1989) and ratPDE4 (PDE4B2) (Lobban et al 1994) have been isolated and studied. Functional and tissue specific expression of PDE4B isoforms have been demonstrated in the rat brain (Lobban et al 1994). DPD was found to be exclusively cytosolic and was selectively expressed in hippocampal, cortex, hypothalamus and striatum regions. ratPDE4 on the other hand was located at the membrane of all brain regions with the exception of the midbrain (Lobban et al 1994).

Analysis of the PDE4B gene (Monaco et al 1994) has shown that DPD and ratPDE4 are splice variants of the same gene, where upon the comparison of the protein sequences it can be seen that ratPDE4 has an extended N-terminus of 48 amino acids. Products larger than DPD can be transcribed according to which methionine initiation codon is utilised. Furthermore, Lobban et al (1994) have shown that DPD and ratPDE4 are likely to be the only products *in vivo* of the PDE4B gene given that only one immunoreactive species is detected with the antisera specific for ratPDE4 and one which recognised ratPDE4 / DPD.

The RD1 clone isolated by Davis et al (1989) was cloned along with two partial clones (RD2 and RD3) which suggested that splice variants of the RD1 gene existed (Davis 1990, Pyne et al 1986). However, upon analysis of rat brain with RD1 specific antisera only one immunoreactive band was detected in rat brain (Shakur et al 1995) with a molecular mass of ~68kDa. This is in agreement with that calculated from the predicted sequence of the cDNA. From this it seems likely that RD1 represents the full length version of the PDE.

The complexity of function of the cyclic AMP specific PDEs encoded by the *dunce* gene of *Drosophila* and its mammalian counterparts RD1 and DPD has been highlighted. It is suffice to say that although these PDEs exhibit a certain sequence homology within a central portion of the protein, the flanking sequences of this conserved region display considerable divergence. However, the amino termini of proteins of each class often contain sequence motifs particular to its own class, for example PDE2 enzymes have a cyclic GMP regulatory domain located at the amino terminal. These sequences surrounding the conserved portion are considered to contain regions which for example interact with other proteins, such as membrane association as seen with RD1 (see section (vii b) above). Bolger et al (1994) have identified two regions present in the amino terminus of the protein translated from the *dnc* and human cDNA homologues isolated in this study. These two regions, which the authors describe as UCR 1 and UCR2 (upstream conserved regions), from both human clones and *Drosophila melanogaster* share significant homology, although UCR 1 and UCR 2 show little homology with each other. The function of these sequences is as yet unknown, however it is thought that the UCR 1 site is likely to undergo alternative splicing. Future work may identify common PDE4 specific motifs, however it is expected that the flanking sequences of the catalytic domain offer unique identifiers eg UCR 1 and UCR2.

1.13 Human Multigene Family Encoding Cyclic AMP Specific Phosphodiesterases

Four human genes have been isolated corresponding to the isozyme subtypes of PDE4A to D (fig 1.13.5). Within each of these PDE4 subtypes there exists further subdivision which has arisen as the result of splice variation of a single gene (Bolger et al 1993). These four human genes have been shown to correspond to the four rat genes representing the PDE4 subclasses isolated by Swinnen et al 1989 (fig 1.10.4, table 1c).

Bolger et al (1993) have shown that 3 of the 4 genes encoded cyclic AMP specific enzymes which were selectively inhibited by rolipram in the μM range of drug concentration. The PDE4 enzymes were also shown to be selectively expressed in particular cell types in a distinctive pattern for each gene. Surprisingly, in contrast to the results obtained from the rat Swinnen et al (1989) have shown that PDE4 activity was not detected in human testes tissue which suggests that the pattern of selective expression is also species specific.

Engels et al (1994) undertook the investigation of the cellular expression of PDE4 isoform subtypes in various human tissues and cell lines, by the isolation of mRNA and reverse transcribing it into cDNA. Using isoform subtype specific primers, tissue expression patterns of the four known human PDE4 genes was determined using PCR in various tissues and in several defined cell lines. A summary of the results of this study is shown in table 1a. In parallel to this study in humans, a comparative study was conducted in the rat where brain, liver, lung, kidney, heart and blood were tested for the expression of each rat isoform subtype. The data clearly demonstrated species specific tissue expression of the various isoform subtypes in rat. In particular PDE4A was expressed in all tissues with the exception of blood, which is in contrast to human PDE4A which was the only isoform found in T cell Jurkat cell line. The conclusions of the study suggest a particular role for PDE4A in T cell functioning in humans. Baeker et al (1994) have isolated a human PDE4D cDNA clone whose mRNA transcript is predominantly found in skeletal muscle.

It is evident that PDE4C is unlikely to be important in controlling the cyclic AMP levels in blood since this isoform subtype was undetectable in the blood from both human and rat species. Cells of the human immune system display a greater selectivity of isoform subtype expression. T-cells selectively express PDE4A, B-cells express only PDE4A and B, neutrophils

predominantly express PDE4B and PDE4C is absent from all of the cells of the immune system. Souness et al (1995) have also shown that it is predominantly PDE4D which is responsible for cyclic AMP hydrolysis in eosinophils. This suggests that specific isoform subtypes are recruited in the particular cell types to control distinct cyclic AMP pools. The reasons as to why cells selectively express one isoform subtype over another can only be understood by determining subcellular localisation and characteristics of these isoform subtypes.

1.14 Cellular Regulation of PDE4

It has been well established that cyclic AMP is at the centre of the control of many cellular functions, therefore enzymes involved in the metabolism of cyclic AMP such as the PDE4 family are poised to play a crucial role in these functions. Evidence suggests that compounds selective for inhibition of PDE4 activity will be particularly important in the treatment of inflammatory disorders (Engels et al 1994). PDE4 activity has been shown to be crucial in the regulation of human monocyte activation (Molnar-Kimber et al 1992) and is elevated in patients with inflammatory disorders (Grewe et al 1982, Chan et al 1993).

Elevation of cyclic AMP PDE activity can be achieved in various cell types by agonists which stimulate adenylyl cyclase and is a homeostatic response by which many cells can regulate responses to hormones and drugs. This PDE activity has been identified as PDE4 (Conti et al 1991). Up regulation of PDE4 activity has been identified in different mammalian cell types. In FRTL-5 cells PDE4 activity is elevated in response to thyroid stimulating hormone, which is known to elevate intracellular cyclic AMP (Sette et al 1994). This hormone dependent cyclic AMP regulation in FRTL-5 cells involves an initial rise in cyclic AMP which is returned to basal level within minutes, despite the constant presence of hormone. This is a feature of many hormone regulated systems where the cell is protected from over stimulation by desensitisation of

the cell, or by an alteration of the sensitivity of the cell to circulating hormone by cell adaptation, such as activation of a protein to remove the stimulus. In FRTL-5 cells the intracellular elevation of cyclic AMP results in an activation of PKA and subsequent phosphorylation and activation of PDE4, which in turn lowers the cyclic AMP level and switches off the hormone signal. Previous reports (Swinnen et al 1989, 1991) had shown that pituitary hormone, in rat sertoli and in FRTL-5 cells, increased the level of mRNA of PDE4, however, thyroid stimulating hormone in FRTL-5 cells appears to cause simply an activation of PDE via phosphorylation.

Isoform subtype induction by cyclic AMP has also been investigated in Jurkats (T-cell like cell line), U937 cells and neuronal cell lines (Engels et al 1994). In U937 cells which express subtypes PDE4A, B and D, only PDE4A and B were up regulated in response to elevated cyclic AMP (Engels et al 1994). In Jurkats which only express subtype 4A a similar up regulatory response was noted. This was shown to be in contrast to the neuronal cell lines tested which express all of the four isoform subtypes and did not show an increase in the levels of either isoform subtype. It is of considerable importance that the induction of PDE4 isoform subtypes can occur in one cell type, and suggests differential control of up regulation dependent on the cell type.

There is also evidence for activation of PDE4 via interaction with the phospholipid signalling system. Increased PDE4 activity was noted in rat thymic lymphocytes (Marcoz et al 1993) in response to mitogenic stimulation, and of PDE4 isolated from U937 cells (DiSanto & Heaslip 1995). In rat thymocytes (Marcoz et al 1993), arachadonic acid and diacylglycerol, phospholipid metabolites formed following mitogenic stimulation, were found to be ineffective. In contrast, the phospholipid metabolite phosphatidic acid was shown to increase the activity of a PDE4. In T cell activation cyclic AMP is

inhibitory, thus lowering the level of the second messenger through activation of PDE allows T cell activation to proceed in response to a mitogenic stimulus.

1.15 Pharmacological Effects of PDE4 Inhibition

(i)(a)PDE4 Inhibition in the Treatment of Asthma

Asthma is a chronic inflammatory condition characterised by inflammation of the airway submucosa as a result of the influx of inflammatory cells in response to an allergen. In the progressive state of the disease the airways become irreversibly obstructed (Giembycz 1992). Current drug therapy uses mainly bronchodilatory agents which are useful in the treatment of the symptoms, but have little effect on the underlying cause of the condition, that is the inflammation. Cyclic AMP elevation produces an anti-inflammatory effect (Bourne et al 1978) by inhibiting the release of inflammatory mediators from cells involved in the immune response (Peachell et al 1992), and achieves bronchodilation through the relaxation of airway smooth muscle (Torphy 1988). An important role for PDE4 activity in regulating the function of mast cells (Torphy et al 1992), neutrophils (Nielsen et al 1990), eosinophils (Dent et al 1991) and basophils (Peachell et al 1992) has also been reported. In patients with inflammatory disorders, up regulation of PDE4 is reported to occur in monocytes (Grewe et al 1982, Chan et al 1993). It would therefore be possible to restore cyclic AMP effects through the selective inhibition of PDE4, providing the inhibitor was specific enough for a particular PDE4 subtype in a specific cell type.

(b)PDE4 in Monocytes

The prevalent role of PDE4 in cells involved in the inflammatory response is an observation which has been credited with much attention. In particular, PDE4 has been shown to be central in the regulation of human monocyte activation (Molnar-Kimber et al 1992). A mediator which has a pivotal role in the inflammatory response is tumour necrosis factor-alpha (TNF-alpha). TNF-alpha along with interleukin-1 (IL-1) recruit polymorphonuclear

leukocytes to the tissues during the inflammatory response (Goto et al 1984). Elevation of cyclic AMP via rolipram has been shown to inhibit TNF-alpha release from monocytes while other cytokines such as Il-1 remain unchanged (Bailly et al 1990, Semmier et al 1993, Prabhakar et al 1994, Klemm et al 1995). The PDE4 subtypes present in monocytes has been studied using the Mono-mac 6 cell line as a model (Verghese et al 1995), in which it was found that mRNA transcripts were present for PDE4A, B and D. On analysis of the protein expression it was noted that PDE4B peaked after 24 hours exposure to dibutyryl cyclic AMP, where PDE4A maintained a high protein level 24 hours after treatment. This data suggests that different PDE4 isotypes are recruited at different time points in the cell cycle and that PDE4A may have a greater role to play in the reduction of cyclic AMP levels.

PDE4 activity in the U937 cell line, which is committed to the human monocyte-macrophage pathway, has been investigated (DiSanto & Heaslip 1993). Two peaks of PDE4 activity were resolved, one of which, Peak2 became activated after 24 hour storage at 4°C in buffer containing a high concentration of sodium acetate and protease inhibitors. The V_{max} of Peak2 PDE4 doubled after the 24 hour storage, and was associated with a shift in the molecular weight. Prior to storage, the molecular weight of Peak2 was determined to be 210 - 250 kDa, whereas after storage there was a larger peak of PDE4 activity corresponding to 45kDa. This could suggest that in U937 cells PDE4 is expressed as a high molecular weight species, which is subsequently cleaved to produce the 45kDa species. Alternatively, the 45kDa species may simply represent a sub-unit of a larger protein.

(c) PDE4 in Eosinophils and T-lymphocytes

Of primary importance in the development of the inflammatory response are eosinophils and T-lymphocytes. The level of blood and lung eosinophils in asthmatics is elevated. Once activated, eosinophils cause cell damage through the release of reactive oxygen species, cationic proteins,

products of the lipooxygenase and cyclooxygenase pathways, cytokines, PAF and eosinophil derived neurotoxin. This release of a barrage of inflammatory mediators not only destroys airway neurones and epithelia, but increases the reactivity of the airways so that the individual is more sensitive to the allergen (Souness et al 1995, Giembycz 1992). PDE4 inhibitors Rolipram and RP734 01 suppressed the production of oxygen radicals from eosinophils and PAF induced airway hyperresponsiveness (Souness et al 1995, Racburn et al 1994). Analysis of the expression of PDE4 subtypes in eosinophils showed that only the PDE4D isoform was present and that it was most likely to be membrane bound *in vivo* (Souness et al 1995).

Evidence suggests that the role of the T-lymphocyte is as an aid in the infiltration of eosinophils and release of cytokines (Giembycz 1992), and that the PDE4 inhibitor RO-20-1724 decreases the cytotoxic effect of these cells (Robicsek et al 1991). Previous analysis of the isoforms of PDE which were present in these cells suggested that there was a cytosolic PDE4 and a membrane bound PDE3 (Robicsek et al 1991). More recently Engels et al (1994) have looked at the PDE4 isoforms expressed and have shown that it is only the PDE4A subtype which is present.

(ii) PDE4 in the CNS

The PDE4 isoform has been shown to be the predominant PDE type expressed in the CNS and human myeloid and lymphoid lineages (Beavo and Reifschneider 1990, McLaughlin et al 1993). Indeed rolipram has been clinically tried as an effective antidepressant (Fleischhacker et al 1992). Multiple sclerosis, the demyelinating disorder, is believed to be a T-cell mediated autoimmune disease (Martin et al 1992), and that TNF-alpha and lymphotoxin-alpha are involved in the demyelination identified in multiple sclerosis lesions (Selmaj 1991). Rolipram was found to inhibit the production of TNF-alpha by autoreactive human and rat T-lymphocytes *in vitro*, and

prevented the clinical signs of encephalomyelitis which is used as an experimental model for multiple sclerosis *in vivo* (Sommer et al 1995).

(iii)PDE4 in Smooth Muscle

The level of PDE4 has been found to increase in the pregnant human uterus, and is thought to be involved in the preparation of the myometrium for contraction at the time of parturition through lowering the level of cyclic AMP (Leroy et al 1994).

Rolipram and RP73401 have both been found to be effective in the relaxation of smooth muscle *in vitro* (Souness et al 1995). Rolipram has also been shown to inhibit non - cholinergic excitatory neurotransmission in guinea pig bronchi (Qian et al 1994). These results suggest that PDE4 inhibitors may have a dual effect in the treatment of asthma as an anti - inflammatory and a bronchodilator, therefore tackling both problems of providing symptomatic relief and treatment of the underlying causes of the condition.

Isolation, purification and characterisation of PDE4 would therefore provide some of the information needed to improve upon current drug therapy, by aiding the development of specific cellular and tissue selective inhibitors. Along with this, molecular biology would aid identification of further subtypes of the PDE4 family and improve and build on our knowledge of the distribution of PDE4 subtypes.

1.16 Isolation of a Human Monocyte Cyclic AMP Specific

Phosphodiesterase - hPDE4A_{Livi}

In addition to the isolation of rat homologues to the *Drosophila* cyclic AMP PDEs, a cDNA clone representing a high affinity, rolipram sensitive cyclic AMP PDE (hPDE4A_{Livi}, Gene Bank descriptor HPDE4A1A) has been isolated from a human monocyte cDNA library using the conserved region of RD1 as a probe (Livi et al 1990, McHale et al 1991). The human cDNA clone hPDE4A_{Livi}, contains significant homology with other cloned PDEs namely RD1, DPD and *Drosophila dunce* PDE. These PDEs have

homologous sequences in two domains, a forty amino acid region located amino terminally and a larger 270 amino acid region in the central portion of the sequence. This larger region is conserved throughout a range of PDEs from other species (Charbonneau 1986) and is proposed to contain the catalytic domain of these PDEs. Amino acid sequence divergence exists at both the NH₂ terminal and at the COOH-terminal of the hPDE4A_{Livi}, sites which most likely serve a regulatory function or define subcellular location.

The recombinant protein hPDE4A_{Livi} has been expressed in both COS-1 cells (Livi et al 1990) and *Saccharomyces cerevisiae* (McHale et al 1991, Torphy et al 1992). A molecular weight of 77kDa was determined for hPDE4A_{Livi} from the predicted amino acid sequence. In COS-1 cells the cDNA was shown to encode a high affinity, cyclic AMP specific PDE which was selectively inhibited by rolipram (Livi et al 1990). Bolger et al (1993) have since isolated the cDNA clone representing the entire sequence of hPDE4A_{Livi} and have shown this PDE to be truncated at the amino terminus. Despite this hPDE4A_{Livi} is a catalytically active enzyme.

Upon the stable transfection of hPDE4A_{Livi} into *Saccharomyces cerevisiae* which lacked endogenous PDE activity, the molecular weight was determined to be 88kDa (Torphy et al 1992). The molecular weight determined from the predicted amino acid sequence was 77kDa (Livi et al 1990). Presumably the discrepancy reflects post translational modification particular to *Saccharomyces cerevisiae*. Yeast expressed hPDE4A_{Livi} displayed similar kinetic characteristics to that of the COS-1 cell expressed enzyme with respect to cyclic AMP hydrolysis and that it was selectively inhibited by PDE4 specific compounds (Torphy et al 1992).

1.17 Isolation of a PDE4 PDE From Human Brain

Since the discovery and isolation of rat homologues of the *drosophila dunce* gene (see section 1.9 iv) attention has focused on the human counterparts, for example hPDE4A_{Livi} described in section 1.12. McLaughlin

et al (1992) have since reported the isolation of another human PDE4 isoform, hPDE4B (Gene Bank descriptor HSPDE4B2A), isolated from a human frontal cortex cDNA library which was cloned by virtue of its homology to the conserved region of hPDE4A_{Livi}. The hPDE4B enzyme was found to be restrictively expressed in human brain, heart, lung and skeletal muscle. In contrast to the study by Engels (1994), McLaughlin et al (1992) were unable to detect PDE4B in placenta, liver or kidney. On the basis of their data McLaughlin et al (1992) stated that since PDE4B activity was undetectable in blood enriched tissue such as placenta then PDE4B does not have a function in monocytes. This must be viewed questionably given the results of the study by Engels 1994, which showed that the PDE4B isoform is present in most circulating blood cells except T-cells, although the differences could be due to the different techniques employed.

McLaughlin et al (1992) classified the PDE4B gene as such due to the observation that it encoded a low K_m , cyclic AMP specific PDE with a predicted molecular weight of 64.2 kDa and was selectively inhibited by rolipram and RO20-1724.

1.18 Isolation of a Human PDE4D

The cDNA for a human PDE4D isoform has been isolated from a human heart cDNA library using a sequence found in the rat PDE4D as a probe (Baecker et al 1994). The cDNA was shown to encode an enzyme which was 604 amino acids long with predicted molecular weight of 68.5kDa, and was found to be 91.4% homologous with the rat PDE4D. The enzyme was engineered for expression in a bacterial system and was shown to be sensitive to rolipram with an IC_{50} of 2.2 μ M. Northern blot analysis found the PDE4D transcript to be most abundant in skeletal muscle but was absent from liver and pancreas.

1.19 Kinetics of Cyclic AMP Hydrolysis and Inhibition by Rolipram of PDE4

(i) Kinetics of Cyclic AMP Hydrolysis

Cyclic AMP hydrolysis via the human PDE4 isoforms which have been reported to date, consistently appear to be of simple, saturation Michaelis-Menten kinetics yielding K_m values which are in the micromolar range characteristic of the PDE4 class. This has shown to be the case for the recombinant monocyte isoform hPDE4A_{Livi} expressed in COS-1 cells (K_m 2.3 μ M, Livi et al 1990) and yeast (K_m 3.1 μ M, Torphy et al 1992), hPDE4B isoform cloned from brain and expressed in yeast (K_m 4.3 μ M, McLaughlin et al 1992) and PDE4 activity isolated and purified from monocytes (K_m 1.6 μ M, Torphy et al 1992).

(ii) Inhibition by Rolipram

The mechanism by which rolipram exerts its inhibitory effect on PDE4 has been less well characterised than that of substrate hydrolysis. Indeed, evidence to date has suggested that the mechanism of inhibition by rolipram may be anomalous based on the observation that log dose response curves showed a shallow profile (Torphy et al 1992, Bolger et al 1993, McLaughlin et al 1993), that is they ranged over several orders of magnitude. Additionally, double-reciprocal plot data of kinetic studies on the hPDE4A_{Livi} enzyme (Livi et al 1990, Torphy et al 1992) and the hPDE4B enzyme (McLaughlin et al 1993) does not fit to simple competitive kinetics. In light of this it has been suggested that PDE4 PDEs may possess a distinct binding site for rolipram (Livi et al 1990, Torphy et al 1992) which could be distinct from the site of catalysis.

(iii) High Affinity Rolipram Binding Site Detected in Rat Brain

High affinity rolipram binding was first reported by Schneider et al (1986) where it was shown that ³H-rolipram bound to sites in rat brain with high affinity (K_d ~2nM) in a saturable, reversible and stereoselective manner. The authors assumed that the rolipram binding site was that of PDE4, either its catalytic site or a distinct allosteric site. Evidence for a distinct rolipram binding

site in rat brain came from studies in which it was shown that there was a difference (~500 fold) in the concentration of rolipram needed to achieve inhibition of catalysis of rat brain PDE4 ($k_i \sim 1\mu\text{M}$ Némoz et al 1989), and the K_d (~2nM Némoz et al 1989, Schneider et al 1986) of rolipram binding to its high affinity site. This suggested that the high affinity rolipram binding site observed by Schneider et al (1986) in rat brain was one distinct from the catalytic site.

Attempts to prove that the high affinity rolipram binding site was associated with PDE4 have been difficult. Schneider et al (1986) have shown that ^3H -rolipram binding is mainly restricted to the brain in the rat, and has failed to show high affinity rolipram binding in tissues outwith the CNS, even although they are known to contain PDE4 activity. Regardless, the nature of the high affinity binding detected by Schneider et al (1986) was shown to be associated with both the soluble and membrane fractions of rat brain homogenates, with K_d values of 2.4nM and 1.2nM respectively. The corresponding Hill coefficients of rolipram binding were near unity, which suggests that rolipram is binding to one site only. Interestingly, rolipram was shown to bind stereospecifically with the (*R*)-rolipram conformation being more potent at displacing ^3H -rolipram, and that binding was dependant upon the presence of divalent cations, particularly magnesium.

The function of the high affinity rolipram binding site in brain is unknown, although it is thought that the site is preferentially associated with neuronal cells as opposed to glial cells (Tohda et al 1994). In addition, ^3H -rolipram binding along with ^3H -cyclic AMP binding has been located to post-synaptic pyramidal cell bodies (Kato et al 1993) in the gerbil brain. In the gerbil hippocampus there is a decrease in the binding of ^3H -cyclic AMP, presumably to PKA, and ^3H -rolipram which precedes the death of pyramidal cells after CNS ischaemia (Kato et al 1993, Murase et al 1993). This suggests that the

cyclic AMP second messenger system has a role to play in post ischaemic neuronal cell death.

(iv) The Rolipram Binding Site of Human PDE4

Analysis of the mechanism by which PDE4 inhibitors effect substrate hydrolysis catalysed by the cloned human PDE4 isoforms has proved to be controversial. Although comparable K_m values for cyclic AMP hydrolysis have been calculated for the monocytic PDE4 activity isolated from purified human monocytes to that of the cloned monocyte PDE hPDE4A_{Livi} (Torphy et al 1992), the kinetics of rolipram inhibition were unclear. Rolipram was shown to be a competitive inhibitor of the PDE4 activity isolated from monocytes but not of the cloned hPDE4A_{Livi} which was also shown to be inhibited stereoselectively by (*R*)-rolipram. With the isolation of human PDE4 it has been questioned that these isoforms may possess such a high affinity binding site for rolipram, as discussed for rat brain, considering the anomalous kinetics observed (Torphy et al 1992, Livi et al 1990, McLaughlin et al 1993).

High affinity rolipram binding was observed in the soluble fraction of yeast expressing hPDE4A_{Livi} with a K_D of 1nM and Hill coefficient 1.01 (Torphy et al 1992) demonstrating that, akin to rat brain, probably only one binding site for rolipram is present on hPDE4A_{Livi}. The two stereoisomers of rolipram were shown to inhibit cyclic AMP hydrolysis of hPDE4A_{Livi} with greater potency than that of human monocytic PDE4, with K_i values of 61nM and 390nM for (*R*) and (*S*)-rolipram respectively. Human monocytic PDE4 hydrolytic activity was not inhibited in a stereospecific manner by rolipram, and was inhibited relatively less potently with a K_i of 0.8 μ M. PDE4 inhibitor (*R*)-rolipram along with RO-20-1724 showed greater potency (10 - 100 fold) for displacing ³H-rolipram from the high affinity site than for inhibition of hPDE4A_{Livi}. Selectivity for competition at the high affinity site over PDE4 inhibition has also been shown for rolipram analogues in mouse brain (Koe et al 1990). This difference of rank order potency between displacement of ³H-

rolipram and inhibition of PDE4, along with the discrepancy between concentrations of rolipram needed to inhibit PDE activity over that needed to displace ^3H -rolipram, could indicate that the high affinity site has a function other than inhibition of catalysis. This idea can only be treated speculatively considering the differences of rolipram inhibition between the recombinant PDE4 and that isolated and purified from human monocytes. One argument for this could be that the groups necessary for high affinity binding are susceptible to cleavage upon the purification procedure. PDE4 isolated from U937 cells (DiSanto & Heaslip 1993, 1995) was shown to be activated by phosphatidic acid (5 - 50 $\mu\text{g} / \text{ml}$). This activation was inhibited by nM concentrations of rolipram which suggested that phosphatidic acid could be interacting with the high affinity rolipram binding site. However, the authors DiSanto and Heaslip (1995) could not detect any high affinity binding in crude, purified or stabilised U937 cells, whereas they could detect such in rat brain homogenates. Thus, the inability to detect high affinity binding seems unlikely to be associated with the purification of PDE4 from U937 cells. The ability of enantiomers of rolipram to show selectivity for the inhibition of PDE4 isolated from guinea pig eosinophils was effected by purification (Souness et al 1993), however, the authors could not detect high affinity binding of rolipram in either purified or crude cell samples.

(v) High Affinity Rolipram Binding Outwith the CNS

High affinity rolipram binding has been associated with stimulation of acid secretion in isolated rabbit gastric glands (Barnette et al 1995) and the accumulation of cyclic AMP in guinea pig eosinophils (Souness et al 1993).

In clinical trials which measured the efficacy of rolipram as an antidepressant, one of the side effects noted was gastrointestinal problems (Horowski & Sastre-Y-Hernandez 1985). PDE4 inhibitors were since found to inhibit cyclic AMP elevation in parietal cells which resulted in the stimulation of

acid secretion via PKA. This was shown to be similar to the acid secretion in response to histamine, an activator of cyclase (Choquet et al 1990). The ability of rolipram to increase acid secretion in isolated gastric glands has been correlated with binding to a high affinity rolipram binding site (Barnette et al 1995). Similar to the study with recombinant PDE4 (Torphy et al 1992), the (*R*)-rolipram enantiomer was more potent than the (*S*)-enantiomer for competition at the high affinity binding site and increase in acid secretion (Barnette et al 1995). (*R*)-rolipram was shown to displace ³H-rolipram with an IC₅₀ of 3nM, to increase acid secretion with an EC₅₀ of 4nM but the IC₅₀ for PDE4 inhibition in these cells was 1.4μM. Thus, there was an ~350 fold difference in the concentration of rolipram needed to compete for the high affinity site and that necessary for inhibition of substrate hydrolysis. However, there was little correlation between increase in acid secretion and PDE4 inhibition, which suggests, according to the author, that the functional effect of rolipram in this tissue is through an interaction with the rolipram high affinity site.

In explanation of this data and the anomolous kinetics observed with rolipram, Torphy et al (1992) and Barnette et al (1995) have suggested that catalysis and inhibitor binding occur at the same site, but that this site exists on two non-interconvertible forms of PDE4 which have similar affinities for cyclic AMP, as shown by the linear kinetics of cyclic AMP hydrolysis, but differ with respect to their inhibition by compounds such as rolipram or RO-20-1724 giving rise to the non-competitive inhibition observed.

In support of the theory by Barnette et al (1995) that the high affinity site is not involved in the inhibition of catalysis, a similar conclusion was reached by Schudt and Hatzelmann (1995). PDE4 isolated from human neutrophils was shown to have both high and low affinity binding components (Schudt and Hatzelmann 1995). Competition studies using ³H-rolipram or ³H-RP73401, a Rhône-Poulenc compound, in the presence of the Syntex compound RS25344 showed that high and low affinity K_i values could be

calculated for several PDE inhibitors. In conclusion of this study in neutrophils, the authors demonstrate that the low affinity binding and inhibition of catalysis are related, whereas high affinity binding and catalysis are not.

The accumulation of cyclic AMP in response to PDE4 inhibitors in guinea pig eosinophils is also thought to be through interaction with a high affinity rolipram binding site (Souness et al 1993). In this study (*R*)-rolipram was shown to inhibit solubilised PDE4 more potently than (*S*)-rolipram, and this stereoselectivity was only evident upon the solubilisation of the membrane bound form. Although high affinity rolipram binding sites could not be detected, the stereoselectivity shown by rolipram upon solubilisation of the enzyme suggested that a high affinity site similar to that detected by Torphy et al (1992) and Barnette et al (1995) was involved. The authors determined a correlation between the ability of PDE4 inhibitors to displace ³H-rolipram from binding sites on rat brain membranes, with the ability to inhibit catalysis of solubilised PDE4 from eosinophil membranes and with the stimulation of cyclic AMP accumulation in whole cells (Souness et al 1993). Souness et al (1993) suggest that upon solubilisation of eosinophil membranes a stereospecific site is exposed, which is similar to that detected in rat brain (Schneider et al 1986) and which allosterically regulates catalysis. Thus, in contrast to Torphy et al (1995), Souness et al (1993) suggest that the functional effect of rolipram on eosinophils, that is, cyclic AMP accumulation, is the result of the interaction of rolipram with a high affinity site and also to the catalytic site.

1.20 PDE7 High Affinity Cyclic AMP Specific PDE

This relatively recent class of cyclic AMP specific PDEs was originally cloned from a human glioblastoma cell line (Michaeli et al 1993). This study used a similar principle to that for the isolation of DPD (Colicelli et al 1989) and the yeast PDE2 gene (Sass et al 1986), where a *ras2 val19* mutation in the yeast expression system resulted in constitutively high cyclic AMP levels and rendered the yeast sensitive to heat shock (see section 1.11(ii) for details).

Michaeli et al (1993) took a slightly different approach in that cyclic AMP levels were elevated by deletion of both of the PDE genes present in *Saccharomyces cerevisiae* *PDE1* and *PDE2* and so the yeast were sensitive to heat shock.

The human gene isolated by this method, *HCP1*, encoded a PDE with significant homology to other cyclic AMP PDEs including the ~270 amino acid region proposed to contain the catalytic site (Chabonneau et al 1986, Chen et al 1986). However, upon biochemical analysis HCP1 activity displayed a high affinity for cyclic AMP (K_m 0.2 μ M), but was distinct from the PDE4 in that HCP1 was insensitive to inhibition by RO20-1724 or rolipram. HCP1 activity was also unaffected by cyclic GMP. Northern blot analysis showed that HCP1 was predominantly expressed in skeletal muscle with less activity expressed in heart and kidney.

PDE7 soluble PDE activity has also been isolated from hepatocytes which is insensitive to inhibition by IBMX and shows an aberrant response to Mg^{2+} , in contrast to PDE4 activity also present in hepatocytes which are activated dose-dependently by Mg^{2+} and Mn^{2+} (Lavan et al 1989).

The novel PDE7 class, their distribution and physiological role remains a topic under current investigation.

In conclusion, PDE4 family is one of great importance and has certain therapeutic potential as the target for specific inhibitors. However, to enable this a greater understanding of this enzyme class is needed, particularly concerning the kinetics of rolipram inhibition and the regulation of the enzyme class, which can be achieved through the study of cloned enzymes efficiently expressed in yeast and mammalian derived cell lines.

Table 1 **Expression of PKA Subtypes I and II**

Tissue	Subtype PKA Expressed Upon Stimulation With Hormone	
	<u>Type I</u>	<u>Type II</u>
Hepatocytes	Glucagon	---
Ovarian	---	HGH
Corpus Luteum	HGH	---
Osteoblasts	Parathyroid Hormone	Prostaglandin E ₂

HGH = Human Gonadotrophic Hormone

Table 1a **Comparison of Characteristics of *Drosophila dunc* PDE with RD1 and DPD**

Enzyme	K_m cyclic AMP (μM)	K_i (μM)	
		Rolipram	RO-20-1724
<i>dunc</i>	2	>100	>100
RD1	4.1 \pm 1.1	0.7 \pm 0.1	4.2 \pm 0.6
DPD	2.9 \pm 0.5	0.5 \pm 0.1	1.7 \pm 0.2

This data was from Henkel - Tigges and Davis 1989

Table 1b Detection of Human PDE4 in Human Tissues and Defined Cell Lines

	PDE4A	PDE4B	PDE4C	PDE4D
Brain	++	++	++	++
Liver	++	++	++	++
Lung	++	++	++	++
Trachea	++	++	++	++
Kidney	++	++	++	++
Placenta	++	++	++	++
Heart	++	++	++	++
Blood	++	++	-	++
U937 cells	++	++	-	++
Jurkat cells	++	-	-	-
Namalwa cells	++	++	-	-
Neutrophils	±	++	-	±
Eosinophils	++	++	-	++
Neuroblastoma cells	++	++	++	++

This data was taken from Engels et al 1994.

++ = expression

± = weak expression

- = no expression

Table 1c **Nomenclature for Rat PDE4 Species**

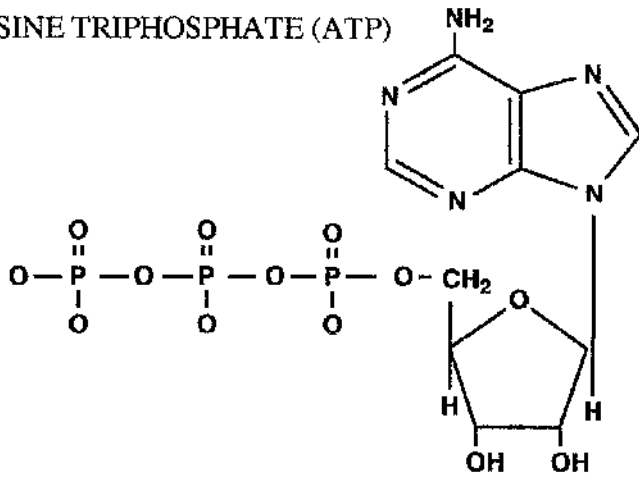
Present Nomenclature	Previous Nomenclature	Conti & Swinnen (1990) Nomenclature
4A	IVA	ratPDE2
4B	IVB	ratPDE4
4C	IVC	ratPDE1
4D	IVD	ratPDE3

Fig. 1.4.1

Reaction Scheme of Adenylyl Cyclase

The figure shows the reaction scheme of adenylyl cyclase with the conversion of adenosine triphosphate to 3'5' - cyclic AMP.

ADENOSINE TRIPHOSPHATE (ATP)



Adenyly cyclase
+ Mg²⁺

3'5' CYCLIC ADENOSINE
MONOPHOSPHATE

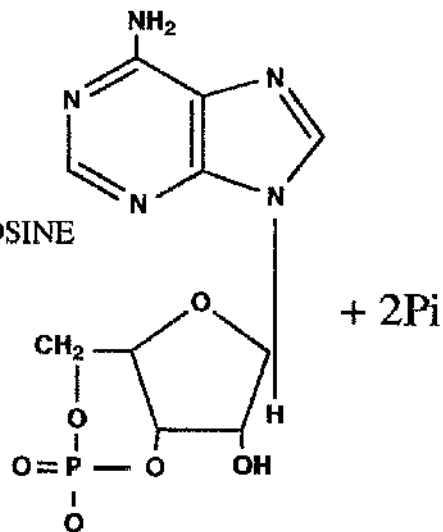


Fig. 1.4.2

Schematic of G-Protein Cycling

Binding of the agonist to the receptor causes dissociation of the beta-gamma complex from the activated alpha subunit, which has exchanged GDP for GTP. The alpha subunit is able to interact with such effector systems as adenylyl cyclase. The intrinsic GTPase activity of the alpha subunit switches off the signal via the hydrolysis of GTP to GDP. The GDP bound alpha subunit can reassociate with the beta-gamma complex.

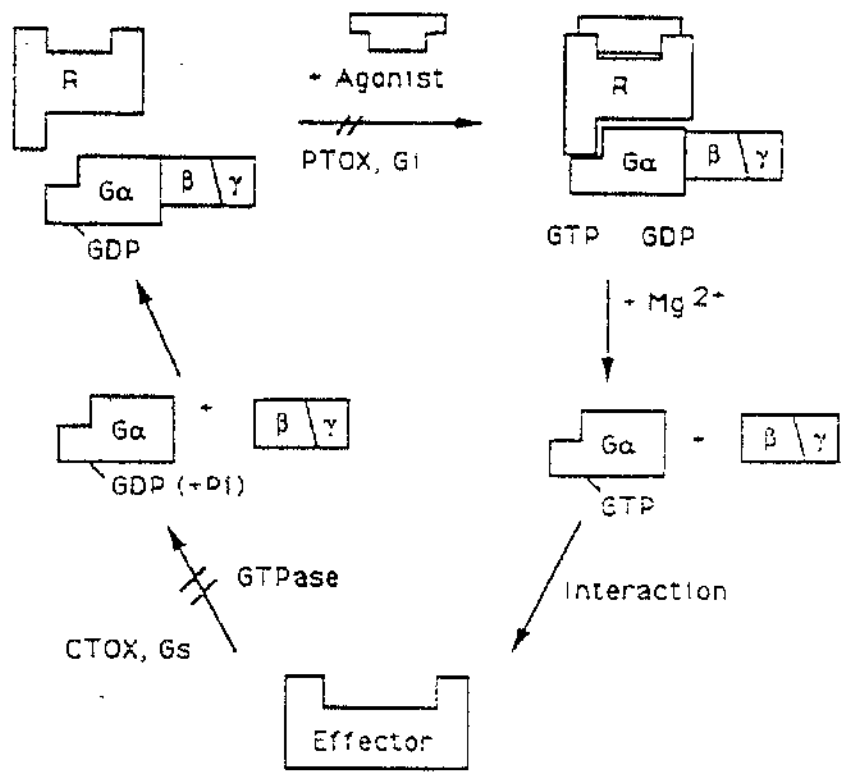
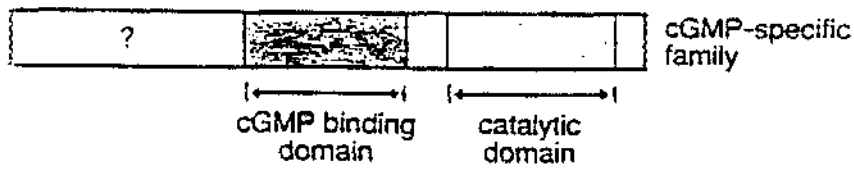
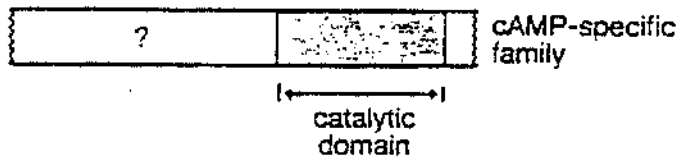
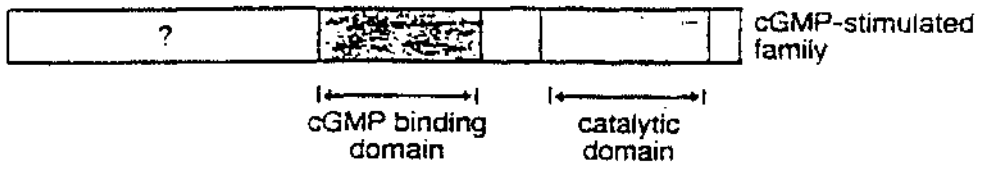
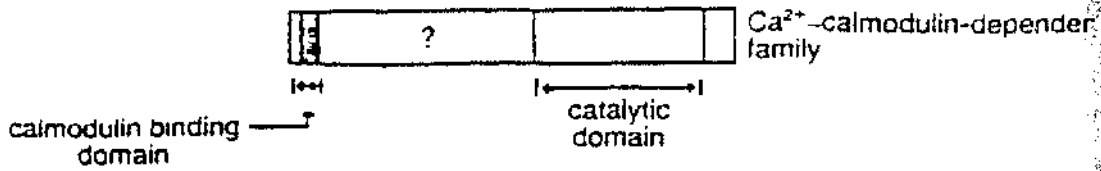


Fig. 1.10.3

**Schematic Alignment of Mammalian PDE
Isoform Families**

This figure diagrammatically shows the structural features of mammalian PDE isoforms. (Beavo & Reifsnyder 1990).



**Fig. 1.10.4 Schematic Representation of the Four Rat PDE
Genes**

Numbers at the right indicate the number of amino acid residues. The highly conserved region is shown by the unshaded area. The less homologous N and C terminal regions are shown by the shaded areas. Filled areas indicated by serine corresponds to the region which is homologous to the cyclic AMP binding domain of PKA. PDE4A, B, C and D isoforms correspond to ratPDE2, 4, 1 and 3 respectively. (Conti & Swinnen 1990).

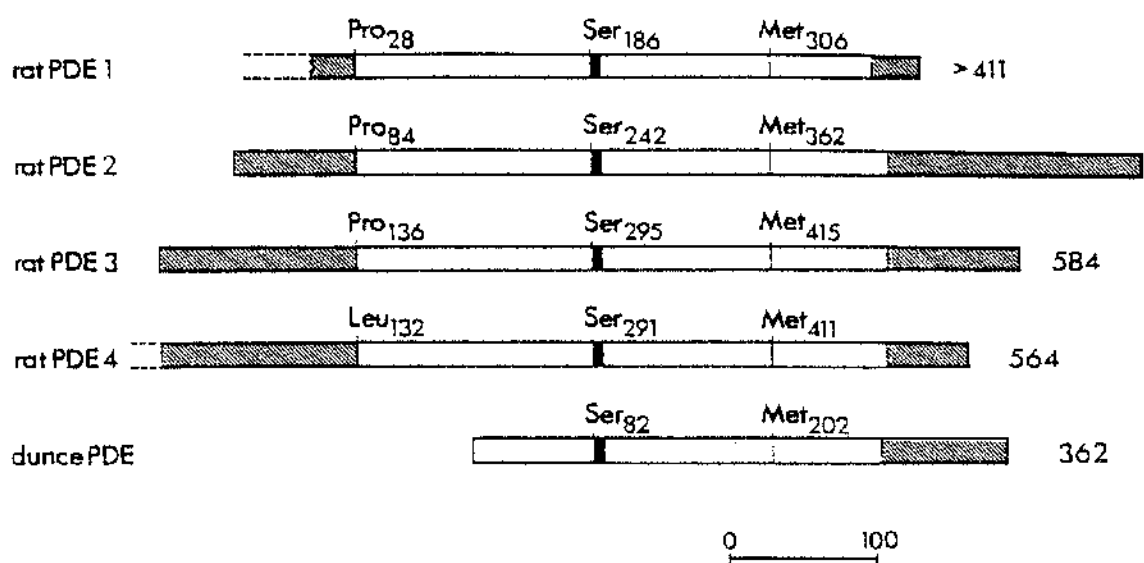
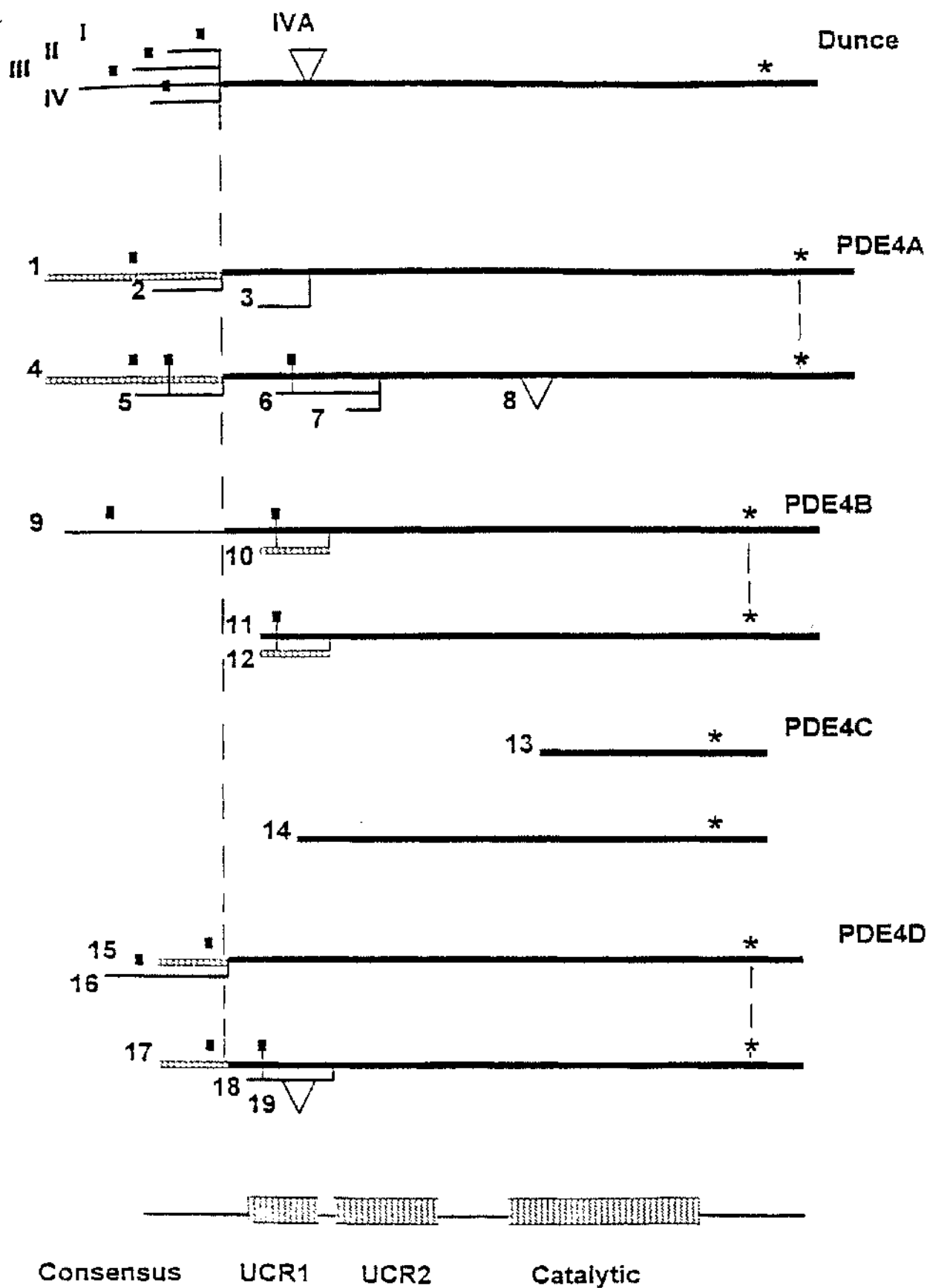


Fig. 1.13.5

Alignment of Human and Rat PDE4 mRNA

Shown is the schematic representation of the four human and rat PDE4 mRNA's, at the top and bottom respectively. Common sequences are shown by heavy merged lines. Areas of unique sequence which are conserved between human and rats, and are unique to any PDE4 subtype are shown by the thin cross hatched lines. Thin solid lines indicate variant sequence which is not conserved between human and rat. Triangles in the rat clones show variants lacking a block of sequence as compared to other transcripts from the same locus. Initiation codons are shown by small boxes and termination codons by *. Vertical dashed lines show splice points that occur in homologous positions in clones from different loci. Roman numerals show various alternative spliced isoforms from the *dunc* locus.

(Bolger et al 1993).



Chapter - 2

Materials and Methods

2. Materials and Methods.

2.1 Solutions

All solutions were prepared in double-distilled deionised water and all pH measurements were determined using an Horiba F.8L pH meter.

2.2 Chemicals

A list of the chemicals used and their suppliers are listed in appendix I.

2.3 Preparation of Soluble and Pellet Associated Enzyme From Yeast

A primary yeast cell culture was made by selecting an isolated yeast colony from a plate of yeast extract peptone dextrose (YPD) agar, using a sterile Eppendorf tip, which was placed into 50ml YPD liquid media and grown for 16 hours in a shaking incubator at 30°C. After this initial 16 hours of growth, the entire 50ml primary culture was used to inoculate 1L of YPD liquid media and grown for 20 hours, at 30°C in a shaking incubator. Following the 20 hour incubation, the cell suspension was centrifuged at 3200rpm (1000g_{av}) for 10 minutes in the Beckman J21 centrifuge with a JA20 rotor. Cell pellets were resuspended in 80mM Triethanolamine - HCl, 5mM MgCl₂ buffer pH 7.4 with KOH containing a mixture of protease inhibitors at a final concentration of 40µg/ml - PMSF, 156µg/ml benzamidine and 1µg/ml each of aprotonin, leupeptin, pepstatin A, and antipain. The protease inhibitors were initially dissolved as a 1000x stock in 100% DMSO before addition to the buffer. Cells were lysed by subjection to 4 passes through a French Pressure Cell Press (SLM Instruments Inc.) at 960 psi. The resultant lysate was centrifuged 48,000rpm (210,000g_{av}) for 45 minutes using the Ti50 rotor in a Beckmann ultracentrifuge. Aliquots of both pellet and supernatant were assayed for PDE activity immediately and residual material stored at -80°C for later analysis.

2.4 Phosphodiesterase Assay

Cyclic nucleotide phosphodiesterase activity was assayed by a modification of the two - step procedure of Thompson and Appleman (1971) and Rutten et al (1973) as described previously by Marchmont and Houslay (1980). Here ^3H -cyclic AMP (8- ^3H -adenosine 3'5'-cyclic phosphate) was diluted in 20mM Tris-HCl, 10mM MgCl_2 pH7.4 and the unlabelled cyclic AMP. 50 μl of this solution (approx. 0.2 μCi) was then added to the tubes containing 15-30 μg protein and the volume made up to 100 μl with 20mM Tris-HCl, 10mM MgCl_2 pH7.4. Samples were incubated at 30 $^\circ\text{C}$ for 10 minutes and boiled for 1 minute to terminate the reaction. The protein concentration used was shown to be within the linear range of the reaction of protein vs activity, as shown in fig 2.4.2. This figure demonstrates that, at 3 μM cyclic AMP, the reaction is linear over the range of 1 - 240 μg protein. That the reaction was linear, shows that substrate is not a limiting factor. To ensure that the 10 minute assay incubation time was in the linear range of the reaction, enzyme activity was assayed over the range of 1 - 10 minutes at 1 - 20 μM cyclic AMP (fig 2.4.1). This analysis showed that a 2 minute lag occurred initially, with the reaction becoming linear after this time.

After allowing the samples to cool, 25 μg of snake venom (Ophiphagus hannah-cobra, 1mg/ml in 20mM Tris-HCl, 10mM MgCl_2 pH7.4) was added, and the samples were incubated again at 30 $^\circ\text{C}$ for 10 minutes. 400 μl of a freshly prepared slurry of Dowex:H $_2$ O:ethanol (1:1:1) was then added, and following incubation on ice for 30 minutes, the samples were centrifuged at 12,000 rpm for 3 minutes in a Jouan MR1812 bench centrifuge. 150 μl of supernatant was then removed into 2ml of 'Ecoscint' scintillation fluid. The amount of ^3H -adenosine present was determined by counting on an LKB scintillation counter. A diagram describing the PDE assay reaction scheme is shown in figure 2.4.3.

For estimation of kinetic parameters, the PDE assays were conducted using cyclic nucleotide concentrations ranging from 0.05 μM -

100 μ M. In order to calculate K_m values, the data were fitted to the Michaelis Menton equation $V_{obs} = (V_{max}[\text{cyclic AMP}] / (K_m + [\text{cyclic AMP}]))$ using the Ultrafit graphical package. This non-linear fitting programme obviates errors in fitting to the Lineweaver-Burke plot using regression analysis, where the spread of errors is not evenly distributed as it is a double-reciprocal plot. In each case, the 'robust weighting' facility was used and the 'goodness of fit' index was no less than 0.99 with each estimation, 1 being a perfect fit..

Inhibitor analysis was performed with 3 μ M cAMP as substrate over a range of inhibitor concentrations as shown in the appropriate figures. PDE inhibitors were dissolved in 100% DMSO as a 10mM stock and diluted in 20mM Tris - HCl 10mM MgCl₂ pH7.4 to provide a range of concentrations for use in the assay. Inhibitors were added at a volume of 25 μ l, which was included in the assay volume of 100 μ l. As such, a 4 times final inhibitor concentration was prepared, of which, 25 μ l was added to the reaction. For each inhibitor, a DMSO control was included in the assay which contained the highest DMSO concentration used. In each case, the DMSO concentration was shown to have no effect.

2.5 Thermal Denaturation.

Pellet and soluble fractions were prepared as described. Each sample was pipetted into pre - warmed 20mM Tris - HCl 10mM MgCl₂ pH7.4 contained in a glass bijoux which had been placed on a stirrer in a water bath set at the temperature for the particular experiment. At the time points shown on the appropriate figure a 100 μ l sample was removed and placed in an Eppendorf microfuge tube which had been kept on ice. PDE activities were then measured at 1 μ M cAMP in the assay mixture described above in section 2.4.

2.6 Protein Determination

Protein was measured by the method of Bradford (1976). Standard solutions of bovine serum albumin were prepared in the range of 0-100 μ g in distilled water. The unknown samples were solubilised by the

addition of 0.2% Triton X-100 and left on ice for 30 minutes. The standard and unknown protein solutions were made up to a volume of 800 μ l with distilled water before the addition of 200 μ l of Bradford reagent. Absorbances were determined at 595nm using an LKB spectrophotometers and the unknown concentrations determined from the standard curve.

2.7 Preparation of Synaptosomes

The method detailed here is as described in Dunkley et al (1988).

i) Tissue preparation

Brain tissue (~1g) was removed from freshly sacrificed adult male Sprague-Dawley rats and placed in ice cold gradient buffer containing 0.32M sucrose, 1mM EDTA and 0.25mM dithiothreitol pH7.4. The tissue was then roughly chopped and homogenised in 10 volumes of gradient buffer using 10 passes at 700rpm (Janke & Kunkel IKA-Labortechnik RW20). Homogenate was then filtered through two layers of guaze before centrifugation at 3200rpm (1000g) for 10 minutes in the Beckman J21 centrifuge with a JA20 rotor. This post nuclear supernatant (S1) was loaded onto the step gradients.

ii) Percoll-Sucrose Solutions

Solutions of 23%, 15%, 10% and 3% Percoll (density 1.129g/l) were made up in gradient buffer and adjusted to pH7.4 with HCl or NaOH before use. Volumes of 2ml of each of the Percoll-Sucrose solutions were layered in 15ml corex tubes using an LKB 2232 Microperspex S peristaltic pump. A 2ml volume of the S1 fraction was then layered onto the gradients which were centrifuged at 20,000rpm (32,500g) for exactly 5 minutes in a Beckmann J21 centrifuge with the JA20 fixed angle head.

iii) Fraction Collection

Interfacial fractions, 4 bands and a pellet, were collected using a pastuer pipette and pooled from each gradient. Fractions were washed twice by resuspension in 10ml gradient buffer and centrifuged for 15 minutes at

13,800rpm (15,000g) using the Beckmann JA20 rotor in the J21 centrifuge. After this final stage the fractions were resuspended in 0.6ml gradient buffer with the exception of experiments where the synaptosomal fractions were hypotonically shocked to prepare pellet and soluble fractions. The hypotonic buffer was the same as the gradient buffer except it did not contain 0.32M sucrose. Protease inhibitor cocktail containing a mixture of protease inhibitors at a final concentration of 40µg/ml - PMSE, 156µg/ml benzamidine and 1µg/ml each of aprotonin, leupeptin, pepstatin A, and antipain was added to the buffer. The protease inhibitors were initially dissolved as a 1000x stock in 100% DMSO before addition to the buffer. The lysate was then centrifuged 48,000rpm for 45 minutes in a Beckmann ultracentrifuge using the TL-100 rotor. The resultant pellet was resuspended in a suitable volume of gradient buffer. All fractions were then aliquoted, frozen in liquid nitrogen and stored at -80°C.

2.8 Subcellular Fractionation of Synaptosomes by Continuous Sucrose Gradients

Subcellular fractionation was carried out essentially as per Shakur et al (1993).

i) Cell Lysis

Synaptosomal fractions were prepared as in chapter section 2.7 iii) except at the final resuspension stage where fractions 2,3 and 4 were pooled and resuspended in 1ml of lysis buffer pH8.1 containing 5mM Tris-HCl and 50µM calcium chloride. Lysate was left on ice for 45 minutes before rehomogenisation and centrifugation at 2000rpm in a Jouan MR1812 bench centrifuge to give a post-nuclear supernatant.

ii) Preparation of Membranes

Gradients were layered using an LKB 2232 Microperspex S peristaltic pump. Post-nuclear supernatant (~1ml) was loaded onto a gradient consisting of 3ml 0.5M sucrose layered onto 1ml of 1.6M sucrose, and

centrifuged 50,000rpm for 30 minutes using an SW55 swing out rotor. Membranes were harvested at the 0.5M/1.6M interface. Solid sucrose was then added to the membranes to give a concentration of >1.6M. All sucrose solutions were made up in lysis buffer (see chapter section 2.8 i) for recipe).

iii) Continuous Sucrose Gradient

A continuous gradient of 0.6M - 1.6M sucrose was prepared using a gradient mixer. Membranes were loaded into the bottom of the tube and centrifuged at 50,000rpm for 18 hours in the SW55 rotor. Samples were collected in 200µl aliquots using the peristaltic pump, frozen in liquid nitrogen and stored at -80°C.

2.9 Acetylcholinesterase Assay

Acetylcholinesterase hydrolyses acetylthiocholine to produce a thiol which exchanges with 5,5'-dithiobis-2nitrobenzoate (DTNB). This compound is yellow and can be measured by following the change in the optical density at 412nm. This method was as described by Ellman et al (1961).

Briefly, activity was measured using the following method. For this experiment an LKB spectrophotometer set at 412nm was linked to a chart recorder. Solutions containing 100µl tissue sample (0.5-2.5mg/ml protein) and 2.7ml of 0.1M phosphate buffer pH8 were set up in 4ml glass tubes and incubated at 37°C for 30 minutes. Solutions were then cooled to room temperature. 0.1ml of 10mM 5,5'-dithiobis-2nitrobenzoate in phosphate buffer and 0.1ml of 15mM acetylthiocholine iodide were then added to the tubes and mixed rapidly. The trace was followed for several minutes.

Activity was calculated using the following:

Molar extinction coefficient = 1.36×10^4

p = protein concentration in mg/ml

Activity = $\frac{\text{Abs. units/min} \times \text{Cuvette vol.} \times 1 \times 10^3}{1.36 \times 10^4 \times \text{Sample vol.} \times p}$

$= \mu\text{moles/min/mg}$

2.10 Lactate Dehydrogenase Assay

Lactate dehydrogenase activity was measured as described by Marchbanks (1967). Enzyme activity was measured by the rate of oxidation of NADH which absorbs at a wavelength 340nm therefore, the rate of decrease of optical density at 340nm is a measure of enzyme activity. Briefly, 1.35ml of 0.15M Tris/HCl pH7.4 and 50 μ l of each 10mM sodium pyruvate and tissue sample were added to a 1.5ml cuvette and used to zero a spectrophotometer set at 340nm and linked to a pen recorder. Free lactate dehydrogenase activity was measured by the addition of 50 μ l of 2mM β -NADH and the trace followed for several minutes. Finally 10% Triton/tris was then added to the cuvette to release entrapped activity and the total activity was calculated from this trace.

Lactate dehydrogenase activity was then calculated using the following:

Occluded lactate dehydrogenase = Total - Free

Molar extinction coefficient = 6.22×10^3

p = protein concentration in mg/ml

Activity = $\frac{\text{Abs. units/min.} \times \text{Cuvette vol.} \times 1 \times 10^3}{6.22 \times 10^3 \text{ Sample vol. } p}$

$\frac{6.22 \times 10^3 \text{ Sample vol. } p}{6.22 \times 10^3 \text{ Sample vol. } p}$

= nmoles/min/mg protein

2.11 5'-nucleotidase Assay

The activity of 5'-nucleotidase was assayed according to the protocol detailed by Newby et al (1975) which was a modification of the radioassay of Avruch (1971).

5'-nucleotidase activity was measured by the release of ^3H -adenosine from ^3H -AMP. Reactions were set up in a 500 μ l volume containing a substrate solution of 200 μ M AMP 'spiked' with 3 μ l/ml of tritiated nucleotide which gave ~25,000 c.p.m. The volume was made up to 500 μ l with 50mM Tris-HCl pH8.0 buffer. Reactions were initiated with the addition of 10 μ l of particulate fraction and incubated for 15 minutes at 37°C, and then terminated

by the addition of 100 μ l of 0.15M ZnSO₄ and subsequently 100 μ l of 0.15M Ba(OH)₂. Samples were then centrifuged for 5 minutes at 12,000rpm in a Jouan MR1812 bench centrifuge. 500 μ l of supernatant was then added to 5ml of 'Ecoscint' and radioactivity was determined in an LKB scintillation counter.

2.12 Assay of Adenylate Cyclase Activity

Adenylate cyclase (E.C. 4.6.1.1) activity was measured as described by Houslay et al (1976). Here an assay cocktail was prepared consisting of an ATP-regenerating system (1.5mM ATP, 7.4mg/ml creatine phosphate, 0.2mg/ml creatine kinase and 0.8mg/ml BSA) in a buffer of 25mM triethanolamine, 5mM MgSO₄, 10mM theophylline, 1mM EDTA and 1mM dithiothreitol, pH7.4. Drugs and membranes (20 - 100 μ g) were then added as appropriate to give a final assay volume of 100 μ l.

Samples were then incubated at 30°C for 10 minutes, and the reaction was terminated by boiling for 2 minutes. The precipitated protein was pelleted by centrifugation for 5 minutes at 12,000rpm in a Jouan MR1812 bench centrifuge and the supernatants were then removed for cyclic AMP determination (see chapter section 2.13).

2.13 Cyclic AMP Determination

Determination of cyclic AMP content was based on the saturation assay of Brown et al (1972) as described by Whetton et al (1983).

This assay depends upon the specific binding ability of the cyclic AMP nucleotide to a cyclic AMP binding protein isolated and purified from bovine adrenal glands (see chapter section 2.14). Samples and binding protein are incubated together until equilibrium occurs and bound cyclic AMP is then separated from unbound by the use of a charcoal/BSA suspension. The charcoal absorbs free nucleotides and therefore estimation of ³H-cyclic AMP bound to the protein can be made.

Using a range of known cyclic AMP concentrations, it is possible to construct a standard displacement curve from which estimations of

cyclic AMP content can be made. This is done by incubating increasing amounts of unlabelled cyclic AMP with a fixed amount of the tritiated nucleotide and binding protein. The portion of cyclic AMP can in this way be reduced, as the unlabelled and tritiated species compete for a finite number of binding sites on the protein.

Total cyclic AMP binding to the protein was determined by incubating the tritiated cyclic AMP in the absence of the unlabelled species, whilst non-specific binding is estimated by the incubation of tritiated cyclic AMP in the absence of binding protein as well as unlabelled cyclic AMP.

For the assay, a series of unlabelled cyclic AMP solutions were prepared ranging from 0-320 pmoles ml⁻¹. This was done by dissolving cyclic AMP in a buffer containing 50mM Tris/5mM EDTA pH7.4. Tritiated cyclic AMP (5.8-³H-adenosine 3'5' cyclic phosphate) in 50% ethanol was diluted in this Tris/EDTA buffer to give approximately 500,000cpm/ml. 100μl of this solution was added to tubes containing 50μl each of assay buffer, standard cyclic AMP solution or supernatant from the unknown samples. After mixing, 100μl of binding protein was added to the samples which were mixed again. Following incubation at 4°C for 2 hours, the binding reaction was terminated by the addition of 0.25ml of a BSA/charcoal suspension. This solution consisted of 2% GSX-100 charcoal and 1% BSA suspended in ice cold assay buffer. The charcoal was pelleted from the samples by centrifugation for 5 minutes at 12,000rpm in a Jouan MR1812 bench centrifuge at 4°C. 400μl of supernatant was removed into 'Ecoscint' scintillation fluid, and the samples counted in an LKB scintillation counter. This counter had an RIA curve fitting programme which produced a standard curve (described above) by plotting cpm of standard sample vs pmol cyclic AMP. Cyclic AMP content in the unknown samples was automatically calculated from the standard curve. The binding assay gave optimum sensitivity between 0.25 and 8 pmoles/sample.

2.14 Preparation of Cyclic AMP Binding Protein from Bovine

Adrenal Glands

The buffer used throughout this procedure contained 250mM sucrose, 25mM KCl, 5mM MgSO₄ and 50mM Tris-HCl pH 7.4 and all operations were performed at 4°C.

i) Dissection

Approximately 30 fresh bovine adrenal glands were used. The surrounding fat was removed and the gland was opened to lie flat. Medulla area (pale brown/pink) was removed by gently scraping with a scalpel. The darker cortex area was retained and the coating of connective tissue was removed from it.

ii) Homogenisation

Tissue was homogenised in 200ml of buffer in a Waring blender.

iii) Centrifugation

Homogenate was filtered through two layers of muslin, which was washed in a small volume of buffer, and centrifuged at 15,000rpm in a JA20 rotor at 4°C for 15 minutes. Supernatant was decanted through filter paper, aliquoted and stored at -20°C.

2.15 SDS-PAGE Electrophoresis

Separation of proteins by electrophoresis was carried out in 10% polyacrylamide gel slabs as described by Laemmli (1970).

Samples (100µg protein) were dissolved in 20µl of Laemmli loading buffer containing 5M urea, 0.18M SDS, 0.38M dithiothreitol, 0.05M Tris/HCl pH8 and bromophenol blue as the tracking dye and boiled for 5 minutes. Electrophoresis was carried out in a 'running buffer' of 0.025M Tris/HCl, 0.19M glycine and 0.0035M SDS. When the dye front reached the edge of the gel electrophoresis was stopped and the proteins transferred to nitrocellulose (see chapter section 2.16)

2.16 Western Blotting

Proteins were transferred from the polyacrylamide gel to nitrocellulose 100% setting for 2 hours in a transblot apparatus (Hoefer Instruments). This method is essentially as detailed by Huff et al (1985). The 'blotting buffer' used here contained 0.025M Tris with 0.19M glycine/methanol (4:1 v/v).

The nitrocellulose was then incubated in 20mM Tris/HCl pH7.5 with 500mM NaCl (ie TBS) and 5% dried milk powder for 2 hours at room temperature. This stage blocks any non-specific protein binding. After 2 hours the 5% dried milk powder/TBS was poured off and the nitrocellulose washed briefly with distilled water before washing twice with TBS containing 0.2% Nonident P40 and twice with TBS each for 5 minutes. The nitrocellulose was then immunoblotted with TBS containing 1% dried milk powder and a 1:500 dilution of the appropriate antisera for 2 hours.

The antisera used in these experiments was 271 which was generated in rabbits against a peptide corresponding to the last 12 amino acids of the RD1 protein ((C)-T-P-G-R-W-G-S-G-G-D-P-A). RD1 (rat '*dunc*-like' cyclic AMP phosphodiesterase) is a type-IVA PDE which was cloned by homology from a rat brain cDNA library using the drosophola *dunc* PDE cDNA as a probe (Davis et al 1989). The peptide was conjugated with keyhole limpet haemocyanin (KLH) facilitated by the synthesis of a cysteine residue at the N terminus of the peptide, according to the procedure of Lerner (1981).

After immunoblotting the nitrocellulose was washed as before and incubated for 2 hours in TBS with 1% dried milk powder plus 10µl of anti-rabbit peroxidase linked IgG. The nitrocellulose was then washed 4 times for 5 minutes each in TBS and labelled bands were detected using the Amersham ECL Western Blotting visualisation protocol.

2.17 Concentration of Protein Samples

If the samples to be used for Western Blotting were too dilute the following precipitation protocol was followed. 100% trichloroacetic acid was added to the samples to give a final concentration of 20%. Samples were left on ice for 10 minutes before centrifugation for 5 minutes at 12,000rpm in a Jouan MR1812 bench centrifuge. Supernatant was discarded and 20 μ l of ice cold 1M Tris-base plus 20 μ l of Laemmli loading buffer (see chapter section 2.15) were added to the samples prior to boiling for 5 minutes.

Results Chapter - 3

Characterisation of Human PDE4A h6.1

3.1 Introduction

The first PDE4 cDNA to be isolated was for the *Drosophila dunc* enzyme (Chen et al 1986). Subsequent studies used this cDNA to probe mammalian cDNA libraries for PDE4 isoforms from rat (Davis 1990, Conti et al 1990, 1991) and human (Livi et al 1990, McHale et al 1991, Bolger et al 1993, Sullivan et al 1994).

The PDE cDNA clone h6.1 (Sullivan et al 1994) described in this chapter was isolated from a human T-lymphocyte cDNA library using a PDE specific probe. This probe was generated by pcr using primers based on the published sequence of hPDE4A_{Livi} (Livi et al 1990), a PDE4A isoform isolated from human monocytes. The pcr primers were for a highly conserved region representing part of the catalytic domain of hPDE4A_{Livi}. This identified two overlapping clones which represented a PDE4 similar to that isolated by Livi et al (1990), but lacked the first 13 amino acids. These first 13 amino acids of hPDE4A_{Livi} were engineered onto the sequence of h6.1 to provide an open reading frame as per that seen in the Livi et al (1990) clone.

Expression of h6.1 was enabled by engineering the cDNA for integration into the genome under the transcriptional control of a constitutive yeast promoter at the *pep4* locus (see Sullivan et al 1994 for details). This was done in a strain of *Saccharomyces cerevisiae* which did not express either of the two endogenous yeast PDE genes. Yeast strains rendered *pde-1/pde-2* display the heat shock phenotype, due to elevated cyclic AMP levels, previously described (section 1.11(ii)). *Saccharomyces cerevisiae* strains *pde-1/pde-2* expressing the h6.1 cDNA clone, strain YMS 6, were shown to be insensitive to heat shock, whereas the *pde-1/pde-2* untransformed control strain YMS 5 did not, therefore it was concluded that the h6.1 cDNA encoded a functional PDE.

Expression of h6.1 in yeast provided an available source of PDE that could be analysed in detail, in a manner which has not previously been

reported for a PDE4 isoform. The emphasis here is on defining the mechanism of inhibition by the PDE4 specific inhibitor rolipram. Previously published data have suggested that the mechanism of rolipram inhibition may be anomalous (McLaughlin et al 1993, Bolger et al 1993). In particular, the studies on the monocytic PDE hPDE4A_{Livi} which appeared to show that the inhibition by rolipram did not comply with simple competitive inhibition. Detailed discussion of the possible sources for this anomalous behaviour is given in chapter 1 section 1.19, which relate to a rolipram binding site distinct from the catalytic site.

This chapter describes the characterisation of a PDE4A isoform h6.1 (proposed GeneBank descriptor HSPDE4A7, accession number U18087). It reports on the kinetics of substrate hydrolysis, the kinetics of inhibition by the PDE4 selective inhibitor rolipram and the non-selective inhibitor IBMX, inhibitor profile to other PDE inhibitors, thermostability, and divalent cation dependency.

3.2

Results

(i) Activity of Yeast Cell Lysates Expressing h6.1 and Yeast Cell Lysate Expressing Control Yeast Strain YMS5

Cell homogenates of the control yeast strain YMS5 and the yeast strain expressing h6.1, YMS6, were disrupted by means of a cell press and assayed for PDE activity at the substrate concentration of $1\mu\text{M}$ cyclic AMP. Control strain cell lysate YMS5 failed to hydrolyse cyclic AMP, whereas YMS6 cell lysate hydrolysed cyclic AMP with specific activity of 5 - 9 pmol cyclic AMP /min / mg over a range of 25 separate preparations.

Characteristically h6.1 behaved as a PDE of the PDE4 isoform class. The cyclic AMP hydrolysing activity of h6.1 was unaffected by the addition of calcium/calmodulin (20ng/ml), low concentration of cyclic GMP ($10\mu\text{M}$) and was unable to utilise cyclic GMP as a substrate (<1% activity seen with cyclic AMP).

(ii) Location of h6.1 to the Pellet or Soluble Fraction of YMS 6 Lysates

Disrupted cell homogenates were centrifuged $210,000g_{\text{AV}}$ for 45min, after which the pellet and supernatant fractions were assayed for PDE activity at a substrate concentration of $1\mu\text{M}$ cyclic AMP. Over a range of 25 observations it was noted that between 22 - 48% of the total PDE activity was present in the supernatant fraction, the residual activity being in the pellet. Specific activities were shown to range from 16.5 - 34.4 pmol cyclic AMP /min / mg for the pellet fraction, and 2.1 - 6.3 pmol cyclic AMP /min / mg for the soluble fraction, over a range of 25 observations. The considerable activity present in the pellet was not removed by recentrifugation or made soluble with either TX100, used over the range (0.1% - 2%) or sodium chloride used at a range of 0.5M - 2M.

(iii) Thermostability of Pellet and Soluble h6.1

The thermostability of both pellet and soluble h6.1 was assessed at 45°C and 50°C. In each case the pellet and soluble forms of h6.1 decayed as a single exponential yielding linear semi-log plots of residual activity against time (fig 3.2.1). At both temperatures studied the pellet form of h6.1 was considerably more stable with $t_{0.5}$ values of >30 minutes and 20 minutes for 45°C and 50°C respectively. The $t_{0.5}$ values calculated for the soluble form were 10 minutes and 2 minutes for the temperatures 45°C and 50°C respectively.

(iv) Bivalent cation Dependency

Addition of the chelating agent EDTA in the PDE assay medium (Mg^{2+} free) resulted in the dose-dependent inhibition of PDE activity. The ability of magnesium chloride, manganese chloride, and calcium chloride to reactivate the PDE activity was assessed (fig 3.2.2). Both magnesium and manganese chloride were able to activate native PDE activity and reactivate PDE activity in the presence of 0.25mM EDTA. However, calcium inhibited the native PDE activity (fig 3.2.2, table 2).

(v) Kinetics of Cyclic AMP Hydrolysis by h6.1

The K_m value for the hydrolysis of cyclic AMP by both the soluble and pellet forms of h6.1 were determined from Lineweaver-Burke plots (fig 3.2.3). In each instance, the double-reciprocal plots of initial rate versus cyclic AMP concentration for h6.1 activity were linear over a wide substrate concentration range of 0.05 - 100 μ M cyclic AMP and displayed simple saturation kinetics. In order to calculate K_m values, the data were fitted to the Michaelis Menton equation $V_{Obs} = (V_{max}[cyclic\ AMP] / (K_m + [cyclic\ AMP]))$ using the Ultrafit graphical package. This non-linear fitting programme obviates errors in fitting to the Lineweaver-Burke plot using regression analysis, where the spread of errors is not evenly distributed as it is a double-reciprocal plot. In each case, the 'robust weighting' facility was used and the 'goodness of fit' index was no less than 0.99 with each estimation, 1 being a perfect fit. This

analysis yielded K_m values of $4.1 \pm 1.7 \mu\text{M}$ for the soluble form and $5.2 \pm 1.5 \mu\text{M}$ for the pellet form of h6.1 ($n=6$ in each case).

(vi) Inhibitor Profile of h6.1

The ability of PDE4 selective compounds rolipram and RO-20-1724, the non-selective compound IBMX and the PDE3 selective compound cilostimide to inhibit substrate hydrolysis of h6.1 activity was assessed. The substrate concentration used in these experiments was $3 \mu\text{M}$, a concentration which reflects that of the K_m value.

The inhibitor profile for h6.1 was typical of a PDE4 isoform, where substrate hydrolysis was more potently inhibited with rolipram (fig. 3.2.4., table 3) and RO-20-1724 (fig. 3.2.5, table 3) than IBMX (fig. 3.2.6, table 3) or cilostimide (fig. 3.2.7, table 3). IC_{50} values (concentration of inhibitor which produced 50% reduction in substrate hydrolysis) were then calculated for each compound from the dose response curves, and K_i (inhibition constant) was calculated by application of the Cheng-Prusoff equation (Cheng and Prusoff 1973) $K_i = IC_{50} / 1 + (S / K_m)$, which assumes competitive inhibition (table 3).

(vii) Kinetics of Inhibition of h6.1 by IBMX and Rolipram

Both the soluble and pellet fractions of h6.1 were competitively inhibited by rolipram (fig. 3.2.8). This was determined from the double-reciprocal plots (fig. 3.2.8) of h6.1 activity versus cyclic AMP concentration in the presence of increasing inhibitor concentration. These Lineweaver-Burke plots and the slope and Dixon (1953) replots of these data (figs. 3.2.8, 3.2.9, 3.2.10) remained linear over a wide range of substrate and inhibitor concentrations, indicative of simple competitive inhibition.

Similarly, IBMX was shown to be a simple competitive inhibitor of the pellet form of h6.1 as shown in the linear Lineweaver-Burke plots (fig. 3.2.11); slope and Dixon replots (fig. 3.2.12, 3.2.13).

The relationship between increasing protein concentration and PDE activity was also shown to be linear, even in the presence of rolipram at a

concentration which gave half-maximal inhibition of activity (fig. 3.2.14). This demonstrates that rolipram is not a tight-binding inhibitor of h6.1.

3.3

Conclusions and Discussion

PDE h6.1 can be characterised as belonging to the PDE4 isoenzyme family. This was evident from the specificity and high affinity for cyclic AMP as substrate (3.2.v, fig 3.2.3). Also, that the hydrolysis of cyclic AMP was unaffected by either calcium / calmodulin or low concentrations of cyclic GMP (3.2.i), further confirms h6.1 as belonging to the PDE4 class. The inhibitor profile of h6.1 was also typical for a PDE of the PDE4 class, in particular the sensitivity to rolipram and RO-20-1724 (table 3, figs 3.2.4, 3.2.5). PDE h6.1 also shares sequence similarities and biochemical characteristics of other PDE4 isoforms, in particular RD1. This suggests that h6.1 can therefore be classified as a member of the PDE4A subclass (Sullivan et al 1994).

The present study showed that h6.1 was present in both the pellet and soluble fractions of YMS6 cell lysates. However, in COS-1 cells (Sullivan et al 1994), h6.1 was present only in the cytosol. Comparison of h6.1 expressed in both yeast and COS-1 cells (table 4) show similar K_M values for cyclic AMP hydrolysis and more importantly, similar IC_{50} and K_i values for inhibition by rolipram. Furthermore, the present study also shows that the pellet and soluble forms of the enzyme are identical with respect to substrate hydrolysis and inhibitor profile, and differ only in their thermostability (table 3). This suggests that the catalytic activity and the inhibitor binding of the pellet insoluble fraction in yeast was unaffected by its location within the cell. Both the soluble and pellet forms of h6.1 activity decayed as a single exponential, suggesting a homogeneous population of enzyme. However, the pellet form was more stable (fig 3.2.1, table 3). Thus, whatever caused h6.1 to become pellet associated in yeast did not affect enzyme activity, but did constrain the enzyme in such a way as to resist thermal denaturation. The pellet form of h6.1 was unaffected by treatment with either TX100 or NaCl. Therefore, h6.1 is not an integral membrane protein or a peripherally bound enzyme but simply

formed an insoluble complex in yeast as a result of its overexpression. Alternatively, the pellet form of the enzyme could have been composed of yeast which had not been properly lysed. Therefore, the pellet associated enzyme could have formed a 'leaky' complex into which cyclic AMP could enter and access PDE. It is likely that the soluble form represents that of the native enzyme because in COS-1 cells h6.1 is exclusively cytosolic.

An engineered version of h6.1, called h6.1_{his5}, was purified by Dr Neil Brown. PDE h6.1_{his5} was engineered with 5 histidine residues to provide a zinc binding motif at the C-terminal end and allow purification by binding specifically to a nickel chelate column. Using this purification procedure a single peak of protein of 74kDa \pm 3 was isolated. This was comparable with the value obtained using a crude soluble fraction of native h6.1 (73kDa \pm 3) and the single protein band observed on a non denaturing gel (73kDa \pm 2). The molecular size determined for h6.1 was as predicted from the DNA sequence. This data was consistent with the observation from the thermostability studies (3.2.1, table 3) in which it was determined that soluble h6.1 was expressed as a single population of enzyme species and not as the product of proteolysis.

Dependency on the presence of bivalent cations for PDE activity has been previously observed by other investigators (Grant & Colman 1984, Lavan et al 1989). This study has shown that treatment of h6.1 with EDTA rendered the PDE inactive which could be overcome in a dose-dependent fashion by either Mg²⁺ or Mn²⁺ (fig 3.2.2, table 2). This suggests that there is a distinct negatively charged site within the PDE active site to which cations bind and enhance substrate hydrolysis. Indeed, Francis et al (1994) have noted a conserved motif in all PDEs, Hx₃Hx-20E, which is thought to function as a zinc binding site and is essential for activity. Of interest, Pyne and coworkers have shown that the inhibitory effect of zaprinast on PDE5 could be due to its ability to chelate zinc (Beavo et al 1994). This bivalent cation binding site on

PDE4 could also be important for inhibitor binding, for it has been reported that the ability of ^3H -rolipram to bind to sites on rat brain membranes is dependant on the presence of divalent cations (Schneider et al 1986). However, it is not simply the case that the more electro-positive an element then the more potent it will be as an activator of PDE activity because Ca^{2+} , which is more electropositive than either Mg^{2+} or Mn^{2+} , dose-dependently inhibited PDE activity.

PDE inhibitors have been developed on the basis of analogy to cyclic AMP. This would suggest that all inhibitors would be competitive against substrate hydrolysis, however, if such an inhibitor was found to be tight binding then it can be expected that anomolous kinetics may occur as a result. Fig. 3.2.14, shows a linear relationship between protein concentration and h6.1 activity in the presence and absence of rolipram, which demonstrates that rolipram is not a tight binding inhibitor.

The mechanism of inhibition by rolipram of PDE4 is one of the least understood aspects of this family of enzymes. It has been suggested on the basis of dose-response curves of PDE4 that the kinetics of rolipram inhibition may be anomolous (McLaughlin et al 1993, Bolger et al 1993). Although analyses of rolipram inhibition have been so far basic, it has been demonstrated that several orders of magnitude (3 log orders in the case of h6.1 (fig 3.2.4, table 3)) are necessary to completely inhibit the enzyme. In addition, kinetic studies on hPDE4A_{Livi} was reported not to fit to simple competitive inhibition (Livi et al 1990). Clearly, rigorous analysis of the kinetics of rolipram inhibition was necessary to determine any kinetic anomolies with h6.1. This study has shown however, that both rolipram and the non-selective inhibitor IBMX acted as simple competitive inhibitors of h6.1 as shown by the linear double-reciprocal plots (fig 3.2.8, 3.2.11), slope replots (fig 3.2.10, 3.2.13) and Dixon replots (fig 3.2.9, 3.2.12). Schematic representation of competitive

inhibition is given in fig (3.2.15) showing that the inhibitor simply competes with substrate for the active site.

Analysis of hPDE4A_{Livi} indicated that rolipram did not serve as a simple competitive inhibitor from the authors double-reciprocal plots (Livi et al 1990, Torphy et al 1992). In support of this, a plot of slope versus rolipram concentration for hPDE4A_{Livi} (fig 3.2.16) was curved in a concave fashion.

This would not occur if more than one molecule of rolipram bound to the enzyme as hypothesised by the authors, as the plot would be upwardly curving.

Further analysis of this data showed that the slope versus rolipram concentration plot for hPDE4A_{Livi} could be linearised by replotting a double-reciprocal of each axis (Dixon and Webb 1979), which is indicative of partial competitive inhibition. A scheme of partial competitive inhibition is shown in fig 3.2.17, in which the inhibitor competes with the substrate to form an EI complex which can interact further with substrate to form an EIS complex. In such a case both complexes break down to form products at the same rate.

Torphy et al (1992) have suggested that the kinetic anomalies seen with hPDE4A_{Livi} are the result of the presence of a high affinity binding site for rolipram, distinct from the site of catalysis (Introduction 1.19(iii)). Thus, the abnormalities seen with the inhibition by rolipram, would be due to more than one molecule of inhibitor binding per molecule of enzyme. However, this study has shown that both rolipram and IBMX are simple competitive inhibitors of substrate hydrolysis by a PDE4A isoform h6.1.

Sequence analysis of hPDE4A_{Livi} and comparison with that of h6.1 (Sullivan et al 1994) have shown the two to be highly related but differ in five amino acids. These amino acids are located within or next to the catalytic domain (Chen et al 1986, Jin et al 1992), Y³¹⁷/D, R⁵²³/M, R⁵²⁷/P, E⁵⁸⁹/A and N⁵⁹⁸/S (chapter 4 fig 4.2.2). It is possible that these sequence changes could explain the kinetic differences seen with h6.1 and hPDE4A_{Livi}, and cause alterations in the way in which the active site of hPDE4A_{Livi} folds

therefore, allowing both the substrate and inhibitor to bind at the same time. An alternative explanation could be that a modification occurred in the preparation of the enzyme.

Sullivan et al (1994) have shown that h6.1 as opposed to hPDE4A_{Livi}, represents that of the native PDE. Several lines of evidence support this. Using commercially available cDNA libraries, human PDE4A clones were isolated which failed to match the sequence of hPDE4A_{Livi}, yet all matched with h6.1. Moreover, the genomic sequence of a human PDE4A gene matches that of h6.1 (Sullivan et al 1994). Sequence differences in hPDE4A_{Livi} may be the result of a mutant enzyme or that there are two PDE4A genes, however it is more probable that they represent sequencing errors.

Addition to chapter 3, paragraph 1, page 80

The dependency of h6.1 catalytic activity on the presence of bivalent cations could be related to the ability of these cations to form a complex with the substrate. In such a case, this complex of substrate and bivalent cation would allow a more efficient interaction between enzyme and substrate. With respect to the bivalent cation dependency results obtained with h6.1 it could be considered that both magnesium and manganese formed a complex with cyclic AMP to stimulate hydrolysis, whereas, calcium was unable to and was therefore inhibitory.

Addition to chapter 3, paragraph 3, page 80

The dose response curves for rolipram inhibition of h6.1 (fig 3.2.4) were shown to spread over several orders of magnitude to completely inhibit enzyme activity. Therefore, the concentration range of rolipram chosen to investigate the drugs inhibitory mechanism (0 - 5 μ M) in figs 3.2.8 a and b on h6.1 activity could have biased the results towards competitive inhibition.

Table 2 IC₅₀ and EC₅₀ Values for Inhibition / Activation of Pellet h6.1 Activity by EDTA and Divalent Cations

Divalent Cation	IC ₅₀ (mM)	EC ₅₀ (mM)	EC ₅₀ (mM) Reactivation
Magnesium Chloride	N.A.	1.8±0.5	2.4±0.5
Manganese Chloride	N.A.	4.1±0.4	1.6±0.2
Calcium Chloride	1.4±0.06	N.A.	N.A.
EDTA	0.08±0.03	N.A.	N.A.

Results are shown as mean values ± the standard deviation for three observations in each case.

IC₅₀ was the concentration which resulted in 50% inhibition of h6.1 activity.

EC₅₀ was the concentration which resulted in 50% activation of h6.1 activity.

N.A. = not applicable.

Table 3 **K_m, Inhibitor Profile and Thermostability Values for Soluble and Pellet Forms of h6.1**

	Soluble h6.1	Pellet h6.1
K _m ^{cAMP} (μM)	5.2±1.5 (n=6)	4.1±1.7 (n=6)
Rolipram IC ₅₀ (μM)	0.51±0.15 (n=6)	1.35±0.5 (n=6)
K _i (μM)	0.4±0.1 (n=6)	0.7±0.3 (n=6)
IBMX IC ₅₀ (μM)	25.6±2.2 (n=3)	37.2±4.5 (n=3)
K _i (μM)	15±3 (n=3)	19±2 (n=3)
Cilostimide IC ₅₀ (μM)	N.D.	129±41 (n=3)
K _i (μM)	N.D.	81.8±26 (n=3)
RO-20-1724 IC ₅₀ (μM)	N.D.	7.2±1.2 (n=3)
K _i (μM)	N.D.	4.5±0.8 (n=3)

Values are given as mean ± the standard deviation for the number of observations in parenthesis.

IC₅₀ was the concentration which resulted in 50% inhibition of h6.1 activity.

The K_i value was the inhibition constant calculated from the Cheng-Prusoff equation as described in results section 3.2.vi.

N.D. = not determined.

Table 4 Comparison of h6.1 Activity Expressed in the Soluble Fractions of COS-1 Cells and *Saccharomyces Cerevisiae*

	<u>COS-1 Cells*</u>	<u><i>Saccharomyces Cerevisiae</i></u>
K_m^{cAMP} (μM)	6 \pm 2 (n=3)	4.1 \pm 1.7 (n=6)
Rolipram IC ₅₀ (μM)	0.6 \pm 0.2 (n=3)	0.51 \pm 0.15 (n=6)
K_i (μM)	0.6	0.4 \pm 0.1 (n=6)

* = Data from Sullivan et al (1994).

Values are shown as the mean \pm standard deviation for the number of observations in parenthesis.

IC₅₀ was the concentration which resulted in 50% inhibition of h6.1 activity.

The K_i value was the inhibition constant calculated from the Cheng-Prussoff equation as described in results section 3.2.vi.

Fig. 3.2.1 a **Thermostability of Soluble and Pellet h6.1 at**
45°C

Thermostability of h6.1 was measured at 45°C. The resultant $t_{0.5}$ values were calculated to be 10 minutes and >30 minutes for soluble and pellet activity respectively.

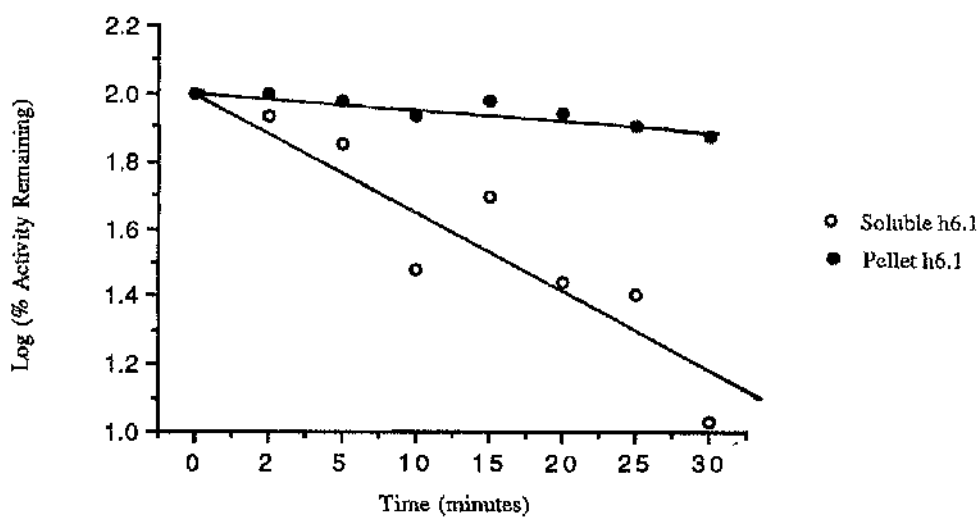


**Fig. 3.2.1 b Thermostability of Soluble and Pellet h6.1 at
50°C**

Thermostability of h6.1 was measured at 50°C. The resultant $t_{0.5}$ values were calculated to be 2 minutes and 20 minutes for soluble and pellet activity respectively.

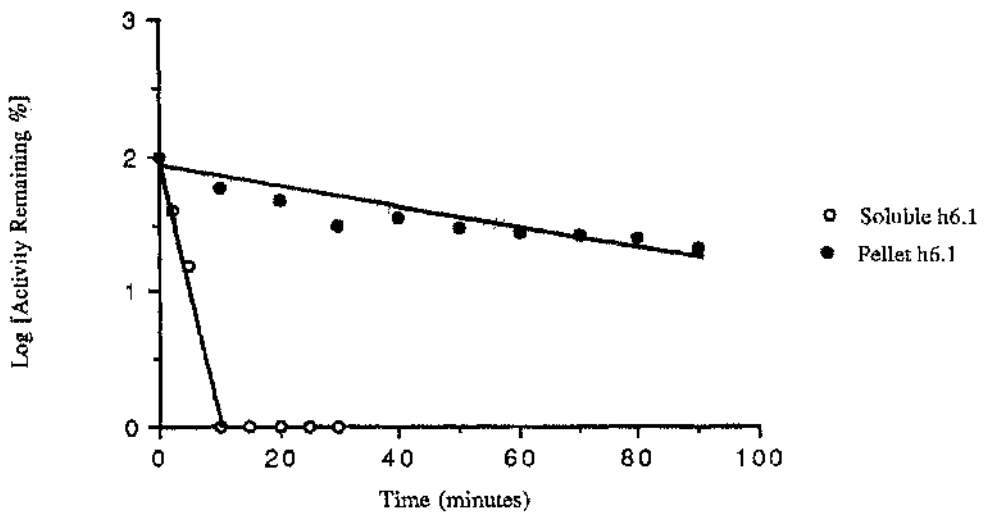


Fig. 3.2.2 a Treatment of Pellet h6.1 with EDTA

h6.1 activity was measured in ion free Tris pH7.4 buffer in the presence of increasing concentration of EDTA, which dose-dependently inhibited activity as shown. Result is shown in table 2.

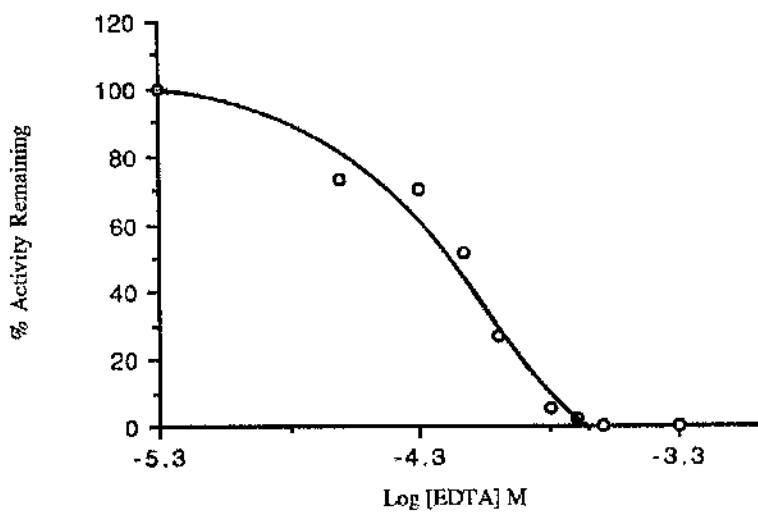


Fig. 3.2.2 b **Dose-Response of Pellet h6.1 to Magnesium Chloride**

h6.1 activity was measured in the presence of increasing concentration of magnesium chloride in Tris pH7.4 buffer, which dose-dependently activated activity as shown. Result is shown in table 2.

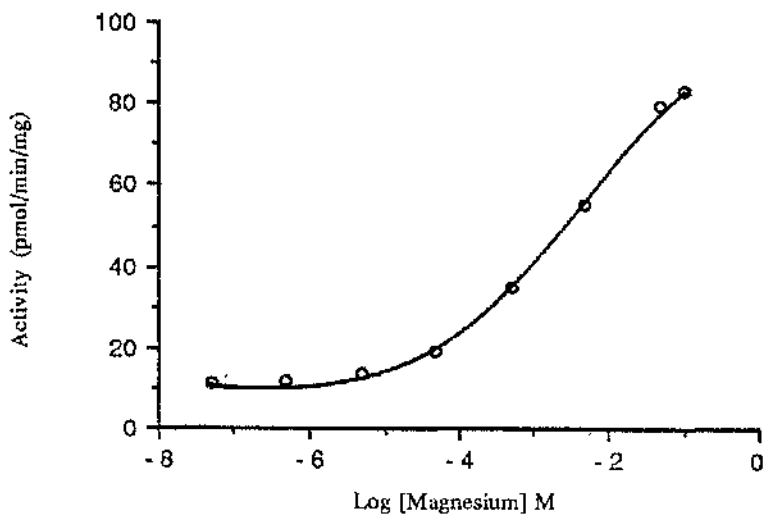


Fig 3.2.2 c

Reactivation of EDTA Treated Pellet h6.1 with Magnesium Chloride

Activation of native pellet h6.1 and reactivation of EDTA treated h6.1 with magnesium chloride is shown. Result is shown in table 2.

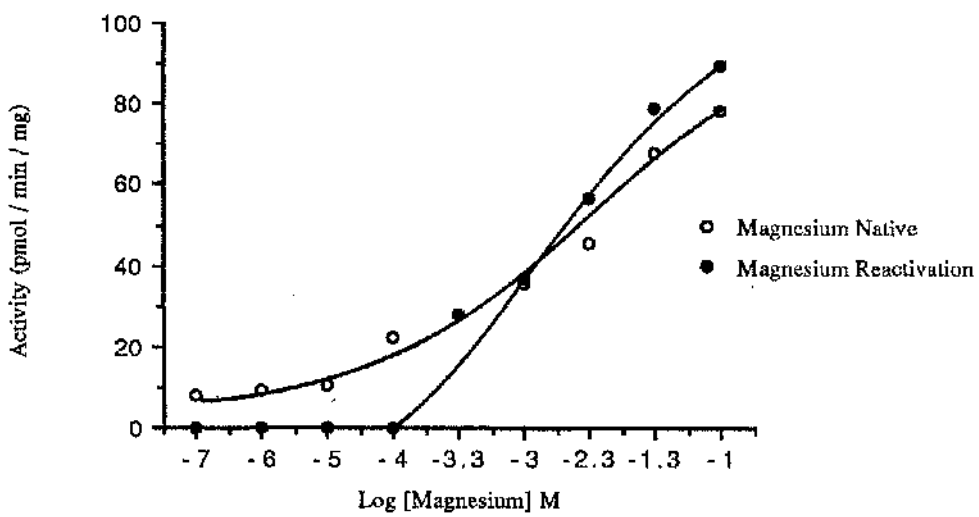


Fig 3.2.2 d

**Reactivation of EDTA Treated Pellet h6.1 with
Manganese Chloride**

Activation of native pellet h6.1 and reactivation of EDTA treated h6.1 with manganese chloride is shown. Result is shown in table 2.

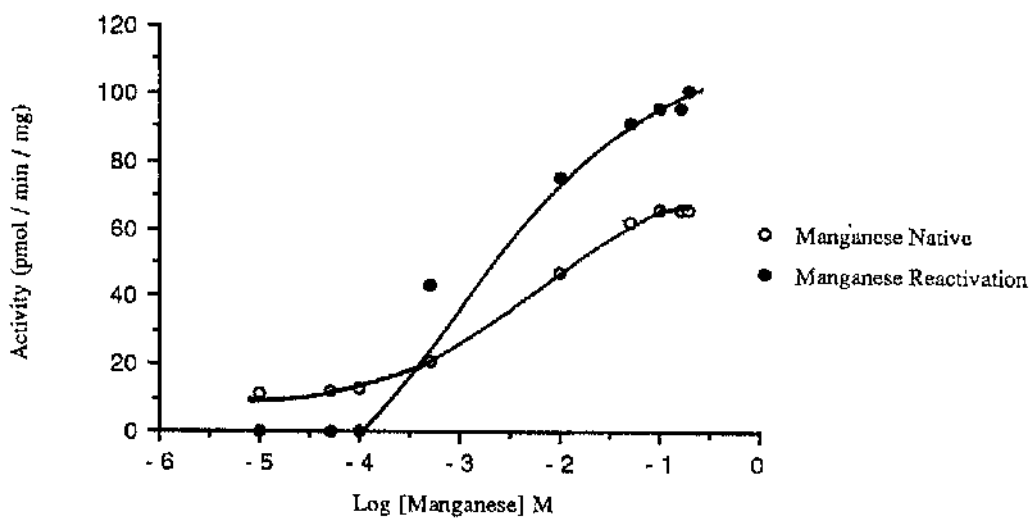
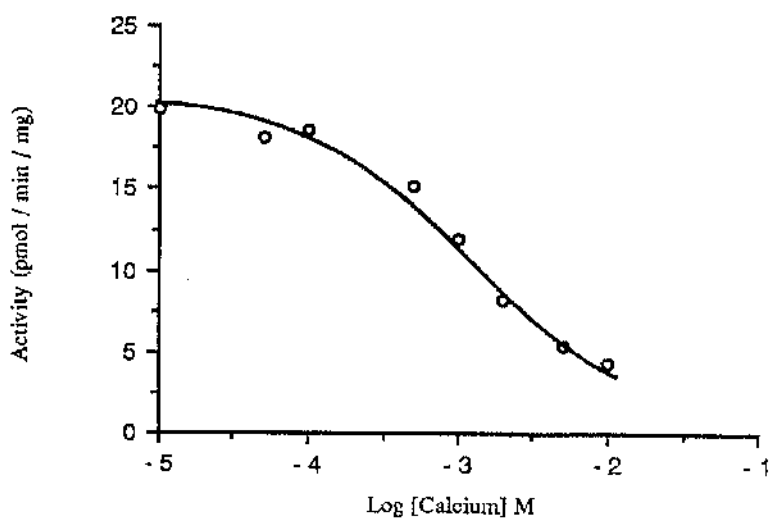


Fig 3.2.2 e

Inhibition of Native Pellet h6.1 with Calcium Chloride

Inhibition of native pellet h6.1 with calcium chloride is shown. Result is shown in table 2.



**Fig. 3.2.3 a Determination of K_m cyclic AMP For Soluble
h6.1**

Lineweaver-Burke plot was constructed by the measurement of soluble h6.1 activity in the presence of increasing cyclic AMP concentrations. Activity was linear over the ranges 0.1 - 100 μ M (insert), and 0.05 - 10 μ M cyclic AMP. K_m values were calculated using the Ultrafit programme as described in results, and the data is shown in table 3.

This experiment is representative of one carried out with at least six different preparations.

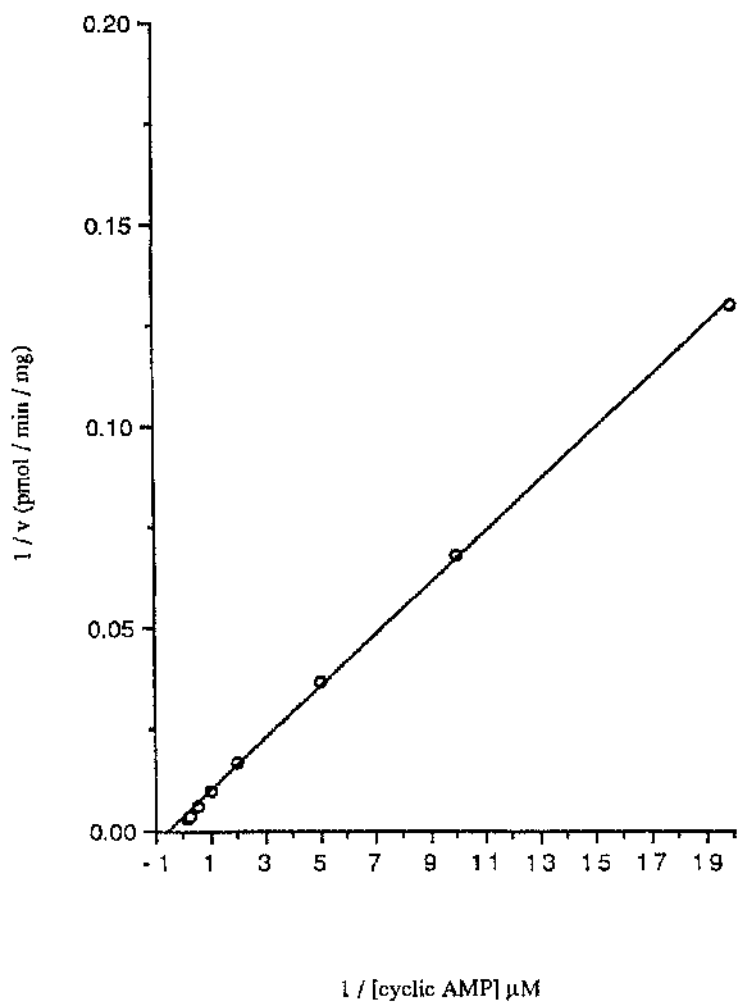
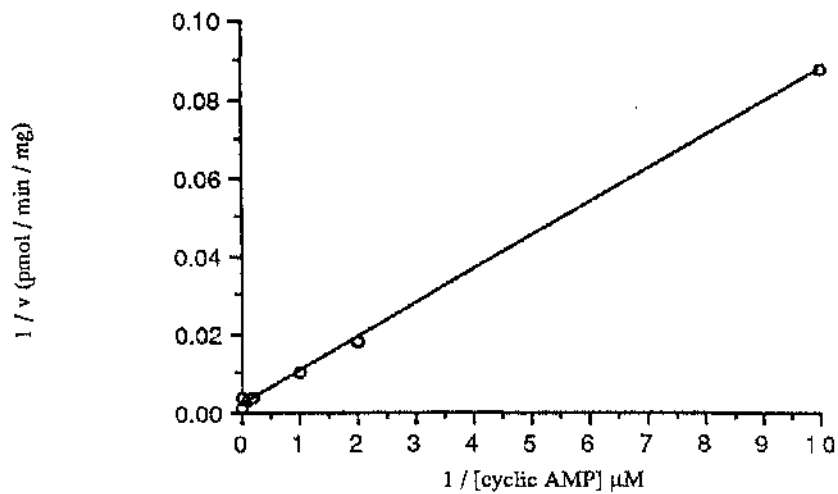


Fig. 3.2.3 b Determination of K_m cyclic AMP For Pellet
h6.1

Lineweaver-Burke plot was constructed by the measurement of pellet h6.1 activity in the presence of increasing cyclic AMP concentrations. Activity was linear over the range 1 - 20 μ M cyclic AMP. K_m value was calculated using the Ultrafit programme as described in results, and the data is shown in table 3. This experiment is representative of one carried out with at least six different preparations.

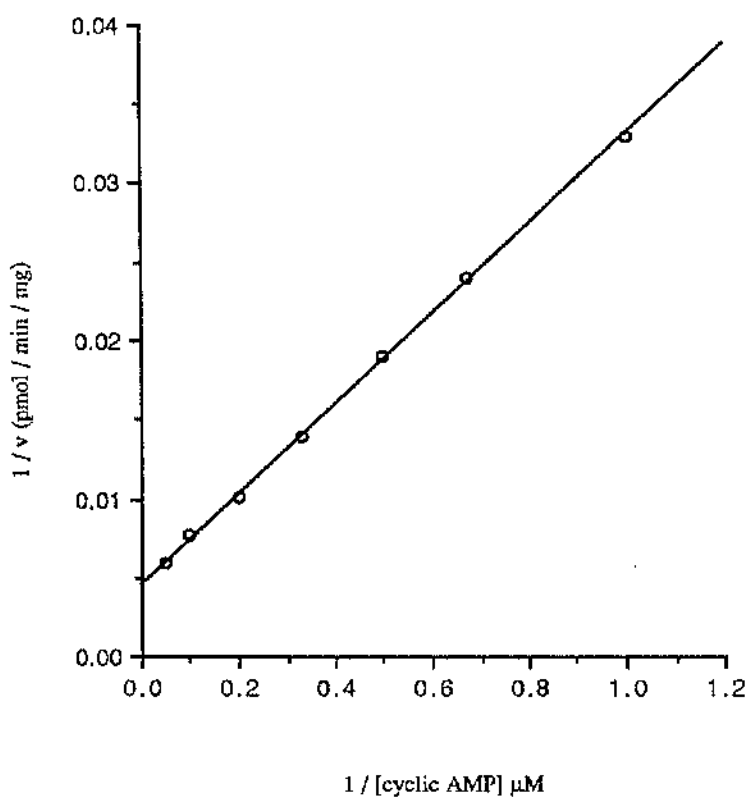


Fig. 3.2.4

Dose-Response to Rolipram of Soluble and Pellet h6.1

Soluble (a) and pellet (b) activity was measured at a fixed concentration of cyclic AMP ($3\mu\text{M}$), which approximated that of the K_m for each enzyme, in the presence of increasing rolipram concentration. Resultant IC_{50} values are given in table 3.

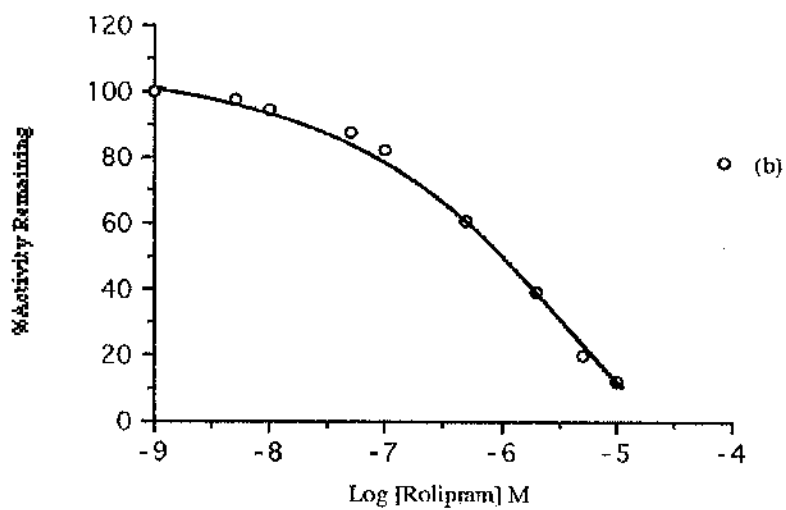
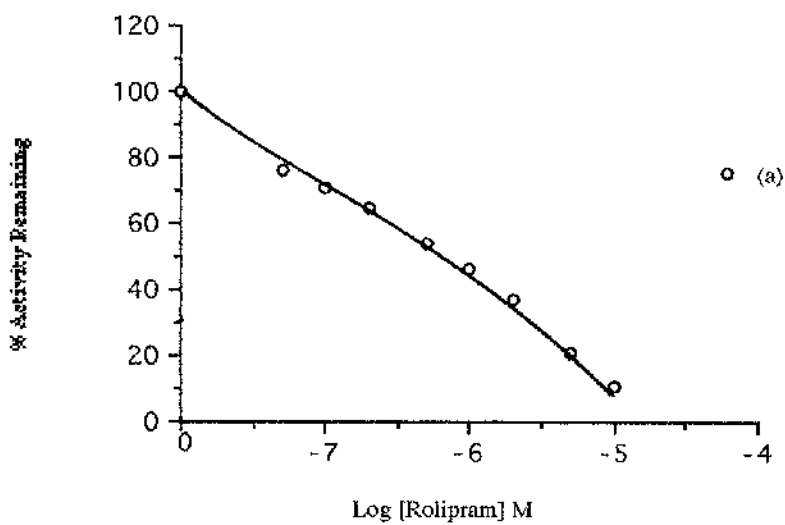


Fig. 3.2.5

Dose-Response to RO-20-1724 of Pellet h6.1

Pellet h6.1 activity was measured at a fixed concentration of cyclic AMP ($3\mu\text{M}$), which approximated that of the K_m , in the presence of increasing Ro-20-1724 concentration. The resultant IC_{50} value is given in table 3.

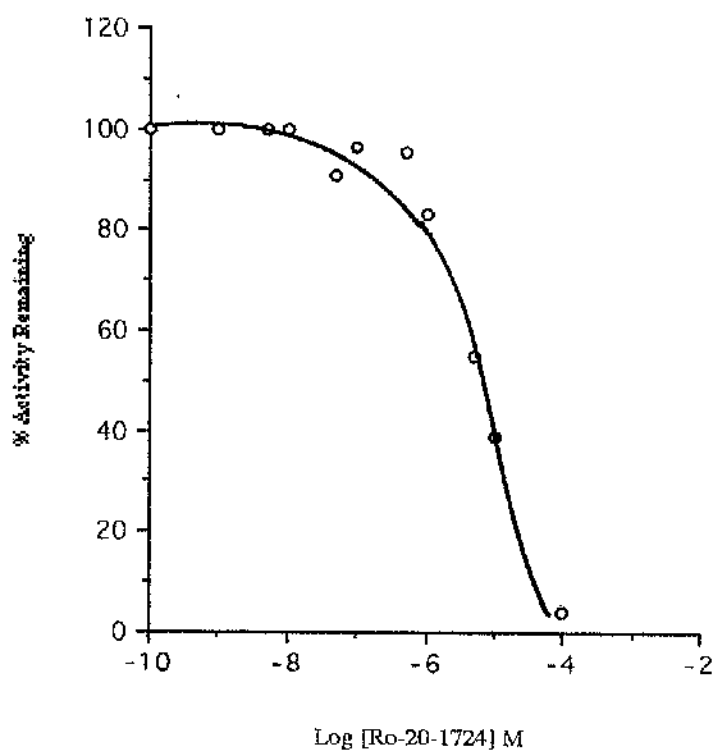


Fig. 3.2.6

Dose-Response to IBMX of Soluble and Pellet h6.1

Soluble (a) and pellet (b) activity was measured at a fixed concentration of cyclic AMP ($3\mu\text{M}$), which approximated the K_m for each enzyme, in the presence of increasing IBMX concentration. Resultant IC_{50} values are given in table 3.

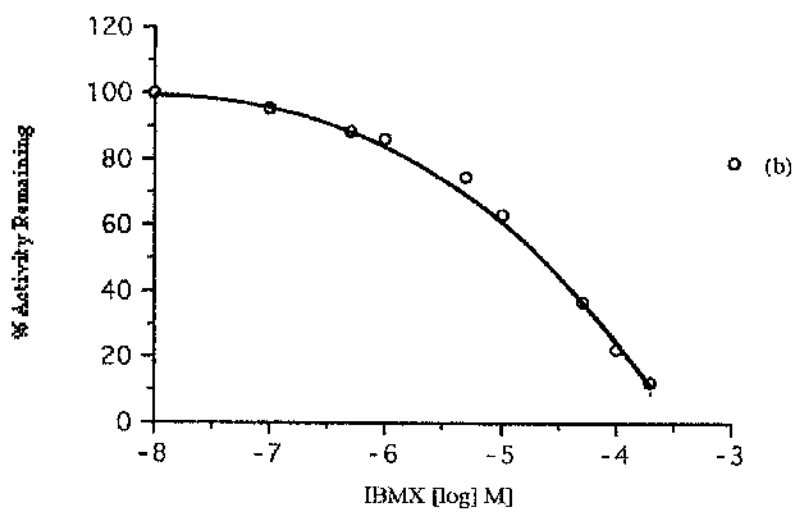
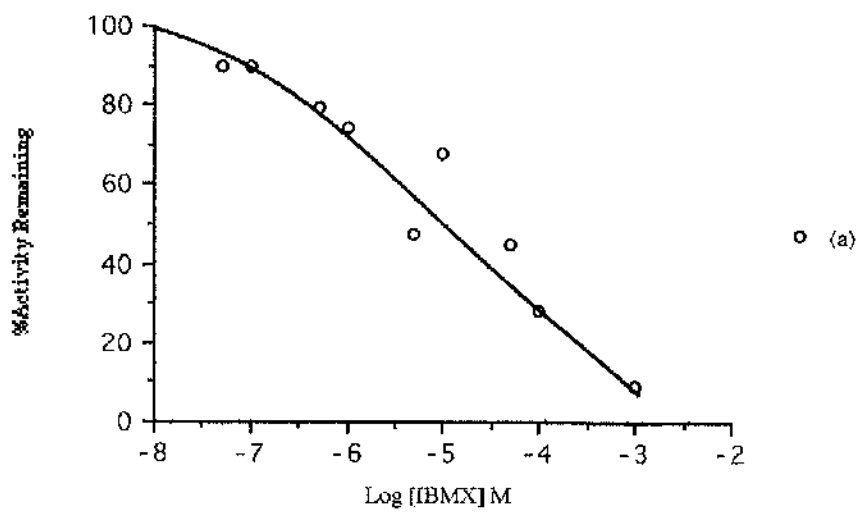


Fig. 3.2.7

Dose-Response to Cilostimide of Pellet h6.1

Pellet h6.1 activity was measured at a fixed concentration of cyclic AMP (3 μ M), which approximated that of the K_m , in the presence of increasing cilostimide concentration. The resultant IC₅₀ value is given in table 3.

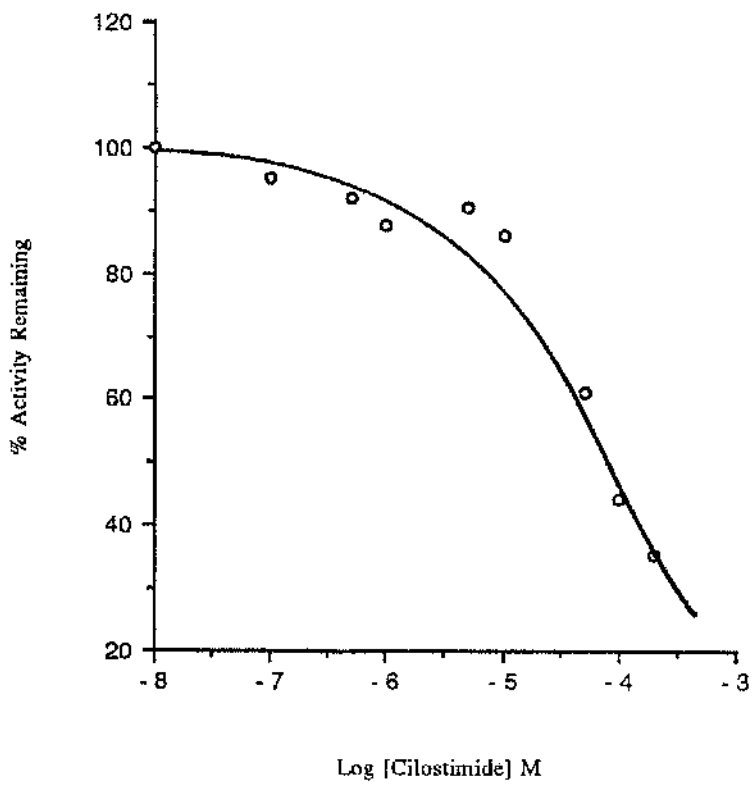


Fig. 3.2.8 a **Kinetics of Rolipram Inhibition of Soluble**
h6.1

Soluble h6.1 activity was measured over the range of 1 - 20 μ M cyclic AMP in the presence of increasing concentration of rolipram. This experiment is representative of one done at least three times.

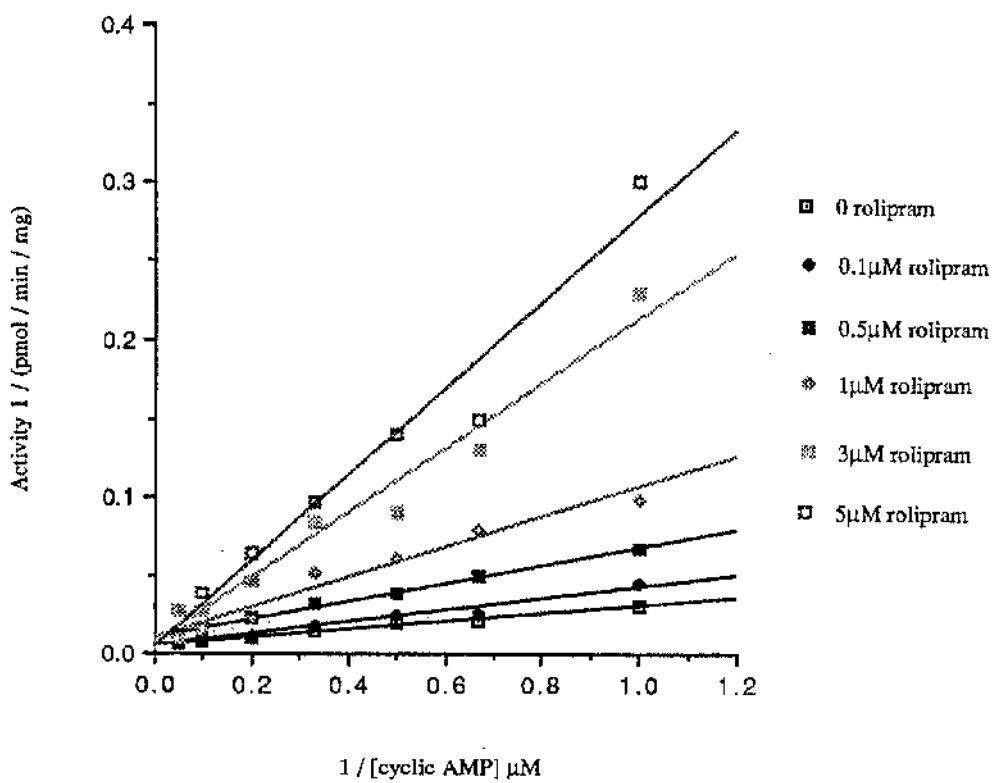


Fig. 3.2.8 b **Kinetics of Rolipram Inhibition of Pellet**
h6.1

Pellet h6.1 activity was measured over the range of 1 - 20 μ M cyclic AMP in the presence of increasing concentration of rolipram. This experiment is representative of one done at least three times.

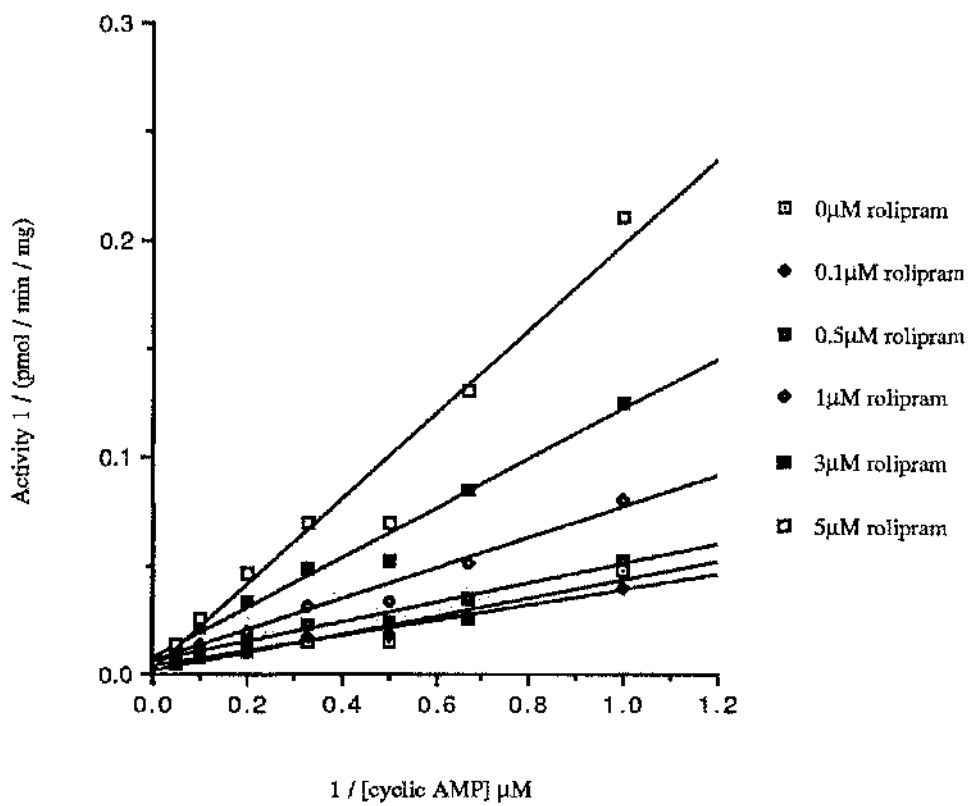


Fig. 3.2.9 a

**Dixon Replot of Rolipram Inhibition of Soluble
h6.1**

Data is shown as the reciprocal of activity versus increasing concentration of rolipram (Dixon and Webb 1979). This experiment is representative of one done at least three times.

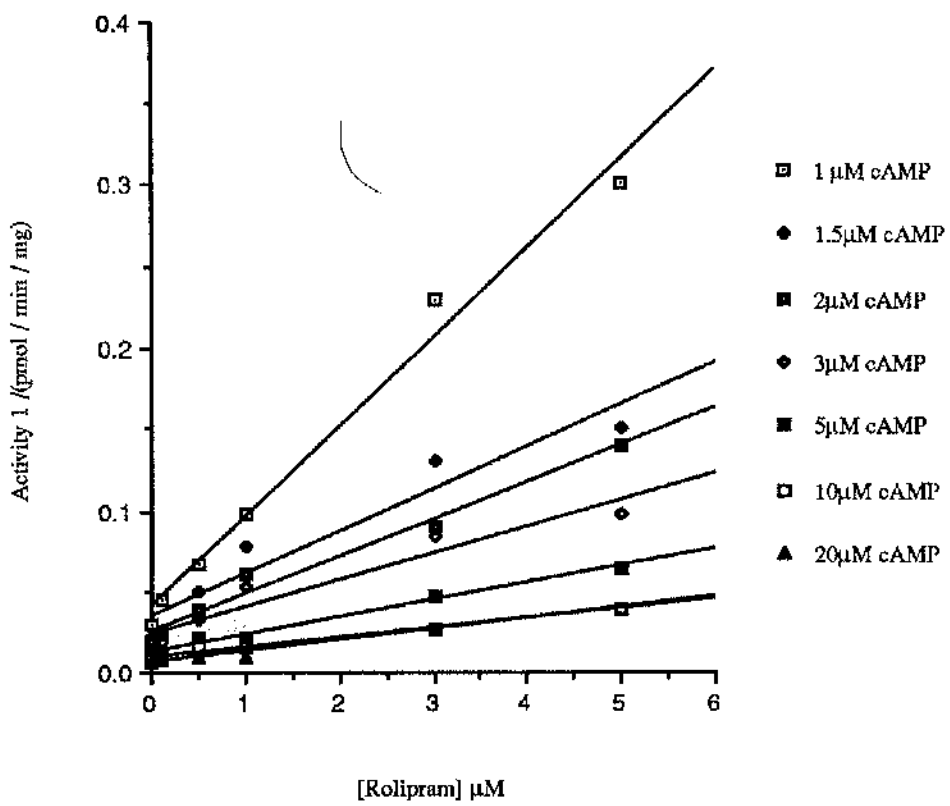
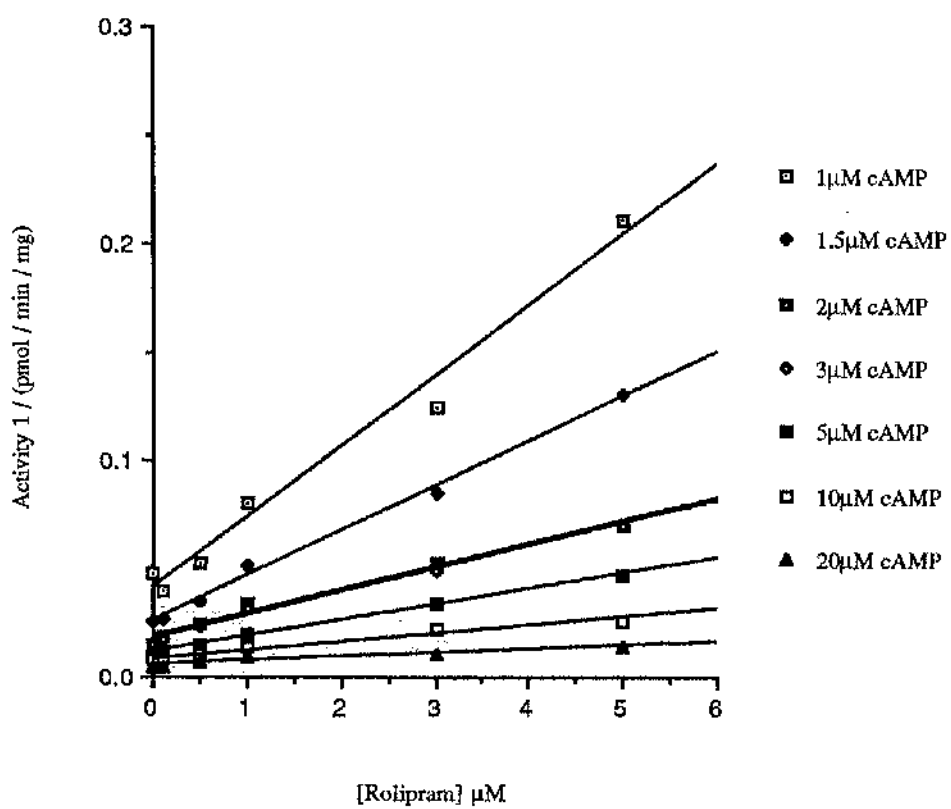


Fig. 3.2.9 b

**Dixon Replot of Rolipram Inhibition of Pellet
h6.1**

Data is shown as the reciprocal of activity versus increasing concentration of rolipram (Dixon and Webb 1979). This experiment is representative of one done at least three times.



**Fig. 3.2.10 a Slope Replot of Rolipram Inhibition of Soluble
h6.1**

Data is shown as the slope replot of activity versus increasing concentration of rolipram. This experiment is representative of one done at least three times.

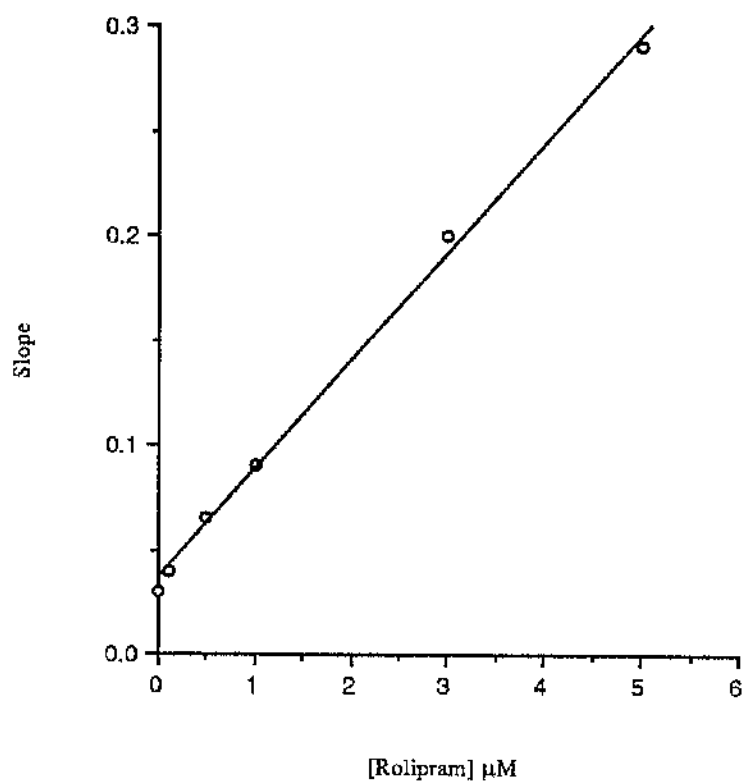


Fig. 3.2.10 b **Slope Replot of Rolipram Inhibition of Pellet**
h6.1

Data is shown as the slope replot of activity versus increasing concentration of rolipram. This experiment is representative of one done at least three times.

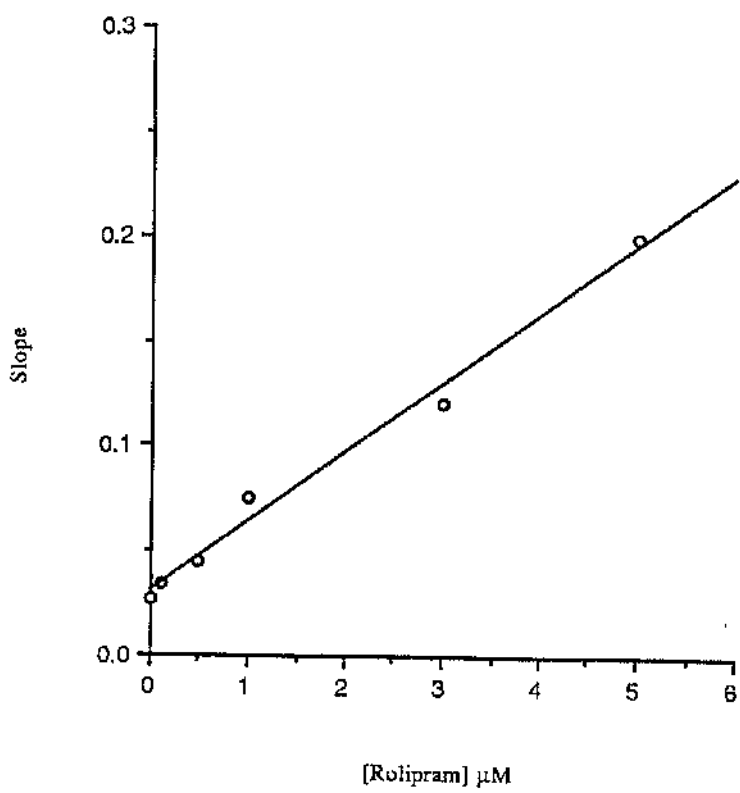


Fig. 3.2.11

**Kinetics of IBMX Inhibition of Pellet
h6.1**

Pellet h6.1 activity was measured over the range of 1 - 20 μ M cyclic AMP in the presence of increasing concentration of IBMX. This experiment is representative of one done at least three times.

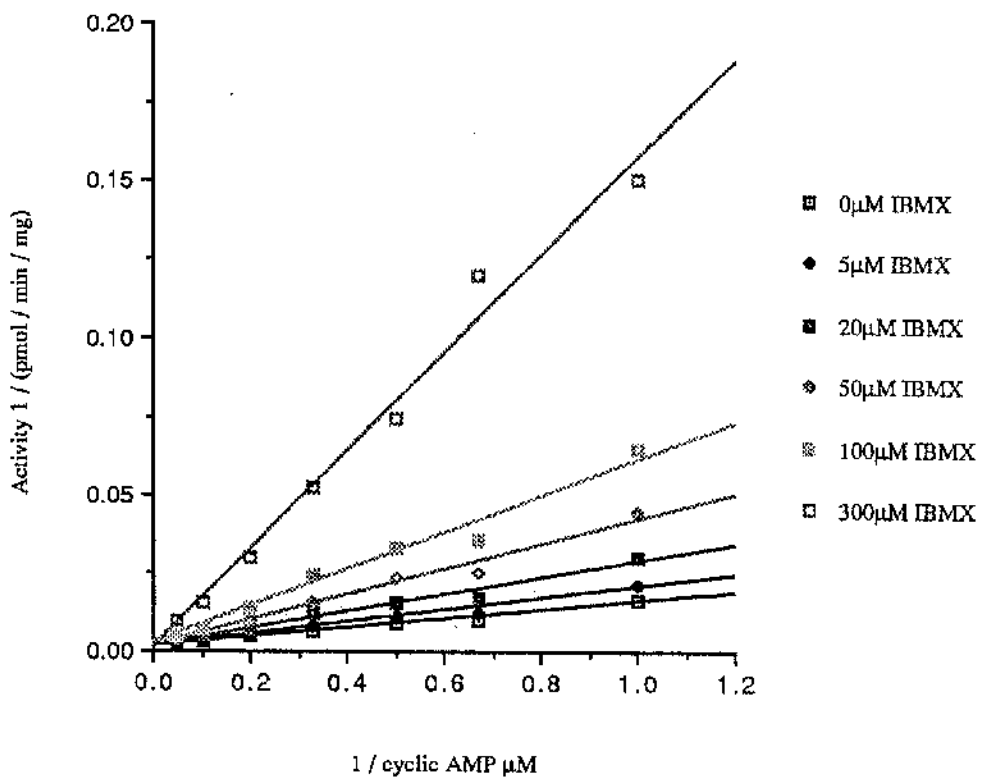


Fig. 3.2.12

**Dixon Replot of IBMX Inhibition of Pellet
h6.1**

Data is shown as the reciprocal of activity versus increasing concentration of rolipram (Dixon and Webb 1979). This experiment is representative of one done at least three times.

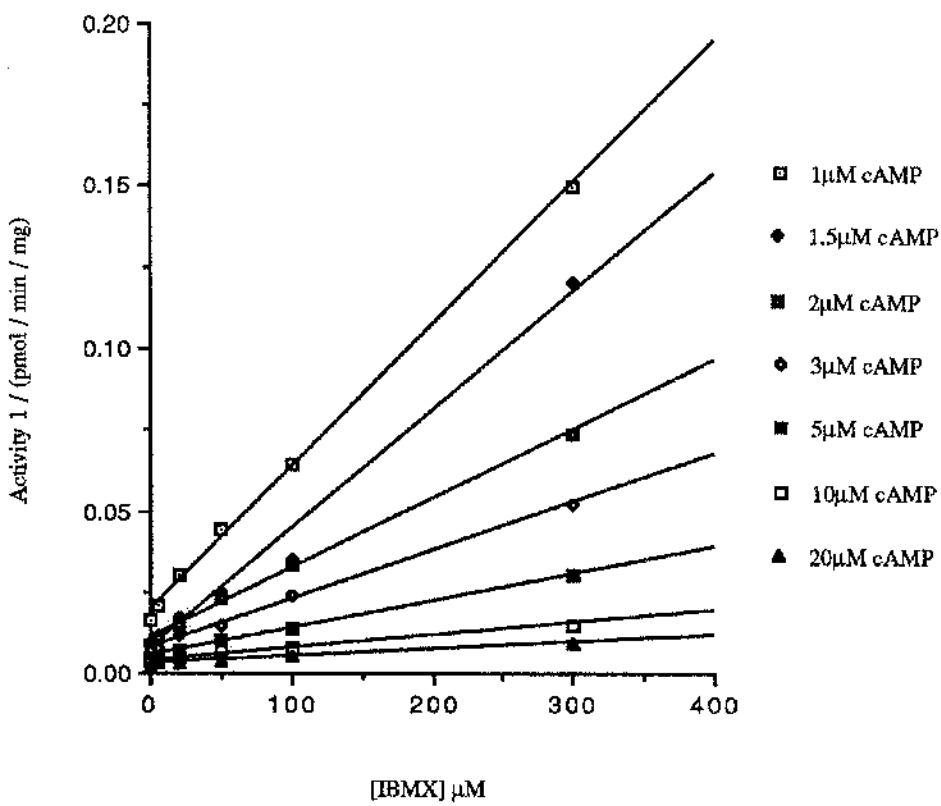


Fig. 3.2.13 **Slope Replot of IBMX Inhibition of Pellet**
h6.1

Data is shown as the slope replot of activity versus increasing concentration of rolipram. This experiment is representative of one done at least three times.

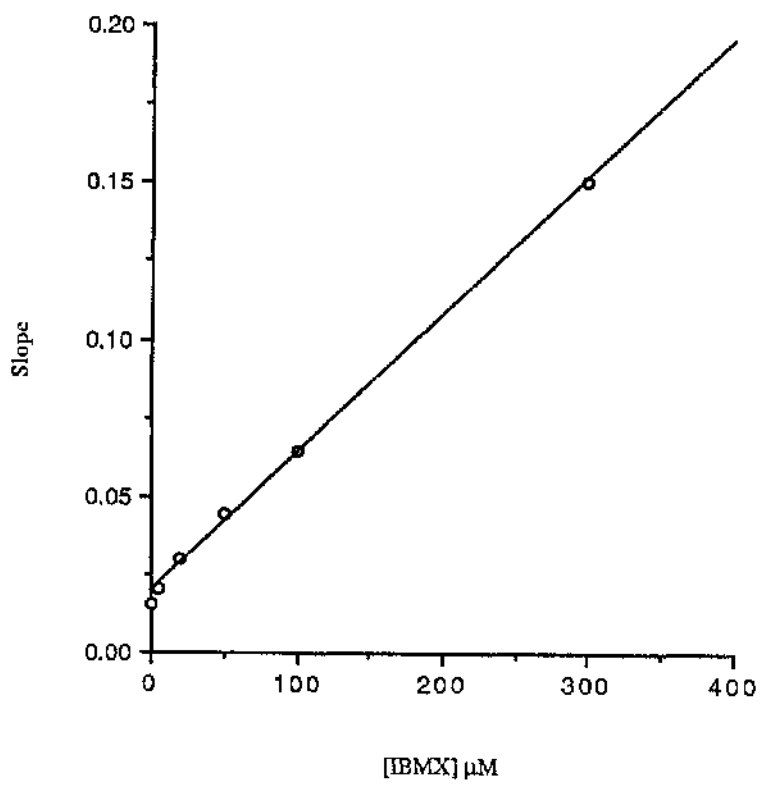
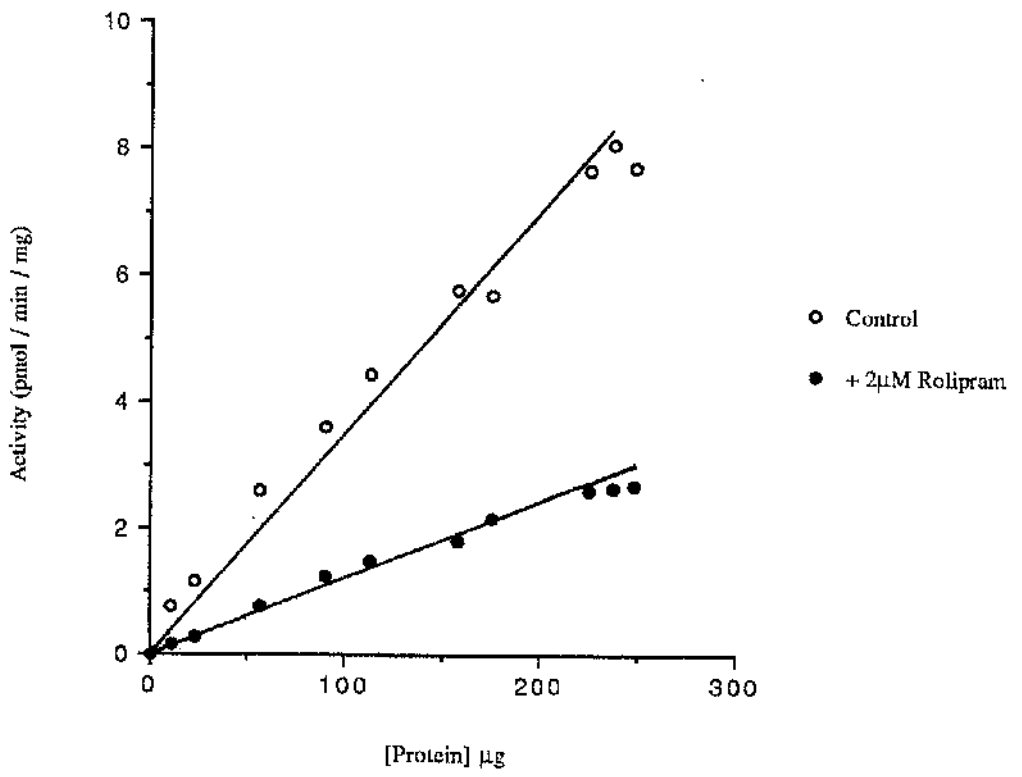


Fig. 3.2.14 **Measurement of Increasing h6.1 Protein**
Concentration vs Activity

h6.1 activity was measured over the protein concentrations shown $\pm 2\mu\text{M}$ rolipram, at a substrate concentration of $1\mu\text{M}$ cyclic AMP.



**Fig. 3.2.15 Schematic Representation of Competitive
Inhibition**

Shown diagrammatically is the scheme of competitive inhibition showing that the inhibitor simply competes with substrate for the active site.

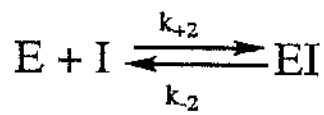
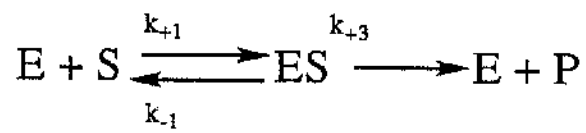


**Fig. 3.2.16 Slope Replot of Rolipram Inhibition of
hPDE4ALivi**

Data is shown as the slope replot of activity versus increasing concentration of rolipram. This data was obtained from Livi et al 1990.

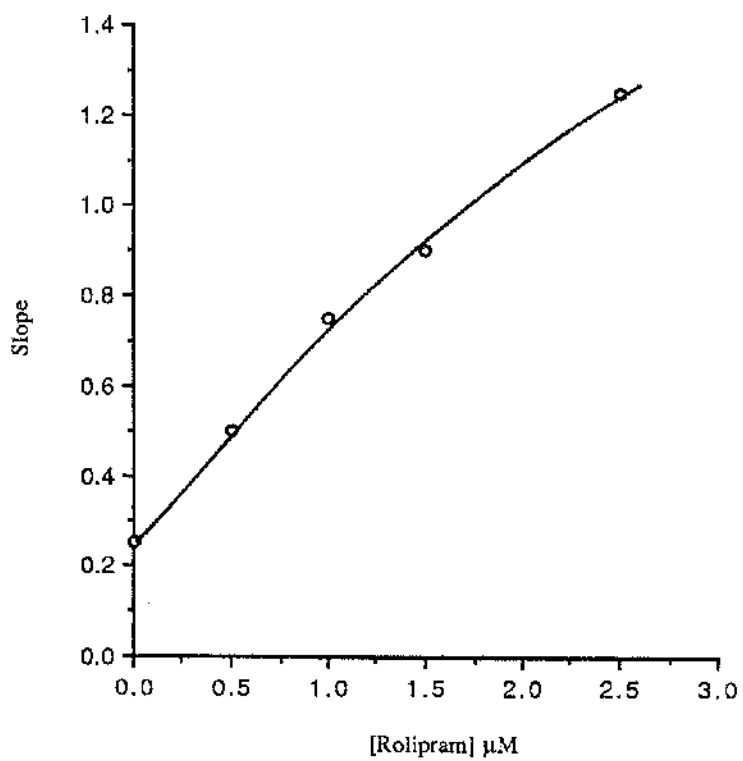
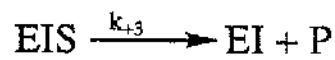
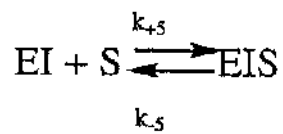
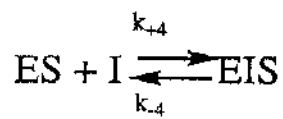
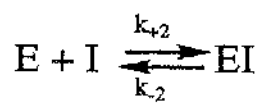
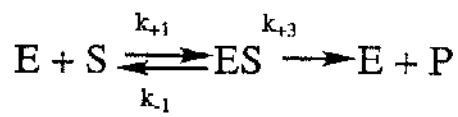


**Fig. 3.2.17 Schematic Representation of Partial
Competitive Inhibition**

Shown diagrammatically is the scheme of partial competitive inhibition. This shows that the inhibitor competes with the substrate to form an EI complex which can interact further with substrate to form an EIS complex. In such a case both complexes break down to form products at the same rate.



Results - Chapter 4

Analysis of Truncated Versions of
h6.1, Chimeric PDE HYB1 and an N-terminal
Domain Extension PDE 10AORF

4.1 Introduction

The cloning and analysis of h6.1, as described in chapter 3, has shown that hPDE4A_{Livi} and h6.1 are highly related proteins but differ with respect to five amino acids contained within, or next to, the catalytic domain (Sullivan et al 1994, Jin et al 1992). The amino acid residues which differ between hPDE4A_{Livi} and h6.1 are shown in fig 4.2.2. At the time of this study, it was thought that the differences between h6.1 and hPDE4A_{Livi} were the result of either cloning errors or mutations, or that h6.1 and hPDE4A_{Livi} represented alternative species. Also, Torphy et al (1992) reported that a high affinity binding site for rolipram, distinct from the catalytic site, was present on hPDE4A_{Livi}. Thus, Torphy et al (1992) proposed that the ability of hPDE4A_{Livi} to bind more than one molecule of rolipram per enzyme molecule was consistent with the kinetic anomalies seen with hPDE4A_{Livi}. As shown in chapter 3, both rolipram and IBMX were simple competitive inhibitors of substrate hydrolysis (figs 3.2.8, 3.2.11), therefore, substrate and inhibitor binding occur at the one site in h6.1. It was anticipated that if h6.1 displayed anomalous kinetics, perhaps through the binding of rolipram to a site other than the catalytic site as proposed by Torphy et al (1992), then trimming of the surrounding sequences of the basic catalytic domain would reveal this.

Analysis of the catalytic domain (Jin et al 1992) has shown that, while members of any one PDE class show 60 - 90% homology in the catalytic region, those belonging to different classes are much less homologous. The catalytic region of PDE4 (Jin et al 1992) can be identified by homology with other PDE species (fig 4.1.1), and is conserved throughout the PDE4 class. However, it is evident that the N and C terminal regions of PDE4 A, B, C and D isoforms, outwith the catalytic region, differ widely (fig 4.1.2) Bolger et al (1993). Thus, these N and C terminal regions presumably perform other functions which could influence enzyme stability or catalysis. In order to address whether the N and C terminal regions of h6.1 influenced enzyme

activity, Dr M. Sullivan (Sandoz), created a series of mutants of h6.1 which were engineered for expression in *Saccharomyces cerevisiae* as per h6.1. These truncations, which refer to the sequence of h6.1, took the form of an N-terminal deletion of residues 1 - 172 (YMS 10 yeast strain), a deletion at the N-terminus of residues 1 - 172, and C-terminus of residues 608 - 692 leaving the basic catalytic domain (YMS11 yeast strain) and a C-terminal deletion of residues 608 - 692 (YMS12 yeast strain) (fig 4.2.1).

In addition, a hybrid form of h6.1 was constructed which involved an N-terminal domain swap of h6.1 with a 33 amino acid unique N-terminal region of a novel PDE4A splice variant, which has been called 2EL (HSPDE4A8, GenBank accession number U18088) (Horton et al 1995) (fig 4.2.2). 2EL was isolated from a human, resting, T cell cDNA library, which was screened with a PDE specific probe generated by pcr as reported for h6.1 (Sullivan et al 1994). Sequence analysis of the putative proteins encoded by 2EL and h6.1 showed that they differed in two regions. 2EL was shown to encode a unique 33 amino acid N-terminal sequence, after which their identity extends over a further 275 amino acids. After this region of homology there is a 34bp insertion, within the putative catalytic region, where premature termination of 2EL would occur as a result of the frameshift of the 2EL ORF. The insertion of the 34bp fragment disrupts the catalytic region of 2EL in such a way as to produce a protein which is inactive when the cDNA is transfected into COS cells (Horton et al 1995). To investigate the function of the unique N-terminal region of 2EL, as the 2EL enzyme was inactive, the hybrid HYB1 was constructed. HYB1 was generated by exchanging the N-terminal region of 2EL with the corresponding region of h6.1 to assess the effect of the N-terminal region of 2EL on catalytic activity.

Studies by Bolger et al (1993) have shown that a longer open reading frame, than that for either h6.1 or hPDE4A_{Livi}, can be generated from the PDE4A gene (fig.1 Bolger et al 1993). The product encoded by the cDNA

isolated, which represented the PDE4A gene, was named PDE46 (GeneBank name HSPDE4A5, GeneBank accession number L20965). PDE46 was shown to be related to hPDE4A_{Livi}, in that hPDE4A_{Livi} was a truncated version. In relevance to this, Dr Mike Sullivan (Sandoz) has isolated a cDNA clone which represented an extended version of h6.1 which has been named 10AORF. The sequence of 10AORF is identical to PDE46, except for a 14 amino acid extension at the N-terminal region (fig 4.2.3).

To analyse the effects of the structural alterations of the truncated enzymes, 10AORF and HYB1 we considered the kinetics of cyclic AMP hydrolysis and the effect of rolipram thereon. The thermostability of the enzymes were also analysed as an indication of alterations to the catalytic unit.

It was hoped that it would be possible to determine the relative amounts of the truncated enzymes, 10AORF and HYB1 as expressed in yeast using antisera which would cross react with each enzyme, and thus, enable the determination of V_{max} values for each of the enzymes. This would have been done, initially, by western blot analysis of increasing protein concentration from the soluble fraction of transfected yeast cells. The resultant blots would then have been scanned to obtain a plot of OD value vs μg protein, in order to estimate the concentration of RD1 in each sample relative to each other. Then, amounts of protein from transfected yeast, which would provide equivalent amounts of RD1 could have been immunoprecipitated. The immunoprecipitates would have been assayed for PDE activity over a range of cyclic AMP concentrations, and the data plotted as a Lineweaver-Burke plot to define the relative V_{max} for each enzyme. From this, it would have been possible to determine any effect on enzyme activity as a result of changes to the N and C terminal regions. However, we were unable to generate an antisera despite repeated attempts using various peptides. This antisera could also have been used to look at the expression and determine the molecular weight, of such proteins *in vivo*.

This chapter describes the characterisation of the truncated enzymes, the 10AORF enzyme which has an extended N-terminal region with respect to h6.1, and the chimeric enzyme HYB1. These experiments were designed to investigate effects on catalysis and enzyme stability induced by the changes to the N and C terminal regions of h6.1.

4.2

Results

(i) Sequence Alignments of h6.1, 10AORF, HYB 1, YMS 10, YMS 11 and YMS 12

The truncations of h6.1, which were created by Dr Mike Sullivan (Sandoz), took the form of an N-terminal deletion of residues 1 - 172 (YMS 10 yeast strain), a deletion at the N-terminus of residues 1 - 172, and C-terminus of residues 608 - 692 leaving the basic catalytic domain (YMS 11 yeast strain) and a C-terminal deletion of residues 608 - 692 (YMS 12 yeast strain). These truncations are shown diagrammatically in fig 4.2.1, and their amino acid sequences are shown in the alignment in fig 4.2.4. The sequences of the truncated enzymes, h6.1 and HYB1 are all aligned to the sequence of PDE46.

The sequence alignment of h6.1, HYB1 and 2EL are shown in fig 4.2.2. Shown in this alignment is the unique N-terminal region of 2EL which has been exchanged for the N-terminal region of h6.1.

The identity of 10AORF with PDE46 is shown in fig 4.2.3. The sequence of 10AORF is identical to PDE46, except for a 14 amino acid extension at the N-terminal region of PDE46. In addition, this alignment shows that the amino acid base changes seen in hPDE4A_{Ljvi} are absent from the sequence of PDE46.

(ii) Expression of 10AORF, HYB1, YMS10, YMS11 and YMS12 in *Saccharomyces cerevisiae*

Cell suspensions of yeast expressing 10AORF, HYB1, YMS10, YMS11 and YMS12 were disrupted by means of a cell press. Cell homogenates were centrifuged 210,000g_{av} for 45 minutes, after which the pellet and supernatant fractions were assayed for PDE activity at a substrate concentration of 1μM cyclic AMP. All yeast strains expressed measurable PDE activity in both the pellet and soluble fractions, with the exception of the YMS10 strain. It is unclear as to why only the YMS10 strain did not express PDE activity,

however, if yeast transfected with plasmid are not placed under any selection pressure, as in this case, then the cells secrete the plasmid. As a result the yeast which do not contain the plasmid grow more rapidly. This could have been the case with YMS10.

The specific activities determined (in pmol cyclic AMP / min / mg \pm standard deviation from the mean) for each of the enzyme preparations expressed in yeast, for pellet and soluble fractions respectively were, HYB1 1.14 ± 0.3 , 1.4 ± 0.4 (n=3), 10AORF 21.7 ± 1.7 , 15.7 ± 1.8 (n=3), YMS11 0.43 ± 0.1 , 0.76 ± 0.2 (n=3) and YMS12 5.99 ± 1.2 , 0.46 ± 0.2 (n=3) (table 5). The control yeast strain for HYB1 was YMS5X and for the truncations and 10AORF the control yeast strain was YMS5. In each case the control strain failed to hydrolyse cyclic AMP.

The activity distribution between the soluble and pellet fractions expressed in yeast (table 5) were similar for HYB1, 10AORF and YMS11 with 40 - 60% of the activity in the soluble fraction. However, considerably less of the YMS12 activity was present in the soluble fraction. The values in table 5 are representative of at least three different preparations.

(iii) Kinetics of Cyclic AMP Hydrolysis by the Soluble Forms of 10AORF, HYB 1, YMS 11 and YMS 12

The K_m value for the hydrolysis of cyclic AMP by the soluble fractions of yeast expressing 10AORF, HYB1, YMS11 and YMS12 were determined from Lineweaver-Burke plots (figs 4.2.5, 4.2.6, 4.2.7 and 4.2.8 respectively). In each instance, the double-reciprocal plots of initial rate versus cyclic AMP concentration for each activity was linear over the substrate concentration range of 0.1 - 50 μ M and displayed simple saturation kinetics. In order to calculate K_m values, the data were fitted to the Michaelis Menton equation $V_{obs} = (V_{max}[\text{cyclic AMP}] / (K_m + [\text{cyclic AMP}]))$ using the Ultrafit graphical package. In each case, the 'robust weighting' facility was used and the 'goodness of fit' index was no less than 0.99 with each estimation, 1 being

a perfect fit. This non-linear fitting programme obviates errors in fitting to the Lineweaver-Burke plot using regression analysis, where the spread of errors is not evenly distributed as it is a double-reciprocal plot. This analysis yielded K_M values for each of the enzyme activities which were all in the low μM range. The K_M values are shown in table 6. Each experiment is representative of that carried out at least three times.

(iv) Dose Response to Rolipram of the Soluble Forms of
10AORF HYB 1, YMS 11 and YMS12

The ability of the PDE 4 selective inhibitor rolipram to inhibit substrate hydrolysis of 10AORF, HYB 1 and the truncated enzyme activities was assessed. To ensure an accurate comparison with h6.1, the dose response curves were constructed using an identical substrate concentration, $3\mu\text{M}$, which reflected that of the K_M value of h6.1. Rolipram was used in the concentration range of $0.05 - 10\mu\text{M}$.

IC_{50} values (concentration of inhibitor which produced 50% reduction in substrate hydrolysis) were then calculated for each enzyme from the dose response curves shown in figs 4.2.9, 4.2.10, 4.2.11 and 4.2.12 for 10AORF, HYB1, YMS11 and YMS12 respectively. The IC_{50} values are shown in table 6.

(v) Kinetics of Inhibition of the Soluble Form 10AORF by
Rolipram

The mechanism of inhibition by rolipram of PDE4A was further investigated in this study. In chapter 3, it was shown that both the non-selective inhibitor IBMX, and the PDE4 inhibitor rolipram, competitively inhibited substrate hydrolysis (figs 3.2.7 & 3.2.10) of h6.1. The isolation of the extended version of h6.1, 10AORF allowed the further analysis of rolipram interaction. In addition, determination of the IC_{50} value of rolipram inhibition of 10AORF, showed a greater potency of inhibition compared to that for h6.1 (table 6). It was necessary, therefore, to investigate whether this shift in

potency was the result of a change in the mechanism by which rolipram inhibited the enzyme.

To address this question, double-reciprocal plots were constructed of soluble 10AORF activity versus cyclic AMP concentration in the presence of increasing concentration of inhibitor. Soluble 10AORF activity, in contrast to h6.1, was partially competitively inhibited by rolipram. Linear Lineweaver-Burke (fig. 4.2.13) and Dixon (1953) (fig. 4.2.14) plots were obtained with 10AORF, which remained linear over a wide range of substrate and inhibitor concentrations. However, a slope replot (fig. 4.2.15) of this data was shown to be curvilinear, indicative of partial competitive inhibition.

(vi) Thermostability of 10AORF, HYB 1 and YMS 12 at 45°C

The thermostability of soluble 10AORF, HYB 1 and YMS 12 were assessed at 45°C. In each case, the enzyme activities decayed as a single exponential yielding linear semi-log plots of residual activity against time (fig 4.2.16). At the temperature studied the extended version of h6.1, 10AORF, was considerably more stable than either of the soluble forms of HYB 1, YMS 12 or h6.1 with a $T_{0.5}$ value of >30 minutes. The values calculated for h6.1, YMS 12 and HYB 1 are shown in table 7.

Analysis of the four human and rat PDE4 genes by Bolger et al (1993) has further highlighted the complexity of this isoenzyme family. With relevance to this present study, analysis of the PDE4A gene revealed that a product, PDE46, could be transcribed which has been shown since to represent the full length version of h6.1 described in Chapter 3. PDE46 (Bolger et al 1993) was shown to contain complete ORFs, with stop codons present in all three reading frames upstream of the putative initiation codon. The isolation of h6.1 from a human T-lymphocyte cDNA library, initially involved the identification of two overlapping clones which represented a PDE4 similar to that isolated by Livi et al (1990), but lacked the first 13 amino acids. These first 13 amino acids of hPDE4A_{Livi} were engineered onto the sequence of h6.1 to provide an open reading frame as seen in the Livi et al (1990) clone. Since non-native amino acids had to be engineered onto the N-terminal region of the sequence of h6.1 to provide an open reading frame, this indicated that the h6.1 sequence isolated was not complete. In addition, Bolger et al (1993) had shown that a longer product, PDE46, could be transcribed. Using a similar strategy to that which resulted in the isolation of h6.1, Dr Mike Sullivan (Sandoz) isolated a clone which represented an N-terminally extended version of h6.1. This clone was named 10AORF, and was found to be an extension of the sequence of h6.1 by ~190 amino acids at the N-terminus. The sequence alignment of PDE46 with 10AORF (fig 4.2.3), shows that 10AORF differs from PDE46 by only a 14 amino acid extension at the N-terminal region.

Originally it was considered (Bolger et al 1993) that the PDE4A enzyme isolated by Livi et al (1990), hPDE4A_{Livi}, represented a partial clone of PDE46 which maintained catalytic activity despite being truncated at the N-terminus. Sequence alignment of 10AORF, PDE46 and h6.1 (fig 4.2.4) have shown the complete identity of their internal amino acid sequence apart from the N-terminal amino acids. The 10AORF enzyme was also shown to be an N-

terminally extended version of h6.1 (fig 4.2.4). The importance of the identity of 10AORF and h6.1 with PDE46, is that it provides confirmation that the sequence of h6.1 is correct. This can be concluded since the amino acid changes seen in the sequence of hPDE4A_{Livi}, were not seen in the sequence of PDE46 isolated by Bolger et al (1993).

Comparison of the sequences of the four human PDE4 genes, and the PDE4 gene of *Drosophila melanogaster* (Bolger et al 1993) has highlighted that the most divergent region found was at the N-terminus. Thus, the catalytic region of PDE4 genes is conserved between species, however, flanking sequences have been shown to be different at both the N and C termini. Indeed, analysis of the human PDE4 genes and the *Drosophila melanogaster dunc* gene (Davis & Davidson 1984), has shown that no homologous sequences are found either between human genes or the *dunc* gene. It is of interest that the mammalian PDE4 isoforms, and not the *dunc* gene product, are inhibited by the characteristic PDE4 inhibitors rolipram and RO-20-1724 (Henkle-Tigges & Davis 1989). This may suggest that the N-terminus of the human PDE4 genes contain the information to allow the interaction with these inhibitors, since this region was shown to be the most divergent.

The observation that the mammalian PDE4 isoforms have unique N and C terminal regions (Bolger et al 1993, Swinnen et al 1989) suggested that these regions could perform specific functions, such as, affecting catalytic activity. In order to investigate such roles for the N and C termini, Dr Mike Sullivan (Sandoz) constructed a series of truncated forms of h6.1 which were analysed in this present study. The truncations of h6.1 took the form of an N-terminal deletion of residues 1 - 172 (YMS10 yeast strain), a deletion at the N-terminus of residues 1 - 172, and C-terminus of residues 608 - 692 leaving the basic catalytic domain (YMS11 yeast strain) and a C-terminal deletion of residues 608 - 692 (YMS12 yeast strain). These truncations are shown

diagrammatically in fig 4.2.1, and their amino acid sequences are shown in the alignment in fig 4.2.4. The N-terminally extended version of h6.1, 10AORF, was similarly investigated. In addition, a chimeric PDE4A was constructed to investigate the function of the N-terminal domain of 2EL (Horton et al 1995). The chimeric PDE4A was called HYB1, and was constructed by swapping the unique N-terminal region of 2EL with the corresponding region of h6.1. The PDE 2EL has been shown by Horton et al (1995) to be a splice variant of the PDE4A gene. The activity of 2EL could not be examined by expression in a cell system because it is inactive catalytically. This catalytic inactivation is due to a 34 bp insert in the presumed catalytic domain, which results in the premature truncation of the protein sequence. The significance, physiologically, of the production of catalytically inactive proteins is unknown. Bolger et al (1993) have isolated a variant of PDE46, called TM3. In this study, Bolger et al (1993) described TM3 as being a product which is expressed only in yeast, and not translated as a protein product in human cells. It has been considered by Horton et al (1995) that the production of non-functional mRNAs, such as 2EL and TM3, in human cells is a type of safety mechanism used to control the expression level of functional PDE activity. However, it could be that such variants influence PDE activity. Here we wanted to know whether 2EL was inactive due to the 34bp insert, or an inhibitory 5' domain. To test the latter, a chimera was made of the 5' domain of 2EL and the complete C-terminal region of h6.1. Of interest in this present study, was the unique N-terminal region of 2EL which was investigated using the chimeric protein HYB1.

Yeast strains YMS11, YMS12, HYB1 and 10AORF all expressed activity which was distributed between the pellet and soluble fractions (table 5). Pelleted h6.1 activity (chapter 3 section 3.2.ii), was shown not to be affected by either centrifugation or treatment with either high concentrations of salt or the detergent TX100. It was anticipated that if h6.1 had a weak interaction with the membrane, then it would be released by

re-centrifugation. Similarly, if the enzyme was either peripherally bound or an integral membrane protein, then the activity would have been released by sodium chloride and TX100 respectively. Irrespective of treatment, the activity remained in the pellet fraction. The insoluble pellet fraction of each YMS11, YMS12, HYB1 and 10AORF could be an artifact of the expression in yeast, as h6.1 expressed in COS-1 cells is exclusively cytosolic (Sullivan et al 1994). The pellet material could also represent either a sediment of partially broken cells which settle upon centrifugation, or simply an aggregate of protein.

Comparison of the catalytic activities of YMS11, YMS12, HYB1 and 10AORF showed that each form hydrolysed cyclic AMP with high affinity and displayed linear kinetics (figs 4.2.5 - 4.2.8, table 6). Statistical analysis (table 6) of the K_m values calculated for each enzyme form, demonstrated that the values were not significantly different from h6.1, with the exception of 10AORF ($p=0.025$). YMS11, YMS12, HYB1, 10AORF and h6.1 all share an identical core catalytic region which would explain the observed similarity in the K_m . The N-terminally extended version of h6.1, 10AORF, hydrolysed cyclic AMP with a significantly lower K_m than that calculated for h6.1 (table 6). This would suggest that the N-terminal region of 10AORF can affect substrate hydrolysis. Shakur et al (1995) have previously shown the regulation of catalytic activity by the N-terminal region of a rat PDE4A enzyme RD1. In this case, the relative V_{max} values calculated for RD1 and the N-terminally truncated species met²⁶RD1, showed that the extended N-terminal region of RD1 was inhibitory. Further studies on a splice variant of RD1, RPDE6 (McPhee et al 1995), in rat brain showed that the alternative splicing of the N-terminus allows a further attenuation of catalytic activity. Thus, it seems likely that the difference found in the K_m value between h6.1 and the N-terminally extended 10AORF is a true observation, considering the evidence reported for the control of catalysis by the N-terminus of proteins encoded by a related rat gene. Whether differences in the V_{max} values exist between enzymes

reported in this present study remains to be determined. It was an aim of this study to calculate such values, using an h6.1 antiserum. The h6.1 antiserum could have been used to immunoprecipitate equal amounts of activity from each of the yeast strains. Thus, one could define relative V_{\max} values, and determine any differences in such, for each yeast strain. This has already been shown for RD1 expressed in COS-1 cells (Shakur et al 1995), to demonstrate a reduced V_{\max} for RD1 as compared to the truncated met²⁶RD1. However, this present study was unable to determine relative V_{\max} values for either YMS11, YMS12, HYB1, 10AORF or h6.1 due to the inability to produce an h6.1 antisera (Dr Neil Brown). Despite repeated attempts using several peptides a suitable antibody could not be produced.

Comparison of the K_m values calculated for YMS11, YMS12 and HYB1 showed that there was no significant difference with that of h6.1 (table 6). The K_m value calculated for 10AORF was found to be significantly different from h6.1, which suggests a role for the N-terminally extended region of 10AORF in catalysis. The next stage in this study was to determine differences, if any, between the various enzyme forms with respect to the inhibition by the PDE4 inhibitor rolipram, and thus, elucidate a possible role for the N and C termini of h6.1 in the interaction with inhibitor. In order to do this, IC₅₀ values were calculated from the dose-response curves to rolipram for each of the enzyme forms (figs 4.2.9 - 4.2.12). Statistical analysis of these values (table 6) have shown a significant difference between the IC₅₀ for each enzyme from h6.1, with the most significant being YMS11, YMS12 and HYB1. This observation indicates that both the N and C termini have a role in the interaction of inhibitor. Of particular importance is the observation that YMS11, which consists of only the catalytic unit, can still bind and interact with inhibitor despite the lack of flanking N and C terminal regions. The most profound difference was shown between the IC₅₀ to inhibit 10AORF as compared to either YMS11, YMS12 or HYB1, where approximately ten fold less inhibitor

was necessary to inhibit 10AORF. Thus, although the C-terminal region does play a role in inhibitor interaction, as shown by the elevated IC_{50} compared to h6.1 for YMS11 and YMS12, the N-terminus is likely to be more important.

The N-terminus of h6.1, and the extended N-terminus of 10AORF must contain specific information for inhibitor interaction. Removal of either the C-terminus only (YMS12), or the N and C termini together (YMS11), have similar effects with respect to the IC_{50} , which suggests that any truncation of the h6.1 sequence disrupts the way in which the protein folds and orientates for interaction with substrate and inhibitor. It is the conclusion of this study, however, that the N-terminus is more important in these functions. Evidence to support this is that the extension of the N-terminus of h6.1 enhances catalysis and interaction with inhibitor, where approximately ten fold less inhibitor is necessary to inhibit substrate hydrolysis of 10AORF than either of the truncates or HYB1. Additionally, substitution of the N-terminus with a different sequence (HYB1) from h6.1, causes an increase in the IC_{50} for rolipram inhibition (table 6). Taken together, this evidence supports a role for the N-terminal region in allowing the optimal orientation and conformation necessary, for catalysis and interaction with inhibitor.

With the observation that 10AORF was more potently inhibited by rolipram than h6.1 (table 6), the next stage was to investigate whether this increased sensitivity arose from an alteration in the kinetics of inhibition. As described in chapter 3, rolipram was shown to be a simple competitive inhibitor of h6.1. In this chapter a comparative analysis for rolipram inhibition was carried out for 10AORF. Linear Lineweaver-Burke (fig. 4.2.13) and Dixon (fig 4.2.14) plots were obtained for 10AORF. Using the Lineweaver-Burke plot data (fig. 4.2.13), slope replots (4.2.15) were constructed which were shown to be curvilinear as found with the hPDE4A_{Livi} enzyme (chapter 3, fig. 3.2.16). It would seem therefore, that 10AORF is partially competitively inhibited by rolipram, whereas h6.1 is competitively inhibited. This data would suggest that

the extended N-terminal domain of 10AORF, alters the conformation of the active site to allow both substrate and inhibitor to bind at the same time. A schematic representation of partial competitive inhibition is shown in chapter 3, fig. 3.2.17.

Measurement of an enzymes thermostability, over a time course, at a fixed temperature, can provide two important pieces of information. Firstly, the $t_{0.5}$ value, that is, the time at which activity decays to half maximal, gives an indication as to how stable the enzyme is. Therefore, it is possible to determine if alterations to the enzyme structure, similarly alter enzyme stability. Secondly, the progress of the time course gives an indication of whether the sample which is being assayed, consists of a single or mixed population of enzyme. Using this experimental method the thermostability, at 45°C, was measured for each 10AORF, YMS12 and HYB1. The resultant $t_{0.5}$ values would reveal if changes to the N-terminal region of h6.1, either the extension of this region (10AORF), or sequence substitution (HYB1), affected the thermostability. In addition, measurement of the thermostability of YMS12 would show if the C-terminal region had any influence. Shown in figure 4.2.16 are the plots of log percentage activity versus time for 10AORF, YMS12 and HYB1. Each enzyme form decayed as a single exponential, thus, the enzyme activity assayed is represented by a single population. Statistical analysis of this data (table 7) has shown that the N-terminus of h6.1 has a vital role in stability of the enzyme. The extension of h6.1 N-terminal region, in 10AORF, increased the thermostability by more than three fold. This $t_{0.5}$ value calculated for 10AORF was significantly greater than that calculated for h6.1 ($p=0.0001$ table 7). Similarly, the domain swop contained within the sequence of HYB1, was shown to cause a significant reduction in the thermostability of h6.1 activity ($p=0.001$ table 7). The truncation of the C-terminal region (YMS12) had the least significant effect on thermostability ($p=0.021$ table 7). The extension of the N-terminal region of h6.1 (10AORF) increased enzyme thermostability,

presumably, by allowing the protein to adopt a conformation in which the enzyme could resist thermal denaturation. By swapping the N-terminal domain of 2EL with h6.1 (HYB1), and therefore changing the sequence of the N-terminal region, the ability to resist thermal denaturation was reduced compared to h6.1. This loss of thermostability presumably occurred, because the protein could not adopt the same conformation as h6.1 due to N-terminal sequence differences. Thus, the $t_{0.5}$ value of HYB1 was reduced significantly lower than that of h6.1 ($p=0.001$ table 7). The observation in this study, that protein N-terminal regions promote stability of enzyme activity is not a novel one. The N-terminal region of the PDE4A RD1 was shown by Shakur et al (1993) to be necessary for enzyme stability. The N-terminal truncate met²⁶RD1 displayed a $t_{0.5}$ value which was less than that calculated for RD1.

Studies on the rat PDE4A species (McPhee et al 1995, Shakur et al 1993, 1995) has highlighted the important contributory role of the N-terminal domain of these enzymes in cell location, thermostability and enzyme activity (see discussion section chapter 5). As described in chapter 5, the N-terminal domain of the rat enzyme had profound effects on V_{max} and thermostability. By analogy to the rat species, this study has determined an important role of the N-terminal domain of the human species in thermostability, substrate hydrolysis and inhibitor interaction. Analysis of the mechanism by which rolipram inhibited 10AORF has indicated that a change in the enzyme conformation had occurred from that of h6.1. This change in conformation allowed a switch from competitive inhibition (h6.1) to partial competitive inhibition (10AORF). Evidence in support of a conformational change is provided by the thermostability data (fig. 4.2.16, table 7). At 45°C, 10AORF was shown to be significantly more thermostable than h6.1, which would indicate that a conformational change had occurred.

Originally it was thought that the amino acid differences seen between hPDE4A_{Livi} and h6.1 were the cause of the differences in mechanism

of inhibition by rolipram. However, this study conducted on 10AORF would dispute this since partial competitive inhibition was seen with rolipram, as per hPDE4A_{Ljvi}. It is the conclusion of this study that a conformational change occurred to the 10AORF enzyme, induced by the N-terminal domain extension. This could account for the difference in kinetics of rolipram inhibition seen with h6.1. The reason for kinetic differences, with respect to inhibition by rolipram, between h6.1 and hPDE4A_{Ljvi} remain unclear. However, it is possible that a modification to hPDE4A_{Ljvi} occurred during the enzyme preparation.

Future studies are likely to focus on the investigation of h6.1 and 10AORF *in vivo*. Indeed, studies are necessary to investigate the functions of the various true splice variants of the human PDE4A gene isolated so far, such as PDE46, TM3 (Bolger et al 1993), 2EL (Horton et al 1995). It will also be necessary to establish if a protein of the size of h6.1 is expressed *in vivo*. This would clarify if h6.1 is a true splice variant of the PDE4A gene, as 2EL is, or simply a truncated protein of the PDE46 sequence. Irrespective of this, h6.1 provides a good model for the pharmacological investigation of PDE4A selective inhibitors, since its sequence includes the catalytic domain.

Table 5 **Specific Activities of PDE Activity in *Saccharomyces cerevisiae* Expressing HYB1, YMS11, YMS12 and 10AORF**

Enzyme Species	Specific Activity (pmol/min/mg)	
	Pellet	Soluble
HYB1	1.14 ± 0.3	1.4 ± 0.4
10AORF	21.7 ± 1.7	15.7 ± 1.8
YMS11	0.43 ± 0.1	0.76 ± 0.2
YMS12	5.99 ± 1.2	0.46 ± 0.2

The results are shown as mean ± standard deviation for three separate preparations.

Table 6 K_m cyclic AMP and IC_{50} rolipram Data for Soluble HYB1, YMS11, YMS12 and 10AORF, in Comparison with h6.1

Enzyme Species	K_m cyclic AMP (μM)	IC_{50} rolipram (μM)
h6.1	4.1 \pm 1.7	0.51 \pm 0.15
HYB1	2.04 \pm 0.2	1.93 \pm 0.23 (p=0.0001)
10AORF	1.9 \pm 0.2 (p=0.025)	0.19 \pm 0.02 (p=0.004)
YMS11	4.3 \pm 1.3	2.4 \pm 0.2 (p=0.0001)
YMS12	5.9 \pm 0.7	1.7 \pm 0.14 (p=0.0001)

Values are shown as mean \pm standard deviation for at least three separate experiments.

Data in parenthesis are significance values calculated using the students t - test. The significance values were calculated to examine differences between h6.1 and the other enzyme species.

IC_{50} was the concentration which resulted in 50% inhibition of enzyme activity.

Table 7 **Thermostability Values Calculated for Soluble YMS12, 10AORF and HYB1 at 45°C, and Comparison with h6.1**

Enzyme Species	Thermostability at 45°C (t _{0.5})	Significance Value Students t-test
h6.1	10 minutes	
YMS12	13 minutes	p=0.021
10AORF	>30 minutes	p=0.0001
HYB1	3 minutes	p=0.001

Significance values were calculated using the students t -test to compare the values for HYB1, YMS12 and 10AORF with h6.1.

Fig. 4.1.1 **Schematic Alignment of Mammalian PDE**
Isoform Families

This figure diagrammatically shows the structural features of mammalian PDE isoforms. (Beavo & Reifsnyder 1990).

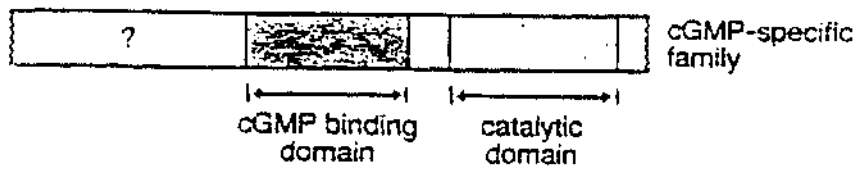
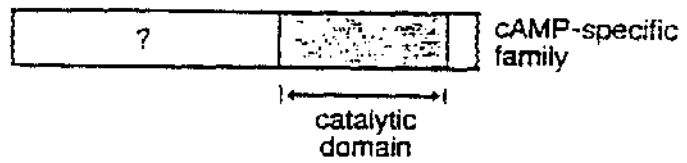
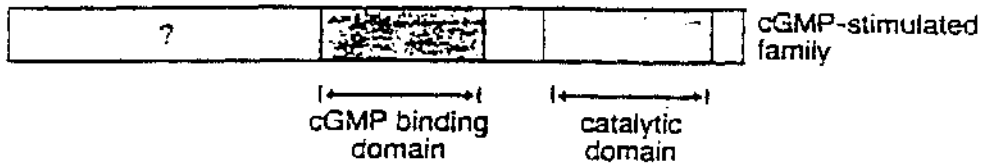
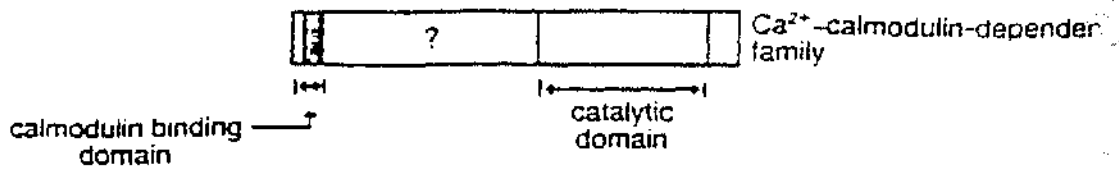
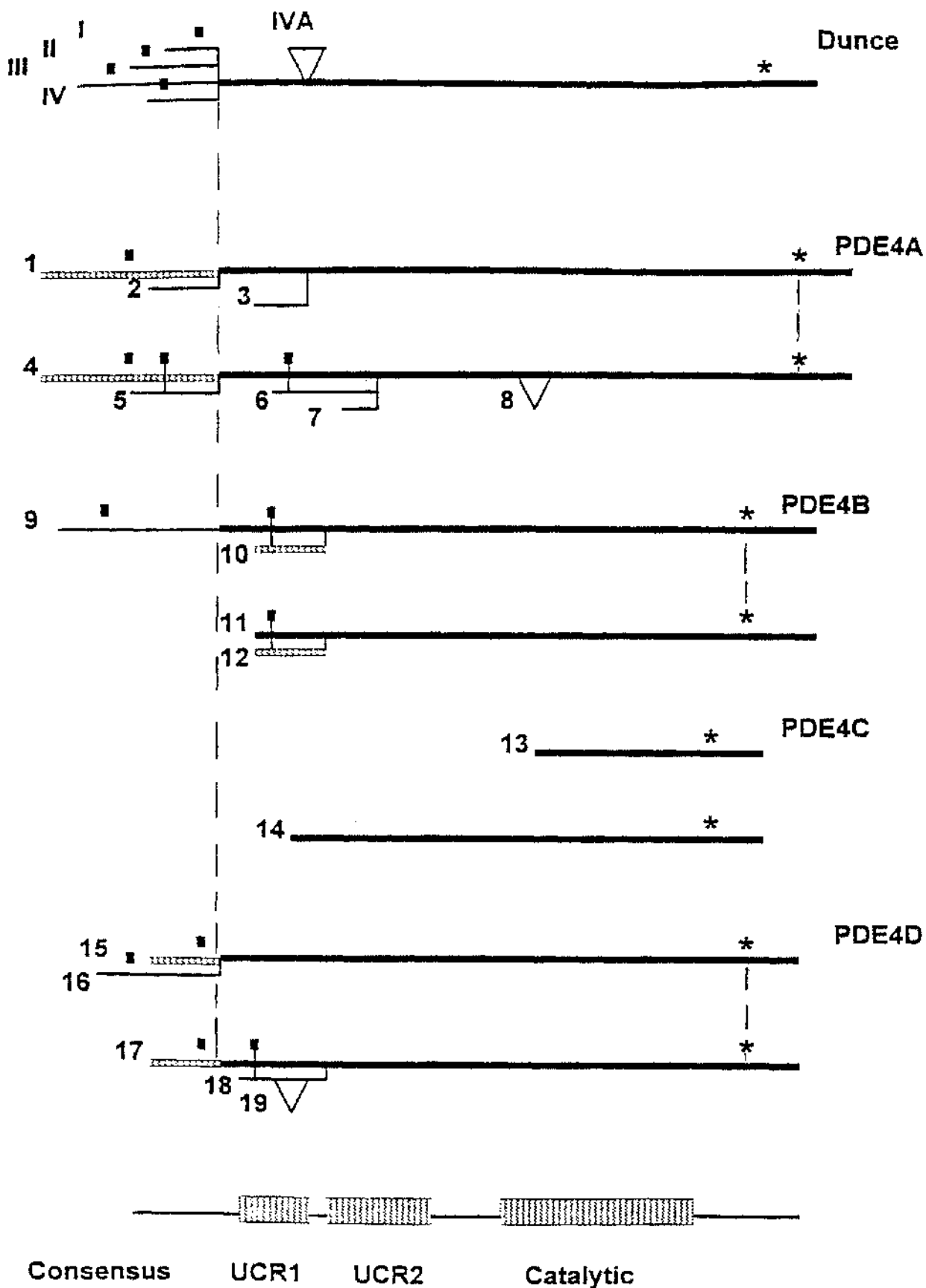


Fig. 4.1.2

Alignment of Human and Rat PDE4 mRNA

Shown is the schematic representation of the four human and rat PDE4 mRNA's, at the top and bottom respectively. Common sequences are shown by heavy merged lines. Areas of unique sequence which are conserved between human and rats, and are unique to any PDE4 subtype are shown by the thin cross hatched lines. Thin solid lines indicate variant sequence which is not conserved between human and rat. Triangles in the rat clones show variants lacking a block of sequence as compared to other transcripts from the same locus. Initiation codons are shown by small boxes and termination codons by *. Vertical dashed lines show splice points that occur in homologous positions in clones from different loci. Roman numerals show various alternative spliced isoforms from the *dunc* locus.

(Bolger et al 1993).



Consensus

UCR1

UCR2

Catalytic

**Fig. 4.2.1 Schematic Representation of Truncations of
h6.1**

Shown diagrammatically are the truncations made to the sequence of h6.1 to obtain YMS10, YMS11 and YMS12.

h6.1

Met ——— Glu ←———— Glu ——— Thr/Stop
1 168 601 686

YMS10

Met/Glu ——— Glu ——— Thr/Stop
168 601 686

YMS11

Met/Glu ——— Glu ——— Thr/Stop
168 601 686

YMS12

Met ——— Glu ——— Glu/Stop
1 168 601

Fig. 4.2.2

**Alignment of the Sequences of h6.1, HYB1
and 2EL**

Sequence alignments were made using the Gene Jockey programme, and were aligned to the sequence of h6.1. The amino acids of h6.1 which are different to that of hPDE4A_{Ljvj} are shown boxed.

10 20 30 40 50

Contig# 1
h6.1 aa ORF engineered MCPFPVTVPLGGPTFPVCKATLSEETCQQLARETLEELDWCLEQLETMQTYRSVSE
HYB 1 pep sandoz
2EL peptide

60 70 80 90 100 110

Contig# 1
h6.1 aa ORF engineered MASHKFKRMLNRELTHLSEMSRSONQVSEYISTTFLDKQNEVEIPSPITMKERERKQQ
HYB 1 pep sandoz
2EL peptide

120 130 140 150 160

Contig# 1
h6.1 aa ORF engineered APRPRPSQPPPPVPHLQPMSSQITGLKKLMHSNSLNNSNIPRFGVKTDQEELLAQE
HYB 1 pep sandoz MVLPDQGFKLLGNVLQGPPEPYRLLTSGLRRLHQE
2EL peptide MVLPDQGFKLLGNVLQGPPEPYRLLTSGLRRLHQE

170 180 190 200 210 220

Contig# 1
h6.1 aa ORF engineered
HYB 1 pep sandoz LENLNKWLNIIFCVSDYAGGRSLTCIMYMIHQERDLLKKFRIPVDITMVTYMLTLED
2EL peptide LENLNKWLNIIFCVSDYAGGRSLTCIMYMIHQERDLLKKFRIPVDITMVTYMLTLED
LENLNKWLNIIFCVSDYAGGRSLTCIMYMIHQERDLLKKFRIPVDITMVTYMLTLED

230 240 250 260 270 280

Contig# 1
h6.1 aa ORF engineered
HYB 1 pep sandoz HYHADVAYHNSLHAADVLOSTHVLLATPALDAVFTDLEILAALFAAAIHDVDHPGV
2EL peptide HYHADVAYHNSLHAADVLOSTHVLLATPALDAVFTDLEILAALFAAAIHDVDHPGV

290 300 310 320 330

Contig# 1
h6.1 aa ORF engineered
HYB 1 pep sandoz SNQFLINTNSELALMYNDESVLNHHLAVGFKLLQEDNCDIFQNL SKRQRQSLRKM
2EL peptide SNQFLINTNSELALMYNDESVLNHHLAVGFKLLQEDNCDIFQNL SKRQRQSLRKM
SNQFLINTNSELALMYNDESVLNHHLAVGFKLLQEDNCDIFQNL SKRQRQSLRKM

340 350 360 370 380 390

Contig# 1
h6.1 aa ORF engineered
HYB 1 pep sandoz VIDMVLATDMSKHM TLLADLKT MVETKKVTSSGVLLLDNYSDRIQVLRNMVHCADL
2EL peptide VIDMVLATDMSKHM TLLADLKT MVETKKVTSSGVLLLDNYSDRIQVLRNMVHCADL
VIDMVLATDMSKHM TLLADLKT MVETKKVTSSGVLLLDNYSDRIQVLRNMVHCADL

400 410 420 430 440

Contig# 1
h6.1 aa ORF engineered
HYB 1 pep sandoz SNPTKPLELYRQWTDRI MAEFFQQGDRERERGMETSPMCDKHTASVEKSQVGFIDY
2EL peptide SNPTKPLELYRQWTDRI MAEFFQQGDRERERGMETSPMCDKHTASVEKSQVGFIDY
SNPTKPLELYRQWTDRI MAEFFQQGDRERERGMETSPMCDKHTASVEKSQVQARGI

450 460 470 480 490 500

Contig# 1
h6.1 aa ORF engineered IVHPLWETWADLVHPDAQEILD TLEDNRDWYSAIRQSPSPPEEESRGGHPPLP
HYB 1 pep sandoz IVHPLWETWADLVHPDAQEILD TLEDNRDWYSAIRQSPSPPEEESRGGHPPLP
2EL peptide DGRAQGGFY

510 520 530 540 550 560

Contig# 1
h6.1 aa ORF engineered DKFQFELTLEEEEEEEI SMAQIFCTAQEALTEQGLSGVEEALDATI AWEASPAQES
HYB 1 pep sandoz DKFQFELTLEEEEEEEI SMAQIFCTAQEALTEQGLSGVEEALDATI AWEASPAQES
2EL peptide

570 580 590 600 610
| | | | |

Contig# 1
h6.1 aa ORF engineered LEVMAQEASLEAELEAVYLTOQAQSTGSA[PVAPDEFSS]REEFWAVSHSSPSALAL
HYB 1 pep sandoz LEVMAQEASLEAELEAVYLTOQAQSTGSA[PVAPDEFSS]REEFWAVSHSSPSALAL
2EL peptide

620 630 640 650 660 670
| | | | | |

Contig# 1
h6.1 aa ORF engineered QSPLLPAWRTL SVSEHAPGLPGLPSTAAEVEAQREHQAAKRACCSACAGTFGEDTSA
HYB 1 pep sandoz QSPLLPAWRTL SVSEHAPGLPGLPSTAAEVEAQREHQAAKRACCSACAGTFGEDTSA
2EL peptide

680
|

Contig# 1
h6.1 aa ORF engineered LPAPGGGGSGGDPT
HYB 1 pep sandoz LPAPGGGGSGGDPT
2EL peptide

Fig. 4.2.3

**Alignment of the Sequences of 10AORF and
PDE46**

Sequence alignments were made using the Gene Jockey programme, and were aligned to the sequence of PDE46 (top sequence).

10 20 30 40 50 60 70
MEPPTVPSERSLSLSLPGPREGQATLKPPPQHLWRQPRTPIRIQQRGYSDSAERAEREROPHRPIERADAMDTSDRP
.....
IPALPGPREGQATLKPPPQHLWRQPRTPIRIQQRGYSDSAERAEREROPHRPIERADAMDTSDRP

10 20 30 40 50 60
80 90 100 110 120 130 140 150
GLRTTRMSWPSSFHGTGTGSGGAGGGSSRRFEAENGPTPSPGRSPLDSQASPLVLHAGAATSQRRESFLYRSDSDY
.....
GLRTTRMSWPSSFHGTGTGSGGAGGGSSRRFEAENGPTPSPGRSPLDSQASPLVLHAGAATSQRRESFLYRSDSDY

150 160 170 180 190 200 210 220 230
DMSPKIMSRNSSVTSEAHAEDLIVTPFAQVLASLRSVRSNFSLLTNVPVPSNKRSPGLGGPTPVCKATLSEETCOOLA
.....
DMSPKIMSRNSSVTSEAHAEDLIVTPFAQVLASLRSVRSNFSLLTNVPVPSNKRSPGLGGPTPVCKATLSEETCOOLA

240 250 260 270 280 290 300
RETLEELDWCLEOLETMQTYRSVSEMA SHKFKRMLNRELTHLSEMSRSGNQVSEYISTTFLDKQNEVEI P SPTMKER
.....
RETLEELDWCLEOLETMQTYRSVSEMA SHKFKRMLNRELTHLSEMSRSGNQVSEYISTTFLDKQNEVEI P SPTMKER

310 320 330 340 350 360 370 380
EKQQAPRPRPSQPPPPVPHLQPM SQITGLK KLMHNSLNN SNIPRFGVKTDQEELLAQEL ENLNK WGLNIFCVSDY
.....
EKQQAPRPRPSQPPPPVPHLQPM SQITGLK KLMHNSLNN SNIPRFGVKTDQEELLAQEL ENLNK WGLNIFCVSDY

390 400 410 420 430 440 450 460
AGGRSLTCIMYMI FQERDLLK KFRIPVD TMV TYMLTLEDHYHADVAYHNSLHAADV LQSTHVLLATPALDAVFTDLE
.....
AGGRSLTCIMYMI FQERDLLK KFRIPVD TMV TYMLTLEDHYHADVAYHNSLHAADV LQSTHVLLATPALDAVFTDLE

470 480 490 500 510 520 530
ILAAALFAAAIHVDVHPGVSNOFLINTINSELALMYNDESVLENHHLAVGFKLLQEDNCDIFQNL SKRQRQSLRKMVID
.....
ILAAALFAAAIHVDVHPGVSNOFLINTINSELALMYNDESVLENHHLAVGFKLLQEDNCDIFQNL SKRQRQSLRKMVID

540 550 560 570 580 590 600 610
| | | | | | | |
MVLATDMSKHMILLADLKTMTVETKKVTS S G V L L L D N Y S D R I Q V L R N M V H C A D L S N P T K P L E L Y R Q W T D R I M A E F F Q Q
.....
MVLATDMSKHMILLADLKTMTVETKKVTS S G V L L L D N Y S D R I Q V L R N M V H C A D L S N P T K P L E L Y R Q W T D R I M A E F F Q Q
| | | | | | | |
530 540 550 560 570 580 590 600

620 630 640 650 660 670 680 690
| | | | | | | |
G D R E R E R G M E I S P M C D K H T A S V E K S Q V G F I D Y I V H P L W E T W A D L V H P D A Q E I L D T L E D N R D W Y Y S A I R Q S P S P P P E E
.....
G D R E R E R G M E I S P M C D K H T A S V E K S Q V G F I D Y I V H P L W E T W A D L V H P D A Q E I L D T L E D N R D W Y Y S A I R Q S P S P P P E E
| | | | | | | |
610 620 630 640 650 660 670 680

700 710 720 730 740 750 760 77
| | | | | | | |
E S R G P G H P P L P D K F Q F E L T L E E E E E E E I S M A Q I P C T A Q E A L T A Q G L S G V E E A L D A T I A W E A S P A Q E S L E V M A Q E A S L
.....
E S R G P G H P P L P D K F Q F E L T L E E E E E E E I S M A Q I P C T A Q E A L T E Q G L S G V E E A L D A T I A W E A S P A Q E S L E V M A Q E A S L
| | | | | | | |
690 700 710 720 730 740 750

780 790 800 810 820 830 840
| | | | | | | |
E A E L E A V Y L T Q Q A Q S T G S A P V A P D E F S S R E E F V V A V S H S S P S A L A L Q S P L L P A W R T L S V S E H A P G L P G L P S T A A E V E
.....
E A E L E A V Y L T Q Q A Q S T G S A P V A P D E F S S R E E F
| | | | | | | |
760 770 780 790

850 860 870 880
| | | |
A Q R E H Q A A K R A C S A C A G T F G E D T S A L P A P C C G G S G C D P T

Fig. 4.2.4

**Alignment of the Sequences of h6.1, HYB1,
2EL, YMS10, YMS11, YMS12, 10AORF and
PDE46**

Sequence alignments were made using the Gene Jockey programme, and were aligned to the sequence of PDE46. The amino acids of h6.1 which are different to that of hPDE4A_{Ljvi} are shown boxed.

10 20 30 40 50
| | | | |
Contig# 1
h6.1 aa ORF engineered
HYB 1 pep sandoz
YMS11/PEPTIDE
HPDE46.PEP MEPPTVPSEERSLSLSLPGPREGQATLKPPFQHLWRQPRTPIRIQQRGYSDSAERAE
YMS12
YMS10/PEPTIDE

60 70 80 90 100 110
| | | | | |
Contig# 1
h6.1 aa ORF engineered
HYB 1 pep sandoz
YMS11/PEPTIDE
HPDE46.PEP RERQPHRPIERADAMDTSDRPGRLRTRMSWPSSFHGTGTGSGGAGGGSSRRFEAEN
YMS12
YMS10/PEPTIDE

120 130 140 150 160
| | | | |
Contig# 1
h6.1 aa ORF engineered
HYB 1 pep sandoz
YMS11/PEPTIDE
HPDE46.PEP GPTPSPGRSPLDSQASPLVLHAGAAATSQRRESFLYRSDSDYDMSPKTMSRNSSVT
YMS12
YMS10/PEPTIDE

170 180 190 200 210 220
| | | | | |
Contig# 1
h6.1 aa ORF engineered MVLPSDQGCFFVTTVPLGGPTPVCKATLSE
HYB 1 pep sandoz
YMS11/PEPTIDE
HPDE46.PEP SEAHAEADLIVTPFAQVLASLRSVRSNFSLLTNVPVPSNKRSPPLGGPTPVCKATLSE
YMS12 MVLPSDQGCFFVTTVPLGGPTPVCKATLSE
YMS10/PEPTIDE

230 240 250 260 270 280
| | | | | |
Contig# 1
h6.1 aa ORF engineered ETCQQLARETLEELDWCLEQLETMQTYRSVSEMASHKFKRMLNRELTHLSEMSRSG
HYB 1 pep sandoz
YMS11/PEPTIDE
HPDE46.PEP ETCQQLARETLEELDWCLEQLETMQTYRSVSEMASHKFKRMLNRELTHLSEMSRSG
YMS12 ETCQQLARETLEELDWCLEQLETMQTYRSVSEMASHKFKRMLNRELTHLSEMSRSG
YMS10/PEPTIDE

290 300 310 320 330
| | | | |
Contig# 1
h6.1 aa ORF engineered NQVSEYISTTFLDKQNEVEIIPSPMKEREKQQAAPRPRPSQPPPPVPVPHLQPMSSIT
HYB 1 pep sandoz
YMS11/PEPTIDE
HPDE46.PEP NQVSEYISTTFLDKQNEVEIIPSPMKEREKQQAAPRPRPSQPPPPVPVPHLQPMSSIT
YMS12 NQVSEYISTTFLDKQNEVEIIPSPMKEREKQQAAPRPRPSQPPPPVPVPHLQPMSSIT
YMS10/PEPTIDE

340 350 360 370 380 390
| | | | | |
Contig# 1
h6.1 aa ORF engineered GLKCLMHSNSLNNSNI PRFGVKT DQEELLAQELLENLNKWLNI FCVSDYAGGRSLT
HYB 1 pep sandoz MFKLLGNVLQGEPEYRLTSGRLRLHQELENLNKWLNI FCVSDYAGGRSLT
YMS11/PEPTIDE MELENLNKWLNI FCVSDYAGGRSLT
HPDE46.PEP GLKCLMHSNSLNNSNI PRFGVKT DQEELLAQELLENLNKWLNI FCVSDYAGGRSLT
YMS12 GLKCLMHSNSLNNSNI PRFGVKT DQEELLAQELLENLNKWLNI FCVSDYAGGRSLT
YMS10/PEPTIDE MELENLNKWLNI FCVSDYAGGRSLT

400 410 420 430 440
| | | | |
Contig# 1
h6.1 aa ORF engineered C I M Y M I F Q E R D L L K K F R I P V D T M V T Y M L T L E D H Y H A D V A Y H N S L H A A D V L Q S T H V L
HYB 1 pep sandoz C I M Y M I F Q E R D L L K K F R I P V D T M V T Y M L T L E D H Y H A D V A Y H N S L H A A D V L Q S T H V L
YMS11/PEPTIDE C I M Y M I F Q E R D L L K K F R I P V D T M V T Y M L T L E D H Y H A D V A Y H N S L H A A D V L Q S T H V L
HPDE46.PEP C I M Y M I F Q E R D L L K K F R I P V D T M V T Y M L T L E D H Y H A D V A Y H N S L H A A D V L Q S T H V L
YMS12 C I M Y M I F Q E R D L L K K F R I P V D T M V T Y M L T L E D H Y H A D V A Y H N S L H A A D V L Q S T H V L
YMS10/PEPTIDE C I M Y M I F Q E R D L L K K F R I P V D T M V T Y M L T L E D H Y H A D V A Y H N S L H A A D V L Q S T H V L

450 460 470 480 490 500
| | | | | |
Contig# 1
h6.1 aa ORF engineered L A T P A L D A V F T D L E I L A A L F A A A I H D V D H P G V S N Q F L I N T N S E L A L M Y N D E S V L E N
HYB 1 pep sandoz L A T P A L D A V F T D L E I L A A L F A A A I H D V D H P G V S N Q F L I N T N S E L A L M Y N D E S V L E N
YMS11/PEPTIDE L A T P A L D A V F T D L E I L A A L F A A A I H D V D H P G V S N Q F L I N T N S E L A L M Y N D E S V L E N
HPDE46.PEP L A T P A L D A V F T D L E I L A A L F A A A I H D V D H P G V S N Q F L I N T N S E L A L M Y N D E S V L E N
YMS12 L A T P A L D A V F T D L E I L A A L F A A A I H D V D H P G V S N Q F L I N T N S E L A L M Y N D E S V L E N
YMS10/PEPTIDE L A T P A L D A V F T D L E I L A A L F A A A I H D V D H P G V S N Q F L I N T N S E L A L M Y N D E S V L E N

510 520 530 540 550 560
| | | | | |
Contig# 1
h6.1 aa ORF engineered H H L A V G F K L L Q E D N C D I F Q N L S K R Q R Q S L R K M V I D M V L A T D M S K H M T L L A D L K T M V
HYB 1 pep sandoz H H L A V G F K L L Q E D N C D I F Q N L S K R Q R Q S L R K M V I D M V L A T D M S K H M T L L A D L K T M V
YMS11/PEPTIDE H H L A V G F K L L Q E D N C D I F Q N L S K R Q R Q S L R K M V I D M V L A T D M S K H M T L L A D L K T M V
HPDE46.PEP H H L A V G F K L L Q E D N C D I F Q N L S K R Q R Q S L R K M V I D M V L A T D M S K H M T L L A D L K T M V
YMS12 H H L A V G F K L L Q E D N C D I F Q N L S K R Q R Q S L R K M V I D M V L A T D M S K H M T L L A D L K T M V
YMS10/PEPTIDE H H L A V G F K L L Q E D N C D I F Q N L S K R Q R Q S L R K M V I D M V L A T D M S K H M T L L A D L K T M V

570 580 590 600 610
| | | | |
Contig# 1
h6.1 aa ORF engineered E T K K V T S S G V L L L D N Y S D R I Q V L R N M V H C A D L S N P T K P L E L Y R Q W T D R I M A E F F Q Q
HYB 1 pep sandoz E T K K V T S S G V L L L D N Y S D R I Q V L R N M V H C A D L S N P T K P L E L Y R Q W T D R I M A E F F Q Q
YMS11/PEPTIDE E T K K V T S S G V L L L D N Y S D R I Q V L R N M V H C A D L S N P T K P L E L Y R Q W T D R I M A E F F Q Q
HPDE46.PEP E T K K V T S S G V L L L D N Y S D R I Q V L R N M V H C A D L S N P T K P L E L Y R Q W T D R I M A E F F Q Q
YMS12 E T K K V T S S G V L L L D N Y S D R I Q V L R N M V H C A D L S N P T K P L E L Y R Q W T D R I M A E F F Q Q
YMS10/PEPTIDE E T K K V T S S G V L L L D N Y S D R I Q V L R N M V H C A D L S N P T K P L E L Y R Q W T D R I M A E F F Q Q

620 630 640 650 660 670
| | | | | |
Contig# 1
h6.1 aa ORF engineered G D R E R E R G M E I S P M C D K H T A S V E K S Q V G F I D Y I V H P L W E T W A D L V H P D A Q E I L D T L
HYB 1 pep sandoz G D R E R E R G M E I S P M C D K H T A S V E K S Q V G F I D Y I V H P L W E T W A D L V H P D A Q E I L D T L
YMS11/PEPTIDE G D R E R E R G M E I S P M C D K H T A S V E K S Q V G F I D Y I V H P L W E T W A D L V H P D A Q E I L D T L
HPDE46.PEP G D R E R E R G M E I S P M C D K H T A S V E K S Q V G F I D Y I V H P L W E T W A D L V H P D A Q E I L D T L
YMS12 G D R E R E R G M E I S P M C D K H T A S V E K S Q V G F I D Y I V H P L W E T W A D L V H P D A Q E I L D T L
YMS10/PEPTIDE G D R E R E R G M E I S P M C D K H T A S V E K S Q V G F I D Y I V H P L W E T W A D L V H P D A Q E I L D T L

680 690 700 710 720
| | | | |
Contig# 1
h6.1 aa ORF engineered E D N R D W Y S A I R Q S P S P P P E E S R G P G H P P L P D K F Q F E L T L E E E E E E E I S M A Q I P C
HYB 1 pep sandoz E D N R D W Y S A I R Q S P S P P P E E S R G P G H P P L P D K F Q F E L T L E E E E E E E I S M A Q I P C
YMS11/PEPTIDE E D N R D W Y S A I R Q S P S P P P E E S R G P G H P P L P D K F Q F E L T L E E E E E E E I S M A Q I P C
HPDE46.PEP E D N R D W Y S A I R Q S P S P P P E E S R G P G H P P L P D K F Q F E L T L E E E E E E E I S M A Q I P C
YMS12 E D N R D W Y S A I R Q S P S P P P E E S R G P G H P P L P D K F Q F E L T L E E E E E E E I S M A Q I P C
YMS10/PEPTIDE E D N R D W Y S A I R Q S P S P P P E E S R G P G H P P L P D K F Q F E L T L E E E E E E E I S M A Q I P C

730 740 750 760 770 780
| | | | | |
Contig# 1
h6.1 aa ORF engineered T A Q E A L T E Q G L S G V E E A L D A T I A W E A S P A Q E S L E V M A Q E A S L E A E L E A V Y L T Q Q A Q
HYB 1 pep sandoz T A Q E A L T E Q G L S G V E E A L D A T I A W E A S P A Q E S L E V M A Q E A S L E A E L E A V Y L T Q Q A Q
YMS11/PEPTIDE T A Q E A L T E Q G L S G V E E A L D A T I A W E A S P A Q E S L E V M A Q E A S L E A E L E A V Y L T Q Q A Q
HPDE46.PEP T A Q E A L T A Q G L S G V E E A L D A T I A W E A S P A Q E S L E V M A Q E A S L E A E L E A V Y L T Q Q A Q
YMS12 T A Q E A L T E Q G L S G V E E A L D A T I A W E A S P A Q E S L E V M A Q E A S L E A E L E A V Y L T Q Q A Q
YMS10/PEPTIDE T A Q E A L T E Q G L S G V E E A L D A T I A W E A S P A Q E S L E V M A Q E A S L E A E L E A V Y L T Q Q A Q

	790	800	810	820	830	840
Contig# 1					
h6.1 aa ORF engineered	STGSAPVAPDEFSSREEFVVAVSHSSPSALALQSPLLPAWRTL SVSEHAPGLPGLF					
HYB 1 pep sandoz	STGSAPVAPDEFSSREEFVVAVSHSSPSALALQSPLLPAWRTL SVSEHAPGLPGLF					
YMS11/PEPTIDE	STGSAPVAPDEFSSREE					
HPDE46.PEP	STGSAPVAPDEFSSREEFVVAVSHSSPSALALQSPLLPAWRTL SVSEHAPGLPGLF					
YMS12	STGSAPVAPDEFSSREE					
YMS10/PEPTIDE	STGSAPVAPDEFSSREEFVVAVSHSSPSALALQSPLLPAWRTL SVSEHAPGLPGLF					

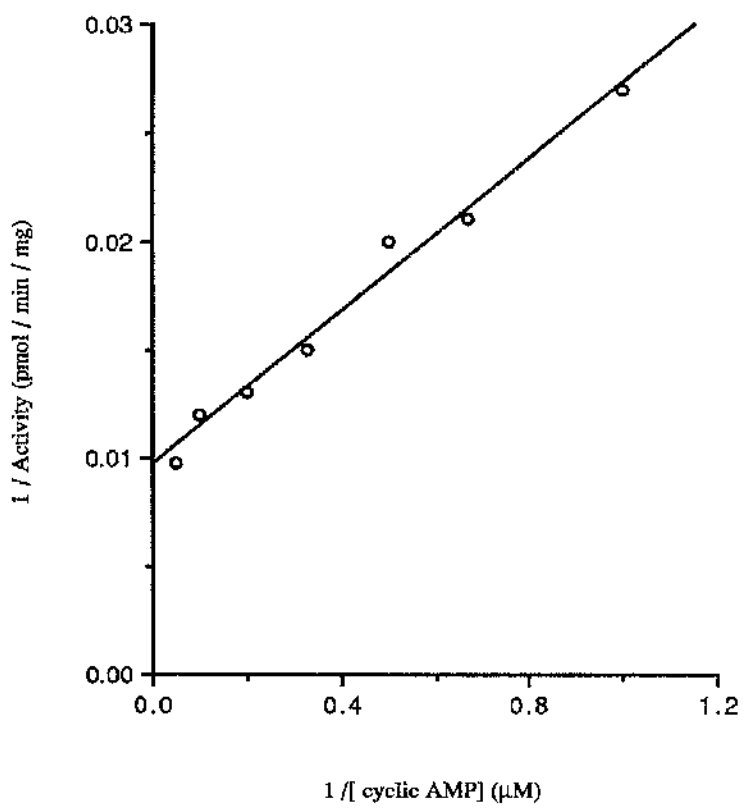
	850	860	870	880
Contig# 1			
h6.1 aa ORF engineered	STAAEVEAQREHQAAKRACCSACAGTFGEDTSALPAPGGGGSGGDPT			
HYB 1 pep sandoz	STAAEVEAQREHQAAKRACCSACAGTFGEDTSALPAPGGGGSGGDPT			
YMS11/PEPTIDE	STAAEVEAQREHQAAKRACCSACAGTFGEDTSALPAPGGGGSGGDPT			
HPDE46.PEP	STAAEVEAQREHQAAKRACCSACAGTFGEDTSALPAPGGGGSGGDPT			
YMS12	STAAEVEAQREHQAAKRACCSACAGTFGEDTSALPAPGGGGSGGDPT			
YMS10/PEPTIDE	STAAEVEAQREHQAAKRACCSACAGTFGEDTSALPAPGGGGSGGDPT			

Fig. 4.2.5

**Determination of K_m cyclic AMP For Soluble
10AORF**

Lineweaver-Burke plot was constructed by the measurement of soluble 10AORF activity in the presence of increasing cyclic AMP concentrations. Activity was linear over the ranges of cyclic AMP shown. K_m values were calculated using the Ultrafit programme as described in results, and the data is shown in table 6.

This experiment is representative of one carried out at least three times.



**Fig. 4.2.6 Determination of K_m cyclic AMP For Soluble
HYB1**

Lineweaver-Burke plot was constructed by the measurement of soluble HYB1 activity in the presence of increasing cyclic AMP concentrations. Activity was linear over the ranges of cyclic AMP shown. K_m values were calculated using the Ultrafit programme as described in results, and the data is shown in table 6. This experiment is representative of one carried out at least three times.

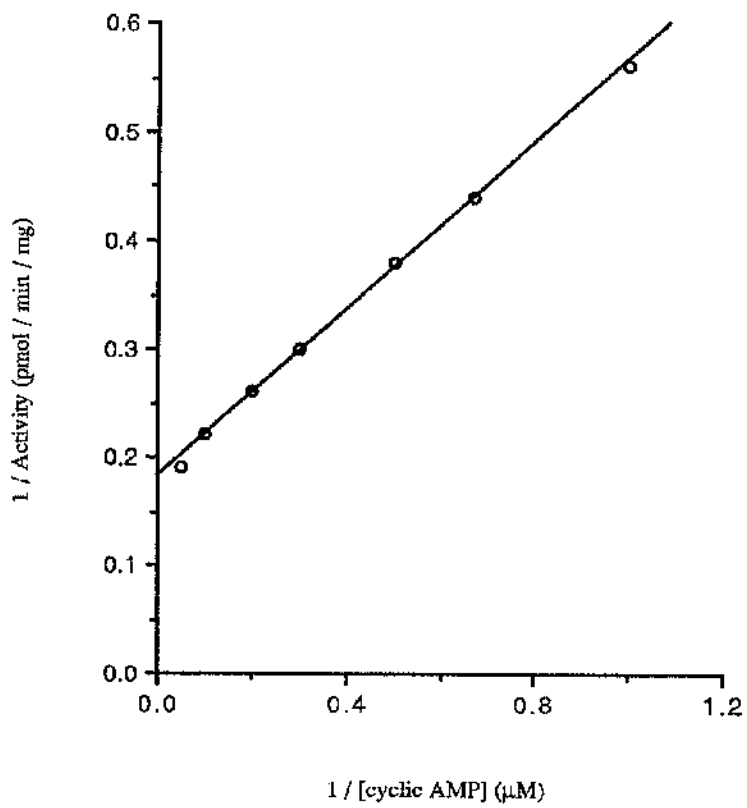


Fig. 4.2.7 Determination of K_m cyclic AMP For Soluble YMS11

Lineweaver-Burke plot was constructed by the measurement of soluble YMS11 activity in the presence of increasing cyclic AMP concentrations. Activity was linear over the ranges of cyclic AMP shown. K_m values were calculated using the Ultrafit programme as described in results, and the data is shown in table 6. This experiment is representative of one carried out at least three times.

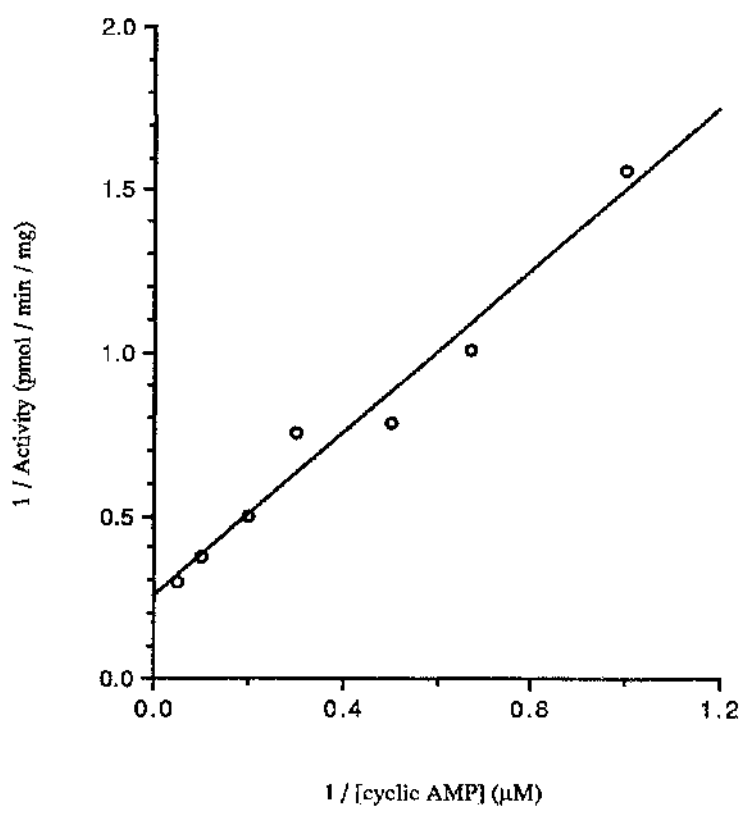


Fig. 4.2.8

**Determination of K_m cyclic AMP For Soluble
YMS12**

Lineweaver-Burke plot was constructed by the measurement of soluble YMS12 activity in the presence of increasing cyclic AMP concentrations. Activity was linear over the ranges of cyclic AMP shown. K_m values were calculated using the Ultrafit programme as described in results, and the data is shown in table 6. This experiment is representative of one carried out at least three times.

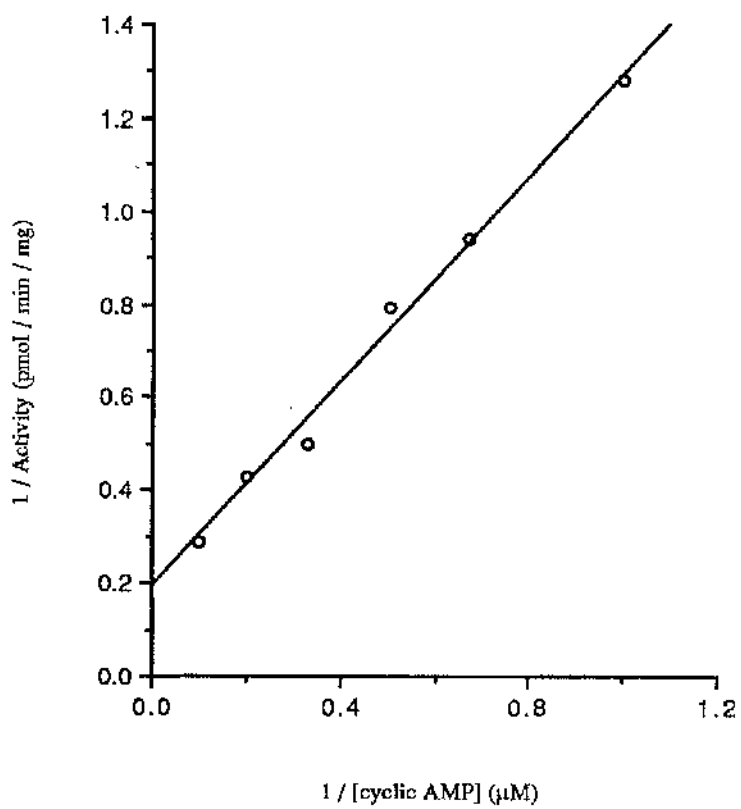


Fig. 4.2.9

Dose-Response to Rolipram of Soluble
10AORF

Soluble 10AORF activity was measured at a fixed concentration of cyclic AMP (3 μ M), which approximated that of the K_m , in the presence of increasing rolipram concentration. The resultant IC₅₀ value is given in table 6.

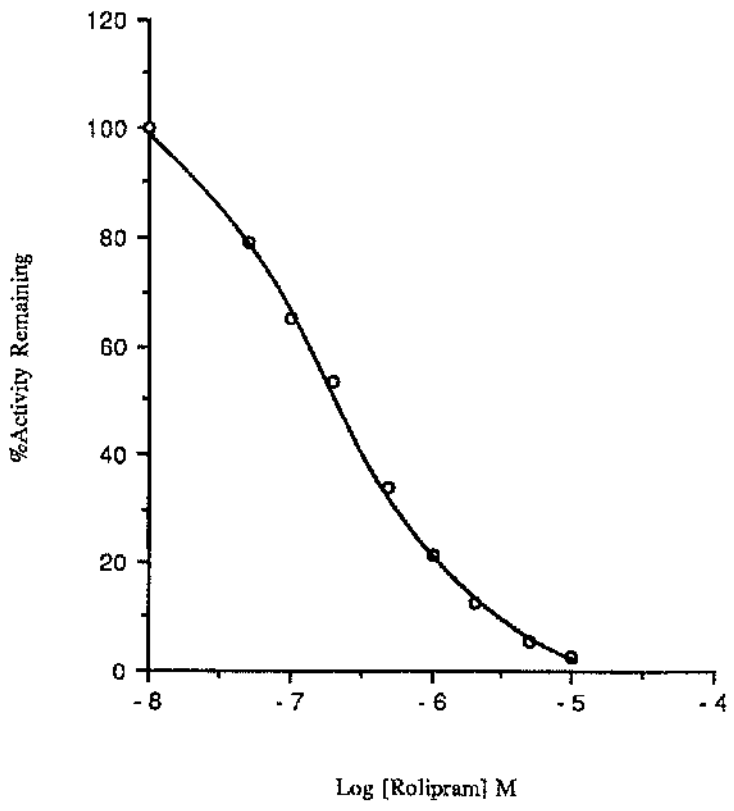


Fig. 4.2.10

**Dose-Response to Rolipram of Soluble
HYB1**

Soluble HYB1 activity was measured at a fixed concentration of cyclic AMP (3 μ M), which approximated that of the K_m , in the presence of increasing rolipram concentration. The resultant IC₅₀ value is given in table 6.

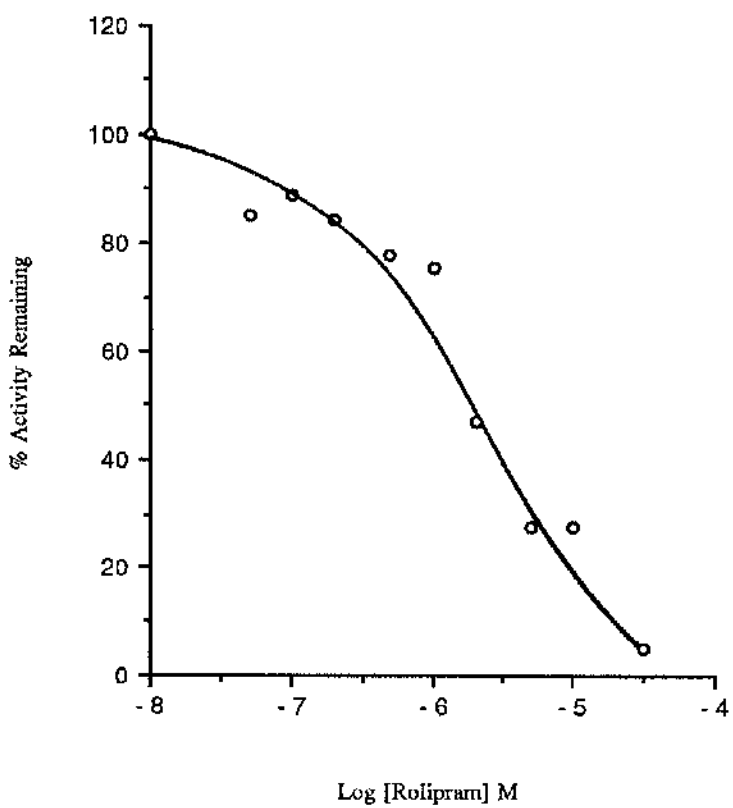


Fig. 4.2.11 **Dose-Response to Rolipram of Soluble**
YMS11

Soluble YMS11 activity was measured at a fixed concentration of cyclic AMP ($3\mu\text{M}$), which approximated that of the K_M , in the presence of increasing rolipram concentration. The resultant IC_{50} value is given in table 6.

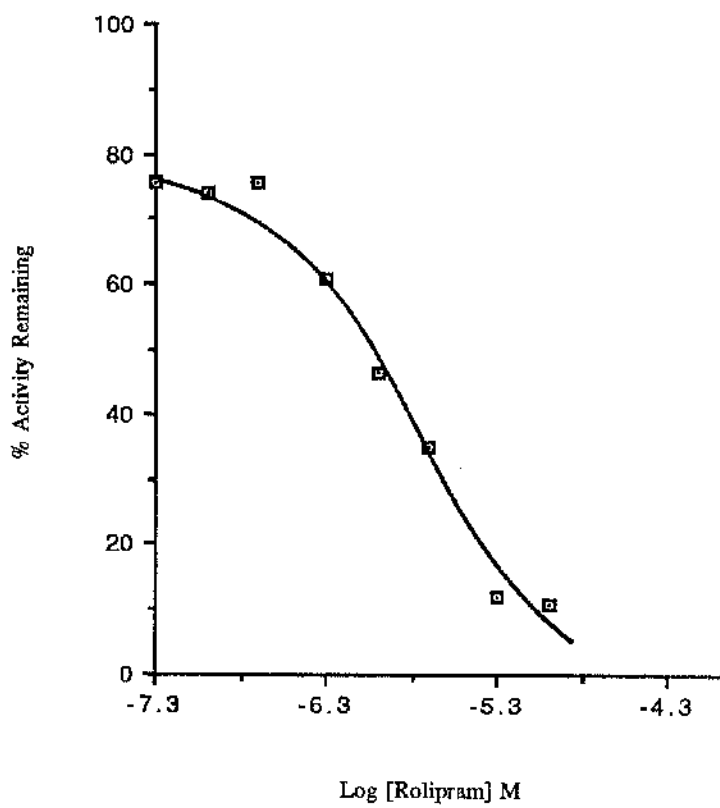


Fig. 4.2.12

**Dose-Response to Rolipram of Soluble
YMS12**

Soluble YMS12 activity was measured at a fixed concentration of cyclic AMP (3 μ M), which approximated that of the K_m , in the presence of increasing rolipram concentration. The resultant IC₅₀ value is given in table 6.

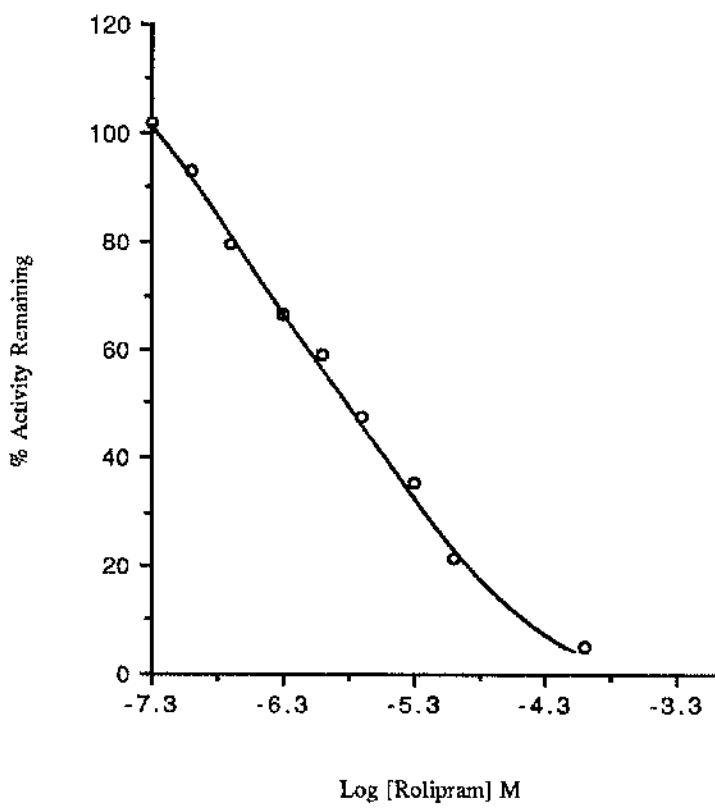


Fig. 4.2.13

**Kinetics of Rolipram Inhibition of Soluble
10AORF**

Soluble 10AORF activity was measured over the range of 1 - 20 μ M cyclic AMP in the presence of increasing concentration of rolipram. This experiment is representative of one done at least three times.

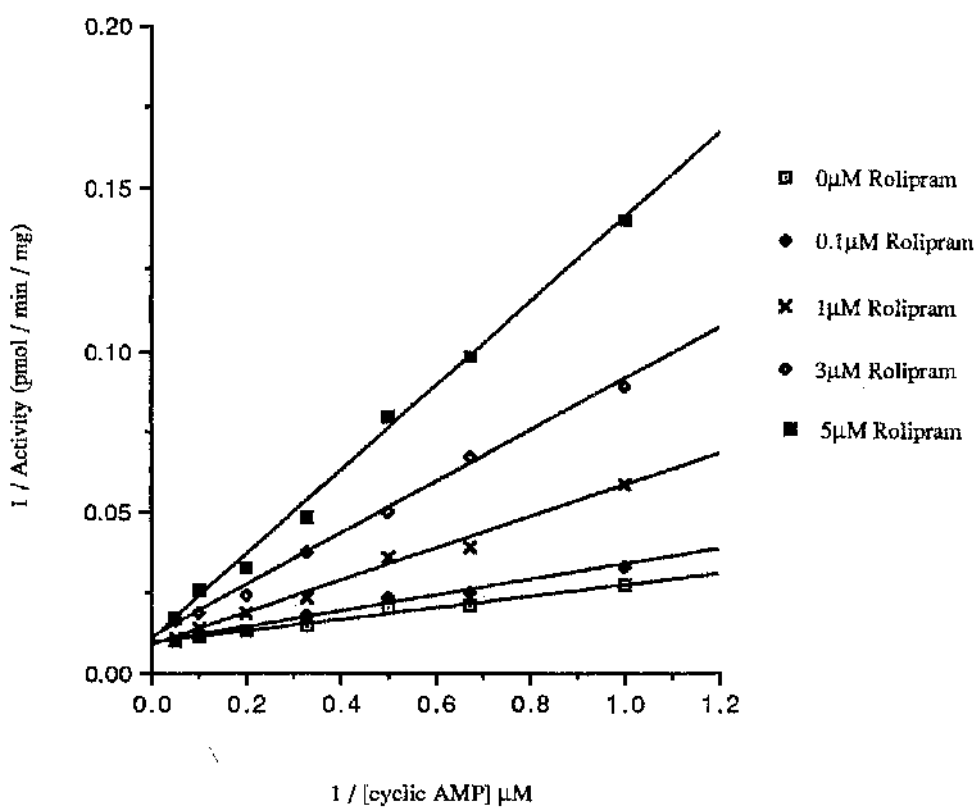


Fig. 4.2.14

**Dixon Replot of Rolipram Inhibition of Soluble
10AORE**

Data is shown as the reciprocal of activity versus increasing concentration of rolipram (Dixon and Webb 1979). This experiment is representative of one done at least three times.

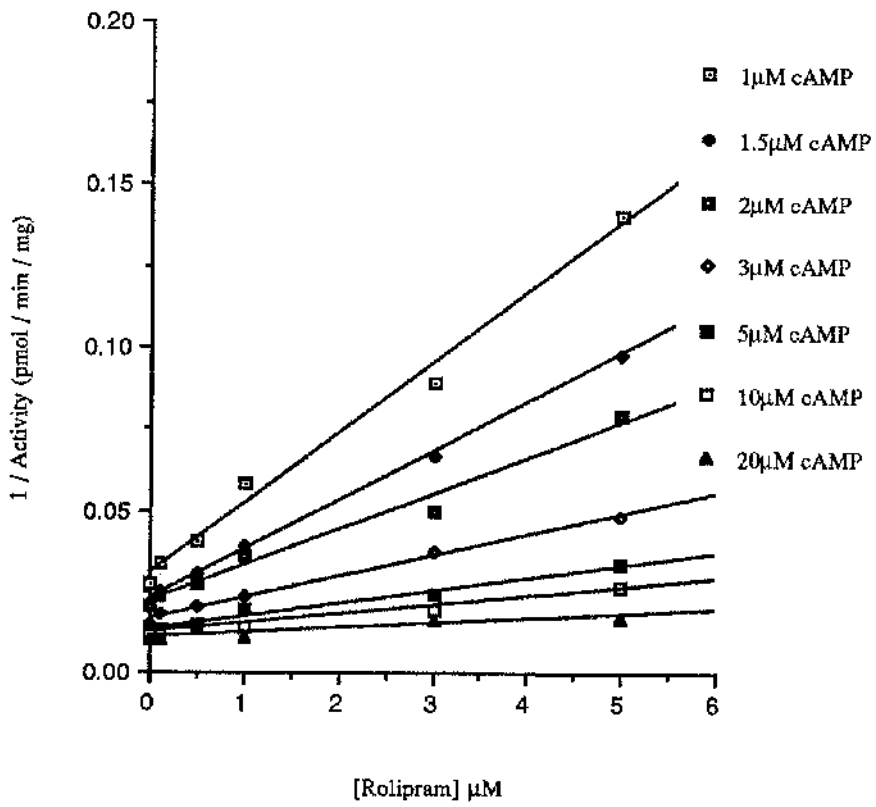


Fig. 4.2.15

**Slope Replot of Rolipram Inhibition of Soluble
10AORE**

Data is shown as the slope replot of activity versus increasing concentration of rolipram. This experiment is representative of one done at least three times.

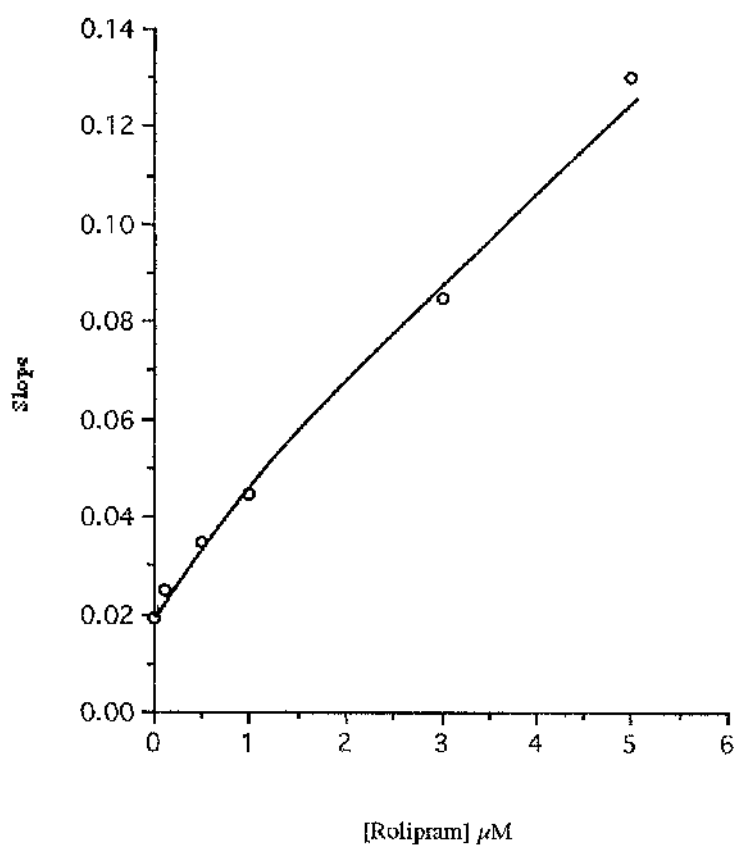
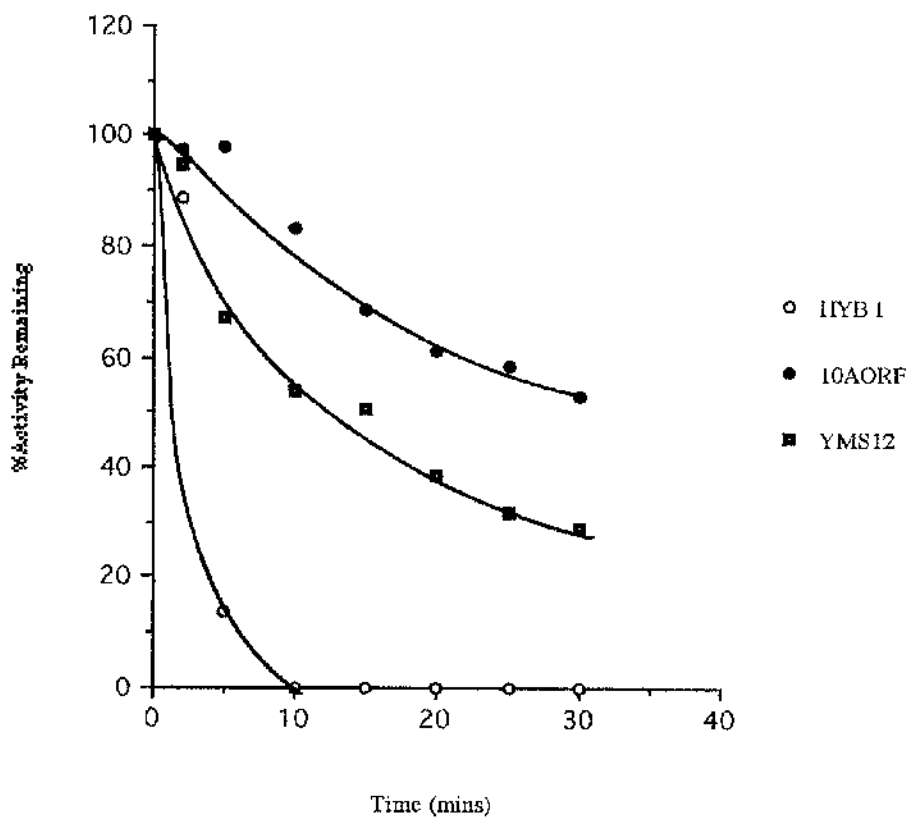


Fig. 4.2.16

**Thermostability of Soluble 10AORE, HYB1
and YMS12 at 45°C**

Thermostability of 10AORE, HYB1 and YMS12 was measured at 45°C. The resultant $t_{0,5}$ values are shown in table 7.



Results - Chapter5

Analysis of Rat PDE4A RD1

5.1 Introduction

Dunc mutants of *Drosophila melanogaster* carry a genetic mutation at the chromomere region 3D3 - 3D4 and display particular phenotypic characteristics which include learning difficulties (Byres et al 1981), and both female (Mohler 1973, 1977) and male (Kiger 1977) infertility. The phenotype of *dunc* mutants is the result of abnormal cyclic AMP metabolism, due to a genetic mutation of the *dunc* gene. Isolation of the *dunc* gene (Davis & Davidson 1984) and the subsequent biochemical, genetic and molecular analysis (Byres et al 1981, Davis & Kiger 1981, Chen et al 1986) have shown that it encodes a cyclic AMP specific PDE.

Given the importance of the dunce gene in *Drosophila melanogaster* it was considered whether the gene was structurally and functionally conserved in mammals. Using a probe representing *dunc*, Davis et al (1989), screened a variety of genomic cDNA libraries, including rat, which led to the isolation of the rat *dunc* -1 gene. A fragment of the rat *dunc* -1 genomic clone, which had a high degree of homology to the *Drosophila melanogaster dunc* gene, was used to probe a rat brain cDNA library. From this screen, three clones RD1, RD2 and RD3 were isolated. RD1 was shown to be the largest clone, with a complete ORF encoding a protein of some 610 amino acids and predicted molecular weight of 68kDa. The RD2 and RD3 clones were smaller, with truncations at the 3' end. However, the isolation of RD2 and RD3 suggested that RD1 may be alternatively spliced *in vivo* and that RD1 may not reflect a full length PDE. The pattern of tissue expression of RD1 was also analysed (Davis et al 1989). The major RNA transcripts detected in the whole rat brain and cerebellum were of a different size (4kb) to that detected in heart, lung and testes (4.4 kb), suggesting different levels of control of RD1 mRNA transcription in different tissues. However, it was found that mRNA for RD1 occurred predominantly in the brain.

The amino acid sequence of RD1 was found to be 76% homologous to the *dunc* gene product within a conserved region suggested to contain the catalytic domain (Charbonneau et al 1986), although limited sequence similarity was seen outside of this region. Expression of RD1 in yeast (Henkel-Tiggas & Davis 1989) allowed the characterisation of the enzyme, with respect to both inhibitor sensitivity and substrate specificity. RD1 was shown to hydrolyse cyclic AMP specifically with a K_m of $\sim 4\mu\text{M}$. It was also highly sensitive to inhibition by the compounds rolipram and RO-20-1724, with IC_{50} values of 0.7 and $4.2\mu\text{M}$ respectively. The inhibition of the cyclic AMP hydrolysing activity of RD1 by rolipram was the factor which distinguished the mammalian enzyme from the *Drosophila melanogaster dunc* gene product. Therefore, the sequences outwith the homologous region of RD1 may allow for the interaction of PDE4 inhibitors. Rolipram, on the basis of studies done on RD1, was suggested as being selective for this group of cyclic AMP specific PDEs now known as the PDE4 family.

It is intriguing that *dunc* mutants lacking the gene which encodes a cyclic AMP specific PDE exhibit a learning and memory defect in *Drosophila melanogaster* (Dudai 1983) whereas, in humans the PDE4 inhibitor rolipram has anti-depressant properties (Watchel et al 1983). In addition, Nighorn et al (1991) found that the *dunc* PDE was concentrated in a brain area in the rat, which has been associated with the processes of learning and memory.

RD1 activity has been analysed upon its expression in COS-1 cells transfected with the recombinant vector pSVL-RD1 (Shakur et al 1993). Isolation of RNA from pSVL-RD1 transfected COS-1 cells and hybridisation with a ^{32}P -labelled RD1 cDNA, revealed a band of 3.1kb. Translation of RD1 mRNA *in vitro* revealed a 68kDa product. Membranes of COS-1 cells transfected with pSVL-RD1 expressed $\sim 75\%$ of the total RD1 activity, with the remainder being found in the cytosol. Engineered deletion of the first 25 N-

terminal amino acids of RD1, yielded a truncated enzyme which was called met²⁶RD1. In COS-1 cells transfected with pSVL-met²⁶RD1, this truncated PDE activity was found as an active species located exclusively in the cytosolic fraction. Subcellular fractionation studies of COS-1 cell membranes showed that RD1 primarily associated with the plasma membrane, but with a fraction which occurred associated with the golgi. This was confirmed with confocal microscopy studies (Shakur et al (1995)). RD1 did not behave as a peripheral membrane protein, but required detergent such as TX-100, to solubilise activity. However, unlike integral membrane proteins there was no evidence for a transmembrane domain. This suggested that it bound to the membrane through some other action. One suggestion made, was that the attachment of RD1 to the membrane might be through the acylation of the N-terminal cysteines found in the 1 - 25 amino acid domain. Recent evidence (McPhee et al 1995) has shown that the 'cytosolic RD1' activity found in COS-1 cells (Shakur et al 1993) was actually the N-terminally truncated protein met²⁶RD1. Expression of met²⁶RD1 resulted from the positioning of the met²⁶ residue of RD1 within a suboptimal Kozak sequence. As such, in systems like COS-1 cells, products could be formed from initiation of the sequence at the met²⁶ residue. A soluble RD1 activity is unlikely to exist *in vivo*, since soluble activity could not be immunoprecipitated from rat cerebellum homogenates (McPhee et al 1995).

Sequence comparison of RD1 with the *Drosophila melanogaster dunc* PDE, and another PDE4 species from the rat called the DPD enzyme (Collicelli et al 1989), shows that they share homology over a central domain containing the catalytic region. However, the N and C terminal regions were shown to be distinctly heterologous (Davis 1990). It was thought, therefore, that the N-terminal region of RD1 might perform a specific function. RD1 and met²⁶RD1 shared similar properties regarding substrate specificity and inhibitor sensitivity (Shakur et al 1993). However, thermostability studies revealed that,

at 50°C, membrane-associated RD1 was more thermostable than either met²⁶RD1 or the membrane-associated activity which had been solubilised. Therefore, the N-terminal domain contains information to locate RD1 to the membrane, which allows the protein to adopt a conformation which increases its thermostability. This N-terminal domain also confers an inhibitory effect on catalytic activity (Shakur et al 1995). The truncate, met²⁶RD1, had a V_{max} value for cyclic AMP hydrolysis which was two fold greater than that for RD1. The unique N-terminal region of RD1 not only determines the location of RD1 within the cell, but also has a regulatory effect on the catalytic activity.

Northern blot analysis of various rat tissues revealed that RD1 transcripts were found predominantly in the brain (Davis et al 1989, 1991). It was an objective of this study to determine if a PDE species of the molecular weight of RD1 was indeed expressed in brain, and to determine the properties that it had. In order to address these questions, this study focused the analysis on a specific membrane region, the cerebellum. In particular, it was investigated as to whether RD1, if it was expressed, was associated with nerve terminals where the receptor / adenylyl cyclase system occurred. In the mammalian CNS the role of cyclic AMP is less well characterised. However, it has been associated with the processes of neurotransmission by virtue of its synaptic localisation (Therien and Mushynski 1979) and in mood regulation (Schneider et al 1986). To look at the role of RD1, the use of rat cerebellum synaptosomes were employed.

Neurones, and their support cells glia, do not survive the process of homogenisation intact. Homogenisation causes the cell bodies to become disassociated from the nerve endings. Synaptosomes form when the post-synaptic cells and pre-synaptic membrane reseal to form osmotically active particles (Dunkley et al 1988). This process of resealing entraps organelles of the synapse (fig 5.1.1), including post-synaptic densities, synaptic vesicles, mitochondria and cytoplasmic enzymes such as lactate dehydrogenase, to form

metabolically active synaptosomes (Gordon-Weeks). Synaptosome preparations were originally described using rat brain (Gray & Whittaker 1962, DeRobertis et al 1962). The subcellular fractions which are enriched in synaptosomes, such as synaptic vesicles, have been used to study aspects of synaptic function, for example, neurotransmitter release of acetylcholine (Thorne et al 1991).

Availability of antisera to RD1 enabled the study of the enzyme in rat brain. In particular, to study whether RD1 was indeed expressed, and if so, determination of its location. This was done with the original intention of extending the study to human tissue had a suitable PDE4A antibody been forthcoming. This proved not to be the case at the time of this study. This chapter describes work carried out on a rat PDE4A species, with the purpose of investigating the distribution between the membrane and soluble fractions of the rat cerebellum, and to determine whether the RD1 activity expressed *in vivo* was of similar molecular weight as found with pSVL-RD1 transfected COS-1 cells. This work was enabled using an antiserum directed against a decapeptide sequence found in the C-terminal region of RD1.

5.2

Results

(i) Preparation and Identification of Synaptosomes From Rat Cerebellum

Rat cerebellum synaptosomes were prepared according to the method described in Dunkley et al (1988) and Thorne et al (1991). Briefly, a post-nuclear supernatant (S1), which was obtained from the centrifugation (1000g x 10min) of a homogenate of rat cerebellum tissue, was loaded onto percoll / sucrose step gradients. After centrifugation of the gradients, as per Dunkley et al (1988), the material that collected at the four interfaces (F1 - F4 inclusive), plus the pellet fraction F5, were carefully removed using a Pasteur pipette. After the washing procedure, as described by Dunkley et al (1988), each of the fractions were analysed for occluded lactate dehydrogenase (LDH) activity (Johnson 1960, modified by Marchbanks 1967). Measurement of occluded LDH, a cytoplasmic enzyme, determines the integrity of the synaptosomes and also provides a means to assess the reproducibility of synaptosome preparation between experiments. Non-occluded LDH activity was assessed, initially, and occluded activity was measured by the addition of Triton X-100 (2%) which resulted in synaptosome rupture. By subtracting the LDH activity prior to the addition of TX-100, from that obtained after the addition of TX-100, the amount of occluded activity could be calculated.

The distribution of LDH activity across the gradient obtained in this study (fig 5.2.2, table 8), resembled that obtained by Thorne et al (1991) (fig 5.2.3), with the exception of the F1 fraction. The F1 fraction was suggested by Dunkley et al (1988) to contain contaminating synaptic membranes as opposed to functional synaptosomes. It could be the case, in this study, that the vesicles found in the F1 fraction, and which gave rise to the elevated occluded LDH activity, were derived simply from membrane fractions which had resealed and were not functional synaptosomes as found in fractions

F2 and F3 (fig 5.2.2). The distribution of occluded LDH activity across the rest of the gradient was comparable to that of Thorne et al (1991) (fig 5.2.3).

The fractions collected, F1 - F5, have been characterised by Thorne et al (1991) and Dunkley et al (1988) by the presence of marker enzymes. Synapsin I, a nerve terminal phosphoprotein which is predominantly found associated with synaptic vesicles (DeCamilli et al 1983), was present in fractions F2 - F4 predominantly. The F5 fraction was characterised as that which mainly contained mitochondria, by the abundance of the marker enzyme pyruvate dehydrogenase (Dunkley et al 1988), and the absence of LDH activity (Thorne et al 1991). In addition, Dunkley et al (1988) have described that this method of synaptosome preparation allowed the separation of synaptosomes with post-synaptic densities attached. Thorne et al (1991) have characterised the fractions further by the distribution of the cholinergic marker acetylcholinesterase, which terminates the action of the neurotransmitter acetylcholine. The distribution of acetylcholinesterase activity obtained by Thorne et al (1991) (fig 5.2.5) was similar to that obtained in this study from rat cerebellum (fig 5.2.4). The similarity of the distribution of marker enzymes, LDH and acetylcholinesterase, suggest that the fractions obtained in this study are comparable to that by Thorne et al (1991) and Dunkley et al (1988).

(ii) Western Blot Analysis of RD1 in Rat Cerebellum

Synaptosomes

Using the anti - RD1 antiserum, the fractions obtained from the gradient used to separate rat cerebellum synaptosomes, including the original post-nuclear supernatant applied to the gradient, were immunoblotted for RD1. The RD1 antisera identified a single band of molecular weight 73 ± 3 kDa. This molecular weight was higher than that determined from the cDNA sequence (~68kDa). However, Shakur et al (1995) have determined that the RD1 immunoreactivity from cerebellum membranes migrated with RD1 immunoreactivity obtained from COS-1 cells transfected with the RD1 cDNA

(fig 1a of Shakur et al 1995). In addition, the RD1 immunoreactivity found in cerebellum was predominantly membrane associated ($92 \pm 3\%$) (Shakur et al 1995), as was the RD1 activity expressed in COS-1 cells ($\sim 75\%$) (Shakur et al 1993).

Densitometric analysis of the distribution of RD1 immunoreactivity in samples from the gradient used to isolate rat cerebellum synaptosomes in this study, showed that RD1 was present to a greater degree in the F2 and F3 fractions (fig. 5.2.6). RD1 was found, to a lesser extent, in the F1 and F4 fractions. In the mitochondrial fraction F5, negligible immunoreactivity was detected.

(iii) Subfractionation of the F2 and F3 Synaptosome Gradient

Fractions

The fractions from the synaptosome gradient which were enriched in RD1 immunoreactivity, F2 and F3, were pooled, lysed and fractionated further on a sucrose density gradient to resolve different membrane populations as described by Shakur et al (1993). The lysate was centrifuged (2000rpm x 5min) to obtain a post-nuclear supernatant which was then applied onto the top of a sucrose step gradient. The step gradient consisted of a step of 0.5M sucrose (3ml) layered onto a step of 1.6M sucrose (1ml). After centrifugation (50,000rpm x 30min), the membranes were harvested from the 0.5 / 1.6M sucrose interface. The membrane fraction ($\sim 200\mu\text{l}$) was supplemented with solid sucrose to give a concentration of $>1.6\text{M}$, which has an equivalent refractive index of >4.5 . The membrane fraction was then loaded under a 0.6 - 1.6M sucrose continuous gradient and centrifuged (50,000rpm x 18hours). Samples were then removed from the gradient in 200 μl aliquots using a peristaltic pump.

(iv) Assay of Subcellular Fractionation Samples for 5'

Nucleotidase and Adenylyl Cyclase Activity

Samples were collected from the subfractionation gradient as described above (section (iii)), and assayed for the plasma membrane markers 5' nucleotidase as described by Newby et al (1975), (fig 5.2.7) and adenylyl cyclase as described by Houslay et al (1986) (fig 5.2.8). The distribution of the plasma membrane markers were similar across the gradient. Samples of similar 5' nucleotidase activity were pooled to provide enough protein for western blotting with the RD1 C-terminal antisera.

(v) Western Blot of Subcellular Fractionation Samples with RD1 Antisera

Densitometric analysis of the western blot of samples from the subcellular fractionation described above (section (iii)), probed with the RD1 antisera, has shown that the peak of RD1 immunoreactivity correlated with the peak of 5' nucleotidase activity (fig 5.2.9). This suggests that *in vivo*, RD1 activity is associated with the plasma membrane. Association of RD1 with the plasma membrane has previously been shown by Shakur et al (1993) for COS-1 cells transfected with RD1 cDNA. Furthermore, the RD1 activity expressed in COS-1 cells is identical in molecular weight to that detected in membranes prepared from rat cerebellum (section (ii) above).

5.3 Conclusions and Discussion

Using a probe representing the *Drosophila melanogaster dunc* gene, Davis et al (1989) isolated the rat *dunc*-1 gene from a rat genomic cDNA library. A fragment of the rat *dunc*-1 genomic clone, which had a high degree of homology to the *Drosophila melanogaster dunc* gene, was used to probe a rat brain cDNA library. From this screen, three clones RD1, RD2 and RD3 were isolated. RD1 was shown to be the largest clone, with a complete ORF encoding a protein of 610 amino acids and predicted molecular weight of 68kDa.

Shakur et al (1993) have demonstrated that upon expression in COS-1 cells, the RD1 cDNA encodes a protein of the PDE4A class which is predominantly associated with the membrane fraction, in particular the plasma membrane. Membrane association was shown to be dependant upon the presence of the first N-terminal 25 amino acids, since the truncated met²⁶RD1 lacking these amino acids was exclusively cytosolic. This N-terminal region was also shown to confer thermostability (Shakur et al 1993) as well as the inhibition of catalytic activity (Shakur et al 1995), in addition to determining the cellular location of the enzyme.

The major RD1 RNA transcripts which were originally detected in the whole rat brain and cerebellum which were of a different size (4kb) from those detected in heart, lung and testes (4.4kb) (Davis et al 1989). This suggested that different levels of control of PDE4A mRNA transcription was occurring in different tissues. However, it was found that RD1 mRNA transcripts were predominantly located in the brain (Davis et al 1989). Thus, although the mRNA data indicated the presence of RD1 in rat brain, it was unknown as to whether an RD1 PDE was actually expressed in such tissues, and to which cellular location the enzyme was targeted.

Shakur et al (1995) have addressed this question, and have investigated the RD1 activity which is expressed in the cerebellum of the rat

brain. Using a C-terminal antisera to RD1, rat cerebellum homogenate, high speed pellet and membrane free cytosol fractions were probed with the antibody. Approximately 92% of the total RD1 immunoreactivity was found to be associated predominantly with the high speed membrane fraction. This correlated with the data obtained from the study with RD1 expressed in COS-1 cells, which showed that ~75% of the RD1 activity associated with the membrane fraction. The difference between the percentage of RD1 activity bound to COS-1 cell membranes and cerebellum membranes, might reflect differences in the availability of membrane attachment sites in foreign host cells, as opposed to that found *in vivo*.

Although RD1 was found associated with the membrane fraction upon expression of the RD1 cDNA in COS-1 cells, the truncated RD1 species met²⁶RD1, was found to be an exclusively cytosolic enzyme (Shakur et al 1993). RD1 and met²⁶RD1 were found to be essentially the same with respect to kinetics of cyclic AMP hydrolysis and inhibitor profile. The existence of kinetically similar membrane / cytosolic associated enzymes has already been reported for other cyclic AMP PDEs. The rat liver 'dense - vesicle', cyclic GMP inhibited PDE, is found both as an integral membrane protein (Pyne et al 1987a), and a kinetically similar soluble enzyme released upon 'hypotonic shock' of hepatocytes (Loten et al 1978). The purified enzyme (Pyne et al 1987a) was shown to have a native molecular weight of 62kDa, 5kDa of which behaved as a membrane anchor and was proteolytically cleaved upon purification. The particulate form, from hepatocyte membranes, was also shown to be a substrate for phosphorylation by PKA (Kilgour et al 1989). Similarly, two closely related but distinct PDE2 isoforms have been identified and purified to apparent homogeneity in rat liver (Pyne et al 1986). Both enzymes were shown to possess similar physical properties, such as, they were of a dimeric form with molecular weight of 134kDa. One isoform was found to be an integral membrane protein found associated with the plasma membrane,

and the other was located to the cytosolic fraction. The two isoforms could be differentially regulated by cyclic GMP, in that, at low cyclic AMP concentrations cyclic GMP was a more potent activator of the particulate enzyme. In rabbit ventricular myocardium particulate and soluble PDE3 isoforms have been identified, with the sarcoplasmic reticulum particulate enzyme more sensitive to inhibition by the inhibitor milrinone (Kithas et al 1988). The partitioning of kinetically similar enzymes to membrane / cytosol compartments, allows the control of the concentration of specific pools of cyclic AMP. In addition, these membrane / cytosol isoforms can be differentially regulated by cyclic GMP (Pyne et al 1986) and PKA (Kilgour et al 1989), and show differences in the potency at which they are inhibited by isoform selective inhibitors (Kithas et al 1988) to exert a further control of localised cyclic AMP levels. This compartmentalisation of cyclic AMP enables the activation of PKA isoforms selectively (Livisey et al 1982, Scott & Carr 1992, Barsony & Marx 1990).

Shakur et al (1995) have shown the *in vivo* expression of RD1 in rat brain. In order to investigate whether RD1 is expressed alongside the receptor / adenylyl signalling system, this present study focused on rat brain synaptosomes. Synaptosomes are the metabolically and osmotically functional vesicles formed upon homogenisation of neuronal tissue. Contained within the synaptosomal membrane itself are the pinched off nerve endings (ie dendrites), synaptic vesicles containing neurotransmitters and mitochondria (fig 5.1.1). In addition, Dunkley et al (1988) have shown that these synaptosomes may have post-synaptic densities attached. The method used for the isolation of synaptosomes in this study, was the sucrose / Percoll gradient system developed by Dunkley et al (1988) and Thorne et al (1991) and used a low speed supernatant fraction (S1) to resolve populations of synaptosomes. The resultant fractionation in this study, was similar to that of Thorne et al (1991) with respect to the distribution of marker enzymes LDH and

acetylcholinesterase (figs 5.2.2, 5.2.3, 5.2.4, 5.2.5). Of the 5 fractions obtained, RD1 was found to be enriched in fractions 2 and 3 (fig 5.2.9), with less RD1 immunoreactivity in fractions 1 and 4, and detected minimally in the mitochondrial fraction F5.

Those fractions which were found to be enriched with RD1, F2 and F3, were lysed and fractionated further on a continuous gradient of 0.5 - 1.6M sucrose (Shakur et al 1993), in order to isolate a plasma membrane fraction. Using markers for the plasma membrane, adenylyl cyclase and 5' nucleotidase, enabled the identification of RD1 with the plasma membrane fraction (figs 5.2.7, 5.2.8, 5.2.9). Fractions 2 and 3 represent those synaptosomes which have post-synaptic densities attached, as opposed to those found in F4 which are predominantly pre-synaptic in origin. This suggests that RD1 may associate with the post-synaptic junction along with the receptor / adenylyl cyclase system thus enabling the transduction of the signal from the receptor to be terminated. This study confirms that the *in vivo* expression of RD1 is predominantly restricted to the plasma membrane, as has been shown both biochemically and with immunofluorescence studies, in COS-1 cells transfected with the RD1 cDNA (Shakur et al 1993, 1995).

In rat brain there is evidence for the PDE4 gene encoding multiple protein products as has been also shown for the PDE4B gene (Lobban et al 1994, Monaco et al 1994). The isolation of transcripts representing RD2 and RD3 in addition to RD1, suggested that the PDE4A gene in rat brain could produce proteins of variant size (Davis et al 1989). Recently, a PDE4A enzyme (RPDE6, Gen Bank name RNPDE4A5, Gen Bank accession number L27057) has been isolated from rat brain which was shown to be related to RD1 (Bolger et al 1994b). Sequence alignment of RPDE6 and RD1 showed that they were identical over the entire C-terminal region, until 23 amino acids from the N-terminus of RD1. This sequence divergence of RPDE6 provided a unique N-

terminal region distinct from that of RD1. This data determined RPDE6 and RD1 as splice variants of the PDE4A gene (McPhee et al 1995).

In whole rat brain homogenates, the antisera directed against the C-terminal region of RD1 detected an ~109kDa band which co-migrated with RPDE6 expressed in COS-7 cell membranes (McPhee et al 1995), as well as an ~79kDa band which co-migrated with RD1 immunoreactivity from COS-1 transfected cell membranes. RPDE6 immunoreactivity was detected in the whole brain homogenate, low speed pellet (P1), high speed pellet (P2) and the supernatant fraction (S1). The RD1 immunoreactive band was detected only in the homogenate and high speed pellet fractions. This suggested that the differences in the N-terminal regions of RD1 and RPDE6, resulting from alternative splicing, removed the region conferring membrane association with RD1, since RPDE6 was found in all fractions. Indeed, the point of alternative splicing occurred at the 5' position which allowed a complete N-terminal exchange.

RPDE6 was characterised as a product of the PDE4A gene (McPhee et al 1995) as has RD1 (Shakur et al 1993). The different N-terminal region of RPDE6 was shown to allow the expression of the enzyme in a membrane and cytosolic associated form (McPhee et al 1995), whereas, that of RD1 confines the enzyme to the membrane fraction (Shakur et al 1993, 1995). Shakur et al (1995) have previously shown a 2-fold difference between the relative V_{\max} value of RD1 and met²⁶RD1, where the extended N-terminal region of RD1 had an inhibitory effect. In this regard, membrane associated RPDE6 had an even lower relative V_{\max} , which was ~10% of that shown by met²⁶RD1, and 67% of that expressed in COS-7 cell cytosol transfected with the cDNA for RPDE6. Thus, the N-terminal region of these PDE4A enzymes attenuated the catalytic activity. Furthermore, membrane-association of the enzyme activity also lead to the inhibition of catalysis, which presumably resulted from a conformational change induced by membrane attachment.

In conclusion, RD1 cDNA transfected into COS-1 cells resulted in the expression of a PDE4A enzyme (Shakur et al 1993), which co-migrated with a species detected in rat brain by an RD1 specific antisera (Shakur et al 1995). This RD1 species was found associated with rat cerebellum membranes, in particular, those which had post-synaptic densities attached. In addition, subfractionation of such synaptosomal membranes resulted in the migration of RD1 with the plasma membrane marker 5' nucleotidase. Thus, RD1 in cerebellum is located to the plasma membrane along with the receptor / adenylyl cyclase machinery, enabling the termination of the cyclic AMP signal.

Other studies have demonstrated the presence of a larger splice variant of RD1, RPDE6, in rat brain (McPhee et al 1995, Bolger et al 1994b). These two splice variants differ with respect to their N-terminal domains, which exert profound effects on their cellular location and enzyme activity (Shakur et al 1995, MCPhee et al 1995). Alternative splicing of the N-terminal region of enzymes from the PDE4A (McPhee et al 1995, Bolger et al 1994b) and PDE4B (Lobban et al 1994) families allow the cellular distribution of PDE4 isoenzymes to both membrane and cytosol compartments, with the ability of the N-terminal region to regulate activity upon membrane attachment. As a consequence, discrete changes in the cyclic nucleotide concentration, either occurring at a membrane or cytosolic site can be controlled efficiently. This evidence for splice variants of the PDE4A (McPhee et al 1995, Bolger et al 1994b) and PDE4B (Lobban et al 1994) isoforms, implies that drug development strategies designed to produce inhibitors for the PDE4A family in mammalian brain, for conditions such as depression, need to consider the effect these inhibitors will have on the variant products of the one gene.

Table 8 **Lactate Dehydrogenase (LDH) Activity Determined**
from Rat Cerebellum Synaptosome Preparation

Fraction	Total LDH (nmol/min/mg)	Occluded LDH (nmol/min/mg)
S1	1.2 ± 0.16	0.15 ± 0.1
F1	0.68 ± 0.06	0.57 ± 0.08
F2	1.00 ± 0.02	0.61 ± 0.01
F3	1.21	0.66 ± 0.04
F4	0.76 ± 0.06	0.37 ± 0.06
F5	0.17 ± 0.03	0.05

Data is shown as mean nmol of NADH oxidised / min / mg protein ± standard deviation for triplicate samples.

The distribution of LDH activity is representative of that done at least three times:

Fraction S1 refers to the supernatant applied to the gradient, fractions F1 - F4 refer to the samples collected at the Percoll / sucrose gradient interface and F5 refers to the pellet collected from the gradient.

Total LDH was measured in the presence of Triton X-100 and occluded LDH was the difference between total and free levels of the enzyme.

Fig. 5.1.1

Formation of Synaptosomes

Shown opposite is a diagrammatic representation of the formation of synaptosomes. (Gordon-Weeks, P.R., Neurochemistry - A Practical Approach).

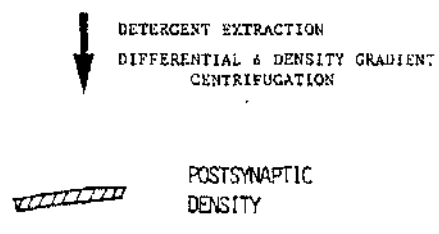
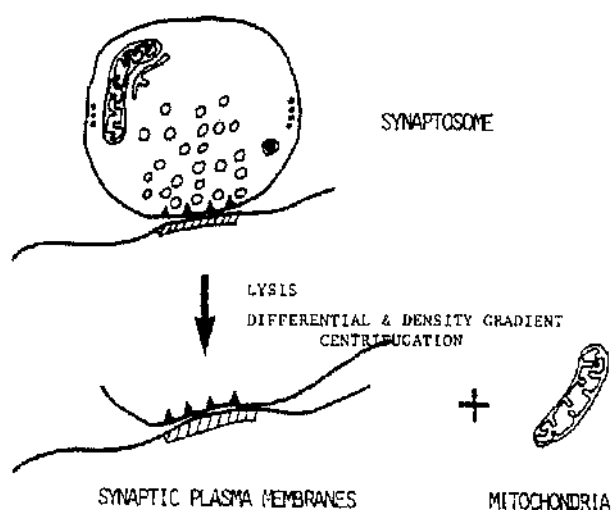
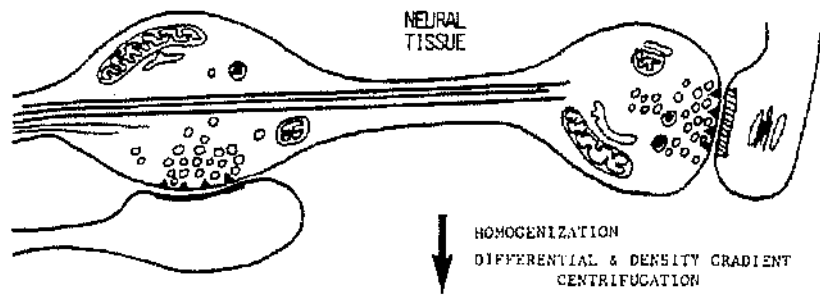


Fig. 5.2.2

**Lactate Dehydrogenase Activity in Rat
Cerebellum Synaptosomal Fractions**

Data is shown as mean nmol of NADH oxidised / min / mg protein \pm standard deviation for triplicate samples. Standard deviation is represented by vertical bars. This graph is representative of one carried out for at least three separate preparations. Fraction S1 refers to the supernatant applied to the gradient, fractions F1 - F4 refer to the samples collected at the Percoll / sucrose gradient interface and F5 refers to the pellet collected from the gradient.

Total LDH was measured in the presence of Triton X-100 and occluded LDH was the difference between total and free levels of the enzyme.

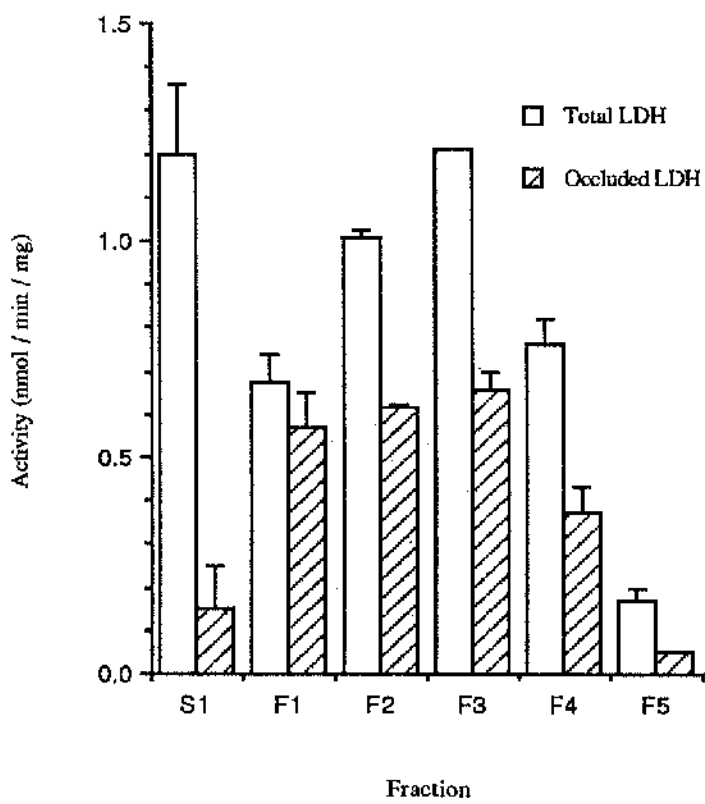


Fig. 5.2.3

**Distribution of Lactate Dehydrogenase Activity
as Determined by Thorne et al (1991)**

The method used to prepare the synaptosomes in this study was as used by Thorne et al (1991). Shown opposite is a comparative distribution of LDH activity obtained by Thorne et al (1991). Data is shown as mean nmol of NADH oxidised / min / mg protein \pm standard deviation for triplicate samples. Fraction S1 refers to the supernatant applied to the gradient, fractions F1 - F4 refer to the samples collected at the Percoll / sucrose gradient interface and F5 refers to the pellet collected from the gradient.

Total LDH was measured in the presence of Triton X-100 and occluded LDH was the difference between total and free levels of the enzyme.

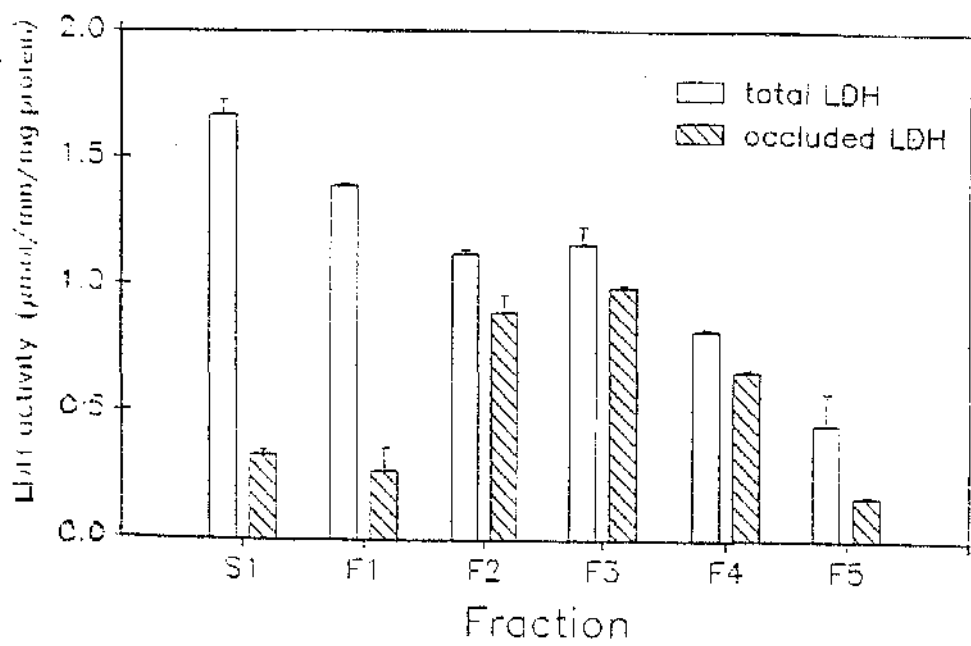


Fig. 5.2.4

**Acetylcholinesterase Activity in Rat
Cerebellum Synaptosomal Fractions**

Data is shown as mean μmol of acetylthiocholine oxidised / min / mg protein \pm standard deviation for triplicate samples with standard deviation shown as vertical error bars. The distribution of acetylcholinesterase activity is representative of that done at least three times. Fractions F1 - F4 refer to the samples collected at the Percoll / sucrose gradient interface and F5 refers to the pellet collected from the gradient.

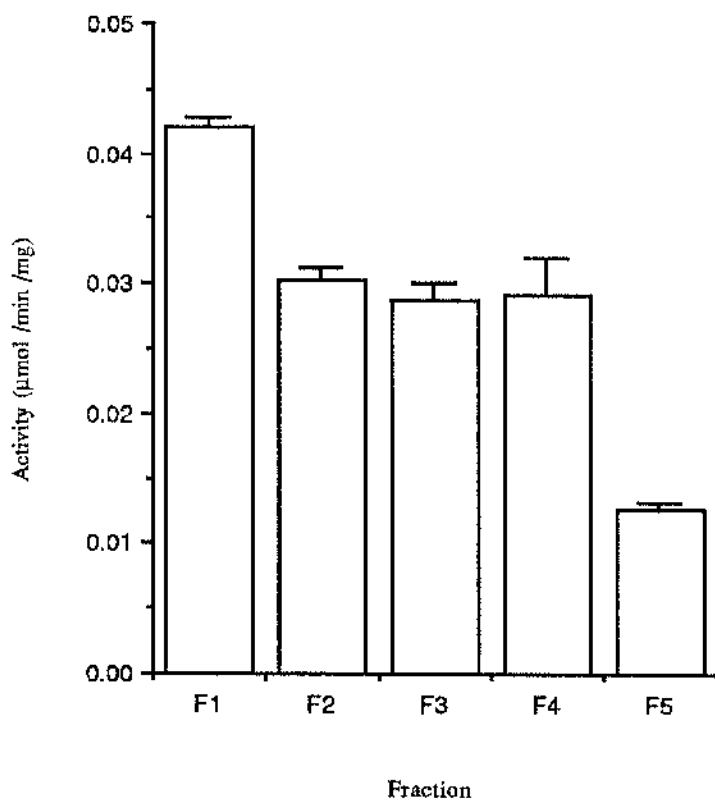


Fig. 5.2.5

**Distribution of Acetylcholinesterase Activity
as Determined by Thorne et al (1991)**

The method used to prepare the synaptosomes in this study was as used by Thorne et al (1991). Shown opposite is a comparative distribution of acetylcholinesterase activity obtained by Thorne et al (1991). Data is shown as mean μmol of acetylthiocholine oxidised / min / mg protein \pm standard deviation for triplicate samples. Fraction S1 refers to the supernatant applied to the gradient, fractions F1 - F4 refer to the samples collected at the Percoll / sucrose gradient interface and F5 refers to the pellet collected from the gradient.

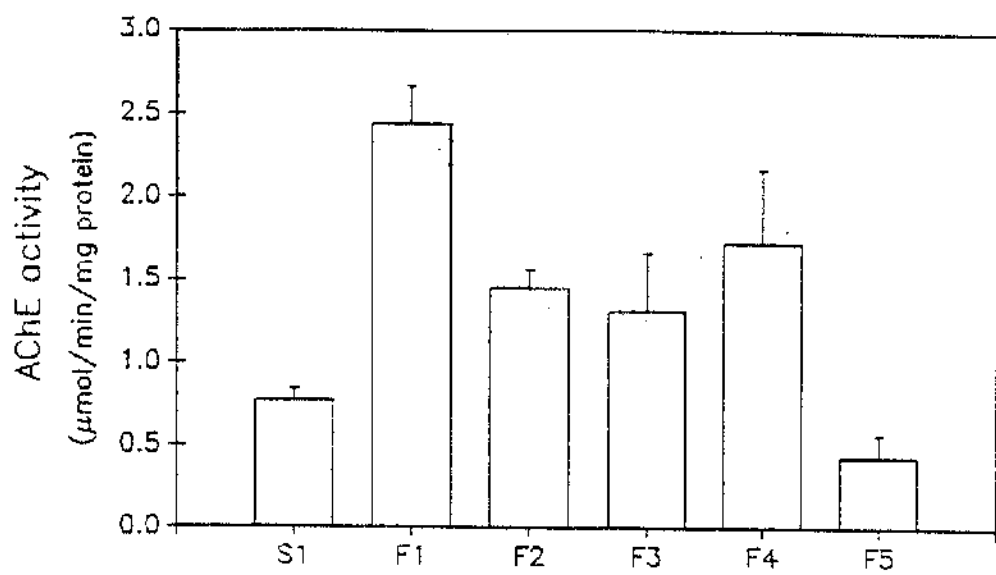


Fig. 5.2.6 **Western Blot of RD1 Immunoreactivity in**
Fractions obtained from Rat Cerebellum
Synaptosomes

Proteins electrophoresed on an SDS-PAGE gel were transferred to nitrocellulose and Western blotted for RD1 immunoreactivity. The antisera was directed against a C-terminal region of RD1. Equal amounts (100 μ g) of protein were loaded on each gel track. Shown are the samples collected at the Percoll / sucrose interface F1 - F4 and the pellet fraction F5. The data is shown as the distribution of RD1 immunoreactivity, mean \pm standard deviation, obtained densitometrically from electrophoresis of samples from a rat cerebellum synaptosome preparation.

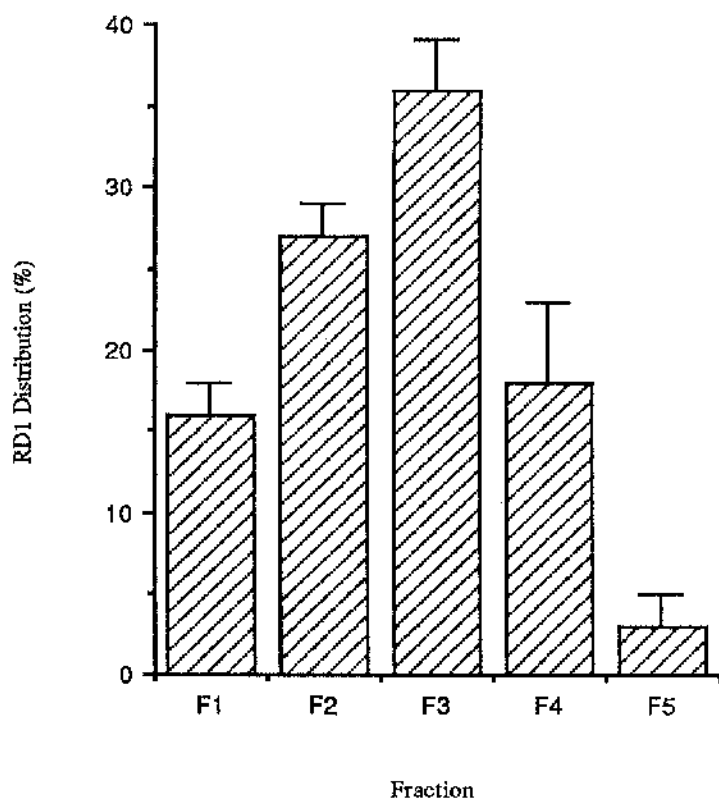


Fig. 5.2.7

**Distribution of 5' Nucleotidase Activity In
Synaptosomal Subcellular Fractions Obtained
from a Sucrose Density Gradient**

5' nucleotidase activity was measured in samples obtained from the subcellular fractionation of synaptosomal samples F2 - F3. Results are shown as nmol substrate hydrolysed per minute \pm standard deviation for triplicate samples.

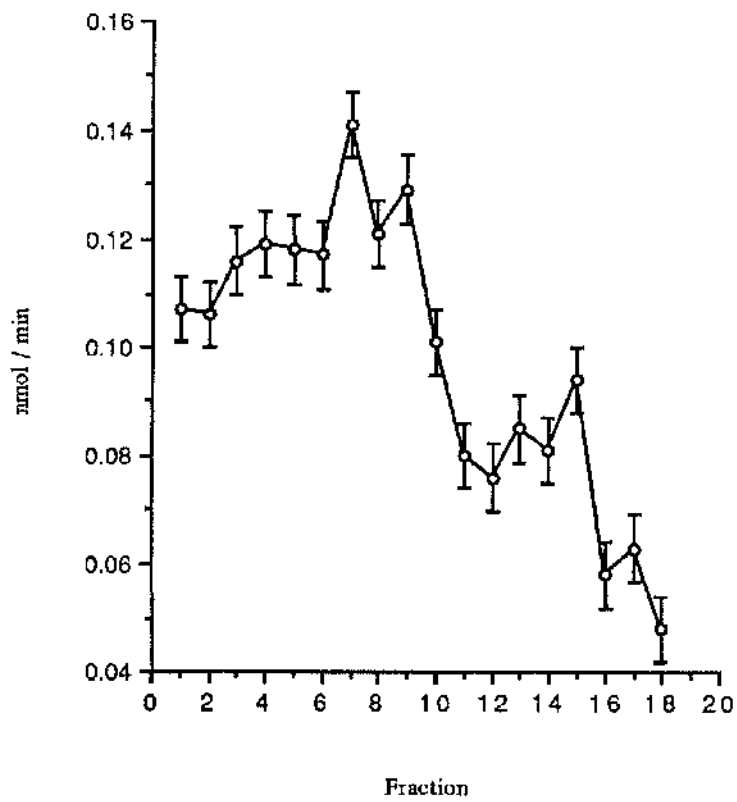
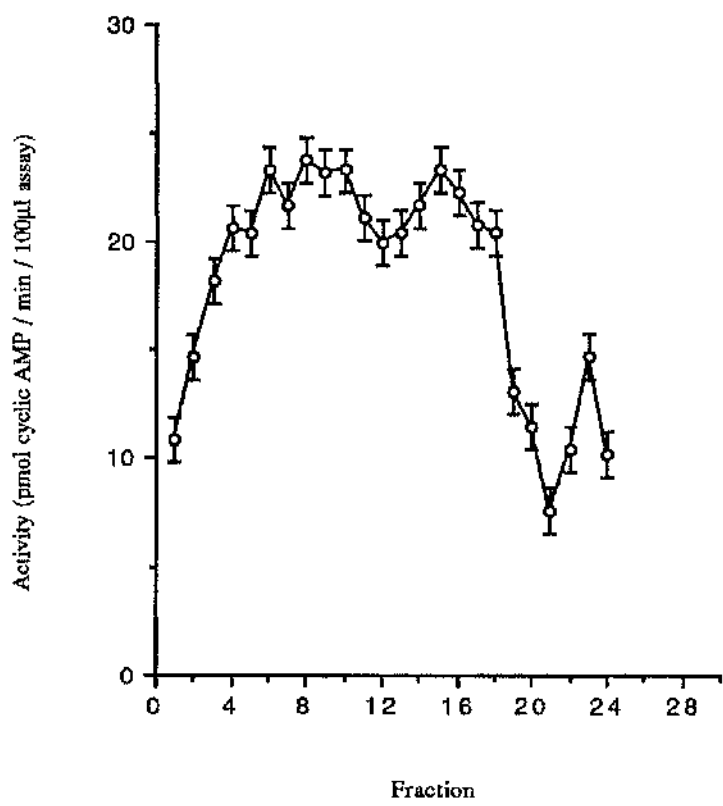


Fig. 5.2.8

**Distribution of Adenylyl Cyclase Activity In
Synaptosomal Subcellular Fractions Obtained
from a Sucrose Density Gradient**

Adenylyl cyclase activity was measured in samples obtained from the subcellular fractionation of synaptosomal samples F2 - F3. Results are shown as pmol cyclic AMP / min / 100 μ l assay \pm standard deviation for triplicate samples.

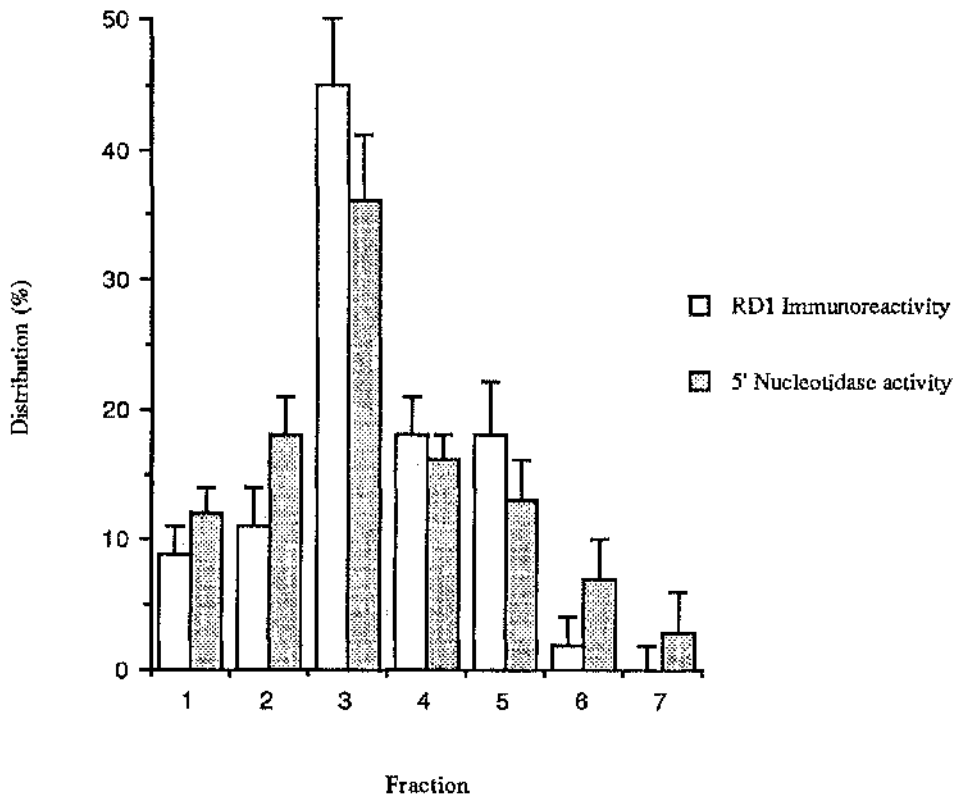


5.2.9

RD1 Immunoreactivity in Fractions Obtained from Subcellular Fractionation of Synaptosomes (F2 & F3)

Proteins electrophoresed on an SDS-PAGE gel were transferred to nitrocellulose and Western blotted for RD1 immunoreactivity. The antisera was directed against a C-terminal region of RD1. Equal amounts (100 μ g) of protein were loaded on each gel track. To obtain sufficient protein for immunoblot analysis, fractions of similar 5' nucleotidase activity were pooled. Shown is the distribution of RD1 immunoreactivity determined by densitometry, alongside the distribution of the plasma membrane marker 5' nucleotidase. Results are shown as mean \pm standard deviation.

Western blot fraction	Fractions pooled from 5' nucleotidase gradient
1	1 - 2
2	3 - 6
3	7 - 9
4	10
5	11 - 12
6	13 - 15
7	16 - 18



Final Discussion and Conclusions

6. Final Discussion and Conclusions

The isolation and characterisation of members of the PDE4 family is a research area which has gained considerable attention. The interest in the PDE4 family of enzymes is a reflection of the important role these enzymes play in the regulation of the intracellular cyclic nucleotide cyclic AMP concentration, and the possibility that selective inhibitors could be used as therapeutic agents.

Of particular interest in this study, was the characterisation of a PDE4A enzyme isolated by Dr Mike Sullivan (Sandoz), from a human T-lymphocyte cDNA library. The importance of the cyclic AMP signalling system in the immune response has been established. In the mammalian immune system, cyclic AMP is known to be an important regulator of such functions as attenuation of lymphocyte blastogenesis (Epstein et al 1984), lymphocyte proliferation and differentiation (Coffey et al 1978, Hadden 1988), inhibition of release of inflammatory mediators histamine and leukotriene C₄ from basophils (Peachell et al, 1992) and the blockade of the cytokine pathway due to the suppression of tumour necrosis factor alpha production from human mononuclear cells (Semmler et al 1993). Quiescent peripheral blood lymphocytes are stimulated to proliferate upon contact with antigen, which triggers the immune response. Sustained, elevated levels of cyclic AMP have been shown to inhibit lymphocyte activation, lymphocyte proliferation and differentiation (Coffey et al 1978, Hadden 1988). Of importance in this crucial role of cyclic AMP is the role of the PDE4 cyclic AMP specific PDEs which catalyse the degradation of the cyclic nucleotide. Engels et al (1994) has already shown that the PDE4A isoform is the only one expressed in the T-cell Jurkat cell line, which implies the importance of this isoform in these cells.

The enzyme isolated from the T-cell cDNA library, studied herein was named h6.1 (HSPDE4A7, GenBank accession number U18087). This present study has characterised h6.1 as a typical member of the PDE4

enzyme family. h6.1 was shown to hydrolyse cyclic AMP specifically and was insensitive to Ca^{2+} / calmodulin and cyclic GMP (chapter 3, 3.2.i). An engineered version of h6.1, called h6.1_{his5}, was used by Dr Neil Brown for the purification and molecular weight determination of the enzyme. h6.1 was shown to appear as a single band on a denaturing gel of $73\text{kDa} \pm 2$. This was comparable to the molecular weight determined from the purification procedure as predicted from the cDNA sequence. DiSanto and Heaslip (1993) have suggested that in the promonocytic cell line U937, PDE4 is expressed as a large molecular weight species of 210 - 250kDa. This large molecular weight protein was cleaved, upon storage, to produce a protein of $\sim 45\text{kDa}$. This was not the case with h6.1 as the purification data, along with the thermostability study (chapter 3, 3.2.iii, fig 3.2.1), has shown that h6.1 was expressed as a single population of enzyme and was not a proteolysis product.

Rolipram has been used as a tool to characterise PDE4 as such, because of the selectivity of the inhibitor for this enzyme class. The mechanism by which rolipram achieves inhibition is a subject which has generated a lot of interest. Several groups have suggested that the kinetics of inhibition by rolipram are anomolous. This was based on the findings that shallow dose response curves were obtained with rolipram, which spread over several orders of magnitude (Torphy et al 1992, Bolger et al 1993, McLaughlin et al 1993). With the isolation of human PDE4, it has been questioned whether these isoforms possess the high affinity rolipram binding site which has been detected in rat brain (Némoz et al 1989, Schneider et al 1986) suggested to be responsible for the anomolous kinetics detected. This high affinity rolipram binding site was suggested as being present in the cloned enzyme isolated from human monocytic cells, hPDE4A_{Livi} (Livi et al 1990), rabbit gastric glands (Barnette et al 1995) and guinea pig eosinophils (Souness et al 1993). This high affinity site has been shown to bind rolipram stereoselectively, with the (*R*) enantiomer being the more potent with a K_d of $\sim 1\text{nM}$. In contrast, the inhibition

Correction to chapter 6, paragraph 2, page 177

Torphy et al (1992) and Barnette et al (1995), have suggested that rolipram binds to only one site on PDE4, the catalytic site. They suggested that different non-interconvertible forms of PDE4 exist which hydrolyse substrate with similar K_m values but differ with respect to the affinity for binding of inhibitors such as rolipram and Ro-20-1724 to the catalytic site. Analysis of hPDE4A_{Livi} indicated that rolipram did not seem to serve as a simple competitive inhibitor (Torphy et al 1992, Livi et al 1990) from the authors double reciprocal plots. In support of this, a replot of slope versus rolipram concentration for hPDE4A_{Livi} (chapter 3, fig 3.2.16) was curved in a concave fashion instead of linear as would be expected of a simple competitive inhibitor. Furthermore, analysis of their data showed that the slope versus rolipram concentration plot for hPDE4A_{Livi} could be linearised by replotting a double-reciprocal of each axis (Dixon and Webb 1979), which is indicative of partial competitive inhibition. In the case of partial competitive inhibition the enzyme active site is able to accommodate both substrate and inhibitor at the same time as shown in fig 3.2.17.

of PDE4 catalysis requires rolipram in the μM range (Torphy et al 1992, Barnette et al 1995). Studies by Torphy et al (1992), Barnette et al (1995) and Schudt and Hatzelmann (1995) all suggest that the high affinity rolipram binding site is not associated with the ability of rolipram to inhibit catalysis. Indeed, more recent evidence has suggested that the irritational, gastric side effects found with the therapeutic dose of rolipram is due to an interaction with this high affinity site (Barnette et al 1995).

Torphy et al (1992) and Barnette et al (1995), have suggested that rolipram binds to only one site. However, they suggest that this site is present on two non-interconvertible forms of PDE4, which catalyse breakdown of cyclic AMP with similar K_M values, but bind rolipram with either low or high affinity. Analysis of hPDE4A_{Livi} indicated that rolipram did not seem to serve as a simple competitive inhibitor from the authors double-reciprocal plots (Livi et al 1990, Torphy et al 1992). In support of this, a plot of slope versus rolipram concentration for hPDE4A_{Livi} (chapter 3, fig 3.2.16) was curved in a concave fashion. However, this would not be expected to occur if more than one molecule of rolipram was binding to the enzyme as hypothesised by the authors, because the plot would be upwardly curving. Furthermore, analysis of their data showed that the slope versus rolipram concentration plot for hPDE4A_{Livi} could be linearised by replotting a double-reciprocal of each axis (Dixon and Webb 1979), which is indicative of partial competitive inhibition.

Kinetic analysis of human PDE4A in this study, with respect to inhibition by rolipram, showed that while inhibition of h6.1 was of a competitive nature (chapter 3, figs. 3.2.8, 3.2.9 and 3.2.10), inhibition of the N-terminally extended enzyme 10AORF was partially competitive (chapter 4, figs 4.2.13, 4.2.14 and 4.2.15). This alteration in the mechanism with which rolipram inhibited 10AORF can be explained by a conformational change in 10AORF induced by the additional N-terminal amino acids. This conclusion is supported by the thermostability data, where at 45°C, 10AORF was

considerably more thermostable than h6.1, which suggests that a conformational change had indeed occurred. In addition, the comparative IC₅₀ data for rolipram inhibition of 10AORF (0.19μM) and h6.1 (0.51μM), demonstrated that 10AORF was more potently inhibited. This decrease in IC₅₀^{rolipram} suggested that an alteration in inhibitor interaction had occurred with 10AORF. It would seem that as with the rat PDE4A species, the N-terminal domain of the human equivalent is important in enzyme thermostability and activity.

Jin et al (1992), has shown that upon analysis of the catalytic domain of PDEs, members of any one class show 60 - 90% homology in this region, while those belonging to different classes are much less homologous. The catalytic region of PDE4 (Jin et al 1992) can be identified by homology with other PDE species (chapter 4, fig 4.1.1) and is conserved throughout the PDE4 class. Bolger et al (1993) has compared the sequences of the four human PDE4 genes, and has shown that outwith the catalytic domain little, or no, sequence similarity occurs. Thus, these N and C terminal regions presumably perform other functions which could influence enzyme stability or catalysis. In order to address whether the N and C terminal regions of h6.1 influence enzyme activity, Dr M. Sullivan (Sandoz), created a series of mutants of h6.1. These truncations, which refer to the sequence of h6.1, took the form of an N-terminal deletion of residues 1 - 172 (YMS 10 yeast strain), a deletion at the N-terminus (residues 1 - 172) and also at the C-terminus (608 - 692) leaving the basic catalytic domain (YMS 11 yeast strain) and a C-terminal deletion (residues 608 - 692) (YMS 12 yeast strain) (chapter 4, fig 4.2.1). Also analysed were the N-terminally extended version of h6.1, 10AORF and the domain swap of N-terminal regions of h6.1 with the catalytically inactive splice variant 2EL described in chapter 4.

The N-terminal region of PDE4 was shown to perform several functions. While the extended N-terminus of 10AORF enhanced catalysis,

inhibitor interaction (chapter 4, table 6) and enzyme stability (chapter 4, table 7) the substitution of the N-terminal region of h6.1 with that of 2EL was shown to be detrimental. This suggests that the sequences involved in forming the catalytic region, and those adjacent to this region, are specific for the optimal functioning of the enzyme with regards to catalysis and inhibitor interaction. In addition, the N-terminal sequence of h6.1 might be specifically involved in the conformational folding of the enzyme in such a way as to resist thermal denaturation, as shown in the different thermostabilities of h6.1 and HYB1 (chapter 4, table 7). The involvement of the N-terminal region in such functions has already been demonstrated for RD1 where the N-terminally truncated enzyme, met²⁶RD1 had a greater V_{max} for cyclic AMP hydrolysis and was less thermostable (Shakur et al 1993, 1995).

Sullivan et al (1994) have suggested that the sequence of h6.1 represents the native PDE. Human PDE4A clones isolated from commercial cDNA libraries corresponded to the sequence of h6.1 and not hPDE4A_{Livi}. In addition, Bolger et al (1993) have isolated what is considered to be the full length sequence encoded by the human PDE4A gene, PDE46. Alignment of the sequences of h6.1 and that of PDE46 (chapter 4, fig 4.2.4), shows that the amino acid differences are not seen in PDE46. This data concludes the sequence of h6.1 at these points to be correct. Transfection of COS-1 cells with pSVL-RD1 (Shakur et al 1993), allowed the analysis of the rat PDE4A gene product RD1. Isolation of mRNA from transfected cells, and *in vitro* translation, showed that the cDNA encoded a 68kDa protein product. Subcellular fractionation studies showed that in transfected COS-1 cells, RD1 associated predominantly with the membrane fraction, in particular the plasma membrane. A small proportion of the activity associated with golgi fraction also. Approximately 75% of the total RD1 activity was membrane located, with the residual being cytosolic. A recent study (McPhee et al 1995) has revealed that the cytosolic RD1 species in COS-1 cells was that corresponding to met²⁶RD1

(Shakur et al 1993). In this study, McPhee et al (1995) showed that the soluble fraction of lysates of RD1 transfected COS-1 cells co-migrated with the that of homogenates from met²⁶RD1 transfected cells. Expression of met²⁶RD1 occurred because the met²⁶ residue of RD1 was within a suboptimal Kozak sequence (Kozak 1986). As a result of the over-expression in COS-1 cells shorter products could be formed by a second initiation start site which occurred at this point. Expression of a met²⁶RD1 like activity did not occur *in vivo*, as has been shown from immunoblot analysis of the pellet and soluble fractions from various rat brain regions (McPhee et al 1995).

Early studies have provided preliminary evidence which suggests a role for a cyclic AMP specific PDE, in the process of neurotransmission. The studies using *Drosophila melanogaster* have shown that genetic mutations of components of the cyclic AMP signalling pathway, result in disruption of the processes of learning and memory (Byres et al 1981, Nighorn et al 1991). These genetic mutations include *dunc*, which encodes a cyclic AMP specific PDE, and *rut* which encodes a calcium-calmodulin stimulated adenylyl cyclase (Dudai 1988, Levin et al 1992, Qiu et al 1991). In the mammalian CNS, Thérien and Mushynski (1979) have demonstrated that a particulate cyclic AMP PDE activity is concentrated over post-synaptic densities in rat brain. The cyclic AMP specific PDE inhibitors, including rolipram and RO-201724, have been evaluated as antidepressants, and studies in rat have demonstrated that a specific behavioural pattern is shown after PDE4 inhibitor administration (Watchel 1982). These behavioural effects were correlated with increased brain cyclic AMP levels in these animals (Kant et al 1980) following PDE4 inhibitor treatment.

Davis et al (1989) provided evidence, using northern blotting, which suggested that RD1 mRNA occurred predominantly in rat brain tissue. However, it was unknown as to whether a protein encoded by RD1 mRNA was translated into protein in rat brain. To address this, the present study questioned

whether RD1 activity was associated with rat cerebellum synaptosomes. Synaptosomes are formed from the resealing of post-synaptic and presynaptic membranes, which have been sheared from the cell bodies upon homogenisation. The resealed membranes have within them organelles of the synapse, such as, post-synaptic densities, synaptic vesicles, mitochondria and enzymes of the cytoplasm (Gray & Whittaker 1962, DeRobertis et al 1962). Synaptosomes therefore provided a source of rat brain neuronal membrane to study. Immunoblotting of rat brain cerebellum membrane / cytosol fractions (Shakur et al 1995), with antiserum directed against a C-terminal region of RD1, showed that ~92% of the activity was membrane associated. Analysis of the rat brain synaptosome preparations with the RD1 antiserum, identified a band of ~73kDa (chapter 5, fig 5.2.6). Shakur et al (1995) demonstrated that RD1 immunoreactivity from rat brain cerebellum membranes, migrated with that of COS-1 cells transfected with RD1 cDNA. Interestingly, those fractions which were enriched in RD1 immunoreactivity (chapter 5, fig 5.2.9), have been shown (Dunkley et al 1988) to have post-synaptic densities attached. This would correlate with the work of Thérien and Mushynski (1979), who have demonstrated that a particulate cyclic AMP PDE activity is concentrated over post-synaptic densities in rat brain.

The particular membrane fraction with which RD1 associated, was revealed upon sub-fractionation of the synaptosomal fractions which were enriched in immunoreactivity. This sub-fractionation procedure identified RD1 immunoreactivity, with the plasma membrane markers adenylyl cyclase and 5'-nucleotidase (chapter 5, figs 5.2.7 - 5.2.9). This study confirmed the observation in COS-1 cells that RD1 associated with the plasma membrane fraction primarily (Shakur et al 1993). The post-synaptic localisation of RD1, and identification of RD1 with those fractions containing adenylyl cyclase and 5'-nucleotidase outline a role for PDE4A in the process of neurotransmission. Indeed, this data correlates with the studies discussed above which implied that

a PDE4 was involved in this process. The recently published data (McPhee et al 1995), on the larger PDE4A rat splice variant, RPDE6, showed that in rat cerebellum only RD1 could be detected. This RD1 activity was found only in the membrane fraction (fig 3 McPhee et al 1995). This would suggest that RD1 is the main PDE4A activity involved in controlling cyclic AMP levels in this region of rat brain.

In conclusion, this thesis has highlighted the prominent role of products of the PDE4A gene, in processes which involve the functioning of T-lymphocytes and neurological events. These enzymes, and variants thereof, are likely to be considered targets for therapeutically useful drugs. Engels et al (1994) has shown that only PDE4A is expressed in the T-cell Jurkat cell line, which suggests that inhibitors of PDE4A will be useful in treating inflammatory disorders. Indeed, elevation of PDE4 activity is considered to be the underlying cause of certain inflammatory disorders (Grewe et al 1982, Chan et al 1993). Current drug therapy in the treatment of asthma relies on symptomatic relief, mainly with bronchodilatory agents, and leaves the underlying cause, the inflammation, unchecked. The ability to restore cyclic AMP levels, through PDE4 inhibition, would be a route to producing an anti-inflammatory effect. Similarly, PDE4 is considered a target for drugs used to treat disorders such as depression. Future studies will presumably focus on the development of more potent inhibitors of these enzymes, which possess few of the side effects which are currently associated with inhibitors such as rolipram (Barnette et al 1995).

References

7. References

- 1 Anant, J. S., Ong, O. C., Yie, H., Clarke, S., O'Brien, P. J. and Fung, B. K. (1992) *J. Biol. Chem.*, **267**, 687 - 690
- 2 Anderson, N. G., Kilgour, E. and Houslay, M. D. (1989) *Biochem. J.*, **262**, 867 - 872
- 3 Appleman, M. M. and Terasaki, W. L. (1975) *Adv. Cyclic Nucleotide Res.*, **5**, 153 - 163
- 4 Baehr, W., Devlin, M. J. and Applebury, M. L. (1979) *J. Biol. Chem.*, **254**, 11669 - 11677
- 5 Baeker, P. A., Obernolte, R., Bach, C., Yee, C. and Shelton, E. R. (1994) *Gene*, **138**, 253 - 256
- 6 Bailey, S. B., Ferrua, B., Fay, M. and Gougerot-Pocidalo, M. A. (1990) *Cytokine*, **2**, 205 - 210
- 7 Barnette, M. S., Grais, M., Cieslinski, L. B., Burman, M., Christensen, B. and Torphy, T. J. (1995) *J. Pharm. Exp. Therap.*, **273**, 1396 - 1402
- 8 Barsony, J. and Marx, S. J. (1990) *Proc. Natl. Acad. Sci.*, **87**, 1188 - 1192
- 9 Beavo, J. A., Hardman, J. G. and Sutherland, E. W. (1970) *J. Biol. Chem.*, **245**, 5649 - 5655
- 10 Beavo, J. A., Hardman, J. G. and Sutherland, E. W. (1971) *J. Biol. Chem.*, **246**, 3841 - 3846
- 11 Beavo, J. A. and Reifsneider, D. H. (1990) *TIPS*, **11**, 150 - 155
- 12 Beavo, J. A. (1990) in *Cyclic Nucleotide Phosphodiesterases : Structure, Regulation and Drug Action*, vol. 2 (Beavo, J. A. and Houslay, M. D., eds.), pp. 3 - 14, John Wiley & Sons
- 13 Beavo, J. A., Conti, M. and Heaslip, R. J. (1994) *Mol. Pharmacol.*, **46**, 399 - 405

- 14 Beebe, S. J. and Corbin, J. D. (1986) in *The Enzymes : Control of Phosphorylation*, vol. A (Krebs, E. G. and Bayer, P. D., eds.), pp. 43 -111
- 15 Black, P. (1988) *J. Pharmacol. Methods*, **20**, 57 - 58
- 16 Bolger, G., Michaeli, T., Martins, T., St. John, T., Steiner, B., Rodgers, L., Riggs, M., Wigler, M. and Ferguson, K. (1993) *Mol. Cell. Biol.*, **13**, 6558 -6571
- 17 Bolger, G. (1994a) *Cell. Signalling*, **6**, 851 - 860
- 18 Bolger, G., Rodgers, L. and Riggs, M. (1994b) , **149**, 237 - 244
- 19 Bordier, C. (1981) *J. Biol. Chem.*, **256**, 1604 - 1607
- 20 Bourne, H. R., Lichtenstein, L. M., Melman, K. M., Henney, C. S., Weinstein, Y. and Shearer, G. M. (1974) *Science*, **184**, 19 - 22
- 21 Bradford, M. M. (1976) *Anal. Biochem.*, **72**, 248 - 254
- 22 Brechler, V., Pavoine, C., Hanf, R., Garbarz, E., Fischmeister, R. and Pecker, F. (1992) *J. Biol. Chem.*, **267**, 1546 - 15501
- 23 Breviario, D., Hinnebusch, A., Cannon, J., Tatchell, K. and Dhar, R. (1986) *Proc. Natl. Acad. Sci. USA*, **83**, 4152 - 4156
- 24 Broek, D., Samiy, N., Fasano, O., Fujiyama, A., Tamanoi, F., Northrup, J. and Wigler, M. (1985) *Cell*, **41**, 763 - 769
- 25 Brunkhorst, T. (1989) *Nauyn Schmeidebergs Arch. Pharmacol.*, **339**, 575 - 583
- 26 Burns, F., Rodger, I. W. and Pyne, N. J. (1992) *Biochem. J.*, **283**, 487 - 491
- 27 Burns, F., Sonnenburg, W. K., Francis, S. H., Corbin, J. D. and Beavo, J. A. (1995) *FASEB J.*, **9**, A1261
- 28 Bushfield, M., Murphy, G. J., Lavan, B. E., Parker, P. J., Hruby, V. J., Milligan, G. and Houslay, M. D. (1990) *Biochem. J.*, **268**, 449 - 457
- 29 Bushfield, M., Lavan, B. E. and Houslay, M. D. (1991) *Biochem. J.*, **274**, 317 - 321

- 30 Butcher, R. W. and Sutherland, E. W. (1962) *J. Biol. Chem.*, **237**, 1244 - 1250
- 31 Byres, D., Davis, R. L. and Kiger, J. A. (1981) *Nature*, **289**, 79 - 81
- 32 Cannon, J. F., Gibbs, J. B. and Tatchell, K. (1986) *Genetics*, **113**, 247 - 264
- 33 Casperson, G., Walker, N., Brasier, A. and Bourne, h. (1983) *J. Biol. Chem.*, **258**, 7911 - 7914
- 34 Chan, F. C., Reifsnnyder, D., Beavo, J. A. and Hanifin, J. M. (1993) *J. Allergy Clin. Immunol.*, **91**, 1179 - 1188
- 35 Charbonneau, H., Beier, N., Walsh, K. A. and Beavo, J. A. (1986) *Proc. Natl. Acad. Sci. USA*, **83**, 9308 - 9312
- 36 Chasin, M. (1972) *Biochem. Pharmacol.*, **21**, 2443 - 2450
- 37 Chen, C. N., Denome, S. and Davis, R. L. (1986) *Proc. Natl. Acad. Sci. USA*, **83**, 9313 - 9317
- 38 Cheng, Y. C. and Prusoff, W. H. (1973) *Biochem. Pharmacol.*, **22**, 3099 - 3108
- 39 Cheung, W. Y. (1967) *Biochem. Biophys. Res. Commun.*, **29**, 478 - 482
- 40 Chinkers, M. and Garbers, D. L. (1991) *Annu. Rev. Biochem.*, **60**, 553 - 575
- 41 Choquet, A., Leonard, A., Magais, R. and Bali, J. P. (1990) *Biochem. Pharmac.*, **39**, 1905 - 1911
- 42 Coffey, R. A., Hadden, E. M., Lopez, C. and Hadden, J. W. (1978) *Adv. Cyclic Nucleotide Res.*, **9**, 661 - 676
- 43 Cohen, P. (1985) *Eur. J. Biochem.*, **151**, 439 - 448
- 44 Colicelli, J., Birchmeier, C., Michaeli, T., O'Neill, K., Riggs, M. and Wigler, M. (1989) *Proc. Natl. Acad. Sci. USA*, **86**, 3599 - 3603

- 45 Conti, M. and Swinnen, J. V. (1990) in Cyclic Nucleotide Phosphodiesterases : Structure, Regulation & Drug Action, vol. 2 (Beavo, J. A. and Houslay, M. D., eds.), John Wiley & Sons
- 46 Conti, M., Jin, S. L. C., Monaco, L., Repaske, D. R. and Swinnen, J. V. (1991) *Endocrine Rev.*, **12**, 218 - 234
- 47 Conti, M., Swinnen, J. V., Tsikalas, K. E. and Jin, S. L. C. (1992) *Adv. Second Messenger Phosphoprotein Res.*, **25**, 165 - 175
- 48 Coquil, J. F. (1983) *Biochim. Biophys. Acta*, **743**, 359 - 369
- 49 Crespo, P., Ningzhi, X., Simmonds, W. F. and Gutkind, J. S. (1994) *Nature*, **369**
- 50 Davis, R. L. and Kiger Jr, J. A. (1978) *Biochem. Biophys. Res. Commun.*, **81**, 1180 - 1186
- 51 Davis, R. L. and Kiger Jr., J. A. (1980) *Arch. Biochem. Biophys.*, **203**, 412 - 421
- 52 Davis, R. L. and Kiger Jr., J. A. (1981) *J. Cell. Biol.*, **90**, 101 - 107
- 53 Davis, R. L. and Davidson, N. (1984) *Mol. Cell. Biol.*, **4**, 358 - 367
- 54 Davis, R. L. and Davidson, N. (1986) *Mol. Cell. Biol.*, **6**, 1464 - 1470
- 55 Davis, R. L., Takayasu, H., Eberwine, M. and Myers, J. (1989) *Proc. Natl. Acad. Sci. USA*, **86**, 3604 - 3608
- 56 Davis, R. L. and Henkle-Tigges, J. (1989) *Molec. Pharmacol.*, **37**, 7 - 10
- 57 Davis, R. L. (1990) in Cyclic Nucleotide Phosphodiesterases : Structure, Regulation and Drug Action, vol. 2 (Beavo, J. A. and Houslay, M. D., eds.), pp. 227 - 238, John Wiley & Sons
- 58 DeCamilli, P., Harris, S. M., Hunter, W. B. and Greengard, P. (1983) *J. Cell. Biol.*, **96**, 1355 - 1373
- 59 DeFoe-Jones, D., Scolnick, M., Koller, R. and Dhar, R. (1983) *Nature*, **306**, 707 - 709

- 60 Degerman, E., Belfrage, P., Newman, A. H., Rice, K. C. and Manganiello, V. C. (1987) *J. Biol. Chem.*, **262**, 5797 - 5807
- 61 Degerman, E., Manganiello, V. C., Newman, A. H., Rice, K. C. and Belfrage, P. (1988) *Adv. Second Messenger Phosphoprotein Res.*, **12**, 171 - 182
- 62 Dent, G., Giembycz, M. A., Rabe, K. and Barnes, P. J. (1991) *Br. J. Pharmacol.*, **103**, 1339 - 1341
- 63 DeRobertis, E., Pellegrino De Iraldi, A., Rodriguez de Lores, A. G. and Salganicoff, L. (1962) *J. Neurochem.*, **9**, 23 - 30
- 64 Deterre, P., Bigay, J., Forquet, F., Robert, M. and Chabre, M. (1988) *Proc. Natl. Acad. Sci. USA*, **85**, 2424 - 2428
- 65 DiSanto, M. E. and R.J., H. (1993) *Biochem. Biophys. Res. Commun.*, **197**, 1126 - 1131
- 66 DiSanto, M. E. and Heaslip, R. J. (1993) *Biochem. Biophys. Res. Commun.*, **197**, 1126 - 1131
- 67 Dixon, M. (1953) *Biochem. J.*, **55**, 170 - 175
- 68 Dixon, M. and Webb, E. C. (1979) in *Enzymes*, Academic Press New York
- 69 Dudai, Y. (1983) *Proc. Natl. Acad. Sci. USA*, **80**, 5445 - 5448
- 70 Dudai, Y. (1988) *Annu. Rev. Neurosci.*, **11**, 537 - 563
- 71 Elks, M. L. and Manganiello, V. C. (1984) *Endocrinology*, **15**, 1262 - 1268
- 72 Engels, P., Abdel'Al, S., Hulley, P. and Lubbert, H. (1995) *J. Neurosci. Res.*, **41**, 169 - 178
- 73 Epstein, P. M. and Hachisu, R. (1984) *Adv. Cyclic Nucleotide Protein Phosphorylation Res.*, **16**, 303 - 324
- 74 Erneux, C., Baeynaems, J. M. and Dumont, E. J. (1980) *Biochem. J.*, **192**, 241 - 145

- 75 Fabiato, A. and Fabiato, F. (1979) *Annul. Rev. Physiol.*, **41**, 473 - 484
- 76 Feinstein, M. B., Rodan, G. A. and Cutter, L. S. (1981) in *Platelets in Biology & Pathology*, vol. 2 (Gordon, G. L., ed.), Elsevier / North Holland Biomedical Press
- 77 Fleischhacker, W. W., Hinterhuber, H., Bauer, H., Pflug, B., Berner, P., Simhandl, C., Wolf, R. G., W., Jakutsch, H., Sastre-y-Hernandez and Schubert, H. (1992) *Neuropsychobiology*, **26**, 59 - 64
- 78 Fraenkel, D. G. (1985) *Proc. Natl. Acad. Sci. USA*, **82**, 4740 - 4744
- 79 Frances, S. H., Lincoln, T. M. and Corbin, J. D. (1980) *J. Biol. Chem.*, **255**, 620 - 626
- 80 Francis, S. H. and Corbin, J. D. (1988) *Methods Enzymol.*, **159**, 722 - 729
- 81 Francis, S. H., Colbran, J. A., McAllister-Lucas, L. M. and Corbin, J. D. (1994) *FASEB J.*, **8**, A371
- 82 Fung, B. K. K., Hurley, J. B. and Stryer, L. (1981) *Proc. Natl. Acad. Sci. USA*, **78**, 152 - 156
- 83 Gibbs, J., Sigal, I., Poe, M. and Scolnick, E. M. (1984) *Proc. Natl. Acad. Sci. USA*, **81**, 5704 - 5708
- 84 Gibbs, J., Sigal, I. and Scolnic, E. M. (1985) *TiPS*, **10**, 350 - 353
- 85 Giembycz, M. A. (1992) *Biochem. Pharmacol.*, **43**, 2041 - 2051
- 86 Gillespie, P. J. and Beavo, J. A. (1988) *J. Biol. Chem.*, **263**, 8133 - 8141
- 87 Gilman, A. G. (1984) *Cell*, **36**, 577 - 579
- 88 Gilman, A. G. (1987) *Annu. Rev. Biochem.*, **56**, 615 - 649
- 89 Goetzel, E. J., Shames, R. S., Yang, J. I., Birke, F. W., Lui, Y. F., Albert, P. R. and An, S. (1994) *J. Biol. Chem.*, **269**, 809 - 812
- 90 Goto, K., Nakamura, S., Goto, F. and Yoshinoga, M. (1984) *Br. J. Exp. Pathol.*, **65**, 521 - 525

- 91 Grab, D. J., Carlin, R. K. and Siekevitz, P. (1981) *J. Cell. Biol.*, **89**, 433 - 439
- 92 Grant, P. and Colman, R. W. (1984) *Biochemistry*, **23**, 1801 - 1807
- 93 Gray, A. G. and Whittaker, V. p. (1962) *J. Anat.*, **96**, 79 - 82
- 94 Grewe, S. R., Chan, S. C. and Hanifin, J. M. (1982) *J. Allergy Clin. Immunol.*, **70**, 452 - 457
- 95 Grieswold, D. E., Webb, E. F., Breton, J., White, J. R., Marshall, P. J. and Torphy, T. J. (1993) *Inflammation*, **17**, 333 - 344
- 96 Hadden, J. W. (1988) *Molec. Immunol.*, **25**, 1105 - 1112
- 97 Hamet, P. and Coquil, J. F. (1978) *J. Cyclic Nucleotide Res.*, **4**, 281 - 290
- 98 Hamet, P., Coquil, J. F., Bosseal - Laforhine, S., Franks, D. G. and Tremblay, J. (1984) *Adv. Cyclic Nucleotide Protein Phosphorylation Res.*, **22**, 1 - 38
- 99 Harrison, S. A., Reifsneider, D. H., Gallis, B., Cadd, C. G. and Beavo, J. A. (1986) *Mol. Pharmacol.*, **25**, 506 - 514
- 100 Heyworth, C. M., Wallace, A. W. and Houslay, M. D. (1983) *Biochem. J.*, **214**, 99 - 110
- 101 Heyworth, C. M. and Houslay, M. D. (1983) *Biochem. J.*, **214**, 547 - 552
- 102 Hidaka, H. and Asano, T. (1976) *Biochim. Biophys. Res. Acta*, **429**, 485 - 497
- 103 Hidaka, H. and Endo, T. (1984) *Adv. Cyclic Nucleotide Protein Phosphorylation Res.*, **16**, 245 - 259
- 104 Horowski, R. and Sastre-Y-Hernandez, M. (1985) *Curr. Therap. Res.*, **38**, 23 - 29
- 105 Horton, Y. M., Sullivan, M. and Houslay, M. D. (1995) *Biochem. J.*, **308**, 683 - 691

- 106 Houslay, M. D. and Marchmont, R. J. (1981) *Biochem. J.*, **198**, 703 - 706
- 107 Houslay, M. D., Wallace, A. V., Wilson, S. R., Marchmont, R. J. and Heyworth, C. M. (1983) *Horm. Cell. Regul.*, **7**, 105 - 120
- 108 Iñiguez-Lluhi, J. A., Simon, M. I., Robishau, J. D. and Gilman, A. G. (1992) *J. Biol. Chem.*, **267**, 23409 - 23417
- 109 Ishikawa, I., Katsudhika, S., Chen, L., Halnon, N. J., Kawake, J. I. and Homoy, C. J. (1992) *J. Biol. Chem.*, **267**, 13553 - 13557
- 110 Johnson, M. K. (1960) *Biochem. J.*, **77**, 610 - 618
- 111 Kakuichi, S., Yamazaki, R., Teshima, Y. and Uenishi, K. (1973) *Proc. Natl. Acad. Sci. USA*, **70**, 3526 - 3530
- 112 Kant, G. J., Meyerhoff, J. L. and Lennox, R. H. (1980) *Biochem. Pharmacol.*, **29**, 369 - 373
- 113 Katada, T., Bokoch, G. M., Nothrup, J. K., Ui, M. and Gilman, A. G. (1984) *J. Biol. Chem.*, **259**, 3568 - 3571
- 114 Kataoka, T., Broek, D. and Wigler, M. (1985) *Cell*, **43**, 493 - 505
- 115 Kato, H., Murase, A. K. and Kogure, K. (1993) *Neuroscience*, **52**, 245 - 253
- 116 Kiger Jr., J. A. (1977) *Genetics*, **85**, 623 - 628
- 117 Kiger Jr., J. A. and Golanty, E. (1979) *Genetics*, **91**, 521 - 535
- 118 Kilgour, E., Anderson, N. G. and Houslay, M. D. (1989) *Biochem. J.*, **260**, 27 - 36
- 119 Kincaid, R. L., Balaban, C. D. and Billingsley, M. L. (1987) *Proc. Natl. Acad. Sci. USA*, **84**, 1118 - 1122
- 120 Kittas, P. A., Artmann, M., Thomson, W. J. and Strada, S. J. (1988) *Circulation Res.*, **62**, 782 - 789
- 121 Klemm, P., Mams, H. J. and Perretti, M. (1995) *Eur. J. Pharm.*, **281**, 69 - 74

- 122 Klotz, W. and Stock, K. (1972) *Nauyn-Schmeidebergs Arch. Pharmacol.*, **274**, 54 - 62
- 123 Koe, B. K., Lebel, L. A., Nielson, J. A., Russo, L. L., Saccomano, N. A., Vinick, F. J. and Williams, I. H. (1990) *Drug Devel. Res.*, **21**, 135 - 142
- 124 Kozak, M. (1986) *Cell*, **44**, 283 - 292
- 125 Krause, D. S. and Deutsch, C. (1991) *J. Immunol.*, **146**, 2285 - 2294
- 126 Krebs, E. G. (1985) *Biochem Soc. Trans.*, **13**, 813 - 820
- 127 Krupinski, J., Lehman, T. C., Frankenfeld, C. D., Zwaagsha, J. C. and Walsan, P. A. (1992) *J. Biol. Chem.*, **267**, 24858 - 24862
- 128 Kukovetz, W. R., Poch, G. and Holzmann, S. (1981) in *Vasodilation* (Vanhoutte, P. M. and Leusen, L., eds.), Raven Press New York
- 129 LaPorte, D. C., Toscano, W. A. and Storm, D. R. (1979) *Biochemistry*, **18**, 2820 - 2825
- 130 Lavan, B. E., Lakey, T. and Houslay, M. D. (1990) *Biochem. Pharmac.*, **38**, 4123 - 4136
- 131 Leroy, M. J., Lugnier, C., Merezak, J., Tanguy, G., Oliver, S., LeBec, A. and Ferre, F. (1994) *Cell. Signal.*, **6**, 405 - 412
- 132 Levin, L. R., Han, P. L., Hwang, P. M., Feinstein, P. G., Davis, R. L. and Reed, R. R. (1992) *Cell*, **68**, 479 - 489
- 133 Lincoln, T. M., Hall, C. L. and Corbin, J. D. (1976) *Proc. Natl. Acad. Sci. USA*, **73**, 2559 - 2563
- 134 Livi, J. P., Kmetz, P., McHale, M., Cieslinski, L., Sathe, G. M., Taylor, D. J., Davis, R. L., Torphy, T. J. and Balcarek, J. M. (1990) *Mol. Cell. Biol.*, **10**, 2678 - 2686
- 135 Livisey, S. A., Kemp, B. E., Re, C. A., Partridge, N. C. and Martin, T.J. (1982) *J. Biol. Chem.*, **257**, 14983 - 14987
- 136 Lobban, M., Shakur, Y., Beattie, J. and Houslay, M. D. (1994) *Biochem. J.*, **304**, 399 - 406

- 137 Locmann, S. M., Walter, U., Miller, P. E., Greengard, P. and DeCamilli, P. (1981) *Proc. Natl. Acad. Sci. USA*, **78**, 653 - 657
- 138 Loten, E. G., Assimacopoulos-Jeannet, F. D., Exton, J. H. and Park, C. R. (1978) *J. Biol. Chem.*, **253**, 746 - 757
- 139 Loten, E. G. (1983) *Int. J. Biochem.*, **253**, 746 - 757
- 140 MacFarland, R. T., Zeles, B. D., Novack, J. P. and Beavo, J. A. (1987) *Adv. Cyclic Nucleotide Calcium Protein Phosphorylation Research*, **23**, 10 - 15
- 141 MacPhee, C. H., Harrison, S. A. and Beavo, J. A. (1986) *Proc. Natl. Acad. Sci. USA*, **83**, 6660 - 6663
- 142 Marchbanks, R. M. (1967) *Biochem. J.*, **104**, 148 - 157
- 143 Marchmont, R. J. and Houslay, M. D. (1980a) *Biochem. J.*, **187**, 381 - 392
- 144 Marchmont, R. J. and Houslay, M. D. (1980b) *Nature*, **286**, 904 - 906
- 145 Marchmont, R. J., Ayad, S. R. and Houslay, M. D. (1981) *Biochem. J.*, **195**, 645 - 652
- 146 Marchmont, R. J., Ayad, S. and Houslay, M. D. (1981) *Biochem. J.*, **195**, 645 - 652
- 147 Martin, R., MacFarland, H. F. and MacFarlin, D. (1992) *Annu. Rev. Immunol.*, **10**, 153 - 187
- 148 Martins, T. J., Mumby, M. C. and Beavo, J. A. (1982) *J. Biol. Chem.*, **257**, 1973 - 1979
- 149 Matsumoto, K., Uno, I., Oshima, Y. and Ishikawa, T. (1982) *Proc. Natl. Acad. Sci. USA*, **79**, 2355 - 2359
- 150 Matthews, G. (1987) *Proc. Natl. Acad. Sci.*, **84**, 299 - 300
- 151 McGrath, J., Capon, D., Goeddel, D. and Levison, A. (1984) *Nature*, **310**, 644 - 655
- 152 McHale, M., Cieslinski, L., Eng, W. K., Johnson, R. K., Torphy, T. J. and Livi, G. P. (1990) *Mol. Pharmacol.*, **39**, 109 - 113

- 153 McLaughlin, M. M., Cieslinski, L. B., Burman, M., Torphy, T. J. and Livi, G. (1993) *J. Biol. Chem.*, **268**, 6470 - 6476
- 154 McPhee, I., Pooley, L., Lobban, M., Bolger, G. and Houslay, M. D. (1995) *Biochem. J.*, **310**, 965 - 974
- 155 Meacci, E., Taira, M., Moos Jr., M., Smith, C. J., Movsesian, M. A., Belfrage, P. and Manganiello, V. C. (1992) *Proc. Natl. Acad. Sci. USA*, **89**, 3721 - 3725
- 156 Méry, P. F., Brechler, V., Pavoine, C., Pecker, F. and Fischmeister, R. (1990) *Nature*, **345**, 158 - 161
- 157 Méry, P. F. and Fischmeister, R. (1994) *FASEB J.*, **8**, A82
- 158 Méry, P. F., Pavoine, C., Pecker, F. and Fischmeister, R. (1995) *Molec. Pharmacol.*, **48**, 121 - 130
- 159 Michaeli, T., Bloom, T. J., Martins, T., Loughney, K., Ferguson, K., Riggs, M., Rodgers, L., Beavo, J. A. and Wigler, M. (1993) *J. Biol. Chem.*, **268**, 12925 - 12932
- 160 Milligan, G. (1988) *Biochem. J.*, **255**, 1 - 13
- 161 Miot, F., Van Haastert, P. and Erneux, C. (1985) *Eur. J. Biochem.*, **149**, 59 - 65
- 162 Mohler, J. D. (1973) *Genetics*, **74**, s184
- 163 Mohler, J. D. (1977) *Genetics*, **85**, 259 - 272
- 164 Molnar-Kimber, K. L., Yonno, L. and Heaslip, R. J. (1992) *Mediators of Inflammation*, **1**, 411 - 417
- 165 Morgan, J. P., Perreault, C. L. and Morgan, K. G. (1991a) *Am. Heart J.*, **121**, 961 - 968
- 166 Morgan, J. P. (1991b) *New England J. Med.*, **325**, 625 - 632
- 167 Moss, J., Manganiello, V. C. and Vaughan, M. (1977) *J. Biol. Chem.*, **252**, 5211 - 5215
- 168 Murase, K., Kato, H., Araki, T. and Kogure, K. (1993) *Brain Res.*, **602**, 234 - 239

- 169 Murphy, G. J., Hraby, V. J., Trivedi, D., Wakelam, M. J. O. and Houslay, M. D. (1987) *Biochem. J.*, **243**, 39 - 46
- 170 Murphy, G. J. and Houslay, M. D. (1988) *Biochem. J.*, **249**, 543 - 547
- 171 Nakane, M., Ichikawa, M. and Deguchi, T. (1983) *Brain. Res.*, **273**, 9 - 15
- 172 Nakatuso, K. and Diamond, J. (1989) *Can. J. Physiol. Pharmac.*, **67**, 251 - 262
- 173 Némoz, C., Mouequet, M., Pritent, A. F. and Pacheco, H. (1989) *Eur. J. Biochem.*, **184**, 511 - 520
- 174 Newby, A. C., Luzio, J. P. and Halses, C. N. (1975) *Biochem. J.*, **146**, 625 - 633
- 175 Nielson, C. P., Vestal, R. E., Sturm, R. J. and Heaslip, R. (1990) *J. Allergy Clin. Immunol.*, **86**, 801 - 808
- 176 Nigg, E. A. (1990) *Adv. Cancer. Res.*, **55**, 271 - 310
- 177 Nighorn, A., Healy, M. J. and Davis, R. L. (1991) *Neurone*, **6**, 455 - 467
- 178 Peachell, P. T., Udem, B. J., Schleimer, R. P., MacGlashan Jr., D. W., Leichtenstein, L. M., Cieslinski, L. B. and Torphy, T. J. (1992) *J. Immunol.*, **148**, 2503 - 2510
- 179 Pitt, G. S., Milena, N., Borleis, J., Lin, K. C., Reed, R. R. and Devreotes, P. N. (1992) *Cell*, **69**, 305 - 315
- 180 Podzuweit, T., Nennsteil, P. and Muller, A. (1995) *Cell. Signal.*, **7**, 733 - 738
- 181 Prabhakar, U., Lupschutz, P., O'Leary-Barkus, J., Slivjak, J., Smith, E. F., Lee, J. C. and Esser, K. M. (1994) *Int. J. Immunopharm.*, **16**, 805 - 816
- 182 Pyne, N. J., M.E., C. and Houslay, M. D. (1986) *Biochem. J.*, **234**, 325 - 334

- 183 Pyne, N. J., Cooper, M. and Houslay, M. D. (1987a) *Biochem. J.*, **242**, 33 - 42
- 184 Pyne, N. J., Anderson, N. G., Lavan, B. E., Milligan, G., Nimmo, H. G. and Houslay, M. D. (1987b) *Biochem. J.*, **248**, 897 - 901
- 185 Pyne, N. J., Murphy, G. J., Milligan, G. and Houslay, M. D. (1989) *Biochem. J.*, **243**, 77 - 82
- 186 Pyne, N. J., Cushley, W., Nimmo, H. G. and Houslay, M. D. (1989) *Biochem. J.*, **261**, 897 - 904
- 187 Pyne, N. J., Freissmuth, M. and Plamer, S. (1992) *Biochem. J.*, **285**, 333 - 338
- 188 Pyne, N. J., Grady, M. and Stevens, P. (1993) *Br. J. Pharmac.*, **108**, 74P
- 189 Qian, Y., Girard, V., Martin, C. A. E., Molimard, M. and Advenier, C. (1994) *Eur. Res. J.*, **7**, 306 - 310
- 190 Qui, Y., Chen, C. N., Malone, T., Richter, L., Beckendorf, S. K. and Davis, R. L. (1991) *J. Mol. Biol.*, **222**, 553 - 565
- 191 Raeburn, D., Underwood, S. L., Lewis, S. A., Woodman, V. R., Bartam, C. H., Tomkinson, A., Sharma, S., Jordan, R., Souness, J. E., Webber, S. E. and Karlsson, J. A. (1994) *Br. J. Pharmac.*, **113**, 1423 - 1431
- 192 Rall, T. W., Sutherland, E. W. and Berthet, J. (1957) *J. Biol. Chem.*, **224**, 463 - 475
- 193 Raymond, J. R., Olsen, J. L. and Gettys, T. W. (1993) *Biochemistry*, **32**, 11064 - 11073
- 194 Reeves, M. L., Leigh, B. K. and England, P. J. (1987) *Biochem. J.*, **241**, 535 - 541
- 195 Repaske, D. R., Corbin, J. B., Conti, M. and Goy, M. F. (1993) *Neuroscience*, **56**, 673 - 686

- 196 Richman, P. J. and Klee, C. B. (1978) *J. Biol. Chem.*, **253**, 6323 - 6326
- 197 Robertson, S. P., Johnson, J. D., Holrayde, M. J., Kranias, E. G., Potter, J. D. and Solaro, R. J. (1982) *J. Biol. Chem.*, **257**, 260 - 263
- 198 Robicsek, S., Blanchard, D. K., Djue, J., Krzanowski, J. J., Szentivani, A. and Polson, J. B. (1991) *Br. J. Pharmac.*, **42**, 869 - 877
- 199 Rodger, I. W. and Pyne, N. J. (1992) in *Asthma : Basic Mechanisms & Clinical Management* (Barnes, P. J., Rodger, I. W. and Thomson, N. C., eds.), pp. 58 - 84, Academic Press London
- 200 Saltiel, A. R. and Steierwalt, R. W. (1986) *Diabetes*, **35**, 698 - 704
- 201 Sass, P., Field, J., Nikawa, J., Toda, T. and Wigler, M. (1986) *Proc. Natl. Acad. Sci. USA*, **83**, 9303 - 9307
- 202 Schmitz-Pfeiffer, C., Reeves, M. and Denton, R. (1992) *Cell. Signalling*, **4**, 37 - 49
- 203 Schneider, R., Schmiechen, R., Brezinski, M. and Seider, J. D. (1986) *Eur. J. Pharmacol.*, **127**, 105 - 115
- 204 Schudt, C. and Hatzelmann, A. (1995) *FASEB J.*, **9**, A1261
- 205 Scott, J. D. (1991) *Pharmacol. Ther.*, **14**, 1 - 24
- 206 Scott, J. D. and Carr, D. W. (1992) *News Physiol. Sci.*, **7**, 143 - 148
- 207 Selmaj, K., Raine, C. S., Canella, B. and Brosnan, C. F. (1991) *J. Clin. Invest.*, **87**, 949 - 954
- 208 Semmler, J., Watchel, H. and Endres, S. (1993) *Int. J. Immunopharm.*, **15**, 409 - 411
- 209 Sette, C., Iona, S. and Conti, M. (1994) *J. Biol. Chem.*, **269**, 9245 - 9252
- 210 Shakur, Y., Pryde, J. G. and Houslay, M. D. (1993) *Biochem. J.*, **292**, 677 - 686

- 211 Shakur, Y., Wilson, M. A., Pooley, L., Lobban, M., Griffiths, S. L., Campbell, A. M., Beattie, J., Daly, C. and Houslay, M. D. (1995) *Biochem. J.*, **306**, 801 - 809
- 212 Sharma, R. K., Wang, T. H., Wirch, E. and Wang, J. H. (1980) *J. Biol. Chem.*, **255**, 5916 - 5923
- 213 Shih, T. Y., Papageorge, A. G., Stokes, P. E., Weeks, M. O. and Scolnick, E. M. (1980) *Nature*, **287**, 686 - 691
- 214 Simpson, P. (1988) *Biochem. Pharmacol.*, **37**, 2315 - 2320
- 215 Simpson, A. W. M. (1988) *Biochem. Pharmacol.*, **37**, 2315 - 2320
- 216 Smith, C. J. and Manganiello, V. C. (1988) *Molec. Pharmacol.*, **35**, 381 - 386
- 217 Smith, C. J., Vasta, V., Degerman, E., Belfrage, P. and Manganiello, V. C. (1991) *J. Biol. Chem.*, **266**, 13385 - 13390
- 218 Smith, C. J., Krall, J., Manganiello, V. C. and Movsesian, M. A. (1993) *Biochem. Res. Commun.*, **190**, 516 - 521
- 219 Sommer, N., Loschmann, P. A., Northoff, G. H., Weller, M., Steinbrecher, A., Steinbach, J. P., Lichtenfels, R., Meyermann, R., Reithmuller, A., Fontana, A., Dichgans, J. and Martin, R. (1995) *Nature Medicine*, **1**, 244 - 248
- 220 Sommler, J., Wachtel, H. and Endres, S. (1993) *Int. J. Immunopharmac.*, **15**, 409 - 413
- 221 Sonnenberg, W. K., Mullaney, P. J. and Beavo, J. A. (1991) *J. Biol. Chem.*, **266**, 917 - 948
- 222 Souness, J. E. and Scott, L. C. (1993) *Biochem. J.*, **291**, 389 - 395
- 223 Souness, J. E., Maslen, C., Webber, S., Foster, M., Raeburn, D., Palfreyman, M. N., Ashton, M. J. and Karlsson, J. A. (1995) *Br. J. Pharmacol.*, **115**, 39 - 46
- 224 Spence, S., Rena, G., Sweeney, G. and Houslay, M. D. (1995) *Biochem. J.*, **310**, 975 - 982

- 225 Ståfors, P., Björgell, P. and Belfrage, P. (1984) *Proc. Natl. Acad. Sci. USA*, **81**, 3317 - 3321
- 226 Steinberg, D., Mayer, S. E., Khoo, J. C., Miller, E. A., Miller, R. E., Fredholm, B. and Eicher, R. (1975) *Adv. Cyclic Nucleotide Res.*, **5**, 549 - 568
- 227 Sullivan, M., Egerton, M., Shakur, Y., Marquardson, A. and Houslay, M. D. (1994) *Cell. Signal.*, **6**, 793 - 812
- 228 Sumners, C. and Myers, L. M. (1991) *Am. J. Physiol.*, **260**, C79 - C80
- 229 Swinnen, J. V., Joseph, D. R. and Conti, M. (1989) *Proc. Natl. Acad. Sci. USA*, **86**, 5325 - 5329
- 230 Swinnen, J. V., Joseph, D. R. and Conti, M. (1989) *Proc. Natl. Acad. Sci. USA*, **86**, 8197 - 8201
- 231 Swinnen, J. V., Joseph, D. R. and Conti, M. (1989) *Proc. Natl. Acad. Sci. USA*, **86**, 8197 - 8201
- 232 Swinnen, J. V., Tsikalas, K. E. and Conti, M. (1991) *J. Biol. Chem.*, **266**, 18370 - 18377
- 233 Tamanoi, F., Walsh, M., Kataoka, T. and Wigler, M. (1984) *Proc. Natl. Acad. Sci. USA*, **81**, 6924 - 6928
- 234 Tang, W. J. and Gilman, A. G. (1991) *Science*, **254**, 1500 - 1503
- 235 Tang, W. J. and Gilman, A. G. (1992) *Cell*, **90**, 869 - 872
- 236 Tatchell, K., Robinson, L. C. and Breitenbach, M. (1985) *Proc. Natl. Acad. Sci. USA*, **82**, 3785 - 3789
- 237 Therien, H. M. and Mushynski, B. (1979) *Biochim. Biophys. Acta*, **585**, 201 - 209
- 238 Thomas, M. K., Francis, S. H. and Corbin, J. D. (1990a) *J. Biol. Chem.*, **265**, 14964 - 14970
- 239 Thomas, M. K., Francis, S. H. and Corbin, J. D. (1990b) *J. Biol. Chem.*, **265**, 14971 - 14978

- 240 Thompson, W. J. and Appleman, M. M. (1971) *Biochemistry*, **10**, 311 - 316
- 241 Thompson, W. J. and Appleman, M. M. (1971) *J. Biol. Chem.*, **246**, 3145 - 3150
- 242 Thompson, W. J., Pratt, M. L. and Strada, S. J. (1984) *Adv. Cyclic Nucleotide Protein Phosphorylation Res.*, **16**, 21 - 30
- 243 Thorne, B., Wonnacott, S. and Dunkley, P. R. (1991) *J. Neurochem.*, **56**, 479 - 484
- 244 Toda, T., Uno, I., Ishikawa, T., Powers, S., Kataoka, T., Broek, D., Cameron, S., Broach, J., Matsumoto, K. and Wigler, M. (1985) *Cell*, **40**, 27 - 36
- 245 Tohda, M., Muryama, T., Hasegawa, H., Noguri, S. and Nomura, Y. (1994) *Neurosci. Lett.*, **175**, 89 - 91
- 246 Torphy, T. J. (1988) in *Direction for New Anti-Asthma Drugs* (O'Donnel, S. R. and Persson, C. G. A., eds.), pp. 37 - 58
- 247 Torphy, T. J. (1991) *Thorax*, **46**, 512 - 523
- 248 Torphy, T. J., Zhou, H. L., Foley, J. J. and Serau, H. M. (1991) *Pharmacologist*, **33**, 189 - 192
- 249 Torphy, T. J., Stadel, J. M., Burman, M., Cieslinski, L. B., McLaughlin, M. M., White, J. R. and Livi, G. P. (1992) *J. Biol. Chem.*, **3**, 1798 - 1804
- 250 Torphy, T. J., Livi, G. P., Balcarek, J. M., White, J. R., Chilton, F. H. and Udem, B. J. (1992) *Adv. Second Messenger Phosphoprotein Res.*, **25**, 289 - 291
- 251 Torphy, T. J., Zhou, H. L. and Cielinski, L. B. (1992) *J. Pharmacol. Exp. Ther.*, **263**, 1195 - 1205
- 252 Truatwein, W. and Heschler, J. (1990) *Ann. Rev. Physiol.*, **52**, 257 - 274

- 253 Udovichenko, I. P., Cunnick, J., Gonzales, K. and Takemoto, D. J. (1993) *Biochem. J.*, **295**, 49 - 55
- 254 Van Blesen, T., Howes, B. E., Luttrell, D. K., Krueger, K. M., Tauhova, K., Porfiri, E., Sakaue, M., Luttrell, L. M. and Lefkowitz, R. J. (1995) *Nature*, **376**, 781 - 784
- 255 Vasta, V., Smith, C. J., Calvo, J., Belfrage, P. and Manganiello, V. C. (1992) *Biochem. Biophys. Res. Commun.*, **183**, 1070 - 1075
- 256 Verghese, M. W., McConnel, R. T., Lenhard, J. M., Hamacher, L. and Jin, S. L. C. (1995) *Molec. Pharmacol.*, **47**, 1164 - 1171
- 257 Wald, G. (1968) *Science*, **162**, 230 - 238
- 258 Wang, J. H., Sharma, R. K. and Mooibroek, M. J. (1990) in *Cyclic Nucleotide Phosphodiesterases : Structure, Regulation & Drug Action*, vol. 2 (Beavo, J. A. and Houslay, M. D., eds.), John Wiley & Sons
- 259 Watchel, H. (1982) *Psychopharmacology*, **77**, 309 - 316
- 260 Watchel, H. (1983) *Neuropharmacology*, **22**, 267 - 272
- 261 Watkins, D. C., Johnson, G. L. and Malbon, C. C. (1992) *Science*, **258**, 1373 - 1375
- 262 Weishaar, R. E., Cain, M. H. and Bristol, J. A. (1985) *J. Med. Chem.*, **28**, 537 - 545
- 263 Wingender-Drissan, R. and Becker, J. U. (1983) *Febs. Lett.*, **163**, 33 - 36
- 264 Wilson, M. A., Sullivan, M., Brown, N. and Houslay, M. D. (1994) *Biochem. J.*, **304**, 407 - 415
- 265 Yamamoto, T., Mumby, M. C. and Beavo, J. A. (1983) *J. Biol. Chem.*, **258**, 12526 - 12533
- 266 Yamazaki, R., Teshima, Y., Uenishi, K., Yasuda, S., Kashiba, A., Sobue, K., Ohshima, M. and Nakajima, T. (1978) *Adv. Cyclic Nucleotide Res.*, **9**, 253 - 264

- 267 Yamazaki, A., Sen, I., Bitenski, M. W., Casnellie, J. E. and Greengard, P. (1980) *J. Biol. Chem.*, **255**, 11619 - 11624
- 268 Yau, K. W. and Nakatani, K. (1985) *Nature*, **317**, 252 - 255
- 269 Zuckermann, R. (1973) *J. Physiol.*, **235**, 332 - 333

Appendix 1

<u>Supplier</u>	<u>Chemical</u>
Amersham International, Amersham, Bucks, England, U.K	8-3H-adenosine 3'5' cyclic monophosphate
B.D.H Ltd., Poole, Dorset, England, U.K.	All other chemical reagents not listed here
Bio-Rad, Hemel Hempstead, Herts, England	Nitrocellulose Bradford reagent
Boehringer Mannheim (UK), Lewes, East Sussex, England, UK	ATP GTP Creatine kinase Tris Triton X-100
Sigma Chemical Co., Poole, Dorset, England, U.K.	Adenosine Bovine serum albumin Creatine phosphate Cyclic AMP Dithiothreitol Dowex EGTA Isobutylmethylxanthine Snake venom Tcmed Thimerosal Phenylmethanesulphonyl fluoride

Aprotinin

Pepstatin A

Antipain

Leupeptin

Magnesium chloride

Peptide Research Foundation

(Scientific Marketing Associates)

Koch-Light Ltd.

Dimethylsulphoxide

Pharmacia (UK)

Percoll

Schering Aktiengesellschaft (Berlin)

Gift of rolipram